



Mountain Acid Deposition Program (MADPro)

Cloud Deposition to the Appalachian Mountains 1994 to 1999



U.S. EPA Headquarters Library
Mail code 3201
1200 Pennsylvania Avenue NW
Washington DC 20460

Mountain Acid Deposition Program (MADPro)

Cloud Deposition to the Appalachian Mountains 1994 to 1999

EPA Contract No. 68-D2-0134

Author: Selma Isil

Contributors: Dr. Volker Mohnen
Dr. Gary Lovett
Dr. Eric Miller
Dr. James Anderson
Thomas F. Lavery
Ralph Baumgardner

Prepared by: Harding ESE, Inc.
Gainesville, Florida

Project Officer: Ralph Baumgardner
U.S. Environmental Protection Agency
Office of Research and Development
Research Triangle Park, NC

U.S. EPA Headquarters Library
Mail code 3201
1200 Pennsylvania Avenue NW
Washington DC 20460

4725-17413

The information in this document has been funded wholly by the U.S. Environmental Protection Agency (EPA) under Contract Nos. 68-02-4451 and 68-D2-0134 to Harding ESE, Inc. (Harding ESE). It has been subjected to the Agency's reviews, and it has been approved for publication as an EPA document.

Any mention of trade names or commercial products does not constitute endorsement or recommendation for use.

Table of Contents

Acknowledgments	iv
Abstract	v
List of Tables	vii
List of Figures	ix
List of Acronyms and Abbreviations	xiv
Executive Summary	xvii
1.0 Introduction	1-1
2.0 Network Description and Methods	2-1
2.1 Network Description	2-1
2.2 Field Operations	2-1
2.3 Laboratory Operations	2-4
2.4 Data Management	2-5
2.5 Quality Assurance	2-6
2.5.1 Field Data Audits	2-6
2.5.2 Laboratory Data Audits	2-7
2.5.3 External Audits	2-7
2.5.4 Precision and Accuracy	2-7
2.5.5 Quality Assurance Experiments	2-8
2.5.5.1 Valente Versus Gerber PVM Field Comparison	2-8
2.5.5.2 Comparison of Two EPA Gerber PVMs	2-8
2.5.5.3 Comparison of EPA versus Colorado State University Gerber PVMs ...	2-9
2.5.5.4 Evaluation of LWC Instruments	2-9
2.5.6 Whitetop Mountain LWC Data	2-10

Table of Contents (continued)

3.0 Liquid Water Content and Cloudwater Chemistry	3-1
3.1 Cloud Frequency and Mean Liquid Water Content	3-1
3.2 Cloudwater Chemistry	3-1
3.2.1 Cloudwater pH	3-2
3.2.2 Cloudwater Anions	3-3
3.2.3 Cloudwater Cations	3-4
3.2.4 Normalized Cloudwater Concentrations	3-4
3.2.5 Slide Mountain and Hunter Mountain Results	3-4
3.2.6 Discussion of Results	3-5
4.0 Cloud Deposition	4-1
4.1 Cloudwater Deposition Model (CLOUD)	4-1
4.1.1 Model Description	4-1
4.1.1.1 Canopy Structure	4-2
4.1.1.2 Modifications from Original Version of the Model	4-2
4.1.1.3 Parameter Adjustments at Whiteface Mountain	4-4
4.1.2 Model Calculations	4-5
4.1.3 Model Sensitivity	4-6
4.1.4 Results of CLOUD Model Calculations	4-7
4.2 MCLOUD Model Calculations	4-7
4.2.1 MCLOUD Model Structure and Parameterization for MADPro Sites	4-8
4.2.1.1 Vertical Distribution of Leaf Area in the Forest Canopy	4-8
4.2.1.2 Representation of Cloud Droplet Size Distributions	4-8
4.2.1.3 Number of Droplet Size Classes in the Models	4-9
4.2.1.4 Height of the Wind Speed Measurement Above the Whiteface Mountain Canopy	4-9
4.2.1.5 Representation of Atmospheric Conditions	4-9
4.2.2 MCLOUD Calculations	4-10
4.2.2.1 Data Screening	4-10
4.2.2.2 Data Aggregation and Summary	4-10
4.2.3 Sensitivity Analysis	4-11
4.2.3.1 Model Response to Variation in Forest Canopy Description	4-12
4.2.3.2 Model Response to Variation in Wind Speed and LWC	4-12
4.2.3.3 Model Layer Thickness	4-12

Table of Contents (continued)

4.2.4 MCloud Model Results	4-13
4.2.5 Conclusions	4-13
4.3 Comparison of Results Between the Cloud and MCloud Models	4-14
4.3.1 Results and Discussion	4-14
4.4 Best Estimates of Seasonal Deposition Rates	4-15
5.0 Total Deposition	5-1
5.1 Procedures	5-1
5.2 Results and Discussion	5-3
6.0 Comparison with Other Networks	6-1
6.1 Concentration of Pollutant Ions in Clouds	6-1
6.1.1 Comparison of Results with European Studies	6-2
6.2 Deposition	6-3
6.2.1 Comparison of Results with European Studies	6-5
7.0 Conclusions and Recommendations	7-1
7.1 Cloudwater Concentrations	7-1
7.2 Cloudwater Depositions	7-2
7.3 Recommendations	7-2
References	REF-1
Appendices	

U.S. EPA Headquarters Library
Mail code 3201
1200 Pennsylvania Avenue NW
Washington DC 20460

Acknowledgements

The success of MADPro is due in large part to the dedication and hard work of the individuals involved with the day-to-day operations at the collection sites. The field operations group and laboratory analysts of Harding ESE, Paul Casson, Dave Patrick, Joe Beeler, Don Ho, Tom Davenport, and Donna Foley, are to be commended for their high-quality work and commitment to the goals of MADPro.

Abstract

The Mountain Acid Deposition Program (MADPro) was initiated in 1993 as part of the research necessary to support the objectives of the Clean Air Status and Trends Network (CASTNet), which was created to address the requirements of the Clean Air Act Amendments (CAAA). The two main objectives of MADPro were to develop cloudwater measurement systems to be used in a network monitoring environment and to update the cloudwater concentration and deposition data collected in the Appalachian Mountains during the National Acid Precipitation Assessment Program (NAPAP) in the 1980s. MADPro measurements were conducted from 1994 through 1999 during the warm season at three 'permanent' mountaintop sampling stations. These sampling stations were located at Whiteface Mountain, New York; Clingman's Dome, Tennessee; and Whitetop Mountain, Virginia. A mobile manual sampling station was also operated at two locations in the Catskill Mountains in New York during 1995, 1997, and 1998.

MADPro cloudwater concentrations (normalized with respect to liquid water content) of major ions (SO_4^{2-} , NO_3^- , NH_4^+ , and H^+) showed statistically significant results for all three sites: Clingman's Dome showed an increase for all four ions for both normalized and non-normalized concentrations; Whiteface Mountain results showed a significant decrease for NH_4^+ and SO_4^{2-} for both normalized and non-normalized concentrations; and Whitetop Mountain normalized concentrations exhibited a significant increase for SO_4^{2-} only. All results refer to temporal trends and are based on trends analyses using simple statistical procedures that did not account for variations in meteorology. Clingman's Dome exhibited the highest mean and median 6-year (1994 to 1999) average concentrations for the four major ions, whereas Whiteface Mountain consistently had the lowest mean and median concentrations for these ions.

Cloudwater deposition estimates were made by applying the cloudwater deposition computer model, CLOUD (Lovett, 1984), parameterized with site-specific cloudwater chemistry and meteorological data. In addition, a semi-independent model (M-CLOUD) was employed to explore alternative parameterizations and additional model components beyond those offered by the primary CLOUD model.

Monthly cloudwater deposition estimates (via CLOUD) were highly variable with deposition values typically peaking in July or August. Seasonal deposition amounts (June through September) were highest for Whiteface Mountain, opposite of results for cloudwater concentrations, because of the higher wind speeds and liquid water content (LWC) experienced at this site. No temporal trend is evident in the deposition estimates.

Dry, wet, and cloud deposition estimates were calculated on a monthly basis for June through September for 1994 through 1998 at all three sites. Between 80 and 90 percent of sulfur (S)

deposition occurs via cloud exposure at all three sites as does 70 to 87 percent of the total H^+ loading. Cloud deposition is also responsible for 90 to 95 percent of NH_4^+ deposition at the southern sites. Dry deposition is a very minor contributor to the total S and NH_4^+ loading, but contributes between 22 and 28 percent of nitrogen (N) deposition and approximately 16 percent of H^+ deposition at the southern sites.

In comparison to nearby low-elevation CASTNet sites, total deposition values from MADPro sites are approximately 6 to 20 times greater for S, N and NH_4^+ while H^+ depositions are from 1.3 to 10 times greater. Dry deposition values from MADPro sites for S, N, and H^+ fall within the range of dry deposition values for CASTNet sites. Wet deposition values for all three species are generally 1 to 3 times higher at the CASTNet sites. Thus, the difference in total deposition between MADPro and CASTNet sites is directly attributable to cloud deposition.

Concentration ranges for the ions reported for MADPro are comparable to concentration ranges reported for the Canadian High Elevation Fog (CHEF) project and the Mountain Cloud Chemistry Program (MCCP). However, the MADPro means are higher for all four major ions for Whiteface and Whitetop Mountains in comparison to MCCP results. In general, the MADPro mean calculated deposition values (CLOUD model) for water and four major ions, when compared to MCCP values and several other studies, fall within the range of those measured previously for Clingman's Dome and Whitetop Mountain, while those from the MADPro Whiteface Mountain site are slightly above the range.

List of Tables

- Table 2-1.** Schedule of Routine QC Checks, Calibrations, and Audits Performed at the CASTNet Laboratory (Harding ESE)
- Table 2-2.** Precision and Accuracy Objectives for CASTNet Laboratory Data
- Table 2-3.** Data Quality Objectives for Continuous Measurements
- Table 2-4.** Results From the QA Testing at ECN Facilities in the Netherlands
- Table 3-1.** MADPro Cloud Frequency Summary
- Table 3-2.** Summary Statistics for Cloudwater Samples Collected at MADPro Sites from 1994 through 1999
- Table 3-3.** Number of Records Accepted for Analysis
- Table 3-4.** Mountain Cloud Linear Regression Results
- Table 3-5.** Summary Statistics of Major Ion Concentrations for June through September 1994 through 1999
- Table 4-1.** Monthly Deposition Estimates Produced with the CLOUD Model
- Table 4-2.** Seasonal Deposition Estimates Produced with the CLOUD Model
- Table 4-3.** Effect of Data Screening on Sample Retention
- Table 4-4.** Combinations of Wind Speed and LWC Evaluated
- Table 4-5.** Alternate Forest Canopy Descriptions
- Table 4-6.** MCLOUD Seasonal Deposition Estimates
- Table 4-7.** Summary of CLOUD Model Sensitivity, Potential Bias, and Expected Differences with MCLOUD Modeling Results
- Table 4-8.** Comparison of Deposition Velocities and Water Depositions
- Table 4-9.** Best Estimates of Seasonal Depositions

List of Tables (continued)

- Table 5-1.** Summary of Cloud, Precipitation, Dry, and Total Deposition Estimates for Whiteface Mountain
- Table 5-2.** Summary of Cloud, Precipitation, Dry, and Total Deposition Estimates for Whitetop Mountain
- Table 5-3.** Summary of Cloud, Precipitation, Dry, and Total Deposition Estimates for Clingman's Dome
- Table 5-4.** Percent Composition of Total Deposition at the Three MADPro Sites
- Table 5-5.** Dry, Wet, and Total Seasonal Depositions (June through September) for Whiteface Mountain and Two Nearby CASTNet Sites for 1995 through 1998
- Table 5-6.** Dry, Wet, and Total Seasonal Depositions (June through September) for Whitetop Mountain and Two Nearby CASTNet Sites for 1996
- Table 6-1.** Warm Season Average Ion Concentrations for the Six MCCP Sites 1986 through 1988
- Table 6-2.** Comparison (RPD) of MCCP versus MADPro Average Ion Concentrations
- Table 6-3.** Mean Chemical Composition Including Minima and Maxima of Cloudwater Collected at Mt. Brocken, Germany
- Table 6-4.** Statistical Characterization of the Chemical Composition of Fog Samples from European Investigations
- Table 6-5.** Comparison of MADPro Cloudwater Deposition Estimates to Previous Studies
- Table 6-6.** A Summary of Cloudwater Chemical Deposition via Droplet Interception for the Eastern United States
- Table 6-7.** Comparison of the Proportion of Total Ion Deposition Delivered by the Dry, Cloudwater, and Precipitation Deposition Estimates for Whiteface Mountain at an Elevation of 1,050 m

List of Figures

- Figure 2-1.** Locations of Mountain Acid Deposition Sites
- Figure 2-2.** Regional Map for Whiteface Mountain, NY
- Figure 2-3.** Regional Map for Whitetop Mountain, VA
- Figure 2-4.** Regional Map for Clingman's Dome, TN
- Figure 2-5.** MADPro Sampling System
- Figure 2-6.** Flowchart of Laboratory Operations for Cloudwater and Precipitation Sample Analyses
- Figure 2-7.** PVM-100 Intercomparison at Whitetop Mountain, VA, 1998
- Figure 3-1.** Monthly Cloud Frequency (1994 through 1999), Whiteface Mountain, NY
- Figure 3-2.** Monthly Cloud Frequency (1994 through 1999), Whitetop Mountain, VA
- Figure 3-3.** Monthly Cloud Frequency (1994 through 1999), Clingman's Dome, TN
- Figure 3-4.** Mean Liquid Water Content of Clouds (1994 through 1999), Whiteface Mountain, NY
- Figure 3-5.** Mean Liquid Water Content of Clouds (1994 through 1999), Whitetop Mountain, VA
- Figure 3-6.** Mean Liquid Water Content of Clouds (1994 through 1999), Clingman's Dome, TN
- Figure 3-7.** Mean Liquid Water Content of Clouds
- Figure 3-8.** Mean pH of Cloudwater Samples at MADPro Sites (1994 through 1999)
- Figure 3-9.** Frequency Distribution for Cloudwater pH at Whiteface Mountain, NY (1994 through 1999)
- Figure 3-10.** Frequency Distribution for Cloudwater pH at Whitetop Mountain, VA (1994 through 1999)

List of Figures (continued)

- Figure 3-11.** Frequency Distribution for Cloudwater pH at Clingman's Dome, TN (1994 through 1999)
- Figure 3-12.** Normalized SO_4^{2-} Concentrations in Cloudwater at Whitetop Mountain, 1994 through 1996 – Calculated as LWC Weighted Means versus Arrival Sector
- Figure 3-13.** Normalized SO_4^{2-} Concentrations in Cloudwater at Whiteface Mountain, 1994 through 1996 – Calculated as LWC Weighted Means versus Arrival Sector
- Figure 3-14.** Annual SO_2 Emissions for 1995
- Figure 3-15.** Mean Normalized SO_4^{2-} Concentrations ($\mu\text{eq/L}$); Segregated by Back Trajectory Arrival Sector
- Figure 3-16.** pH of Cloudwater Samples, Whiteface Mountain, NY (1995)
- Figure 3-17.** pH of Cloudwater Samples, Whiteface Mountain, NY (1997)
- Figure 3-18.** pH of Cloudwater Samples, Whiteface Mountain, NY (1999)
- Figure 3-19.** pH of Cloudwater Samples, Whitetop Mountain, VA (1995)
- Figure 3-20.** pH of Cloudwater Samples, Whitetop Mountain, VA (1997)
- Figure 3-21.** pH of Cloudwater Samples, Whitetop Mountain, VA (1999)
- Figure 3-22.** pH of Cloudwater Samples, Clingman's Dome, TN (1995)
- Figure 3-23.** pH of Cloudwater Samples, Clingman's Dome, TN (1997)
- Figure 3-24.** pH of Cloudwater Samples, Clingman's Dome, TN (1999)
- Figure 3-25.** Mean Hydrogen Ion Concentrations of Cloudwater Samples at MADPro Sites (1994 through 1999)
- Figure 3-26.** Mean Hydrogen Ion Concentrations of Cloudwater Samples at MADPro Sites (1994 through 1999)

List of Figures (continued)

- Figure 3-27.** Monthly Variation in H^+ Concentrations in Cloudwater (Means Across All Years, 1994 through 1999)
- Figure 3-28.** Mean SO_4^{2-} Concentrations of Cloudwater Samples at MADPro Sites (1994 through 1999)
- Figure 3-29.** Mean SO_4^{2-} Concentrations of Cloudwater Samples at MADPro Sites (1994 through 1999)
- Figure 3-30.** Monthly Variation in SO_4^{2-} Concentrations in Cloudwater (Means Across All Years, 1994 through 1999)
- Figure 3-31.** Mean NO_3^- Concentrations of Cloudwater Samples at MADPro Sites (1994 through 1999)
- Figure 3-32.** Mean NO_3^- Concentrations of Cloudwater Samples at MADPro Sites (1994 through 1999)
- Figure 3-33.** Monthly Variation in NO_3^- Concentrations in Cloudwater (Means Across All Years, 1994 through 1999)
- Figure 3-34.** Mean NH_4^+ Concentrations of Cloudwater Samples at MADPro Sites (1994 through 1999)
- Figure 3-35.** Mean NH_4^+ Concentrations of Cloudwater Samples at MADPro Sites (1994 through 1999)
- Figure 3-36.** Average Minor Ion Concentrations from 1994 to 1999
- Figure 3-37.** Normalized Mean Hydrogen Ion Concentrations of Cloudwater Samples at MADPro Sites (1994 through 1999)
- Figure 3-38.** Normalized Mean SO_4^{2-} Concentrations of Cloudwater Samples at MADPro Sites (1994 through 1999)
- Figure 3-39.** Normalized Mean NO_3^- Concentrations of Cloudwater Samples at MADPro Sites (1994 through 1999)

List of Figures (continued)

- Figure 3-40.** Normalized Mean NH_4^+ Concentrations of Cloudwater Samples at MADPro Sites (1994 through 1999)
- Figure 3-41.** Concentrations for SLD/HUN301 (1995, 1997, 1998)
- Figure 3-42.** CLD303 1994 through 1999 Regressions Using All Data Points - Non-Normalized Concentrations
- Figure 3-43.** CLD303 1994 through 1999 Regressions Using All Data Points - Normalized Concentrations
- Figure 3-44.** WFM300 1994 through 1999 Regressions Using All Data Points - Non-Normalized Concentrations
- Figure 3-45.** WFM300 1994 through 1999 Regressions Using All Data Points - Normalized Concentrations
- Figure 3-46.** WTM302 1994 through 1999 Regressions Using All Data Points - Normalized Concentrations
- Figure 4-1.** Relationship Between Square of the Mean Droplet Diameter (D) and LWC for Clouds on Whitetop Mountain
- Figure 4-2.** Relative Percent Difference Versus Total Anion Concentration for Each Sample
- Figure 4-3.** Sensitivity of Deposition Velocity to Wind Speed
- Figure 4-4.** Sensitivity of Deposition Velocity to LWC
- Figure 4-5.** Results of Numerical Experiments with Model Layer Thickness and Shifts in the Vertical Distribution of Leaf Area
- Figure 4-6.** Difference in Cloudwater Deposition Rate between Model Runs Using the Whitetop Mountain Cloud Droplet Size Distribution and the Whiteface Mountain Cloud Droplet Size Distribution for a Range of LWC and Wind Speed
- Figure 4-7.** Frequency Distribution of Sample Water Deposition for Clingman's Dome 1997 Data Set Calculated with Either 500 or 20 Droplet Size Classes Representing the Continuous Droplet Size Distribution

List of Figures (continued)

- Figure 4-8.** Comparison of Estimated Cloudwater Fluxes Using Four Potential Model Scenarios at Whiteface Mountain, 1997
- Figure 4-9.** Frequency Distributions of LWC and Wind Speed Scaled to Values Representative of 1,225-m Elevation on Whiteface Mountain
- Figure 4-10.** Percent Deviation of Model Response to a Hypothetical Pure Balsam Fir Canopy from Model Response to an Observed Average Canopy at 1,225-m Elevation on Whiteface Mountain over a Range of Wind Speed and LWC Values
- Figure 4-11.** Percent Deviation of Model Response to Several Canopy Height Specifications from Model Response to the Observed Height of 17 m at 1,225-m Elevation
- Figure 4-12.** Percent Deviation of Model Response to Variations in LAI with a Constant Canopy Height of 10 m
- Figure 4-13.** Model Response (Hourly Water Flux) to Variation in Wind Speed for a Range of Cloud LWC
- Figure 5-1.** Areas in the Eastern United States with Elevations Above 800 Meters
- Figure 5-2.** Percent Composition of Total Deposition at MADPro Sites
- Figure A-1.** Mean Liquid Water Content of Clouds with Scaled 1998 WTM LWC
- Figure A-2.** Normalized Mean Hydrogen Ion Concentrations of Cloudwater Samples at MADPro Sites (1994 through 1999) with Scaled 1998 WTM LWC
- Figure A-3.** Normalized Mean NH_4^+ Concentrations of Cloudwater Samples at MADPro Sites (1994 through 1999) with 1998 WTM LWC
- Figure A-4.** Normalized Mean NO_3^- Concentrations of Cloudwater Samples at MADPro Sites (1994 through 1999) with 1998 WTM LWC
- Figure A-5.** Normalized Mean SO_4^{2-} Concentrations of Cloudwater Samples at MADPro Sites (1994 through 1999) with 1998 WTM LWC

List of Acronyms and Abbreviations

AIRMoN	Atmospheric Integrated Research Monitoring Network
AIRS	Aerometric Information Retrieval System
ARS	Air Resource Specialists
ASRC	Atmospheric Sciences Research Center
°C	degrees Celsius
Ca ²⁺	calcium
CAAA	Clean Air Act Amendments
CASTNet	Clean Air Status and Trends Network
CDM-D	cloud deposition model – deciduous
CDM-S	cloud deposition model – spruce
CE	collection efficiency
CHEF	Chemistry of High Elevation Fog
Cl ⁻	chloride
CLASS TM	Chemistry Laboratory Analysis and Scheduling System
CLD303	Clingman's Dome, Tennessee Sampling Station
cm	centimeter
cm/sec	centimeters per second
cond.	conductivity
CSU	Colorado State University
CVS	continuing verification sample
CWP	Cloudwater Project
DAS	data acquisition system
DEC	New York Department of Environmental Conservation
ECEB	eddy covariance-energy budget
ECN	Energy Center for the Netherlands
EPA	U.S. Environmental Protection Agency
EPRI-IFS	Electric Power Research Institute-Integrated Forest Study
ft	foot
g/cm ² /min	grams per square centimeter per minute
g/m ³	grams per cubic meter
H ⁺	hydrogen
Harding ESE	Harding ESE, Inc.
HNO ₃	nitric acid
HUN301	Hunter Mountain, New York Mobile Sampling Station
IC	ion chromatography
ICAP-AE	inductively coupled argon plasma - atomic emission
K ⁺	potassium
K ₂ CO ₃	potassium carbonate

List of Acronyms and Abbreviations (continued)

kg/ha/mo	kilograms per hectare per month
kg/ha/yr	kilograms per hectare per year
km	kilometer
L	liter
LAI	leaf area index
Lpm	liters per minute
LWC	liquid water content
m ² /m ²	square meter per square meter
m	meter
m/sec	meters per second
MADPro	Mountain Acid Deposition Program
MCCP	Mountain Cloud Chemistry Program
MFC	mass flow controller
Mg ²⁺	magnesium
mL	milliliter
MLM	multi-layer model
mm	millimeter
mm/hr	millimeters per hour
MmaD	mass median aerodynamic diameter
N	nitrogen
Na ⁺	sodium
NADP/NTN	National Atmospheric Deposition Program/National Trends Network
NAPAP	National Acid Precipitation Assessment Program
NH ₄ ⁺	ammonium
NIST	National Institute for Standards and Technology
nm	nanometer
NO ₂	nitrite
NO ₃	nitrate
NOAA	National Oceanic and Atmospheric Administration
NPS	National Park Service
O ₃	ozone
Ogden	Ogden Environmental and Energy Services, Inc.
ppb	parts per billion
PVM	particle volume monitor
QA	quality assurance
QC	quality control
%RD	percent relative deficit
Rh	relative humidity

List of Acronyms and Abbreviations (continued)

RPD	relative percent difference
S	sulfur
SLD301	Slide Mountain, New York Mobile Sampling Station
SO ₄ ²⁻	sulfate
SO ₂	sulfur dioxide
SOP	standard operating procedure
TRAACS	Technicon Random Access Automated Chemistry System
µeq/L	microequivalent per liter
µg/filter	microgram per filter
µm	micrometer
UV	ultraviolet
WFM	Whiteface Mountain, New York Sampling Station
WFML	Whiteface Mountain lower
WFMS	Whiteface Mountain summit
WTM302	Whitetop Mountain, Virginia Sampling Station

Executive Summary

The 1990 Clean Air Act Amendments (CAAA) required a reduction in sulfur dioxide (SO_2) emissions by approximately 10 million tons annually to occur in two phases. The first phase was implemented in 1995 when large electric generating facilities reduced emissions. The second phase is scheduled for 2000 and targets other power plants. Title IX of the CAAA also mandated the deployment of a comprehensive research and monitoring program. This program would track the effectiveness of emission reduction programs with respect to deposition, air quality, and changes to affected ecosystems. The Clean Air Status and Trends Network (CASTNet) was implemented in 1991 in response to this mandate.

The Mountain Acid Deposition Program (MADPro) was initiated in 1993 as part of the research necessary to support the objectives of CASTNet. The two main objectives of MADPro were to develop cloudwater measurement systems to be used in a network monitoring environment and to update the cloudwater concentration and deposition data collected in the Appalachian Mountains during the National Acid Precitation Assessment Program (NAPAP) in the 1980s. MADPro measurements were conducted from 1994 through 1999 during the warm season at three 'permanent' mountaintop sampling stations. These sampling stations were located at Whiteface Mountain, New York; Clingman's Dome, Tennessee; and Whitetop Mountain, Virginia. A mobile manual sampling station was also operated at two locations in the Catskill Mountains in New York during 1995, 1997, and 1998. The two main objectives of MADPro have been successfully met. The results of the first objective are summarized in Baumgardner *et al.* (1997) and Anderson *et al.* (1999). The results of the second objective are provided in this report.

This report summarizes the analysis and interpretation of MADPro measurements collected from 1994 through 1999. Summary statistics, analyses of cloud frequency, liquid water content (LWC), cloud chemistry, and cloud and total deposition are presented for the three permanent sites. A summary of European and other cloud studies, their comparison to MADPro results, and comparisons to the Mountain Cloud Chemistry Program (MCCP) results are included along with conclusions and recommendations for future studies.

MADPro cloudwater concentrations (normalized with respect to liquid water content) of major ions (SO_4^{2-} , NO_3^- , NH_4^+ , and H^+) showed statistically significant trend results for all three sites: Clingman's Dome showed an increase for all four ions for both normalized and non-normalized concentrations; Whiteface Mountain results showed a significant decrease for NH_4^+ and SO_4^{2-} for both normalized and non-normalized concentrations; and Whitetop Mountain normalized concentrations exhibited a significant increase for SO_4^{2-} only. All results refer to temporal trends and are based on trends analyses using simple statistical procedures that did not account for variations in meteorology. Clingman's Dome exhibited the highest mean and median 6-year (1994 and 1999) average

concentrations for the four major ions, whereas Whiteface Mountain consistently had the lowest mean and median concentrations for these ions.

The lack of any discernible temporal trends for some of the major ions and the increasing SO_4^{2-} temporal trend exhibited at Whitetop Mountain is inconsistent with the downward trend in SO_2 emission levels in the eastern United States [U.S. Environmental Protection Agency (EPA), 2000]. Given the magnitude of the decrease in the SO_2 emission levels, stronger decreasing temporal trends might also be expected at Whiteface Mountain. These results indicate that cloudwater concentrations of SO_4^{2-} may not be linearly related to SO_2 emission reductions because SO_4^{2-} production in clouds is oxidant-limited. More research and monitoring is necessary before any solid conclusions can be made as the lack of trends, weak trends, or increasing trends, within this period may also be a function of, or influenced by, year-to-year variations in air mass trajectories and regional and local meteorology. Depending on the year, variations in LWC are also shown to have an effect, although not large, on the results.

Cloudwater deposition estimates were made by applying the cloudwater deposition computer model, CLOUD (Lovett, 1984), parameterized with site-specific cloudwater chemistry and meteorological data. In addition, a semi-independent model (MCLOUD) was employed to explore alternative parameterizations and additional model components beyond those offered by the primary CLOUD model. MCLOUD was used to produce an alternative set of cloudwater deposition estimates for eight site-by-year combinations as well as deposition estimates for all 1999 data.

Monthly cloudwater deposition estimates (via CLOUD) were highly variable with depositions typically peaking in July or August. Seasonal deposition values (June through September) were highest for Whiteface Mountain, opposite of results for cloudwater concentrations, because of the higher wind speeds and LWC experienced at this site. No temporal trend is evident in the deposition estimates.

Deposition velocities and cloudwater deposition estimates produced by the CLOUD model were approximately 45 percent higher than the MCLOUD runs for the same site-year combinations. Differences in model formulation and parameterizations, input data, and data screening and data aggregation procedures all contribute to the differences seen in the results from both models. The 1999 deposition estimates produced by MCLOUD were, therefore, scaled up by 1.45 to account for these differences.

Total deposition consists of three components: 1) dry, 2) wet, and 3) cloud depositions. Estimates for all three components were calculated on a monthly basis for June through September for 1994 through 1998 at all three sites. The multi-layer model (MLM) was used to estimate dry deposition (Meyers *et al.*, 1998; Finkelstein *et al.*, 2000). Estimates of wet deposition were made using onsite or nearby precipitation chemistry measurements. These results show that clouds are the largest source

for deposition of pollutants to high-elevation ecosystems. Between 80 and 90 percent of S deposition occurs via cloud exposure at all three sites as does 70 to 87 percent of the total H^+ loading. Cloud deposition is also responsible for 90 to 95 percent of NH_4^+ deposition at the southern sites. Dry deposition is a very minor contributor to the total S and NH_4^+ loading, but contributes between 22 and 28 percent of N deposition and approximately 15 to 16 percent of H^+ deposition at the southern sites.

In comparison to nearby low-elevation CASTNet sites, total deposition values from MADPro sites are approximately 6 to 20 times greater for S, N and NH_4^+ , while H^+ depositions are usually 1.3 to 10 times greater. Dry deposition values from MADPro sites for S, N, and H^+ fall within the range of dry deposition values for CASTNet sites. Wet deposition values for all three species are generally 1 to 3 times higher at the CASTNet sites. Thus, the difference in total deposition between MADPro and CASTNet sites is directly attributable to cloud deposition.

The uncertainties in the calculations of cloud deposition values are estimated to range from at least 50% to 100% or more based on the comparison of the results from the CLOUD and MCLLOUD models and on an analysis of evaluation studies for resistance type models. The model comparisons suggest that the CLOUD model overestimates cloud deposition.

The uncertainties in the calculations of dry and wet deposition values are more variable. The uncertainties in the dry deposition values generated using the MLM model for Whitetop Mountain and Clingman's Dome are estimated as less than 100% for seasonal fluxes based on model evaluation studies. These model calculations are considered underestimates (Finkelstein *et al.*, 2000). The uncertainty in the estimate of wet deposition for Clingman's Dome is unknown. Wet deposition data from nearby Mt. Mitchell were used for this site. The estimates of both dry and wet deposition for Whiteface Mountain are also considered underestimates due to the difference in elevation of the sampling locations. These underestimates may be as high as 400% for dry deposition while the amount of underestimation for wet deposition is unknown.

Concentration ranges for the ions reported for MADPro are comparable to concentration ranges reported for the Canadian High Elevation Fog (CHEF) project and the MCCP. However, the MADPro means are higher for all four major ions for Whiteface and Whitetop mountains in comparison to MCCP results. In general, the MADPro mean calculated deposition values (CLOUD model) for water and four major ions, when compared to MCCP values and several other studies, fall within the range of those measured previously for Clingman's Dome and Whitetop Mountain, while those from the MADPro Whiteface Mountain site are slightly above the range.

Since the commencement of operation in 1994, MADPro has produced a 6-year data set that is comparable to data produced by past networks. Although not designed for ecological studies, results from this program will aid ecologists in damage assessment of high-elevation ecosystems through the provision of a data set of known uncertainty.



1.0 Introduction

Cloudwater droplets have been shown to contain high concentrations of acidic and other dissolved ions depending on back or past trajectories (Mohnen and Vong, 1993). Cloudwater is typically 5 to 20 times more acidic than rain water (Mohnen *et al.*, 1990; Vong *et al.*, 1991). Thus, clouds can be the primary pathway for exposure and deposition of pollutants to high-elevation ecosystems (Aneja and Kim, 1993). Subalpine, high-elevation forests of the eastern United States receive some of the largest air pollution loadings of any rural environment in North America (Miller *et al.*, 1993b; Lindberg, 1992; Lovett and Kinsman, 1990). This large loading of pollutants is due to a combination of factors including high frequency of cloud immersion, high wind speeds, orographic enhancement of precipitation, and the large leaf areas of tree species typical of these environments (Miller and Friedland, 1999). There has been consistent evidence that exposure to acidic cloudwater, which reduces cold tolerance, is one of the causal factors leading to the recent decline of red spruce (*Picea rubens*) in the northeastern United States (Eager and Adams, 1992). Other possible mechanisms of forest damage from acidic deposition include extensive leaching of cations and amino acids from the foliage (Scherbatskoy and Klein, 1983), nitrogen overload, aluminum toxicity, and the combined effect of acid rain, acid fog, oxidants, and heavy metals (Schemenauer, 1986; McLaughlin *et al.*, 1990, 1991).

Previous cloud monitoring efforts that have characterized cloudwater chemistry in North America include:

1. The Cloudwater Project (CWP), Weathers *et al.* (1986, 1988, 1995) – Studied rain and cloudwater chemistry on mountain ranges from Puerto Rico to Alaska;
2. The U.S. Environmental Protection Agency's (EPA's) Mountain Cloud Chemistry Program (MCCP) – Collected and analyzed cloudwater samples and estimates of cloud deposition from the mountains of the eastern United States from 1986 to 1989 (Mohnen and Kadlec, 1989; Saxena *et al.*, 1989; Vong *et al.*, 1991; Li and Aneja, 1992; Mohnen and Vong, 1993); and
3. Canada's Chemistry of High Elevation Fog (CHEF) Project – Measured cloud chemistry on three mountains in southern Quebec from 1985 to 1991 (Schemenauer, 1986; Schemenauer and Winston, 1988; Schemenauer *et al.*, 1995).

Data collected by these projects were used by the National Acid Precitation Assessment Program (NAPAP) to evaluate the role of airborne chemicals on the changing conditions of forests. The NAPAP Integrated Assessment of 1990 concluded that a limited number of forest ecosystems were at risk from acidic deposition and additional ecosystems would be at risk in the future. The 1990 Clean Air Act Amendments (CAAA) required a 10 million ton reduction of sulfur dioxide (SO₂) emissions to occur in two phases. The first phase was to be completed by the year 2000 and the second phase by 2010. Title IX of the CAAA also mandated the deployment of a national monitoring network to

track the effectiveness of emission reduction programs with respect to deposition, air quality, and changes to affected ecosystems. The Clean Air Status and Trends Network (CASTNet) was implemented in 1991 in response to this mandate.

The Mountain Acid Deposition Program (MADPro) was initiated in 1993 as part of the research necessary to support the objectives of CASTNet. The two main objectives of the program were to develop cloudwater measurement systems to be used in a network monitoring environment and to update the cloudwater concentration and deposition data collected in the Appalachian Mountains during NAPAP in the 1980s. MADPro measurements were conducted from 1994 through 1999 during the warm season at three 'permanent' mountaintop sampling stations. These sampling stations were located at Whiteface Mountain, New York; Clingman's Dome, Tennessee; and Whitetop Mountain, Virginia. A mobile manual sampling station was also operated at two locations in the Catskill Mountains in New York during 1995, 1997, and 1998.

The two main objectives of MADPro have been met. The results of the first objective are presented in Baumgardner *et al.* (1997) and Anderson *et al.* (1999). The results of the second objective are provided in this report.

The report includes a detailed network description in Chapter 2.0. Summary statistics and analyses of cloud frequency, liquid water content (LWC), and cloud chemistry are presented in Chapter 3.0. Modeled cloud deposition estimates are discussed in Chapter 4.0. Estimates of cloud, wet, dry, and total depositions are discussed in Chapter 5.0. A summary of European and other cloud studies, their comparison to MADPro results, and comparisons to MCCP results are presented in Chapter 6.0. Conclusions and recommendations for future programs are presented in Chapter 7.0.

2.0 Network Description and Methods

2.1 Network Description

The three permanent MADPro sites were widely dispersed along the Appalachian Mountains (Figure 2-1). Whiteface Mountain (44°21'58"N, 73°54'10"W) is located in the northeastern Adirondacks in upstate New York (Figure 2-2). The cloudwater sampling research station was above the tree line at 1,483 meters (m). The instrumentation was located on the top floor of a four-story observatory at the summit, with the cloudwater collector, particle volume monitor (PVM), and meteorological sensors mounted on the flat circular roof.

Whitetop Mountain (36°38'20"N, 81°36'19"W) is located in the Mount Rogers National Recreation Area of the Jefferson National Forest in southwestern Virginia (Figure 2-3). It is 6 kilometers (km) southwest of Mount Rogers, the highest peak in Virginia. The MADPro research station was at 1,686 m on the main ridge line of the Appalachian range.

Clingman's Dome (35°33'47"N, 83°29'55"W) is the highest mountain in the Great Smoky Mountains National Park (Figure 2-4). The solar-powered MADPro site was situated at an elevation of 2,014 m approximately 50 m southwest of the summit spiral tourist tower. Electronic instrumentation was housed in a small National Park Service (NPS) building and the cloudwater collector, PVM, and meteorological sensors were positioned on top of a 50-foot (ft) scaffold tower.

Collection at the sites was initiated each spring, as soon as local weather conditions would allow, and continued through autumn. Collection ran June through September for Whiteface Mountain, and May through October for Whitetop Mountain and Clingman's Dome.

A mobile site was located on Slide Mountain in the Catskill Mountains of New York in 1995. A semi-automated system was relocated to Hunter Mountain in 1997 and collected samples during 1997 and 1998. The Hunter Mountain site also collected wind speed and wind direction data measured with a portable Davis anemometer.

2.2 Field Operations

The MADPro cloud collection system consisted of an automated cloudwater collector for hourly cloudwater sampling, a PVM for continuous determination of cloud LWC, a meteorological station for continuous measurements of wind speed, wind direction, temperature, relative humidity, solar radiation, and precipitation, and a data acquisition system (DAS) for collection and storage of electronic information from the various monitors and sensors (Figure 2-5). The Clingman's Dome and Whitetop Mountain sites also had a filter pack system for dry deposition estimation, with an

additional wet deposition system consisting of a precipitation collector and rain gauge at Whitetop Mountain. The filter pack and additional wet deposition systems were not used at Whiteface Mountain because the National Oceanic and Atmospheric Administration (NOAA) and the National Atmospheric Deposition Program/National Trends Network (NADP/NTN) were measuring these parameters in the vicinity of the cloudwater collection site. Likewise, the Cingman's Dome site had access to the data collected by a nearby wet deposition system operated by the NPS.

The Whitetop Mountain site was also equipped with a continuous ozone (O_3) monitor. In addition, continuous O_3 data [through Aerometric Information Retrieval System (AIRS)] and SO_2 data [through the New York Department of Environmental Conservation (DEC)] are available for Whiteface Mountain.

The core of the automated cloud collection system is a passive string collector [also known as the Mohnen collector or the Atmospheric Sciences Research Center (ASRC) design] previously used in the MCCP study. Collection occurs when ambient winds transport cloudwater droplets onto 0.4-millimeter (mm) Teflon® wires strung between two circular disks (Falconer and Falconer, 1980; Mohnen and Kadlec, 1989). Once impacted, the droplets slide down the strings into a funnel and through Teflon® tubing into sample bottles in a refrigerated carousel. The development and design of this system is described in detail in Baumgardner *et al.* (1997).

The PVM-100 by Gerber Scientific (Gerber, 1984) measures LWC and effective droplet radius of ambient clouds by directing a narrow laser beam from a 780-nanometer (nm) diode along a 40-centimeter (cm) path. The forward scatter of the cloud droplets in the open air along the path is measured, translated, and expressed as grams of water per cubic meter (g/m^3) of air. This system was programmed so that the collector would be activated and projected out of the protective housing when threshold levels for LWC ($0.05 g/m^3$), wind speed [>2.5 meters per second (m/sec)], and ambient air temperature [2 degrees Celsius ($^{\circ}C$)] were reached. In addition, the system was activated only when no precipitation was measured. Within the context of MADPro, therefore, a cloud was defined by a LWC of $0.05 g/m^3$ or higher, as measured by the PVM. This threshold was established to have comparability with the MCCP measurements, which were made for the most part with Mallant Optical Cloud Detectors set at a threshold of approximately $0.04 g/m^3$ (Mohnen *et al.*, 1990). The wind speed threshold of 2.5 m/sec was established because cloudwater collection is erratic and inefficient at lower wind speeds. Higher wind speeds were necessary to yield the minimum 30 milliliters (mL) of cloudwater required for sample analysis. The temperature limit served to protect against damage from rime ice formation. The absence of rainfall was required because within the objectives of this study, as well as MCCP, only samples from non-precipitating clouds were collected. If a rain detector was activated, the string collector retracted into the protective case and collection was suspended.

Collection of cloud samples only when these criteria were met did not result in loss of cloud frequency and cloud duration information due to continuous data collection by the PVM. All LWC values of 0.05 g/m³ or greater, independent of the type of cloud (i.e. precipitating or non-precipitating), were used to calculate cloud frequency and cloud duration information. It is possible that cloud deposition estimates presented later on in Chapter 4 may be biased by not sampling for the cloud deposition that occurs during precipitating clouds. Collection of cloud water samples during precipitating clouds with an ETH cloud impactor as deployed by Collett *et al.* (1993) was not within the scope of this project. However, the bias due to this lack of sampling during precipitating clouds is offset by the fact that cloud deposition totals were estimated by multiplying the duration-weighted mean chemical fluxes by the cloud-hours for the month. The cloud-hours were calculated as the cloud frequency times the total hours in the month. See Chapter 4 for a detailed discussion on estimation of cloud depositions.

Hourly samples of cloudwater were gathered from the collector cooler by the site operator within 24 hours of each cloud event. The time, date, and volume of each sample were recorded on a report form by the site operator. The site operator also measured pH and conductivity and decanted samples into 250-mL bottles for shipment in coolers to the Harding ESE, Inc. (Harding ESE) laboratory. A rinse/sample blank was also included with each shipment to the Harding ESE laboratory. According to MADPro protocols, the cloud collector was rinsed with deionized water after each cloud event until the conductivity of the rinsate measured < 10 μ S (micro Siemens). The rinse/sampler blank consisted of a portion of this 'clean' rinsate.

Filter packs were prepared and shipped to the field on a weekly basis and exchanged at the Clingman's Dome and Whitetop Mountain sites every Tuesday. For a description of the filter pack set-up, types of filters used and the fraction collected on each filter, refer to the draft CASTNet Quality Assurance Project Plan (CASTNet QAPP) (Harding ESE, 1999) and/or the CASTNet Deposition Summary Report (EPA, 1998). A discussion on filter pack sampling artifacts can be found in Anlauf *et al.* (1986).

Filter pack flow was maintained at 1.50 liters per minute (Lpm) with a mass flow controller (MFC) through the middle of the 1998 season, at which time the flow was increased to 3.0 Lpm for the duration of the project. During 1994 and 1995, a continuous flow was drawn through the filter pack. In 1996, the flow was programmed to shut off during a cloud or rain event to allow for determination of truly dry deposition. Since the total hours of flow and, hence, volume were substantially reduced depending on the weekly weather conditions, an increase in flow to 3.0 Lpm was implemented in 1998 to increase the volume of flow through the filter pack to better detect the lower concentrations of analytes.

A wet deposition sample from Whitetop Mountain was also collected on a weekly basis (according to NADP/NTN protocols) in precleaned polyethylene buckets using an Anderson Model precipitation

sampler. Buckets were placed on the sampler on Tuesday and removed, whether or not rainfall had occurred, the following Tuesday. Buckets were weighed in the field, decanted to a 1-liter (L) polyethylene bottle, sealed, and shipped to Harding ESE for chemical analysis. In addition, precipitation amount (depth) was monitored at Whitetop Mountain with a Belfort rain gauge.

O₃ was measured at Whitetop Mountain (as well as Whiteface Mountain via the DEC) via ultraviolet (UV) absorbance with a Thermo-Environmental Model 49-103 analyzer operating in the 0- to 500-parts per billion (ppb) range. Ambient air was drawn from the air quality tower through a 3/8-inch TFE Teflon® sampling line. The analyzer and Teflon® filters housed at the tower inlet prevented particle deposition within the system. Periodic checks indicated that online losses through the inlet system were consistently less than 3 percent. Zero, precision (60 ppb), and span (400 ppb) checks of the O₃ analyzer were performed every third day using an internal O₃ generator. The O₃ data collected from Whitetop Mountain will not be presented in this report. The data have been validated and are available, however, through the EPA.

All field equipment received start-up calibrations during site initialization each field season and end-of-season calibrations. Calibration checks were performed on the PVM throughout the field season and the results were used to adjust the instrument immediately after the calibration check. Calibrations on the remaining instruments were conducted using standards traceable to the National Institute for Standards and Technology (NIST). In addition, independent equipment audits were performed in 1997 by Ogden Environmental and Energy Services, Inc. (Ogden), and by Air Resources Specialists (ARS) in 1999. Results of the end-of-season calibrations were used to assess sensor accuracy and to flag, adjust, or invalidate data.

2.3 Laboratory Operations

Cloudwater and wet deposition samples were analyzed for pH, conductivity, sodium (Na⁺), potassium (K⁺), ammonium (NH₄⁺), calcium (Ca²⁺), magnesium (Mg²⁺), chloride (Cl⁻), nitrite (NO₂⁻), nitrate (NO₃⁻), and sulfate ion (SO₄²⁻) in the Harding ESE laboratory. Wet deposition samples were filtered before analysis and also analyzed for acidity. During the first 2 years of the project, all cloudwater samples were analyzed for pH and conductivity. Starting in 1996, every tenth sample was analyzed in the Harding ESE laboratory for these two parameters to reduce redundancy but to still provide quality control (QC) data.

Cloud water and wet deposition samples were stored at 4° C until analysis. All analyses were performed within 30 days of sample receipt at the laboratory. The effects of storage on wet deposition samples have been addressed in NAPAP Report #6 (Sisterson *et al.*, 1991). This discussion applies, for the most part, to cloud water samples as well.

Concentrations of the four anions were determined by micromembrane-suppressed ion chromatography (IC). Analysis of Na^+ , Mg^{2+} , and Ca^{2+} was performed with a Perkin-Elmer P-2 inductively coupled argon plasma atomic emission (ICAP-AE) spectrometer, whereas K^+ was analyzed via atomic emission in 1994 and subsequently via ICAP. NH_4^+ concentrations were determined by the automated indophenol method using a Technicon II or Technicon Random Access Automated Chemistry System (TRAACS)-800 autoanalyzer system. Titration to a pH of approximately 8.3 was used for acidity measurements. Figure 2-6 depicts the sequence of laboratory operations for cloudwater and wet deposition samples.

Filter pack samples were loaded, shipped, received, extracted, and analyzed by Harding ESE personnel at the Harding ESE laboratory. For specific extraction procedures refer to Anlauf *et al.* (1986) and the draft CASTNet QAPP (Harding ESE, 1999). Filter packs contained three filter types in sequence: a Teflon® filter for collection of aerosols, a nylon filter for collection of nitric acid (HNO_3), and dual potassium carbonate (K_2CO_3)-impregnated cellulose filters for collection of sulfur dioxide (SO_2). Following receipt from the field, exposed filters and blanks were extracted and analyzed for anions and NH_4^+ , as described previously for cloudwater and wet deposition samples.

Refer to the draft CASTNet QAPP (Harding ESE, 1999) for detailed descriptions of laboratory receipt, breakdown, storage, extraction and analytical procedures for all three sample types.

Results of all valid analyses were stored in the laboratory data management system [Chemistry Laboratory Analysis and Scheduling System (CLASS™)]. Atmospheric concentrations were calculated based on the volume of air sampled following validation of the hourly flow data. Atmospheric concentrations of particulate SO_4^{2-} , NO_3^- , and NH_4^+ were calculated based on analysis of Teflon® filter extracts; HNO_3 was calculated based on the NO_3^- found in the nylon filter extracts; and SO_2 was calculated based on the sum of SO_4^{2-} found in nylon and cellulose filter extracts.

2.4 Data Management

Continuous data (meteorological, LWC, flow, and O_3) were collected from the three permanent sites in hourly and 5-minute averages. Hourly data were collected by nightly polling via telephone modem, and 5-minute data were downloaded to diskettes from the DAS cartridge at least once weekly. The polling software also recovered status files, power failure logs, and automated calibration results (O_3 only) from the previous 7 days. The hourly data and associated status flags were ingested into Microsoft Excel™ spreadsheets. The continuous data were validated (flagged, adjusted, or invalidated) based on the end-of-season calibration results, periodic calibration check results (PVM only), and information provided by status flags and logbook entries.

Discrete data (filter pack, wet deposition, and cloudwater sample results) were managed by CLASS™. In CLASS™, the analytical batches were processed through an automated QC check routine. For each analytical batch, an alarm flag was generated if any of the following occurred:

1. Insufficient QC data were run for the batch;
2. The correlation coefficient of the standard curve was less than 0.995;
3. The 95-percent confidence limit of the Y-intercept exceeded the limit of quantitation;
4. Sample response exceeded the maximum standard response in the standard curve (i.e., sample required dilution);
5. Continuing verification samples (CVSs) exceeded recovery limits; or
6. Reference samples exceeded accuracy acceptance limits.

A batch of one or more flags was accepted only if written justification was provided by the Laboratory Operations Manager.

Atmospheric concentrations for filter pack samples were calculated by merging validated continuous flow data with the laboratory data [micrograms per filter ($\mu\text{g}/\text{filter}$)].

For cloudwater and wet deposition samples, a second laboratory check involved three interparameter consistency checks:

1. Percent difference of cations versus anions (ion balance),
2. Percent difference of predicted versus measured conductivity, and
3. pH versus conductivity relationship of the sample compared to the expected relationship when rainfall is assumed to be controlled by strong inorganic acid.

Evaluation of these interparameter consistency checks provided a method for determining whether the analysis should be repeated or verified.

2.5 Quality Assurance

The quality assurance (QA) program for MADPro consisted of routine audits performed for CASTNet, if applicable, and testing/comparisons of instruments unique to MADPro.

2.5.1 Field Data Audits

The following audits were conducted for field data:

1. Review of all reported problems with sensors and equipment at the sites and the actions taken to solve such problems.

2. Review of calibration files for completeness and adherence to standard operating procedures (SOPs). Certification results for transfer standards were also reviewed, and transfer sensor serial numbers were cross-referenced with the transfer sensor serial numbers on the calibration forms.
3. Comparison of final validated data tables to the raw data tables for identification and verification of all changes made to the data. Summary statistics and results of diagnostic tests for assessment of data accuracy were also reviewed.

2.5.2 Laboratory Data Audits

Laboratory data audits consisted of:

1. Review of all media acceptance test results,
2. Review of chain-of-custody documentation, and
3. Review of all QC sample results associated with analytical batches.

Table 2-1 lists the routine QC checks, calibrations, and audits performed at the Harding ESE laboratory for CASTNet analyses. Table 2-2 lists the laboratory precision and accuracy objectives for CASTNet and MADPro.

2.5.3 External Audits

As discussed in Section 2.2, external audits were performed at all three sites in 1997 by Ogden. Spot reports summarizing sensor and system performance were submitted to Harding ESE within 72 hours of a site audit. In 1999, ARS performed an external audit on the Whiteface Mountain site only, and results were reviewed on a real-time basis with an official final report submitted within 1 month.

2.5.4 Precision and Accuracy

Accuracy of field measurements was determined by challenging instruments, with the exception of the automated cloud sampler and Gerber PVM, with standards that were traceable to NIST. Continuing accuracy was verified by end-of-season calibrations by Harding ESE personnel and by external audits. No certified standards are currently available to determine the accuracy of the cloud sampler and the PVM on a routine basis. Accuracy objectives for the rest of the field measurements are listed in Table 2-3.

Overall precision of field measurements is best determined by collocating instruments and assessing the difference between simultaneous measurements. Even though collocated sampling was not conducted at MADPro sites, it was conducted at CASTNet sites. Since the meteorological instrumentation and O₃ analyzers at MADPro sites were identical to those used at CASTNet sites, precision of these instruments can be inferred from the CASTNet Deposition Summary Report (EPA, 1998), and the CASTNet Annual Reports may be referenced for precision and accuracy results for 1994 through 1999. Precision objectives for field measurements are listed in Table 2-3.

Accuracy of laboratory measurements was determined by analyzing an independently prepared reference sample in each batch and calculating the percent recovery relative to the target value. The percent recovery was expected to meet or exceed the acceptance criteria listed in Table 2-2. When possible, the references were traceable to NIST or obtained directly from NIST. On occasion, references were ordered from other laboratories.

Analytical precision within sample batches was assessed by calculating the relative percent difference (RPD) and percent recovery of CVSs run within that batch. CVSs are independently produced standards which approximate the midpoint of the analytical range for an analyte and are run after every tenth environmental sample. Precision within a batch was also assessed by replicating 5 percent of the samples within a run. Replicated samples were selected randomly.

2.5.5 Quality Assurance Experiments

During the course of MADPro, several field and laboratory tests were conducted for QA purposes and for comparability to other studies. The following sections briefly describe these comparisons.

2.5.5.1 Valente Versus Gerber PVM Field Comparison

The Valente Method, described in Valente, *et al.* (1989), was used in MCCP (Mohnen *et al.*, 1990) to estimate cloud LWC. During the MCCP program, a field intercomparison of a number of instruments was conducted. The results of the tests indicated that the Valente Method provided accurate estimates of cloud LWC. The Gerber PVM was under development during MCCP. A comparison of the Valente Method for LWC and the current Gerber PVM for LWC provides an additional check of the comparability of the two studies.

During the 1997 field season, a comparison of the Valente Method and PVM-100 was conducted at the Whiteface Mountain and Whitetop Mountain sites. Hourly LWC values measured during cloud events from both sites yielded differences of approximately 50 percent, with the Gerber PVM recording the higher readings. The differences between the two methods were not affected by variation in LWC values. The same Valente instrument was used at both sites whereas the Gerber PVM was the instrument assigned to the specific site. Since the differences between the two methods were the same at two different sites using different Gerber PVMs, the differences were attributed to differences between the two methods and not specific instruments.

2.5.5.2 Comparison of Two EPA Gerber PVMs

In May 1998, the PVM assigned to Whiteface Mountain was collocated with the PVM at Whitetop Mountain for approximately 3 weeks. The PVMs measured LWC values within 5 percent of each other during all cloud events within this time period (Figure 2-7). This collocation was conducted to check the precision between the PVMs used on the project. Similar precision (± 5 percent) between PVM-100s was obtained in a European study (Pahl and Winkler, 1995).

2.5.5.3 Comparison of EPA Versus Colorado State University (CSU) Gerber PVMs

In January of 1999, three Gerber PVMs were destroyed in a fire at the Harding ESE Calibration Laboratory, leaving only two PVMs for the three sites for the upcoming 1999 field season. A Gerber PVM was leased from CSU for use at the Whiteface Mountain site. Prior to deployment at the site, the CSU PVM was collocated with the Whitetop Mountain EPA PVM during May 1999 for approximately 3 weeks. During the first half of this time period, the CSU PVM was reading approximately 45 percent lower with respect to the EPA PVM. The LWC values measured with the EPA PVM ranged from 0.04 to 0.63 g/m³. The PVMs were collocated 5 m apart, at the same height and alignment. However, to rule out any differences due to location, the two PVMs were switched around. The same difference (45 percent) was observed.

Since the difference between the EPA and CSU PVMs was very similar to the difference observed between the Valente and EPA PVMs, the accuracy of the EPA PVMs was questioned.

2.5.5.4 Evaluation of LWC Instruments

The Energy Center for the Netherlands (ECN) was contacted to verify the accuracy of the PVMs used in MADPro. The cloud chamber at ECN has the capability to generate clouds of known LWC and was used to calibrate the Mallant cloud detector used during MCCP. The facility is described in detail in Gerber *et al.* (1993) and is summarized below.

The fogs are characterized in the test section (or chamber) by measuring the LWC with a filter method and measuring the droplet spectra with an FSSP-100. Two filter systems are run side by side as a check of the measurement procedure. The filters consist of hydrophobic Pall filters placed in housings that face the flow. Air is drawn through the filters isokinetically at a flow rate of 2.15 m/sec. The filters are conditioned in the operating chamber for at least 2 hours before LWC is measured by weighing the filter both before and after a specified time interval, generally about 1 hour. The constant high relative humidity (Rh) in the chamber and filter-sampling procedures minimizes LWC measurement errors due to evaporation or growth of droplets collected in the filter. Such errors may be important when the filter method is used under ambient conditions where Rh can be subsaturated or supersaturated (e.g., see Valente *et al.*, 1989). The estimated accuracy of filter measurements of LWC in the chamber is 10 percent. The FSSP-100 was located near the filters in the test section.

The MADPro QA testing was conducted in February 2000 and included the two EPA PVMs and the Valente Method used in the 1997 comparison. The CSU PVM was unavailable at the time of the test. The tests included a series of cloud LWC from 0.1 to 0.9 g/m³ at cloud droplet sizes of 10 and 25 mass median aerodynamic diameter (MmaD). The test concentrations were replicated on different test days and different runs. A summary of the results is provided in Table 2-4. The two EPA PVMs measured within 5 to 8.4 percent of the calibration standard over the entire test range of

LWCs and droplet sizes. The Valente instrument measured within 18.2 percent of the Pall filters. This result is contrary to the performance of the Valente during field tests when it consistently measured the LWC approximately 50 percent lower with respect to the PVM-100.

Based on the ECN results and results obtained from field testing (Section 2.5.5.2), the precision between the EPA PVMs is within ± 5 percent. This precision value also agrees with the results found by Pahl and Winkler (1995) in a German inter-comparison study of PVM-100s. Due to the consistency of test results for the EPA PVMs, the LWC values collected with the CSU PVM at Whiteface Mountain during 1999 were adjusted by +35.0 percent.

The ECN results for the Valente, however, did not agree with results of field testing between the PVM-100s and the Valente. The difference is most likely caused by evaporation of water from the instrument when deployed in the field and/or faulty technique during removal and taring of the cartridge. Before any conclusions can be made with any certainty, however, further field testing by collocation of the Valente and the PVM-100 is essential. Once the field accuracy of the Valente instrument is quantified, the MCCP LWC data may require adjustment and cloud deposition estimates may need to be recalculated based on the adjusted LWC to provide a database that would provide better comparison with MADPro results.

2.5.6 Whitetop Mountain LWC Data

During validation of the 1998 MADPro data, it was noticed that Whitetop Mountain LWC values never rose above $0.41 \mu\text{g}/\text{m}^3$ after mid-June. Before this time period the LWC data exhibited the normal range of values for this parameter (0.0 to $0.98 \mu\text{g}/\text{m}^3$). Review of the site logbook entries and of the LWC data showed that the PVM began to malfunction on June 13, 1998. Data were invalidated from June 13 through 16 when repairs were conducted on the PVM. However, from this point on, the LWC values did not rise above $0.41 \mu\text{g}/\text{m}^3$ as stated above. Based on analysis of LWC data (range, average, time series plots, etc.) from Whitetop Mountain from previous and subsequent years, the accuracy of the LWC data from June 17 until the end of the season on October 7 is suspect. The documentation describing the instrument repair procedures does not provide enough information to confidently adjust the data to correct for this suspected error. What can be confidently inferred from the documentation and review of the data is that the zero reading was accurate as well as readings at the calibration span value of approximately $0.16 \mu\text{g}/\text{m}^3$. The site operator had performed monthly calibrations which checked the zero and span values. No problems were reported with calibration results. Review of the data also indicate that around the $0.05 \mu\text{g}/\text{m}^3$ value, indicative of the existence of a cloud, the PVM results agree with logbook comments and other meteorological parameters. Values below $0.05 \mu\text{g}/\text{m}^3$ also correlate with recorded weather conditions (clear, no clouds) in the logbook as well as weather conditions indicated by the meteorological data.

Since there was no reliable information to adjust data points above the calibration span value of $0.16 \mu\text{g}/\text{m}^3$, the analyses contained within the main body of this report use the 1998 LWC data from

Whitetop Mountain as reported. The accuracy of cloud frequency and duration information is not affected since for calculation of these values, accuracy of the PVM at $0.05 \mu\text{g}/\text{m}^3$ is most important. The accuracy of the values above this point is not relevant as the individual values are not used. Only the number of cloud hours are important and useful. The analyses which may be affected are those in which the Whitetop Mountain hourly LWC values are used: time series plot of LWC, normalized (with respect to LWC) concentration values, and linear regressions of normalized concentrations.

Review of maximum LWC values from previous and subsequent years indicate that at Whitetop Mountain the maximum values range from $0.66 \mu\text{g}/\text{m}^3$ (1995) to $1.01 \mu\text{g}/\text{m}^3$ (1997). Given that the zero and span values were accurate, several slope/intercept adjustments were applied to the data collected after June 16. The observed maximum (after June 16) of $0.41 \mu\text{g}/\text{m}^3$ was set to equal values of 0.75, 0.80, 0.85, 0.90, and $0.95 \mu\text{g}/\text{m}^3$ to generate slope/intercept values with which to adjust the data. Analysis of the data after application of each of these adjustment factors showed the $0.85 \mu\text{g}/\text{m}^3$ maximum set-point to yield the most reasonable results based on comparison to data from other years as well as data from the Clingman's Dome site. As can be seen in Figure 3-7, the LWC data from Whitetop Mountain and Clingman's Dome track each other closely, with a few exceptions, up until July of 1998 and then again in 1999.

Even though this report uses the unadjusted data, the slope/intercept adjustment, using $0.85 \mu\text{g}/\text{m}^3$ as the maximum set point, was applied (for investigative purposes) to the 1998 LWC data collected after June 16. The LWC time series plot and the normalized concentration bar charts (Figures 3-37 through 3-40) were replotted with this adjusted data for comparison purposes. These results are presented in Appendix A as Figures A-1 through A-5.

3.0 Liquid Water Content and Cloudwater Chemistry

3.1 Cloud Frequency and Mean Liquid Water Content

Mean monthly cloud frequencies by year for the three sites are summarized in Table 3-1. The monthly cloud frequencies by month and year are also depicted as bar charts in Figures 3-1 through 3-3. Monthly cloud frequencies were determined by calculating the relative percent of all hourly LWC values equal to or greater than 0.05 g/m^3 , or:

$$CF = \frac{100 * (\# \text{ of valid hourly LWC values } \geq 0.05 \text{ g / m}^3)}{n} \quad (3-1)$$

where n is the number of valid hourly LWC values per month.

Any month with less than 70 percent valid LWC data was not considered representative of the monthly weather conditions for that month and was not used in any analyses. Cloud frequencies vary from month-to-month, year-to-year, and from site-to-site. Generally, Whitetop Mountain exhibits slightly lower cloud frequencies with respect to Whiteface Mountain and Clingman's Dome.

Monthly mean LWC values for each year and site are shown in Figures 3-4 through 3-6. Mean LWC was calculated by taking the average of all hourly LWC values equal to or greater than 0.05 g/m^3 during the month. Only those monthly values that passed the 70 percent completeness criteria were plotted. Figure 3-7 depicts the same information as a line graph with all three sites plotted together. In this figure it is apparent that Whiteface Mountain experiences clouds with significantly higher LWCs than the two southern sites, usually 1.5 to 2 times greater.

Height above cloud base could be a significant factor in determining the LWC values at the collection location. Even though the height above cloud base is not quantitatively known for the three sites, it is estimated that cloud base is lower at Whiteface Mountain with respect to the two southern sites (Mohnen *et.al.*, 1990). Since LWC increases vertically from cloud base up through the cloud, height above cloud base could account for the higher LWC values at Whiteface Mountain.

3.2 Cloudwater Chemistry

Annual summary cloudwater chemistry and LWC statistics are presented in Table 3-2. Table 3-3 lists the total number of samples or 'records' that were collected each season of operation at the three sites. Samples were accepted and used for all subsequent analyses if they met an acceptance criteria

based on the cation-to-anion ratio. Samples were eliminated if:

1. Both the anion sum and the cation sum were ≤ 100 microequivalents per liter ($\mu\text{eq/L}$) and the absolute value of the RPD was >100 percent; or
2. Either the anion sum or the cation sum was $> 100 \mu\text{eq/L}$ and the absolute value of the RPD was >25 percent.

The RPD was calculated from the following formula:

$$\text{RPD} = 200 * (\text{cations}-\text{anions})/(\text{cations}+\text{anions})$$

Applying this acceptance criteria eliminated 694 out of 6,186 samples, or 11.8 percent.

3.2.1 Cloudwater pH

The mean annual pH of cloudwater samples for 1994 through 1999 for all three sites is shown in Figure 3-8. Mean pH was obtained by first calculating the mean of the hydrogen ion (H^+) concentration and then converting this value back to pH units by taking the negative log. A steady decrease in mean annual pH is evident for Clingman's Dome.

The pH values are also depicted as frequency distributions averaged over all years in Figures 3-9 through 3-11. The frequency distribution for Whiteface Mountain (Figure 3-9) shows a greater spread of pH values over the range of pH, 3.4 to 5.0, than either Whitetop Mountain or Clingman's Dome. Whitetop Mountain (Figure 3-10) exhibits a relatively normal distribution with most pH values falling in the 3.6 to 3.8 range; whereas, the majority of pH values for Clingman's Dome are in the 3.4 to 3.6 range with very few samples above a pH of 4.0 (Figure 3-11).

The difference in the distribution of pH values may be related to the prevailing wind directions and upwind sources. Figures 3-12 and 3-13 show cloudwater SO_4^{2-} concentrations versus arrival sector for each of the three years 1994 through 1996 for Whitetop Mountain and Whiteface Mountain, respectively. Arrival sector is defined as one of eight upwind directions estimated from 36-hour back trajectories (Heffler, 1983). Arrival sector 1 represents winds from approximately north-northeast. Figure 3-12 shows that the highest cloudwater SO_4^{2-} concentrations at Whitetop Mountain are related to winds from the north. Similarly, Figure 3-13 shows that the highest cloudwater sulfate concentrations at Whiteface Mountain are associated with winds from the southwest. Figure 3-14 provides information on annual SO_2 emissions by state for the eastern U.S. for 1995, the mid-year of the three-year period.

The information in Figures 3-12 and 3-13 is shown as pollution roses in Figure 3-15. The pollution roses were constructed by plotting cloudwater concentrations by arrival sector for 1994 first, then for 1995, and finally for 1996. This procedure obscures 1994 and 1995 data if, for example, 1996 observed the highest concentration. This is the situation for arrival sector 8 for Whitetop Mountain.

In any event, Figure 3-15 relates cloudwater concentrations to upwind source regions. Whiteface Mountain experiences relatively high concentrations with trajectories originating from Pennsylvania, western New York, and the Ohio Valley, areas with high SO_2 emissions (Figure 3-14). Relatively low concentrations are observed with trajectories passing over Vermont and northern New England. Whitetop Mountain experiences high cloudwater concentrations with trajectories from the Ohio Valley.

The data in Figures 3-12 and 3-13 are relatively consistent over the three years. Consequently, the concentrations reported for 1997 through 1999 are probably associated with polluted air masses from the southwest in the case of Whiteface Mountain and from the north for Whitetop Mountain. Annual variability in cloudwater concentrations can be at least partially explained by backward trajectories and upwind source regions.

Figures 3-16 through 3-24 show the pH measurements from all accepted samples as a time series for the years 1995, 1997, and 1999 for the three sites. These time series plots are useful for illustrating seasonal differences in pH values within a site and differences between sites within the same year.

The pH values are also plotted as mean annual hydrogen concentrations in Figure 3-25 and as a line chart with the values for all three sites plotted together for easier comparison in Figure 3-26. From these figures it can be seen that the H^+ concentrations at Clingman's Dome have steadily increased since 1996. A definite pattern is not discernible for either Whiteface Mountain or Whitetop Mountain.

In Figure 3-27, H^+ concentrations are plotted as monthly means averaged across all years (1994 through 1999) to show monthly variations: Whitetop Mountain shows a definite peak in August; Clingman's Dome exhibits higher monthly H^+ concentrations earlier in the season (June and July); and there is no obvious peak for Whiteface Mountain.

3.2.2 Cloudwater Anions

Figures 3-28 through 3-30 show annual means and monthly variations for SO_4^{2-} and Figures 3-31 through 3-33 show the annual and monthly statistics for NO_3^- . A slow but steady increase in SO_4^{2-} means can be seen for Clingman's Dome with no evident pattern at the other two sites. It is interesting to note the divergence between Clingman's Dome, Whitetop Mountain, and Whiteface Mountain in 1999. Clingman's Dome continues the pattern of steady increase, but the other two sites show a decline, which is rather sharp for Whitetop Mountain, in the annual cloudwater SO_4^{2-} concentrations. Back trajectory analyses for 1999 would be useful in determining causes for the difference observed at Clingman's Dome.

A similar pattern is observed for NO_3^- except that, in this case, Clingman's Dome also exhibits a decline in NO_3^- values in 1999 (Figure 3-32).

An early season peak during June and July, like the results for H^+ , is seen for SO_4^{2-} and NO_3^- at Clingman's Dome. Whitetop Mountain shows a peak in August for SO_4^{2-} and NO_3^- which mirrors the results for H^+ . The number of months sampled and the smaller magnitude of differences from month to month at Whiteface Mountain does not allow for any such observations.

3.2.3 Cloudwater Cations

Mean annual NH_4^+ concentrations for 1994 through 1999 for the three sites are presented in Figures 3-34 and 3-35. The Whiteface Mountain and Whitetop Mountain sites follow the same annual pattern from 1995 through 1999. Clingman's Dome shows a steady increase until a decline in 1999, similar to the decline exhibited by the other two sites.

The minor cation annual mean concentrations (Ca^{2+} , Na^+ , Mg^{2+} , and K^+) are shown in Figure 3-36. Cl^- annual means are plotted in this figure as well. The most notable observation is the steady increase in annual Ca^{2+} concentrations at Clingman's Dome.

3.2.4 Normalized Cloudwater Concentrations

Since cloudwater analyte concentrations may be influenced by year-to-year variations in LWC, the concentrations presented in sections 3.2.1 through 3.2.3 were normalized for LWC by multiplying each sample concentration (for H^+ , SO_4^{2-} , NO_3^- , and NH_4^+) by its respective LWC value. These results are presented in Figures 3-37 through 3-40. Normalizing the concentrations with respect to LWC had no effect on results from Whiteface Mountain except for NH_4^+ in 1998 (Figure 3-40) where the normalized value is slightly lower than the 1997 value instead of higher as in Figure 3-34 (non-normalized NH_4^+ concentrations). For Clingman's Dome, the 1996 normalized values for H^+ , SO_4^{2-} and NO_3^- exhibit a different pattern (a decrease with respect to 1995) than the non-normalized concentrations. Also, the 1998 SO_4^{2-} value (Figure 3-38) is lower with respect to the 1997 value instead of slightly higher as in the non-normalized concentrations (Figure 3-28). There was no change in the pattern of normalized concentrations compared to the non-normalized concentrations for H^+ and SO_4^{2-} at Whitetop Mountain. The NO_3^- and NH_4^+ results (Figures 3-39 and 3-40) however, exhibit the same change in pattern for 1996 and 1998 with respect to the non-normalized concentrations. The 1996 normalized values are higher than the 1995 values rather than a little lower as in the non-normalized concentrations, and the 1998 normalized results are lower than the 1997 results rather than higher as exhibited by the non-normalized values (Figures 3-31 and 3-34).

3.2.5 Slide Mountain and Hunter Mountain Results

Figure 3-41 presents results from the 3 years of operation of the mobile site in the Catskill Mountains of New York. In 1995, collection was conducted on Slide Mountain, and during 1997 and 1998 on Hunter Mountain. The two locations are within approximately 30 miles of each other and experience the same weather regime. Therefore, data from the 3 years are comparable.

A large increase in SO_4^{2-} values is evident between 1997 and 1998. In 1995 and 1997, the SO_4^{2-} means were lower than the seasonal SO_4^{2-} means for the three permanent sites. In 1998, however, the SO_4^{2-} value is noticeably higher than the Whiteface Mountain mean, slightly higher than the Whitetop Mountain mean, and just slightly lower than the Clingman's Dome mean for 1998. The NO_3 values are lower with respect to the other sites in 1995 and 1997, but are similar to the Clingman's Dome seasonal mean and surpass the Whiteface Mountain and Whitetop Mountain means in 1998. The NH_4^+ means are lower than the other three sites across all 3 years.

These results, especially the SO_4^{2-} mean concentrations, indicate that the Slide Mountain and Hunter Mountain sites experience somewhat different weather patterns or different types of clouds than Whiteface Mountain.

3.2.6 Discussion of Results

Linear regression analyses were performed for the three sites for the four major ions from 1994 through 1999 to check for statistically significant increases or decreases in concentrations over time. The data were analyzed for both the normalized and non-normalized data sets using all sample concentrations rather than monthly or seasonal averages. The p-values from these analyses are presented in Table 3-4. For Clingman's Dome, the p-values for all four analytes for both data sets (normalized and non-normalized) show a statistically significant increase. The p-values for normalized NH_4^+ and SO_4^{2-} concentrations exhibit greater significance. Whiteface Mountain p-values were significant for NH_4^+ and SO_4^{2-} for both data sets and show a decrease in these concentrations. The p-values for only normalized SO_4^{2-} concentrations show a statistically significant increase at Whitetop Mountain.

The regression plots for those sites and analytes with significant p-values are shown in Figures 3-42 through 3-46. The individual sample points have been removed from these plots since the large number of points (>5000 in some cases) when plotted, visually obscure the information. The very low R^2 values for these regressions indicate that, even though the p-values show high statistical significance (in most cases), the increases or decreases are not linear. The low R^2 statistics are also a result of the scatter from the large number of samples analyzed. Linear regression may not be the most appropriate analytical tool for this particular data set. However, for the purposes of providing a preliminary look at statistical significance in temporal trends, the linear regression results are useful. More appropriate statistical analyses (e.g., Mann-Kendall trend test, etc.) should be performed to further elucidate the nature of the temporal trends exhibited by this data.

Even though there were statistically significant temporal trends discernible for the major ions from 1994 through 1999, 6-year average concentrations were calculated and are presented in Table 3-5 for information purposes only. For all four major ions (SO_4^{2-} , NO_3^- , H^+ , and NH_4^+), Clingman's Dome exhibits the highest mean and median values. Whiteface Mountain, on the other hand, consistently has the lowest mean and median concentrations for all four ions.

Clingman's Dome also exhibited statistically significant upward trends in seasonal SO_4^{2-} , NO_3^- , H^+ , and to a lesser extent, NH_4^+ values as depicted in Figures 3-42 and 3-43. To fully understand the consistently higher concentrations at this site, back trajectory analyses are recommended. Back trajectory analyses for Whiteface Mountain and Whitetop Mountain from 1994 through 1996 (see Figure 3-15) clearly show the different air masses experienced at these two sites. More local emission sources and the possible resulting effect on the air quality of Clingman's Dome should also be investigated (see Mueller, 2000). Butler *et al.* (in press) suggest that the lack of improvement, and even an increase in the vicinity nearby Clingman's Dome, may be attributed to several large coal-fired electric generating facilities that were not required to reduce SO_2 or NO_x emissions under CAAA.

Since SO_2 emission levels in the eastern United States have decreased (EPA, 2000), a stronger decreasing correlation might be expected at Whiteface Mountain. The increasing temporal trend for SO_4^{2-} and the lack of discernible trends for the other three analytes at Whitetop Mountain, combined with the results from Whiteface Mountain, indicate that cloudwater concentrations may not be linearly related to SO_2 emission reductions. Clouds may not contain sufficient amounts of the necessary oxidants for a complete conversion of all available SO_2 . At the cloud water pH levels usually observed at the MADPro sites, hydrogen peroxide (H_2O_2) is the primary, if not the only, oxidant of significance (Seinfeld, 1986). The research of Dutkiewicz *et al.* (1995) at Whiteface Mountain, NY indicates that, at SO_2 concentrations above 1 ppb, H_2O_2 is not present in sufficient quantities to oxidize all of the SO_2 present. The situation is further complicated by the fact that sources of SO_2 and H_2O_2 in the atmosphere are unrelated and large variations in atmospheric concentrations of H_2O_2 are observed (Guns and Hoffmann, 1990). However, more research and monitoring must be conducted before any solid conclusions can be made since the lack of temporal trends within this period may also be a function of, or influenced by, year-to-year variations in air mass trajectories and regional and local meteorology.

4.0 Cloud Deposition

This chapter summarizes the modeled cloudwater deposition estimates for the three MADPro sites for the period 1994 through 1998. The deposition estimates were made by applying the cloudwater deposition computer model (CLOUD) (Lovett, 1984), parameterized with site-specific cloudwater chemistry and meteorological data. The structure of the model, the input parameters, and the sensitivity of the model to several parameters and assumptions are described in Section 4.1. Deposition estimates for the three sites are also reported for monthly, seasonal, yearly, and multi-year periods.

In addition, a semi-independent model (MCLLOUD) was employed to explore alternative parameterizations and additional model components beyond those offered by the primary model. MCLLOUD was used to produce an alternative set of cloudwater deposition estimates for eight site-by-year combinations as well as deposition estimates for all 1999 data. These findings are discussed in Section 4.2. A comparison of the results between the CLOUD and MCLLOUD models is presented in Section 4.3.

4.1 Cloudwater Deposition Model (CLOUD)

4.1.1 Model Description

The CLOUD model was originally described by Lovett (1984). Briefly, it uses an electrical resistance network analogy to model the deposition of cloudwater to forest canopies. The model is one-dimensional, assuming vertical mixing of droplet-laden air to the canopy from the top. Turbulence mixes the droplets into the canopy space, where they cross the boundary layers of canopy tissues by impaction and sedimentation. Sedimentation rates are strictly a function of droplet size. Impaction efficiencies are a function of the Stokes number, which integrates droplet size, obstacle size, and wind speed (Lovett, 1984). The impaction efficiency as a function of the Stokes number is based on wind tunnel measurements by Thorne *et al.* (1982).

A resistance or deposition velocity type model does not solely represent the important atmospheric dynamics controlling deposition. It also simulates the properties of the receptor surface and the depositing substance. This model is the most common type found in the literature for simulating atmospheric deposition. A resistance model is used because it simulates the relationship between atmospheric concentration and flux to a surface.

The forest canopy is modeled as stacked 1-m layers containing specified amounts of various canopy tissues such as leaves, twigs, and trunks. Wind speed at any height within the canopy space is determined based on the above-canopy wind speed and an exponential decline of wind speed as a function of downward-cumulated canopy surface area. The wind speed determines the efficiency of

mixing of air and droplets into the canopy and also the efficiency with which droplets impact onto canopy surfaces. The model is deterministic and assumes a steady state, so that for one set of above-canopy conditions it calculates one deposition rate. The model requires the following as input data:

1. Leaf area index (LAI) of canopy tissues in each height layer in the canopy,
2. Zero-plane displacement height and roughness length of the canopy,
3. Wind speed at the canopy top,
4. LWC of the cloud above the canopy, and
5. Mode of the droplet diameter distribution in the cloud.

From these input parameters, the model calculates the deposition of cloudwater, expressed both as a water flux rate [grams per square centimeter per minute ($\text{g}/\text{cm}^2/\text{min}$)] and as a deposition velocity [flux rate/LWC, in units of centimeters per second (cm/sec)]. Deposition rates of ions are calculated by multiplying the water flux rate by the ion concentration in cloudwater above the canopy. In the original version of the model, a calculation of the evaporation rate from the canopy was also included to estimate net deposition of cloudwater. For this report, only gross deposition rate was estimated, so the evaporation routine was not invoked.

4.1.1.1 Canopy Structure

Comparing cloud deposition rates across sites is difficult because canopy structure (e.g., height and LAI), which has an effect on deposition rates, can vary between locations even within a single site. To focus on meteorological and chemical controls on the deposition process, a "standard" canopy structure was used for all model runs at all sites. The structure chosen was described by Lovett (1984). It is a monospecific Balsam Fir canopy with the following parameters: maximum structure height of 1061 cm, zero-plane displacement of 837 cm, roughness length of 97 cm, and LAI of 7.6 square meters per square meter (m^2/m^2). While this canopy parameterization was originally developed for subalpine forests of New Hampshire, it is similar to forests that can be found at high elevations on Whiteface Mountain (Miller *et al.*, 1993a). Forests near the summits of Whitetop Mountain and Clingman's Dome are similar in structure but may be somewhat taller (e.g., Mueller *et al.*, 1991). Nevertheless, the CLOUD model was executed with the same parameters at all sites. Furthermore, the deposition model calculations represent the deposition expected to a forest stand with the canopy structure specified as homogeneous throughout the stand. If that stand were at a forest edge, the deposition would be greater. However, no information is available on the gap and edge distribution in the forests at the three MADPro sites. Consequently, deposition estimates were made only for homogeneous canopies.

4.1.1.2 Modifications from Original Version of the Model

Several changes in the model were made to improve its performance and tailor it to the sites under study. The model calculates the droplet size distribution associated with each measured LWC according to the formula of Best (1951). The calculation requires specifying the mode of the

distribution. Because droplet size information was not collected at the sites, the droplet size at all sites was assumed to be a function of LWC as reported by Joslin *et al.* (1990) for the Whitetop Mountain site. A regression was run based on the data in Figure 2 of the Joslin *et al.* paper (see Figure 4-1), and the following equation was calculated:

$$D^2 = 49.9874 + 308.1664 \times LWC \quad (4-1)$$

where D is the mean droplet diameter (adjusted $r^2 = 0.94$, $n = 6$). The mean diameter, calculated by taking the square root of both sides of Equation 4-1, was assumed to be identical to the mode diameter used in the Best (1951) distribution, which is a good assumption because of the roughly normal-shaped distribution of cloud droplet diameters. Equation 4-1 was used for all sites.

In summary, the Best (1951) paper provides a method for calculating the droplet size distribution when the modal droplet diameter is known. Data from Whitetop Mountain were used to estimate the mode of the size distribution as a function of LWC. The Best function was then used to calculate the full droplet size distributions.

Another issue concerning the droplet size distribution is the discretization of the distribution in the model simulations. In the original model, three droplet diameter classes were used: 0 to 10, 10 to 20, and 20 to 30 micrometers (μm). Miller *et al.* (1993a) suggested that as many as 500 droplet size classes may be necessary to simulate the deposition rate to within 0.1 percent. Simulations were run with different numbers of droplet size classes and it was found that the deposition velocity using 20 classes was within <1 percent of the deposition velocity using 500 classes. The accuracy of <1 percent was considered sufficient, given the error inherent in calculating or measuring a droplet size distribution; and 20 droplet size classes (in the range of 0 to 100 μm) were used for all simulations.

The model uses canopy-top wind speed as an input parameter; however, in practice wind speed is usually measured some distance above the canopy to avoid shadowing by surrounding tree crowns. Assuming a logarithmic wind profile above the canopy, the canopy-top wind speed (u_h) can be calculated from the wind speed at any height z (u_z) by the following equation:

$$u_h = u_z \frac{\ln[(h - d) / z_0]}{\ln[(z - d) / z_0]} \quad (4-2)$$

where h is the height above the canopy where wind speed was measured, d is the zero-plane displacement height, and z_0 is the roughness length. The anemometers at Clingman's Dome and Whitetop Mountain were 3.2 m above the canopy, and that information was used to calculate canopy-top wind speed using Equation 4-2. The anemometer at Whiteface Mountain was on the roof of a building above tree line, so this site required a more complicated adjustment, described below.

4.1.1.3 Parameter Adjustments at Whiteface Mountain

The cloud chemistry, LWC, and wind speed measurements at Whiteface Mountain were made on the roof of the summit observatory building at an elevation of 1,483 m. This elevation is above the tree line. Miller *et al.* (1993a) report an elevational gradient of canopy structure on Whiteface Mountain, and their highest site, at an elevation of 1,350 m, closely resembles the height and species composition of the forest used in the deposition calculations. Therefore, 1,350 m was used as the target elevation for the model application at Whiteface Mountain.

Wind speed, LWC, and cloud chemistry all change with elevation and, hence, the measured values at the top must be scaled if they are used for modeling at lower elevations. Miller *et al.* (1993a) describe the elevational wind profile $u(z)$ with the function:

$$u(z) = u_{fa} / (1 + [(u_{fa} - u_0) e^{-r(z-z_i)}]) \quad (4-3)$$

where u_0 is the above-canopy wind speed at the 1,050-m measurement site, $u_{fa} = 3.2 u_0$ and is the projected free-air wind speed above the mountain, $z_i = 1,000$ m and is the elevation of the inflection point of the wind profile, and $r = 0.003675$. Evaluating Equation 4-3 with $z = 1,350$ (for the chosen elevation of 1,350 m), and again with $z = 1,483$ (the summit elevation), and then taking the ratio of the two, yields:

$$u(1,350) = 0.854 u(1,483) \quad (4-4)$$

Equation 4-4 was used to calculate the above-canopy wind speed for the 1,350 m site. Equation 4-2 was then used to scale that to the canopy-top wind speed, assuming the above-canopy wind speed estimated by Equation 4-4 corresponds to a point 3.2 m above the canopy.

Based on data from the summit and a site at 1,050 m on Whiteface Mountain, Miller *et al.* (1993a) estimated that cloud LWC decreases linearly with elevation on Whiteface Mountain, from a growing-season average of 0.50 g/m^3 at the summit to 0.39 g/m^3 at the 1,050-m site. This represents a 22-percent decrease in LWC over a 433-m elevational drop. A linear function was calculated to describe the proportional decrease in LWC with elevation as follows:

$$LWC(z) = LWC(s)[1 - (0.22 / 433)(1,483 - z)] \quad (4-5)$$

where $LWC(s)$ is the LWC at the summit. For $z = 1,350$ m, Equation 4-5 reduces to:

$$LWC(1,350) = 0.932 LWC(s) \quad (4-6)$$

All LWC values reported for Whiteface Mountain were adjusted by Equation 4-6 to calculate the LWC at the modeled site.

Following Mohnen *et al.* (1990) and Miller *et al.* (1993a), the elevational change in cloudwater chemistry was also modeled as a dilution process in which higher values of LWC result in lower ion concentrations in cloudwater. Consequently, in correspondence to Equation 4-6, chemical concentrations C in cloudwater at the 1,350-m target site were calculated as:

$$C(1,350) = C(s) / 0.932 \quad (4-7)$$

where $C(s)$ is the ion concentration at the summit (1,483 m) site.

In reality, cloud pollutant concentrations vary as a function of droplet size. However, MADPro did not collect size-resolved concentration data. Instead, cloud water was deposited onto a passive collector thereby measuring deposition-weighted pollutant concentrations (see Section 2.2). These concentration measurements are precisely the type of concentrations required by the CLOUD model for simulating deposition to forest canopies. Consequently, not using size-resolved concentration data will produce no bias in the calculations.

Chemical and meteorological parameters were estimated for two separate sites on Whiteface Mountain:

- Whiteface Mountain Summit (WFMS) which represents the summit data; and
- Whiteface Mountain Lower (WFML), which represents the 1,350-m site for which deposition was modeled.

4.1.2 Model Calculations

The CLOUD model was run for all samples from the three MADPro sites for which wind speed and LWC data were available. The modeled cloudwater flux data were merged with the chemical data and were used to make the following calculations:

1. The Whiteface Mountain data were processed to create results for two sites, WFMS (summit site) and WFML (1,350-m site). Deposition fluxes were calculated only for WFML.
2. Chemical fluxes were calculated as the product of modeled water fluxes and chemical concentrations for all observations for which chemical data were available.
3. The data set was screened for ion balance in the chemical data. The chemical data were screened based on the anion and cation sums and the RPD between anions and cations presented in Section 3.2. Figure 4-2 shows the RPD plotted against the anion sum and illustrates the screening criteria as lines on the plot. All calculations on Figure 4-2 were made on the screened data set.

4. Monthly means were calculated for each site and year, weighted by duration of the sample to give the most appropriate mean for calculating deposition. These data were merged with monthly data on cloud frequency from each site.
5. Deposition totals were calculated by site, year, and month by multiplying the duration-weighted mean chemical fluxes by the cloud-hours for the month. The cloud-hours were calculated as the cloud frequency times the total hours in the month.
6. Deposition fluxes for each sampling season were calculated. To compare equitably across sites, the deposition season was considered to be June through September. Data outside that period were almost never available for the Whiteface Mountain site and were spotty at the other sites. Even within the June through September period, the monthly deposition for each site could not be summed to calculate the seasonal totals because some months had no available data due to equipment failures or data screening. Therefore, the seasonal deposition totals were calculated as the duration-weighted mean chemical fluxes for all observations in the 4-month period multiplied by the total cloud-hours for the 4-month period. Seasonal deposition totals were not calculated unless at least 3 months of valid cloud frequency data were available for that season.

4.1.3 Model Sensitivity

Before the production runs for the three MADPro sites are presented, the sensitivity of the CLOUD model is discussed. The sensitivity of the CLOUD model to various input parameters, including wind speed, droplet size, and canopy structure, has been reported in several publications (Lovett, 1984; Lovett and Reiners, 1986; Mueller, 1991; Miller *et al.*, 1993a). The modeled deposition velocity shows a nearly linear response to changes in canopy-top wind speed in the range of wind speeds commonly encountered (Figure 4-3). This indicates that the model estimates of cloudwater deposition are very sensitive to the correct specification of wind speed at the canopy top.

The slight flattening of the slope of the curve at low wind speeds in Figure 4-3 results from the increased importance of sedimentation flux of droplets when the wind speed decreases. The relationship shown in the figure has little to do with turbulence. Deposition velocity increases with wind speed primarily because increasing wind speeds increase the momentum of the cloud droplets, causing more efficient impaction on vegetation surfaces.

In principle, there should be no sensitivity of the cloud deposition velocity to LWC, if all other parameters are held constant, because the deposition velocity is the deposition flux normalized by the LWC. (Another way of expressing this is that the deposition flux is directly proportional to the LWC, and the deposition velocity is the constant of proportionality.) However, in reality, other parameters are not always held constant. It has been shown many times that the droplet size distribution varies with the LWC [e.g., Mohnen *et al.* (1990) and Mueller (1991)], and the deposition

velocity does depend on the droplet size distribution. This creates a *de facto* dependence of the deposition velocity on the LWC as shown in Figure 4-4. In Figure 4-4, the data in parentheses are the modes of the droplet size distributions corresponding to each LWC, calculated from Equation 4-1.

With less than a two-fold increase in deposition velocity resulting from a five-fold increase in LWC, the deposition velocity is much less sensitive to the LWC than to wind speed. The cloudwater flux rate, however, is the product of the deposition velocity and the LWC, and, as such, has a greater than 1:1 sensitivity to LWC. In other words, doubling the LWC will result in more than doubling the modeled water flux rate.

The model sensitivity to canopy structure has been examined in detail by Lovett and Reiners (1986) and Mueller (1991). However, canopy structure was not varied in this study. This version of the model does not depend on temperature, Rh, solar radiation, or evaporation.

Two other parameters, although not used in the calculations of instantaneous deposition rates in the model, are important in the final calculations of cloud deposition values. These include cloud chemistry and cloud frequency (the percent of hours that the site is immersed in cloud). Calculated cloud deposition totals are directly proportional to both of these factors. For example, if other parameters are held constant, doubling the cloud SO_4^{2-} concentration will double the calculated cloud SO_4^{2-} deposition, and doubling the cloud frequency will double the calculated deposition of all ions.

4.1.4 Results of CLOUD Model Calculations

Monthly deposition estimates are given in Table 4-1. Monthly variability is significant [e.g., sulfate deposition varies from approximately 16 kilograms per hectare per month (kg/ha/mo) to less than 1.0 kg/ha/mo]. Monthly deposition values typically peak in July or August. The highest fluxes were modeled for Whiteface Mountain and the lowest for Clingman's Dome. Depositions of pollutants are generally related to cloudwater deposition.

Seasonal deposition estimates are provided in Table 4-2. For this purpose, a season is defined as the period from June through September. At least three valid months were required to calculate the seasonal deposition value. The highest seasonal fluxes were modeled for Whiteface Mountain. The highest seasonal deposition amount was modeled for Whiteface Mountain because of higher wind speeds and LWC (e.g., see Figure 3-7). No temporal trend is evident in the data.

4.2 MCLOUD Model Calculations

In addition to the model results discussed in Section 4.1, a second model (MCLOUD) was run to explore uncertainties related to the structure and parameterization of inferential deposition models and to assess how these uncertainties affect estimates of water and chemical fluxes. The strategy for

MADPro cloudwater deposition modeling is to use this general sensitivity analysis to better interpret the results of the CLOUD model used to provide the deposition estimates. Specifically, this analysis investigated differences in results between MCLOUD (Miller *et al.*, 1993a) and CLOUD (Lovett, 1984). To maintain a partially blind comparison of model calculations, MCLOUD used most (but not all) of the model parameterization information employed in CLOUD. The scope of the MCLOUD modeling effort was limited to the following site-year data sets: Clingman's Dome, TN (1997); Whitetop Mountain, VA (1995 and 1997); and Whiteface Mountain, NY (1994 through 1998).

The MCLOUD deposition model used for these additional analyses is described in detail by Miller *et al.* (1993a). MCLOUD is an expansion of the Lovett (1984) CLOUD model and is, therefore, only semi-independent of the primary CASTNet model. Differences between the two models are discussed below. The MCLOUD model permits alternative representations of the physical processes involved in cloudwater deposition as well as alternative "dimensions" for computational analysis. Potential differences in model results that might occur because of differences in model parameter systems are discussed in the following subsections.

4.2.1 MCLOUD Model Structure and Parameterization for MADPro Sites

4.2.1.1 Vertical Distribution of Leaf Area in the Forest Canopy

The LAI varies vertically within a forest canopy. Since the actual variation is not known for the three sites, the vertical distribution of leaf area from a similar Balsam Fir forest at 1,350-m elevation on Whiteface Mountain (Miller *et al.*, 1993a) was scaled to the LAI of the CLOUD standard canopy (Section 4.1.1.1) to parameterize MCLOUD. Consequently, the two models use different vertical distributions of leaf area; and model results appear to be fairly sensitive to the vertical distribution of leaf area (Figure 4-5). Therefore, it is expected that differences between the modeling results of ± 10 percent will exist on this basis alone.

4.2.1.2 Representation of Cloud Droplet Size Distributions

For the MCLOUD deposition modeling, the CLOUD assumptions regarding droplet-size distributions were used for Whitetop Mountain and Clingman's Dome sites, and the Miller *et al.* (1993a,b) assumptions were used for Whiteface Mountain. The CLOUD model used the distribution of droplet sizes using the Whitetop Mountain distribution parameters for all three sites.

The consequences of the use of the Whitetop Mountain droplet-size distribution for the Whiteface Mountain site were evaluated by both sensitivity analysis and by running MCLOUD for the WFM-97 data set under both sets of assumptions. Sensitivity analyses suggested a complicated pattern of model response to different combinations of LWC and wind speed using the two different dropsizes distributions (see Figure 4-6). The model runs using the Whitetop Mountain distribution underpredicted the results obtained with the Whiteface Mountain distribution by 1 to 24 percent for

all LWCs at wind speeds below 10 m/sec. At wind speeds > 10 m/sec, use of the Whitetop Mountain distribution increased deposition rates from 1 to 6 percent over the results obtained with the Whiteface Mountain distribution. This complicated model response tended to average out over the broad range of combinations of wind speed and LWC encountered at Whiteface Mountain. Seasonal average cloudwater fluxes (millimeters of water) differed by ~3 percent.

4.2.1.3 Number of Droplet Size Classes in the Models

Five-hundred droplet size class "bins" were used to represent the continuous droplet size distribution in a cloud for MCLOUD. This is a practical compromise between computational efficiency and effective description of the continuous droplet size distribution (see Miller *et al.*, 1993a, Figure 1, for more explanation). CLOUD employed 20 droplet size classes, so comparative runs with 20 droplet size classes were also performed.

The consequences of the number of size classes chosen to represent the continuous size distribution was previously discussed by Miller *et al.* (1993a, Figure 1). Miller *et al.* (1993a) report that 500 droplet size classes are required to arrive at a deposition velocity within 0.1 percent of the limiting value. The consequences of these two different numerical parameterizations (20 versus 500) were explored with MCLOUD using data from Clingman's Dome for 1997. Droplet fluxes were ~10 percent less using 20 droplet size classes compared to 500 classes (Figure 4-7). This degree of deviation is consistent with the previous analysis of Miller *et al.* (1993a) for 20 droplet classes.

4.2.1.4 Height of the Wind Speed Measurement Above the Whiteface Mountain Canopy

The CLOUD model was assigned the reference height of the wind speed versus elevation function presented by Miller *et al.* (1993a) as 3.2 m above the canopy. The actual reference height for this function is 1.0 m above the canopy (Miller *et al.*, 1993a, Figure 3). The 3.2-m reference height is the height of the wind speed measurement above the forest canopies at Whitetop Mountain and Clingman's Dome. The effect of choosing a 3.2-m wind speed reference height versus a 1.0-m height at Whiteface Mountain was explored.

CLOUD uses a reference height of the wind speed versus elevation function as 3.2 m above the canopy. Using a 3.2-m wind speed reference height (versus 1.0-m) at Whiteface Mountain results in a lower cloudwater deposition of ~20 percent (Figure 4-8).

4.2.1.5 Representation of Atmospheric Conditions

Atmospheric pressure, temperature, and the non-condensed water vapor content of the air have subtle effects on droplet deposition due to their effects on the density and kinematic viscosity of the air. Variation in the acceleration due to gravity with distance affects large droplet sedimentation velocities and particle rebound effects. The MCLOUD model includes these subtle effects. CLOUD

does not include these effects (Lovett, 1984). Evaporation is not being considered by either model. The more accurate representation of atmospheric conditions such as the density and kinematic viscosity of air in the model has < 1 percent effect on modeled fluxes.

4.2.2 MCLOUD Calculations

4.2.2.1 Data Screening

Data provided for each site and year were screened according to the following criteria:

1. If LWC was missing, the sample was discarded because water deposition could not be determined.
2. If wind speed was missing, the sample was discarded because water deposition could not be determined.
3. If no sample duration information was available, the sample was discarded because deposition could not be calculated.
4. If a sample duration of greater than 3 hours was required to obtain a satisfactory sample volume for chemical analysis, the sample was discarded because of the potential for evaporation of droplets on the cloudwater collector.
5. If the total measured ionic content was > 200 $\mu\text{eq/L}$ and the percent relative ion deficit (%RD) was > 25 percent, the sample was discarded due to suspect chemical analysis [$\%RD = (\text{sumcations} - \text{sumanions}) / \text{total ions} * 200$].
6. If the total measured ionic content was < 200 $\mu\text{eq/L}$ and the %RD was > 100 percent, the sample was discarded due to suspect chemical analysis.

Table 4-3 illustrates the effect of data screening on sample retention in the data sets. The predominant cause for sample rejection was lack of a valid wind speed measurement. In the WFM-95 data set, unacceptable ion balance was the primary reason for sample rejection, but missing wind speed observations were still significant. Sample retention rates ranged from 47 percent for WFM-95 to 83 percent for WTM-97.

Water flux to the forest canopy for individual samples was calculated using the cloudwater deposition model, parameterized as described above, and using the LWC, wind speed, and duration values for each sample that passed the data screening process. Water flux was combined with the chemical concentrations to calculate individual sample ion fluxes to the forest canopy. Ion concentrations in cloudwater were adjusted to account for LWC scaling for the 1,350-m site on Whiteface Mountain.

4.2.2.2 Data Aggregation and Summary

Individual sample water and ion fluxes were summed for each month. Monthly sums were divided by the amount of time represented by all samples from that month to arrive at an estimate of the

average flux per hour of cloud duration for a given month. The average flux rate was multiplied by the cloud frequency (Table 3-1) for each month to estimate monthly deposition. Monthly deposition fluxes were summed over the June to September growing season.

4.2.3 Sensitivity Analysis

A sensitivity analysis was also performed using only Whiteface Mountain data. Due to the lack of vegetation at the Whiteface Mountain summit measurement site, it was necessary to choose a "representative" elevation on Whiteface Mountain to develop a forest canopy description and to establish a range of environmental conditions that would be meaningful with respect to modeling such a canopy. Placing a simulated forest canopy in the atmospheric conditions characteristic of the summit measurement location would result in calculated deposition rates many times the rates likely to be experienced by actual forest canopies in the northeastern United States. Consequently, a representative elevation of 1,225 m was selected to define the conditions for the model sensitivity analysis. The CLOUD modeling was based on an elevation of 1,350 m. The 1,225-m canopy is considered similar enough to the CLOUD specification that the sensitivity analysis remains very informative.

The atmospheric conditions observed at the Whiteface Mountain summit station during the 1996 measurement campaign were scaled to the 1,225-m elevation. For the purpose of evaluating variations in the model canopy description, the 10th percentile, median, and 90th percentile values of the scaled wind speed distribution were selected to represent model response over a range of wind conditions (Figure 4-9). Similarly, the 25th percentile, median, and 90th percentile values of the scaled LWC were selected to test the range of model response to varying cloud conditions. Model simulations of cloudwater deposition rates were conducted using the nine combinations of wind speed and LWC (Table 4-4) with a range of possible canopy descriptions (Table 4-5). To simplify the interpretation of the simulation results, the instantaneous cloud droplet deposition velocities simulated by the model were extrapolated to a growing season water deposition value (centimeters of water deposited). This extrapolation assumed that the simulation conditions (LWC and wind speed) were constant during cloud immersion over a growing season of 3 months. Cloud immersion frequency was fixed at 25 percent of the period (typical for Whiteface Mountain, see Miller *et al.*, 1993a), except for one analysis which explicitly explored the effect of scaling cloud frequency with elevation.

The range of wind speeds and LWC selected from Figure 4-9 were used to investigate the sensitivity of 3-month, growing-season water depositions to changes in canopy structure and meteorological conditions. Generally, the cloud frequency was assumed constant at 25 percent. Several figures were prepared to illustrate MCloud model sensitivity; they are discussed in the following subsections.

4.2.3.1 Model Response to Variation in Forest Canopy Description

Observed Versus Pure Fir Canopy

Replacing 16 percent of the leaf area attributed to broad-leaf vegetation in the observed canopy with a needle-leaf representation produced a minor effect (Figure 4-10). Generally, the pure needle-leaf canopy had a 1.5 to 2.5 percent higher collection efficiency (CE) than the observed canopy with the exception of high wind speed combined with moderate and high LWC conditions. The slightly increased "openness" of a canopy with some broad-leaf foliage allows both momentum and droplets to penetrate to deeper layers of the canopy. Under lower wind speed (lower turbulence) regimes, CE is reduced rapidly as wind speed decreases in the upper part of the canopy. In lower LWC conditions, a majority of droplets are scavenged in the upper canopy, therefore reducing the effective LWC in the lower canopy space to near zero and reducing deposition, so the increased "openness" has little effect.

Canopy Height

For a canopy with $10 \text{ m}^2/\text{m}^2$ LAI, decreasing the canopy height from the observed value of 17 m resulted in decreasing cloudwater deposition (Figure 4-11). At a height of 10 m, the reduction was generally less than 2.5 percent, except in low LWC conditions where the reduction approached 3.5 percent.

Leaf Area Index

For a 10-m canopy, variation in LAI from the observed value of $10 \text{ m}^2/\text{m}^2$ resulted in a mixed response, depending on the combination of LWC and wind speed (Figure 4-12). Generally, deviations were in the range of +2 to -4 percent. However, conditions of low wind speed, combined with medium and high LWC, produced deviations of -6.5 and -9.8 percent, respectively, at $6 \text{ m}^2/\text{m}^2$ LAI.

4.2.3.2 Model Response to Variation in Wind Speed and LWC

The MCLLOUD deposition model, parameterized with the standard MADPro canopy (described previously) and 1-m thick layers, has a moderately non-linear response to both increasing wind speed and increasing LWC (Figure 4-13). For example, a 50 percent reduction in wind speed produces a 30 to 40 percent reduction in flux for constant LWC. Similarly, doubling the LWC produces almost twice the level of the cloudwater flux for a constant wind speed.

4.2.3.3 Model Layer Thickness

Previous applications of 1-dimensional turbulent diffusion models for cloud droplet flux have used a 1-m layer thickness to describe the vertical structure of the forest canopy and meteorological parameters within the forest canopy (Lovett, 1984; Lovett and Reiners, 1986; Mohnen, 1988; Mueller and Weatherford, 1988; Saxena *et al.*, 1989; Saxena and Lin, 1990; Joslin *et al.*, 1990; Mueller *et al.*, 1991; Mueller, 1991; Miller *et al.*, 1993a and b). Natural forest canopies are

heterogeneous enough, however, for a 1-m layer thickness description of the vertical distribution of leaf area to introduce significant uncertainty for the value of any given layer. Regressions of model results with selected layer thicknesses against results from the 1-m thickness yielded a maximum bias of 0.92 (Figure 4-5). The use of 1-m layers to describe the standard canopy may result in a systematic underestimation of cloudwater flux by 8 percent.

4.2.4 MCLOUD Model Results

MCLOUD seasonal deposition estimates are provided in Table 4-6. Again, a season was defined as the period from June through September and at least three valid months were required to calculate the seasonal deposition value. Except for a few instances, ion deposition was higher at Whiteface Mountain. Total ion deposition estimates could only be compared among the three sites for 1997, due to the limited scope of the MCLOUD runs. Monthly and seasonal totals of cloudwater deposition estimates tended to be highest at Whiteface Mountain due to the higher wind speed and LWC regime of that site. Ion deposition was also higher at Whiteface Mountain than at the southern sites. Whitetop Mountain had somewhat higher ion deposition rates than Clingman's Dome.

4.2.5 Conclusions

The relationship between general model sensitivity and potential bias and uncertainty in CASTNet cloudwater deposition estimates has been assessed for several key model parameters and input data streams. Table 4-7 provides a summary of this assessment.

Uncertainty in estimates of cloudwater deposition is nearly directly proportional to uncertainty in wind speed and LWC measurements, both of which are thought to be small for most site-year data sets. Deposition estimates are directly proportional to cloud frequency, a parameter that is also well known at each site for the majority of the months of the study. Whiteface Mountain is an exception because scaling of wind speed, LWC, and cloud frequency from the summit observations to canopy elevations is required. Therefore, selection of the "representative elevation" for deposition calculations at Whiteface Mountain has a significant effect on how the results from that site will compare to the other observation sites with forested summits.

The response of the cloudwater model appears to be the least sensitive to the least well-constrained parameters such as canopy species composition, height, LAI, and vertical distribution of leaf area. Model response is ± 12 percent or less for 10- to 40-percent changes in these parameters.

Estimates at all three sites are subject to a constant -8 percent bias resulting from numerical error introduced into the models by the choice of a 1-m layer thickness. There is some potential uncertainty (generally $< \pm 10$ percent in LWC, wind speed, and ion concentrations) introduced in a small number of years from the rejection of observations in the data screening process. There is

some potential for an unknown but significant uncertainty in the estimates arising from limited representation of meteorological and chemical conditions during cloud periods. Generally, less than 50 percent of observed cloud periods were represented in each site-year final data set.

4.3 Comparison of Results Between the CLOUD and MCLLOUD Models

Monthly deposition velocities and cloudwater deposition estimates generated by the CLOUD model were compared with those generated by MCLLOUD. Estimates from all three CASTNet MADPro sites were evaluated. Comparisons were made using monthly aggregation of the data.

Monthly average cloudwater and chemical deposition rates were highly correlated between the two semi-independent estimates. Correlations, as measured by the r^2 value, were generally greater than 0.8. Despite the high correlations, differences between estimates were often as large as 50 percent. Most of the differences (including outlier months) appear to be the result of differences in data screening or the aggregation of results to monthly averages. Other important sources of differences between the estimates include the effect of different vertical distributions of leaf areas used to parameterize the models as well as different approaches to scale cloud frequency from the summit to the lower model canopy elevation at Whiteface Mountain.

4.3.1 Results and Discussion

Overall, there was good general agreement between the two semi-independent cloudwater deposition estimates and underlying data aggregated at monthly intervals. After the removal of outliers, all parameters were highly correlated between the two data sets with adjusted r^2 values greater than 0.8.

Table 4-8 presents estimates of deposition velocities and cloudwater fluxes for the 13 months that both models were run. The table shows significant differences between results from Whiteface Mountain and results from Whitetop Mountain and Clingman's Dome. Deposition velocities from the two models are comparable for Whiteface Mountain, i.e., within 15%. Differences in deposition velocities from the two models for Whitetop Mountain and Clingman's Dome range from about 20% to 50%. Cloudwater deposition estimates were approximately 35 to 55 percent higher for the CLOUD runs for all three sites.

Model formulation and parameterizations, input data, and data screening and data aggregation procedures all contribute to the differences between the two sets of model calculations. The approximate 45-percent difference between the model results characterizes the uncertainty inherent in modeling procedures (including data screening and data aggregation procedures). The CLOUD and MCLLOUD results have not been evaluated with field measurements. This type of evaluation could help explain model uncertainties and improve overall model performance.

Resistance type models that simulate dry deposition have been evaluated (e.g., Meyers *et al.*, 1998; Finkelstein *et al.*, 2000) using field measurements. These evaluation studies have shown that the resistance models have little bias for relatively flat, open settings and tend to underestimate deposition velocities for forested, complex settings. Resistance models also have considerable scatter based on modeling individual periods (i.e., ½-hour flux measurements). The scatter shows differences as high as a factor of 2.0 for individual simulations. However, the differences and scatter decrease for aggregated periods – monthly, seasonal, and annual events. Assuming these uncertainties apply to the CLOUD and MCLOUD models, typical uncertainties of at least 50% to 100% or more can be assigned to monthly and seasonal simulations.

4.4 Best Estimates of Seasonal Deposition Rates

Table 4-9 provides the best estimates of seasonal deposition rates for the three MADPro sites. The CLOUD model is considered the primary model and was used to provide most of the information shown in the table. However, because CLOUD model results were not available for 1999 and for 1994 for Whiteface Mountain, MCLOUD results were used for these periods. The MCLOUD results were multiplied by 1.45 to account for the uncertainties discussed in the previous section.

The results show generally higher deposition rates at Whiteface Mountain. The 1997 estimates show a south – north gradient in depositions. The 1999 data are different, however, in that Clingman's Dome has the highest deposition values.

U.S. EPA Headquarters Library
Mail code 3201
1200 Pennsylvania Avenue NW
Washington DC 20460

100

101

102

103

104

105

106

107

108

109

110

111

112

113

114

115

116

117

118

119

120

121

122

123

124

125

126

127

128

129

130

131

132

133

134

135

136

137

138

139

140

141

142

143

144

145

146

147

148

149

150

151

152

153

154

155

156

157

158

159

160

161

162

163

164

165

166

167

168

169

170

171

172

173

174

175

176

177

178

179

180

181

182

183

184

185

186

187

188

189

190

191

192

193

194

195

196

197

198

199

200

201

202

203

204

205

206

207

208

209

210

211

212

213

214

215

216

217

218

219

220

221

222

223

224

225

226

227

228

229

230

231

232

233

234

235

236

237

238

239

240

241

242

243

244

245

246

247

248

249

250

251

252

253

254

255

256

257

258

259

260

261

262

263

264

265

266

267

268

269

270

271

272

273

274

275

276

277

278

279

280

281

282

283

284

285

286

287

288

289

290

291

292

293

294

295

296

297

298

299

300

301

302

303

304

305

306

307

308

309

310

311

312

313

314

315

316

317

318

319

320

321

322

323

324

325

326

327

328

329

330

331

332

333

334

335

336

337

338

339

340

341

342

343

344

345

346

347

348

349

350

351

352

353

354

355

356

357

358

359

360

361

362

363

364

365

366

367

368

369

370

371

372

373

374

375

376

377

378

379

380

381

382

383

384

385

386

387

388

389

390

391

392

393

394

395

396

397

398

399

400

401

402

403

404

405

406

407

408

409

410

411

412

413

414

415

416

417

418

419

420

421

422

423

424

425

426

427

428

429

430

431

432

433

434

435

436

437

438

439

440

441

442

443

444

445

446

447

448

449

450

451

452

453

454

455

456

457

458

459

460

461

462

463

464

465

466

467

468

469

470

471

472

473

474

475

476

477

478

479

480

481

482

483

484

485

486

487

488

489

490

491

492

493

494

495

496

497

498

499

500

501

502

503

504

505

506

507

508

509

510

511

512

513

514

515

516

517

518

519

520

521

522

523

524

525

526

527

528

529

530

531

532

533

534

535

536

537

538

539

540

541

542

543

544

545

546

547

548

549

550

551

552

553

554

555

556

557

558

559

560

561

562

563

564

565

566

567

568

569

570

571

572

573

574

575

576

577

578

579

580

581

582

583

584

585

586

587

588

589

590

591

592

593

594

595

596

597

598

599

600

601

602

603

604

605

606

607

608

609

610

611

612

613

614

615

616

617

618

619

620

621

622

623

624

625

626

627

628

629

630

631

632

633

634

635

636

637

638

639

640

641

642

643

644

645

646

647

648

649

650

651

652

653

654

655

656

657

658

659

660

661

662

663

664

665

666

667

668

669

670

671

672

673

674

675

676

677

678

679

680

681

682

683

684

685

686

687

688

689

690

691

692

693

694

695

696

697

698

699

700

701

702

703

704

705

706

707

708

709

710

711

712

713

714

715

716

717

718

719

720

721

722

723

724

725

726

727

728

729

730

731

732

733

734

735

736

737

738

739

740

741

742

743

744

745

746

747

748

749

750

751

752

753

754

755

756

757

758

759

760

761

762

763

764

765

766

767

768

769

770

771

772

773

774

775

776

777

778

779

780

781

782

783

784

785

786

787

788

789

790

791

792

793

794

795

796

797

798

799

800

801

802

803

804

805

806

807

808

809

810

811

812

813

814

815

816

817

818

819

820

821

822

823

824

825

826

827

828

829

830

831

832

833

834

835

836

837

838

839

840

841

842

843

844

845

846

847

848

849

850

851

852

853

854

855

856

857

858

859

860

861

862

863

864

865

866

867

868

869

870

871

872

873

874

875

876

877

878

879

880

881

882

883

884

885

886

887

888

889

890

891

892

893

894

895

896

897

898

899

900

901

902

903

904

905

906

907

908

909

910

911

912

913

914

915

916

917

918

919

920

921

922

923

924

925

926

927

928

929

930

931

932

933

934

935

936

937

938

939

940

941

942

943

944

945

946

947

948

949

950

951

952

953

954

955

956

957

958

959

960

961

962

963

964

965

966

967

968

969

970

971

972

973

974

975

976

977

978

979

980

981

982

983

984

985

986

987

988

989

990

991

992

993

994

995

996

997

998

999

1000

5.0 Total Deposition

Total deposition, as the term is used most of the time, is defined as dry and wet (or precipitation) deposition summed together. In the eastern United States, frequent cloud exposure usually occurs at elevations above 800 m (Mohnen *et al.*, 1990). Land area above this elevation has been determined to total approximately 25 million hectares. These locations, shown in Figure 5-1, cover a considerable portion of the Appalachian chain, illustrating that the impact of cloud deposition reaches beyond state boundaries and is not unique to a few isolated areas. Total deposition in such areas of frequent cloud exposure then is the sum of cloud, wet, and dry deposition. The extra deposition of pollutants via cloud exposure in these areas is often the cause of environmental damage, especially to red spruce (Eager and Adams, 1992). An analysis of total deposition shows the contribution of each fraction (i.e., cloud, wet, dry) to the total loading at a location. Total deposition from high-elevation sites can be compared to locations where total loading results mostly from dry and wet depositions. Such analyses may result in a better understanding of the processes involved that lead to ecological damage.

5.1 Procedures

Cloud, wet, and dry deposition estimates were calculated on a monthly basis from 1994 through 1999 for the months of June through September at all three sites. Cloud deposition values at the three sites for 1994 through 1998 were estimated by the CLOUD model and for 1999 by the MCLOUD model. Total deposition amounts were calculated for the years 1994 through 1998.

The multi-layer model (MLM) was used to estimate dry depositions from filter pack concentration data (Meyers *et al.*, 1998; Finkelstein *et al.* 2000) for Whitetop Mountain and Clingman's Dome. At both sites, the filter packs were collocated with the automated cloud sampler. The dry deposition values for Whiteface Mountain were obtained from NOAA Atmospheric Integrated Monitoring Network (AIRMoN) and were also estimated by the MLM. The MLM calculations are considered reasonable and representative for Clingman's Dome and Whitetop Mountain because onsite meteorological measurements were used directly in the model. Although the MLM was developed and evaluated using measurements from flat terrain settings, the model evaluation results are considered roughly applicable to these two sites. The data from Meyers *et al.* (1998) show little overall bias and up to 100% differences for individual ½-hr simulations. More recent data (Finkelstein *et al.*, 2000) suggest the MLM underestimates deposition velocities for SO₂ for complex, forested sites. The differences are expected to be lower for longer averaging times, i.e., monthly and seasonal periods. Consequently, the uncertainty in the dry deposition estimates is approximately 100% or lower, and the MLM calculations probably underestimate the dry fluxes.

Wet deposition values for Whitetop Mountain were calculated by Harding ESE from data collected at the site. Wet deposition data for Whiteface Mountain and Clingman's Dome were obtained from

NADP/NTN. Data from Mt. Mitchell were used for Clingman's Dome since the wet deposition data collected at Clingman's Dome by NPS were not available.

The location of the filter pack and wet/dry bucket at Whiteface Mountain differed by approximately 750 m in elevation from the location of the cloud deposition estimates. The difference in elevation also results in a difference in forest canopies and wind speed regimes which are very different from the 1,350-m cloud-modeling site. Higher wind speeds and greater LAI's tend to increase dry deposition of HNO_3 at higher elevations on Whiteface (Miller *et al.*, 1993a). Also, the orographic increase in precipitation over 750 m is significant (approximately 20 percent). It is estimated, therefore, that wet and dry deposition values may be underestimated significantly in each case with respect to cloud deposition values at the 1,350-m cloud-modeling site. CASTNet estimates (EPA, 1998) of dry deposition fluxes for two high elevation sites near Coweeta, NC show differences up to a factor of 4.4 for weekly averages. Again, differences in seasonal averages are expected to be lower. In short, dry and wet deposition calculations for Whiteface Mountain are considered underestimates, maybe as high as 400% for dry deposition.

Monthly total deposition values were calculated by summing the monthly cloud, wet, and dry deposition values for June through September. Tables 5-1 through 5-3 present the monthly cloud, wet, and dry deposition values, when available or when data completeness permitted, for 1994 through 1999 for Whiteface Mountain, Whitetop Mountain, and Clingman's Dome. Monthly total deposition amounts were calculated and presented only if all three fractions for a month were available. As presented in these tables, data completeness for all three fractions for a month was not high for Whitetop Mountain and Clingman's Dome. To determine the composition of total deposition from its three constituents in a statistically meaningful way, the following procedures were employed:

1. For Whiteface Mountain and Whitetop Mountain, the percent that each fraction contributed to the total deposition was calculated for those months when data for all three fractions were available. An overall mean percent value was then calculated from the monthly percentages of each fraction. For Whiteface Mountain, overall mean percentages were calculated for sulfur (S), nitrogen (N), and H^+ . Dry deposition estimates for NH_4^+ were not available from NOAA. For Whitetop Mountain, overall mean percentages were calculated for S, N, NH_4^+ , and H^+ .
2. The above procedure was not suitable for Clingman's Dome because there was only 1 month in 1998 when data from all three fractions were available. Therefore, deposition values of each fraction for all months when data were available from 1994 through 1999 were averaged to yield a fractional mean. The overall fractional means were then summed to yield an overall total deposition value. The percent each fraction contributed to the total deposition was then calculated.

Procedure 2 was tested by calculating the overall percent composition for Whiteface Mountain and Whitetop Mountain using this same procedure. The percent composition values produced by procedures 1 and 2 for the two sites were almost identical for cloud deposition and only differed by 1 to 2 percent for the dry and wet fractions. It was deemed suitable, therefore, to use procedure 2 to produce fractional mean percentages of S, N, NH_4^+ , and H^+ for Clingman's Dome. The percent composition results determined by procedure 1 for Whitetop Mountain and Whiteface Mountain, and by procedure 2 for Clingman's Dome are presented in Table 5-4.

Seasonal deposition values (June through September) were calculated by summing the monthly values for each fraction when data for all 4 months for a given year were available. If data for only 3 of the 4 months were available for a given fraction, then the fractional value was estimated by scaling up from the average of the three available monthly values. A seasonal fractional deposition amount was not calculated if data were not available for at least 3 months in the season. The fractional seasonal deposition values were then summed to yield a seasonal total deposition value. Seasonal total deposition estimates for Whiteface Mountain and Whitetop Mountain are presented in Tables 5-5 and 5-6, respectively. The lack of data completeness at Clingman's Dome did not allow for calculation of seasonal deposition estimates for any ions.

5.2 Results and Discussion

Tables 5-1 through 5-4 show that clouds are, by far, the largest source for deposition of pollutants to high-elevation ecosystems. Between 80 and 90 percent of S deposition occurs via cloud exposure at all three sites as does 70 to 87 percent of the total H^+ loading. Cloud deposition is also responsible for 90 to 95 percent of NH_4^+ deposition at the southern sites. Dry deposition is a very minor contributor to the total S and NH_4^+ loading, but contributes between 22 and 28 percent of N deposition and approximately 15 to 16 percent of H^+ deposition at the southern sites. The percent composition of total deposition at the MADPro sites is depicted in Figure 5-1.

It is important to reiterate here that the dry and wet deposition values for Whiteface Mountain are probably underestimated due to the elevation difference in sampling locations. The uncertainties in the mean estimates of dry deposition for Whitetop Mountain and Clingman's Dome are estimated to be less than 100% for seasonal fluxes based on model evaluation studies. These calculations probably underestimate fluxes.

Seasonal dry, wet, and total deposition estimates for the major ions for Whiteface Mountain and two nearby CASTNet sites are presented in Table 5-5. The same information is presented in Table 5-6 for Whitetop Mountain and two nearby CASTNet sites. Total deposition values from the MADPro sites are approximately 6 to 20 times greater for S, N, and NH_4^+ (NH_4^+ results refer to Whitetop Mountain only) when compared to the CASTNet sites. With one exception, Whiteface Mountain H^+

deposition values are 1.3 to 2.4 times greater than the CASTNet H⁺ depositions. Whitetop Mountain H⁺ deposition values for 1996 are 6.5 to 10 times greater than H⁺ deposition amounts at the CASTNet sites.

Dry deposition values at Whiteface Mountain fall within the range of dry deposition values for the CASTNet sites for S, N, and H⁺. Wet deposition values for all three species are 1 to 3 times higher at the CASTNet sites, except for 1998 when the Whiteface Mountain values were slightly higher for S and nearly equal for N and H⁺.

Even though total seasonal deposition estimates could only be calculated for 1996 for Whitetop Mountain, similar relationships can be ascertained for dry and wet deposition estimates when compared to the closest CASTNet sites.

It is evident from the data presented in Tables 5-5 and 5-6 that the total deposition at MADPro sites is much greater due to cloud exposure than total deposition at lower elevation sites that experience mostly dry and wet depositions.

6.0 Comparison with Other Networks

6.1 Concentration of Pollutant Ions in Clouds

Two major networks for collecting long-term data on cloud chemical composition and concentration have been operated in eastern North America: the CHEF project, which began with field measurements in southern Quebec in 1985; and MCCP, which began in the eastern mountains of the United States in 1986. Protocols for the two programs were closely linked, with the objective of having comparable databases covering eastern North America. Results from CHEF have been published by Schemenauer (1986), Schemenauer and Winston (1988), and Schemenauer *et al.* (1995). Results from MCCP projects have been published by Mohnen and Kadlec (1989) and Saxena *et al.* (1989). Other recent reviews of the results from MCCP have been prepared by Vong *et al.* (1991), Li and Aneja (1992), and Mohnen and Vong (1993).

For the CHEF sample set as a whole (including the main sites at Roundtop, Mont Tremblant, and Montmorency, and the subsites at Mont Tremblant mid-level and Roundtop summit), the mean volume-weighted fog composition for all seasons ($n = 599$) is as follows (in $\mu\text{eq/L}$):

SO_4^{2-}	279.8
NO_3^-	163.3
Cl^-	14.7
NH_4^+	210.3
Ca^{2+}	67.9
Mg^{2+}	14.2
Na^+	15.8
K^+	4.5
H^+	162.2

The total anion concentration is $457.8 \mu\text{eq/L}$ and the total cation concentration is $474.9 \mu\text{eq/L}$. The ion balance was calculated to be 1.8 percent, indicating that it is unlikely that other stable ions are present in significant concentrations.

The CHEF cloud chemistry data are of high quality and are comparable to MCCP data presented in Table 6-1 for 1986 through 1988. The results from MADPro for the sample set as a whole (warm season June through September) during the 1994 through 1999 time period are presented in Table 3-5.

The comparison of regionally and temporally averaged mean ion concentrations indicate that the concentration of major ions in clouds for northern versus southern sites in eastern North America

(North Carolina to Quebec and altitudes of 3,000 to 6,000 feet) fall within the minimum and maximum ranges listed below:

	<u>Northern Sites</u>	<u>Southern Sites</u>
SO_4^{2-}	280-300 $\mu\text{eq/L}$	380-450 $\mu\text{eq/L}$
NO_3^-	120-170 $\mu\text{eq/L}$	170-190 $\mu\text{eq/L}$
H^+	160-230 $\mu\text{eq/L}$	290-370 $\mu\text{eq/L}$
NH_4^+	160-220 $\mu\text{eq/L}$	210-250 $\mu\text{eq/L}$

There is a distinct north-south gradient in cloud ion concentrations that has already been detected in all previous studies. Based on the largest combined data set on cloud chemistry now available, this north-south gradient has been well established.

The MADPro project means are higher for all four major ions for Whiteface Mountain and Whitetop Mountain in comparison with MCCP project means for these same sites. The MADPro Clingman's Dome means, when compared to MCCP's Mt. Mitchell means (the closest MCCP site), were higher for the nitrogen compounds but lower for H^+ and SO_4^{2-} . Table 6-2 presents the relative percent differences between the MCCP and MADPro overall project means.

Significant variations occur during and between individual cloud events both with altitude (height above cloud base), cloud LWC, and origin of air masses (proximity of emission sources) as indicated by the wide spread of maximum and minimum concentrations observed at the monitoring sites.

All CHEF, MCCP and MADPro concentrations that are discussed in this section are volume-weighted means, but have not been normalized for LWC.

6.1.1 Comparison of Results with European Studies

A long-term cloud chemistry monitoring program was operated from 1991 through 1993 at Mt. Brocken, Germany [Möller *et al.* (1994, 1996) and Acker *et al.* (1999)]. For the manual cloudwater collection, the same collector and SOP were used as in MCCP. Therefore, the hourly samples collected at this mountain site are directly comparable to MCCP and MADPro cloud results. LWC was measured with the Gerber PVM-100. The overall results of cloud chemical composition are presented in Table 6-3.

Additional fog collection was performed at other European sites, although for a shorter duration. These investigations are summarized in Table 6-4.

In general, the concentrations of major and minor ions reported by European investigators are higher than those measured in eastern North American networks. This is particularly true for NO_3^- and NH_4^+ , which is indicative of the higher atmospheric pollution burden over Europe and the closer proximity

of major emission sources to the European measurement sites. Most sites also show lower LWC due to the lower elevation of the sampling sites where ground-level fog occurs frequently.

6.2 Deposition

Assessment of atmospheric pollutant transfer is essential for informed ecosystem management of mountain forests to preserve their biological, recreational, and aesthetic value.

Cloud droplet capture by the forest canopy is the principal transfer mechanism. Its magnitude can be obtained from cloud deposition models, cloud deposition measurements by eddy correlation, or estimated from the hydrological mass balance using direct measurement of evapotranspiration by the eddy covariance-energy-budget (ECEB) method [Herckes *et al.* (1999), Kalina *et al.* (1998), and Wrzesinsky and Klemm (2000)]. The latter two approaches are used mostly for short term field research projects; results from such studies will not be discussed here.

All three approaches provide as output the flux rate of liquid cloudwater [millimeters per hour (mm/hr)] and, after adjusting for the time the forest is immersed in clouds (cloud frequency), the monthly or annual total amount of cloudwater (millimeters of water). Incorporating the cloudwater chemical concentration subsequently yields the chemical deposition kg/ha/mo or kilograms per hectare per year (kg/ha/yr).

The best documented estimates of cloudwater chemical deposition prior to MADPro are from MCCP [Mohnen (1988) and Mohnen *et al.* (1990)]. The MCCP collected hourly cloudwater data (solute and LWC concentrations) and meteorological data (winds, cloud frequency, relative humidity, and solar radiation) for about 5 months each summer (May through September) over 3 years (1986 through 1988). The MADPro mean calculated deposition values (CLOUD model) for water and four major ions are compared to MCCP values as well as to values ascertained by Lovett *et al.* (1982) and Miller *et al.* (1993a) in Table 6-5. In general, the values from the MADPro Clingman's Dome and Whitetop Mountain sites fall within the range of those measured previously, while those from the MADPro Whiteface Mountain site are slightly above the range. The calculated values for the MADPro Whitetop Mountain site are similar to those calculated for the Whitetop Mountain (B) site in the MCCP project (Mohnen *et al.* 1990), which had a similar canopy structure to the stand used in the CLOUD model. The calculated values for the MADPro WFML site are higher than those modeled for the MCCP Whiteface Mountain site, although it is not clear from the MCCP report what sort of canopy was modeled for this site or at what elevation. The MCCP report (p. 4-61, Mohnen *et al.*, 1990) suggests that the low deposition estimated for the Whiteface site resulted from a low canopy surface area used for the calculations.

More relevant, perhaps, are the results of Miller *et al.* (1993a) calculations for the 1,350-m elevation on Whiteface Mountain, which is listed as Whiteface Mountain (M) in Table 6-5. The MADPro

water deposition rates are significantly higher than those of Miller *et al.*, but Miller *et al.* were simulating the entire year, including the winter season which they suggest has deposition rates of less than half those of the warm season. They report a mean warm season deposition velocity (45.3 cm/sec) that was actually higher than the MADPro result of 37.2 cm/sec. Miller *et al.* also reported lower chemical concentrations in cloudwater (132 $\mu\text{eq/L}$ of SO_4^{2-} versus 347 $\mu\text{eq/L}$ of SO_4^{2-}). This difference may be due to temporal variation, different sampling locations, or different data treatment (e.g., data screening).

In other studies, the cloud deposition model-spruce (CDM-S) and the cloud deposition model-deciduous (CDM-D) (Sigmon *et al.*, 1989; Mueller *et al.*, 1991) were used to predict deposition to the forests on six eastern United States mountains (Table 6-6). The other large network reporting data for eastern North America is the CHEF project. Deposition estimates from the CHEF project (1985 through 1991) are not available because cloud sampling time extended over several hours and no concurrent LWC measurements were made.

MCCP researchers have estimated that cloudwater deposition provides a substantial fraction of the total chemical deposition to the forests that they studied in the eastern United States. Lindberg and Johnson (1989) estimated that cloudwater contributes approximately 25 to 50 percent of total (rain + cloud + dry) SO_4^{2-} , N, and H^+ deposition at sites on Whiteface Mountain, New York, and in the Great Smoky Mountains National Park, North Carolina. MCCP results indicate that cloud SO_4^{2-} , NO_3^- , H^+ , and NH_4^+ deposition exceeded wet deposition via precipitation for three sites located above 1,400 m. Two sites located near 1,000-m elevation received cloudwater chemical inputs that were at least 50 percent of precipitation chemical deposition.

From a decade of observations (1986 through 1996) [using data from MCCP, MADPro CLOUD, and Electric Power Research Institute-Integrated Forest Study (EPRI-IFS)], Miller and Friedland (1999) estimated the atmospheric deposition at the Whiteface Mountain 1,050-m site for total nitrogen to average 17.2 kg/ha/yr (37 percent deposited as NH_4^+ and 63 percent as NO_3^-) and sulfur deposition to average 18.3 kg/ha/yr. Precipitation and cloudwater deposition contributed nearly equally to total sulfate deposition at the lower (1,050 m) Whiteface Mountain site (Table 6-7).

In a separate study, Miller *et al.* (1993a) determined that cloudwater contributed 2, 39, and 73 percent of total annual SO_4^{2-} deposition at 600-, 1,025-, and 1,350-m elevation, respectively, on Whiteface Mountain. Cloudwater contributed 1, 28, and 59 percent of total annual NO_3^- deposition at 600-, 1,025-, and 1,350-m elevation, respectively, in that study. This shift in the fraction of deposition contributed by cloudwater deposition at high elevations is confirmed by the results from MADPro (Table 5-4). The MADPro results from the 1,350-m elevation at Whiteface Mountain show that almost 91 percent and 84 percent of SO_4^{2-} and NO_3^- deposition, respectively, are from cloudwater interception. Again, the dry and wet deposition estimates from Whiteface Mountain are underestimated, at the very least, by a probable factor of 2 due to the elevation difference in sampling

locations. Scaling the dry and wet deposition estimates to the 1,350-m cloud-modeling site would reduce the percent composition of total deposition from cloud deposition to approximately 84 percent for SO_4^{2-} and 71 percent for NO_3 . This provides a better agreement with the results of Miller *et al.* (1993a).

The two southern sites also receive most of their deposition from clouds. Dry deposition has a larger influence in NO_3 deposition at the southern sites than at Whiteface Mountain. However, more than 65 percent of NO_3 deposition at the southern sites is still received from clouds. The influence of dry deposition may be even greater at the southern sites due to the limitations of the MLM model in estimating deposition velocities and fluxes over complex and high-elevation terrain.

The variation in cloudwater interception with cloud frequency thus produces an elevational gradient in total chemical deposition (Miller *et al.*, 1993a). A summary by Lovett and Kinsman (1990) suggests that eastern United States sites at elevations below 1,000 m receive less than 20 percent of total SO_4^{2-} deposition via cloudwater, but sites above 1,500 m receive 45 to 80 percent of total SO_4^{2-} deposition via cloudwater. These estimates are in agreement with independent summaries by NAPAP (Hicks *et al.*, 1991; Sisterson *et al.*, 1991) and with the MADPro results presented here.

6.2.1 Comparison of Results with European Studies

European studies also suggest substantial chemical fluxes from cloud droplet deposition. In Germany, Kroll and Winkler (1988) estimated that intercepted cloudwater contributed 25 to 150 percent of the water amount and 1 to 4 times the chemical deposition that occurs via rain for two mountain sites at elevations of 840 and 1,440 m (cloud frequencies were 20 percent and 30 percent, respectively). Harvey and McArthur (1989), using a gradient technique, estimated that fog droplet deposition accounted for about 2 to 12 percent of total chemical deposition to moors in central England. At another site in Great Britain with a cloud frequency of 23 percent, Fowler *et al.* (1990) calculated that droplet deposition to moors would increase wet deposition of SO_4^{2-} , NO_3 , H^+ , and NH_4^+ by 12 percent, but if the site were forested, the increase might be 44 percent (based on differences in aerodynamic roughness).

All investigations to date demonstrate the significant variability of the deposition rate with location and time of year, which depends on several spatial and temporal factors, including:

- Seasonal and air mass (trajectories) dependence of pollutant ion-concentration in cloud droplets;
- LWC variations with type of cloud, height above cloud base, and cloud droplet size distribution (which in turn influences droplet interception);
- Wind velocity at any location and its variation within the forest canopy; and
- Type of vegetation and associated LAI at any location.

Consequently, cloud droplet capture by the forest canopy varies substantially from year to year in response to changing meteorological conditions. These fluctuations impart significant variances to total atmospheric deposition rates of all ions. Dry deposition is not an efficient delivery process at high-elevation montane forests.

The observed deposition values for sulfur and nitrogen at high-elevation forest ecosystems represent some of the highest sustained air pollution loadings reported for eastern United States forests.

The lack of a temporal trend in MADPro results for cloudwater ion deposition indicates that sensitive mountain forest ecosystems may continue to experience high levels of sulfur and nitrogen input even as lower elevation forests of the region may experience steady reductions in sulfur and nitrogen deposition as a result of declining emissions.

7.0 Conclusions and Recommendations

Since the onset of its operation in 1994, MADPro has produced a 6-year data set that is comparable to data produced by past networks. The field SOPs, QA program, and laboratory analytical methods for MADPro were designed, when possible, with this objective of comparability in mind.

Differences in equipment with respect to past networks consisted mainly of the use of an automated cloudwater sampler and a continuous LWC measurement system (PVM-100). These changes were implemented as improvements identified as necessary from past experience. Two of the three permanent MADPro sites were identical to sites operated in past studies and all three sites collected samples during the warm season, which also mirrored past networks. Over 5,300 valid hourly samples were collected over the 6-year period of operation.

Therefore, MADPro has successfully achieved its two main objectives of development and implementation of cloudwater measurement systems to be used in a network monitoring environment and to update the cloudwater and deposition data collected in the Appalachian Mountains during NAPAP. MADPro has produced the most substantial amount of cloudwater data (based on the number of samples collected from 1994-1999) in the world. This high-quality data set enables representative conclusions to be drawn.

7.1 Cloudwater Concentrations

Statistically significant decreasing temporal trends were exhibited at Whiteface Mountain for NH_4^+ and SO_4^{2-} for both the normalized and non-normalized concentrations. Whitetop Mountain exhibited a statistically significant, but increasing, temporal trend for normalized SO_4^{2-} concentrations, even though ambient SO_2 levels have declined (Lavery *et al.*, 2000). Since MADPro was not designed as a trends/process study, no definitive conclusions are drawn as to the lack of trends for some or all of the analytes at both Whitetop and Whiteface Mountains, or the SO_4^{2-} trend in the opposite direction at Whitetop Mountain. It can be speculated, however, that the lack of trends, weak trends, or trends in the opposite direction, may be due to chemical non-linearity between emissions and cloudwater concentrations. This non-linearity is probably due to oxidant limitation in clouds and/or year-to-year variability in air mass trajectories, LWC, and local and regional meteorology (Miller and Friedland, 1999).

The Clingman's Dome site exhibits statistically significant temporal trends in concentrations of all the major ions for both normalized and non-normalized results, but these trends are also in the opposite direction (increasing) from what is expected given the SO_2 emission reductions. The trends at this site may, in part, be due to the increase in regional summertime SO_4^{2-} concentrations as documented by Mueller (2000). More research and analysis, especially that which involves back trajectories, needs to be conducted to fully understand the pattern at Clingman's Dome.

For the major ions, Whiteface Mountain exhibited the lowest mean and median normalized values and Clingman's Dome exhibited the highest mean and median concentrations. This is indicative of the north-south gradient noted during the MCCP (Anderson *et al.*, 1999; EPA, 1990). This gradient is probably an effect of the different meteorological conditions experienced at northern versus southern sites as well as a difference in the back trajectories of air masses reaching the sites.

Overall, 6-year mean concentrations at the three sites ranged from 289 to 456 $\mu\text{eq/L}$ for SO_4^{2-} , 125 to 182 $\mu\text{eq/L}$ for NO_3^- , 168 to 237 $\mu\text{eq/L}$ for NH_4^+ , and 225 to 359 $\mu\text{eq/L}$ for H^+ .

7.2 Cloudwater Depositions

MADPro results have clearly demonstrated the significance of the additional deposition of SO_4^{2-} and NO_3^- compounds to high-elevation forests subjected to cloud exposure. These sites experience additional loading on the order of 6 to 20 times greater for SO_4^{2-} and NO_3^- compared to lower elevation CASTNet sites. Approximately 80 to 90 percent of this extra loading is from cloud deposition. The dry and wet deposition fraction estimates from the MADPro sites are relatively comparable to dry and wet deposition amounts experienced at the CASTNet sites. The magnitude of deposition and/or exposure at high elevation sites is substantial enough to cause ecological damage (Eager and Adams, 1992).

A clear north-south pattern in total deposition amounts is not evident from the data presented here. However, data completeness for deposition values for the southern sites must be improved before further statements can be made. A review of the available monthly cloud and total deposition values from 1994 through 1999 does show that, unlike cloudwater concentrations, Whiteface Mountain experiences as much, if not greater, amounts of cloud and total deposition as the southern sites. This increase in deposition rates at Whiteface Mountain with respect to cloudwater concentrations is due in large part to the higher wind speeds and LWC experienced at this site.

Although MADPro was not designed for ecological studies, results from this program will aid ecologists in damage assessment of high-elevation ecosystems through the provision of a data set of known uncertainty.

7.3 Recommendations

1. To determine a trend in cloudwater concentrations and depositions, a longer measurement period than 6 years is necessary, as well as application of more sophisticated statistical procedures on the existing data set.
2. More back trajectory analyses are needed to elucidate any trends corresponding to upwind source regions.

3. Cloud deposition model intercomparisons and evaluations should be conducted via field studies of throughfall and eddy correlation.
4. Collection of spatial distribution of wind speed, cloud LWC, and cloud immersion time information for expansion of cloud deposition modeling to a regional scale.
5. To further increase regional representativeness of the cloud deposition values, canopy structure must be ascertained accurately and very specifically throughout the eastern United States frequently impacted by clouds. Use of satellite sensors for this purpose is recommended. This information will enable a more refined estimate of deposition values than the homogenized deposition estimates provided in this report.
6. Collocated field testing of the Valente method and the PVM-100 is necessary to determine whether MCCP LWC data need adjustment. If MCCP LWC data require adjustment, then the MCCP deposition estimates need to be recalculated using the adjusted LWC to allow better comparison with MADPro deposition estimates.
7. Cloudwater collection efforts must be collocated with ecological studies to further elucidate the processes involved at these locations.
8. To establish an east-west gradient, additional sites in the Green or White Mountains of New England are recommended. An additional site in West Virginia is also recommended due to its proximity and location with respect to Ohio River pollutant sources.
9. Extend the program from seasonal to year-round for estimation of winter time deposition values and comparison to other networks. The program should include other impacted mountainous regions in the western United States (e.g., the Cascades downwind of Seattle, the Sierra Nevadas downwind of the San Joaquin Valley, the San Gabriels and/or San Bernadinos downwind of Los Angeles, etc.).
10. Continuous SO_2 measurements and $\text{PM}_{2.5}$ sampling should be added to the suite of measurements to better address questions on SO_4^{2-} trends or lack thereof.

References

- Acker, K., Möller, D., Wieprecht, W., Auel, R., and Kalass, D. 1999. The Mt. Brocken Air and Cloud Water Chemistry Program and the QA/QC of Its Data. *In: Workshop on Quality Assurance of EMEP Measurements and Data Reporting. EMEP/CCC-Report 1/99*, pp. 161-165.
- Anderson, J.B., Baumgardner, R.E., Mohnen, V.A., and Bowser, J.J. 1999. Cloud Chemistry in the Eastern United States, as Sampled from Three High-Elevation Sites along the Appalachian Mountains. *Atmospheric Environment*, 33:5105-5114.
- Aneja, V.P. and Kim, D.S. 1993. Chemical Dynamics of Clouds at Mt. Mitchell, North Carolina. *Air & Waste*, 43:1074-1083.
- Anlauf, K.G., Wiebe, H.A., and Fellin, P. 1986. Characterization of Several Integrative Sampling Methods for Nitric Acid, Sulphur Dioxide and Atmospheric Particles. *JAPCA*, 36:715-723.
- Baumgardner, R.E., Kronmiller, K.G., Anderson, J.B., Bowser, J.J., and Edgerton, E.S. 1997. Development of an Automated Cloudwater Collection System for Use in Atmospheric Monitoring Networks. *Atmospheric Environment*, 31(13):2003-2010.
- Best, A.C. 1951. Drop-Size Distribution in Cloud and Fog. *Quarterly Journal of the Royal Meteorological Society*, 77:418-426.
- Butler, T.J., Likens, G.E., and Souder, B.J.B. (in press). Regional-Scale Impacts of Phase I of the Clean Air Act Amendments: The Relation Between Emissions and Concentrations, Both Wet and Dry. *Atmospheric Environment*.
- Collett, Jr., J., Oberholzer, B., and Staehelin, J. 1993. Cloud Chemistry at Mt. Rigi, Switzerland: Dependence on Drop Size and Relationship to Precipitation Chemistry. *Atmos. Environ.*, 27A:33-42.
- Dasch, J.M. 1988. Hydrological and Chemical Inputs to Fir Trees from Rain and Clouds During a 1-month Study at Clingman's Peak, NC. *Atmospheric Environment*, 22:2255-2262.
- Dollard, G.J. and Unsworth, M.H. 1983. Field Measurements of Turbulent Fluxes of Wind-Driven Fog Drops to a Grass Surface. *Atmospheric Environment*, 17:775-780.
- Dutkiewicz, V.A., Burkhard, E.G., and Husain, L. 1995. Availability of H₂O₂ for Oxidation of SO₂ in Clouds in the Northeastern United States. *Atmos. Environ.*, 29(22):3281-3292.

- Eager, C. and Adams, M.B., eds. 1992. Ecology and Decline of Red Spruce in the Eastern United States. *Springer Ecological Series*, Vol. 96. pp.395-411. Springer. Berlin.
- Falconer, R.E. and Falconer, P.D. 1980. Determination of Cloudwater Acidity at a Mountain Observatory in the Adirondack Mountains of New York State. *JGR*, 85(C):7465-7470.
- Finkelstein, P.L., Ellestad, T.G., Clarke, J.F., Meyers, T.P., Schwede, D.B., Herbert, E.O., and Neal, J.A. 2000. Ozone and Sulfur Dioxide Dry Deposition to Forests: Observations and Model Evaluation. *Atmos. Environ.*, 105:D12:15,365-15,377.
- Fowler, D., Morse, A.P., Gallagher, M.W., and Choularton, T.W. 1990. Measurements of Cloudwater Deposition on Vegetation Using a Lysimeter and Flux Gradient Technique. *Tellus*, 42B:284-293.
- Gerber, H., Arends, B.G., and Ackerman, A.S. 1993. New Microphysics Sensor for Aircraft Use. *Atmospheric Research*, 00:1-18.
- Gerber, H. 1984. Liquid Water Content of Fogs and Hazes from Visible Light Scattering. *Journal of Climatology and Applied Meteorology*, 23:1247-1252.
- Gunz, D.W. and Hoffman, M.R. (1990). *Atmospheric Chemistry of Peroxides: A Review*. *Atmos. Environ.*, 24A:1601-1633.
- Harding ESE, Inc. (Harding ESE). 1999. *Clean Air Status and Trends Network (CASTNet) Quality Assurance Project Plan (Draft)*. Prepared for the U.S. Environmental Protection Agency (EPA). Contract No. 68-D-98-112. Gainesville, FL.
- Harding ESE, Inc. (Harding ESE). 1997. *Clean Air Status and Trends Network (CASTNet) Mountain Acid Deposition Program Data Report – 1996 Monitoring Season*. Prepared for the U.S. Environmental Protection Agency (EPA), OAQPS, Research Triangle Park, NC 27711. Contract No. 68-D2-0134, Work Assignment No. 2. Gainesville, FL.
- Harvey, M.J. and McArthur, A.J. 1989. Pollution Transfer to Moor by Occult Deposition. *Atmospheric Environment*, 23(5):1073-82.
- Heffler, J.L. 1983. *Branching Atmospheric Trajectory (BAT) Model*. NOAA Technical Memorandum, ERL ARL-121. Air Resources Laboratory, Rockville, MD.

- Herckes, P., Wortham, H., Wendling, R., and Mirabel, P.H. 1999. *Cloudwater Studies at an High Elevation Site in the Voges Mountains (France)*, (poster presentation). Sixth Scientific Conference of the International Global Atmospheric Chemistry Organization, September 13-17, 1999. Bologna, Italy.
- Herterich, R. 1987. *Eignung und Anwendung von Rotating Arm Collectoren zur Bestimmung von Nebel Eigenschaften Flüssigwasser-gehalt, ionische Spurenstoffe, Wasserstoffperoxid*. Diploma thesis. 85 p. Chair of Hydrology, University of Bayreuth. Bayreuth, Germany.
- Hicks, B.B., Draxler, R. R., Albritton, D. L., Fehsenfeld, F. C., Davidson, C. I. 1991. *Atmospheric Processes Research and Process Model Development*. State of Science and Technology Report Number 2. National Acid Precipitation Assessment Program, Washington, DC.
- Joslin, J.D., Mueller, S.F., and Wolfe, M.H. 1990. Test of Models of Cloudwater Deposition to Forest Canopies Using Artificial and Living Forest Canopies and Living Collectors. *Atmospheric Environment*, 24A:3007-3019.
- Kalina, M.F., Zambo, E., and Puxbaum, H. 1998. Assessment of Wet, Dry and Occult Deposition of Sulfur and Nitrogen at an Alpine Site. *Environ. Sci. Pollut. Res.*, 1:53-58.
- Kroll, G. and Winkler, P. 1988. Estimation of Wet Deposition via Fog. In: *Environmental Meteorology*. pp. 227-36. K. Grefen and J. Lobel, eds. Kluwer. Dordrecht, Netherlands.
- Lavery, T.F., Costakis, C., and Rogers, C.M. 2000. *Trends in Atmospheric Deposition of Acid Gases and Particles*. Paper No. 1017. Annual Meeting of the Air and Waste Management Association. June 2000.
- Li, Z. and Aneja, V.P. 1992. Regional Analysis of Cloud Chemistry at High Elevations in the Eastern United States. *Atmospheric Environment*, 26A:2001-2017.
- Lindberg, S.E. 1992. Atmospheric Deposition and Canopy Interactions of Sulfur. In: *Atmospheric Deposition and Forest Nutrient Cycling*. pp.74-89. S. E. Lindberg and D. W. Johnson, eds. Springer-Verlag. New York.
- Lindberg, S.E. and Johnson, J.W. 1989. *1988 Annual Report to the Integrated Forest Study*. ORNL/TM-11121. Report to EPRI (RP2621), Oak Ridge National Laboratory, Oak Ridge, TN.

- Lindberg, S.E., Silsbee, D., Schaefer, D.A., Owens, J.G., and Petty, W. 1988. A Comparison of Atmospheric Exposure Conditions at High- and Low- Elevation Forests in the Southern Appalachian Mountain Range. In: *Acid Deposition at High Elevation Sites*. pp. 321-44. Unsworth, M.H. and Fowler, D., eds. NATO ASI Series C. Vol. 252. Kluwer Academic Publishers, Boston.
- Lovett, G.M. 2000. *Modeling Cloudwater Deposition to the Sites of the CASTNet Cloud Network*. Prepared for Harding ESE, Inc. (Harding ESE). Gainesville, FL.
- Lovett, G. M., and Kinsman, J. D. 1990. Atmospheric Pollutant Deposition to High-Elevation Ecosystems. *Atmospheric Environment*, 24A:2767-2786.
- Lovett, G.M. and Reiners, W.A. 1986. Canopy Structure and Cloudwater Deposition in Subalpine Coniferous Forests. *Tellus*, 38B:319-327.
- Lovett, G.M. 1984. Rates and Mechanisms of Cloudwater Deposition to a Subalpine Balsam Fir Forest. *Atmospheric Environment*. 18:361-371.
- Lovett, G. M., Reiners, W.A., and Olson, R. K. 1982. Cloud Droplet Deposition in Subalpine Balsam Fir Forests: Hydrological and Chemical Inputs. *Science*, 218:1303-1304.
- McLaughlin, S.B., Anderson, C.P., Hanson, P.J., Tjoelker, M.G., and Roy, W.K. 1991. Increased Dark Respiration and Calcium Deficiency of Red Spruce in Relation to Acidic Deposition at High Elevation Southern Appalachian Mountain Sites. *Canadian Journal of Forest Research*, 21:1234-1244.
- McLaughlin, S.B., Anderson, C.P., Edwards, N.T., Roy, W.K., and Layton, P.A. 1990. Seasonal Patterns of Photosynthesis and Respiration of Red Spruce Saplings from Two Elevations in Declining Southern Appalachian Stands. *Canadian Journal of Forest Research*, 20:485-495.
- Meyers, T.P., Finkelstein, P., Clarke, J., Ellestad, T.G., and Sims, P.F. (1998). A Multilayer Model for Inferring Dry Deposition Using Standard Meteorological Measurements. *J. Geophys. Res.*, 103:22,645-22,661.
- Miller, E.K. and Friedland, A.J. 1999. Local Climate Influences on Precipitation, Cloudwater, and Dry Deposition to an Adirondack Subalpine Forest: Insights from Observations 1986-1996. *Journal of Environmental Quality*, 28:270-277.

- Miller, E.K., Friedland, A.J., Arons, E.A., Mohnen, V.A., Battles, J.J., Panek, J.A., Kadleccek, J., and Johnson, A.H. 1993a. Atmospheric Deposition Along an Elevational Gradient at Whiteface Mountain, New York, USA. *Atmospheric Environment*, 27A:2121-2136.
- Miller, E.K., Panek, J.A., Friedland, A.J., Kadleccek, J., and Mohnen, V.A. 1993b. Atmospheric Deposition to a High-Elevation Forest at Whiteface Mountain, New York, USA. *Tellus*, 45B:209-227.
- Mohnen, V.A., and Vong, R.J. 1993. A Climatology of Cloud Chemistry for the Eastern United States Derived from the Mountain Cloud Chemistry Project. *Environ. Rev.*, 1:257-272.
- Mohnen, V.A., Aneja, V., Bailey, B., Cowling, E., Goltz, S.M., Healey, J., Kadleccek, J.A., Meagher, J., Mueller, S.M., and Sigmon, J.T. 1990. *An Assessment of Atmospheric Exposure and Deposition to High-Elevation Forests in the Eastern United States*. Report EPA/600/3-90/058 Edition. U.S. Environmental Protection Agency (EPA), Office of Research and Development, Washington, DC.
- Mohnen, V.A. and Kadleccek, J.A. 1989. Cloud Chemistry Research at Whiteface Mountain. *Tellus*, 41B:79-91.
- Mohnen, V.A. 1988. *Mountain Cloud Chemistry Project: Wet, Dry and Cloudwater Deposition*. EPA/600/3-89-003, U.S. Environmental Protection Agency (EPA), OAQPS, Research Triangle Park, NC.
- Möller, D., Acker, K., and Wieprecht, W. 1994. Cloud Chemistry at Mt. Brocken/Harz. In: *Proceedings of the 6th European Symposium on Physico-Chemical Behavior of Air Pollutants*, pp. 968-974. Rep. EUR 15609/2 EN. Brussels.
- Möller, D., Acker, K. and Wieprecht, W. 1996. A Relationship Between Liquid Water Content and Chemical Composition in Clouds. *Atmos. Res.*, 41:321-335
- Mueller, S.F. 2000. *Recent Air Quality Trends in the Great Smoky Mountains*. 11th Joint Conference on the Applications of Air Pollution Meteorology. Co-sponsored by American Meteorological Society and Air, Waste, and Management Association.
- Mueller, S.F. 1991. Estimating Cloudwater Deposition to Subalpine Spruce-Fir Forests – I. Modifications to an Existing Model. *Atmospheric Environment*, 25A:1093-1104.
- Mueller, S.F., Joslin, J.D., and Wolfe, M.H. 1991. Estimating Cloudwater Deposition to Subalpine Spruce-Fir Forests – II. Model Testing. *Atmospheric Environment*, 25A:1105-1122.

- Mueller, S.F. and Weatherford, F.P. 1988. Chemical Deposition to a High Elevation Red Spruce Forest. *Water, Air and Soil Pollution*, 38:345-363.
- Pahl, S, and Winkler, P. 1995. Höhenabhängigkeit der Spurenstoffdeposition durch Wolken auf Wälder. Abschlussbericht BMFT Nr. 07EU726A8.
- Saxena, V.K. and Lin, N.H. 1990. Cloud Chemistry Measurements and Estimates of Acidic Deposition on an Above Cloudbase Coniferous Forest. *Atmospheric Environment*, 24A:329-352.
- Saxena, V.K., Stogner, R.E., Hendler, A.H., DeFelice, T.P., Yeh, R.J.Y., and Lin, N.H. 1989. Monitoring the Chemical Climate of the Mt. Mitchell State Park for Evaluation of its Impact on Forest Decline. *Tellus*, 41B:92-109.
- Schemenauer, R.S., Banic, C.M., and Urquizo, N. 1995. High Elevation Fog and Precipitation Chemistry in Southern Quebec, Canada. *Atmospheric Environment*, 29: 2235-2252.
- Schemenauer, R.S. and Winston, C. 1988. *The 1986 Chemistry of High Elevation Fog (CHEF) Project*. pp. 1-16. 81st Annual Meeting of the Air Pollution Control Association. Dallas, TX. 88-129.6.
- Schemenauer, R.S. 1986. Acidic Deposition to Forests: the Chemistry of High Elevation Fog (CHEF) Project. *Atmosphere-Ocean*, 24:303-328.
- Scherbatskoy, T., and Klein, R.M. 1983. Response of Red Spruce and Birch Foliage to Leaching by Acidic Mists. *Journal of Environmental Quality*, 12:189-195.
- Schrimpf, E., Klemm, O., Eiden, R., Frevert, T., and Herrmann, R. 1984. Anwendung Eines Grunow-nebelfängers Zur Bestimmung von Schadstoffgehalten in Nebelniederschlägen. Staub-Reinh. *Luft*, 44:72-75.
- Seinfeld, J.H. 1986. *Atmospheric Chemistry and Physics of Air Pollution*. Wiley, New York.
- Shuttleworth, W.J. 1977. The Exchange of Wind-Driven Fog and Mist Between Vegetation and the Atmosphere. *Boundary-Layer Meteorology*, 12:463-489.
- Sigmon, J.T., Gilliam, F.S., and Partin, M.E. 1989. Precipitation and Throughfall Chemistry for Montane Hardwood Ecosystem: Potential for Contributions from Cloud Water. *Can. J. For. Res.*, 19:1240-47.

- Sisterson, D.L., Bowersox, V.C., Meyers, T. P., Simpson, J.C., Mohnen, V. 1991. *Deposition Monitoring Methods and Results*. State of Science and Technology Report Number 6. National Acid Precipitation Assessment Program, Washington, DC.
- Stogner, R.E. and Saxena, V.K. 1988. *Acidic Cloud: Forest Canopy Interactions: Mt. Mitchell, NC*. *Environ. Pollut.*, 53:456-58.
- Thorne, P.G., Lovett, G.M., and Reiners, W.A.. 1982. Experimental Determination of Droplet Deposition on Canopy Components of Balsam Fir. *J. Appl. Meteorol.*, 21:1413-1416.
- Trautner, F. 1988. *Entwicklung und Anwendung von Meßsystemen zur Untersuchung der chemischen und physikalischen Eigenschaften von Nebelwasser und dessen Deposition auf Fichten*. Dissertation. 160 pp. University of Bayreuth. Bayreuth, Germany.
- U.S. Environmental Protection Agency (EPA). 2000. *National Air Quality and Emission Trends Report, 1998*. EPA 454/R-00-003. March 2000.
- U.S. Environmental Protection Agency (EPA). 1990. *An Assessment of Atmospheric Exposure and Deposition to High Elevation Forests in the Eastern United States*. EPA/600/3-90/058. September 1990.
- U.S. Environmental Protection Agency (EPA). 1998. *Clean Air Status and Trends Network (CASTNet) Deposition Summary Report (1987-1995)*. EPA/600/R-98/027. OAQPS, Research Triangle Park, NC 27711.
- Valente, R.J., Mallant, R.K.A.M., McLaren, S.E., Schemenauer, R.S., and Stogner, R.E. 1989. Field Intercomparison of Ground-based Cloud Physics Instruments at Whitetop Mountain, Virginia. *Journal of Atmospheric and Oceanic Technology*, 6:396-406.
- Verhoeven, W., Herrmann, R., Eiden, R., and Klemm, O. 1987. A Comparison of the Chemical Composition of Fog and Rainwater Collected in the Fichtelgebirge, F.R. of Germany, and the South Island of New Zealand. *Theor. Appl. Clim.*, 38:210-221.
- Vong, R.J. and Kowalski, A.S. 1995. Eddy Correlation Measurements of Size-Dependent Cloud Droplet Turbulent Fluxes to Complex Terrain. *Tellus*, 47B:331-352.
- Vong, R.J., Sigmon, J.T., and Mueller, S.F. 1991. Cloudwater Deposition to Appalachian Forests. *Environmental Science and Technology*, 25:1014-1021.

- Weathers, K.C., Lovett, G.M., Likens, G.E. 1995. Cloud Deposition to a Spruce Forest Edge. *Atmospheric Environment*, 29:665-672.
- Weathers, K.C., Likens, G.E., Bormann, F.H., Bowden, W.B., Andersen, J.L., Cass, D.A., Galloway, J.N., Keene, W.C., Kimball, K.D., Huth, P., and Smiley, D. 1988. Cloudwater Chemistry from Ten Sites in North America. *Environmental Science and Technology*, 22:1018-1026.
- Weathers, K.C., Likens, G.E., Bormann, F.H., Bowden, W.B., Andersen, J.L., Cass, D.A., Galloway, J.N., Keene, W.C., Kimball, K.D., Huth, P., and Smiley, D. 1986. A Regional Acidic Cloud/Fog Water Event in the Eastern United States. *Nature*, 319:657-658.
- Wrzesinsky, T. and Klemm, O. 2000. Summertime Fog Chemistry at a Mountainous Site in Central Europe. *Atmos. Environ.*, 34:1487-1496. Abstract.

Tables

10

11

12

13

14

15

16

17

Figures

Appendix

Tables

100

101

102

103

104

105

106

107

108

109

110

111

112

113

114

115

116

117

118

119

120

121

122

123

124

125

126

127

128

129

130

131

132

133

134

135

136

137

138

139

140

141

142

143

144

145

146

147

148

149

150

151

152

153

154

155

156

157

158

159

160

161

162

163

164

165

166

167

168

169

170

171

172

173

174

175

176

177

178

179

180

181

182

183

184

185

186

187

188

189

190

191

192

193

194

195

196

197

198

199

200

201

202

203

204

205

206

207

208

209

210

211

212

213

214

215

216

217

218

219

220

221

222

223

224

225

226

227

228

229

230

231

232

233

234

235

236

237

238

239

240

241

242

243

244

245

246

247

248

249

250

251

252

253

254

255

256

257

258

259

260

261

262

263

264

265

266

267

268

269

270

271

272

273

274

275

276

277

278

279

280

281

282

283

284

285

286

287

288

289

290

291

292

293

294

295

296

297

298

299

300

301

302

303

304

305

306

307

308

309

310

311

312

313

314

315

316

317

318

319

320

321

322

323

324

325

326

327

328

329

330

331

332

333

334

335

336

337

338

339

340

341

342

343

344

345

346

347

348

349

350

351

352

353

354

355

356

357

358

359

360

361

362

363

364

365

366

367

368

369

370

371

372

373

374

375

376

377

378

379

380

381

382

383

384

385

386

387

388

389

390

391

392

393

394

395

396

397

398

399

400

401

402

403

404

405

406

407

408

409

410

411

412

413

414

415

416

417

418

419

420

421

422

423

424

425

426

427

428

429

430

431

432

433

434

435

436

437

438

439

440

441

442

443

444

445

446

447

448

449

450

451

452

453

454

455

456

457

458

459

460

461

462

463

464

465

466

467

468

469

470

471

472

473

474

475

476

477

478

479

480

481

482

483

484

485

486

487

488

489

490

491

492

493

494

495

496

497

498

499

500

501

502

503

504

505

506

507

508

509

510

511

512

513

514

515

516

517

518

519

520

521

522

523

524

525

526

527

528

529

530

531

532

533

534

535

536

537

538

539

540

541

542

543

544

545

546

547

548

549

550

551

552

553

554

555

556

557

558

559

560

561

562

563

564

565

566

567

568

569

570

571

572

573

574

575

576

577

578

579

580

581

582

583

584

585

586

587

588

589

590

591

592

593

594

595

596

597

598

599

600

601

602

603

604

605

606

607

608

609

610

611

612

613

614

615

616

617

618

619

620

621

622

623

624

625

626

627

628

629

630

631

632

633

634

635

636

637

638

639

640

641

642

643

644

645

646

647

648

649

650

651

652

653

654

655

656

657

658

659

660

661

662

663

664

665

666

667

668

669

670

671

672

673

674

675

676

677

678

679

680

681

682

683

684

685

686

687

688

689

690

691

692

693

694

695

696

697

698

699

700

701

702

703

704

705

706

707

708

709

710

711

712

713

714

715

716

717

718

719

720

721

722

723

724

725

726

727

728

729

730

731

732

733

734

735

736

737

738

739

740

741

742

743

744

745

746

747

748

749

750

751

752

753

754

755

756

757

758

759

760

761

762

763

764

765

766

767

768

769

770

771

772

773

774

775

776

777

778

779

780

781

782

783

784

785

786

787

788

789

790

791

792

793

794

795

796

797

798

799

800

801

802

803

804

805

806

807

808

809

810

811

812

813

814

815

816

817

818

819

820

821

822

823

824

825

826

827

828

829

830

831

832

833

834

835

836

837

838

839

840

841

842

843

844

845

846

847

848

849

850

851

852

853

854

855

856

857

858

859

860

861

862

863

864

865

866

867

868

869

870

871

872

873

874

875

876

877

878

879

880

881

882

883

884

885

886

887

888

889

890

891

892

893

894

895

896

897

898

899

900

901

902

903

904

905

906

907

908

909

910

911

912

913

914

915

916

917

918

919

920

921

922

923

924

925

926

927

928

929

930

931

932

933

934

935

936

937

938

939

940

941

942

943

944

945

946

947

948

949

950

951

952

953

954

955

956

957

958

959

960

961

962

963

964

965

966

967

968

969

970

971

972

973

974

975

976

977

978

979

980

981

982

983

984

985

986

987

988

989

990

991

992

993

994

995

996

997

998

999

1000

Table 2-1. Schedule of Routine QC Checks, Calibrations, and Audits Performed at the CASTNet Laboratory (Harding ESE)

Observable	Measurement Device	Performance Test Frequency	Performance Standard	Calibration Frequency	Calibration Standard	Audit Frequency	Audit Standard	Primary
Total Acidity	Titration	One per batch or daily	Blanks, standards	Daily	NIST-traceable pH 4 and pH 7 potassium hydrogen phthalate (as primary standard)	Annual	Reference standards	EPA/NIST reference standards
Ca ²⁺ , Mg ²⁺ , Na ⁺ , K ⁺	Atomic absorption	One per batch or daily	Blanks, standards, replicates, independent reference standards	Daily	Reagent-grade chemicals	Annual	Reference standards	EPA/NIST reference standards
NH ₄ ⁺	Automated wet chemical	One per batch or daily	Blanks, standards, replicates, independent reference standards	Daily	Reagent-grade chemicals	Annual	Reference standards	EPA/NIST reference standards
NO ₃ ⁻ , NO ₂ ⁻ , Cl ⁻ , SO ₄ ²⁻	Suppressed ion chromatography	One per batch or daily	Blanks, standards, replicates, independent reference standards	Daily	Reagent-grade chemicals	Annual	Reference standards	EPA/NIST reference standards
Fine/Coarse Aerosol Mass	Gravimetric (micro-balance)	One per batch or daily	Class S weight	Daily	Class S weight	Annual	Class S weight	NIST reference weight

Source: Harding ESE.

Table 2-2. Precision and Accuracy Objectives for CASTNet Laboratory Data

Analyte	Medium	Method	Acceptance Criteria		
			Precision (RPD)	Accuracy (%)	Nominal Detection Limits
PH	W	Electrometric	12	85 - 115	N/A
Conductivity	W	Electrometric	10	85 - 115	0.2 μ ohms/cm
Acidity	W	Titrimetric	15	N/A	5 μ eq/L
Ammonium (NH_4^+)	W/F	Automated colorimetry	10	90 - 110	0.02 mg-N/L
Sodium (Na^+)	W/F	ICAP-AE	10	90 - 110	0.005 mg/L
Potassium (K^+)	W/F	ICAP-AE	10	90 - 110	0.005 mg/L
Magnesium (Mg^{2+})	W/F	ICAP-AE	10	90 - 110	0.003 mg/L
Calcium (Ca^{2+})	W/F	ICAP-AE	10	90 - 110	0.003 mg/L
Chloride (Cl^-)	W	Ion chromatography	5	95 - 105	0.02 mg/L
Nitrite (NO_2^-)	W	Ion chromatography	5	N/A	0.004 mg/L
Nitrate (NO_3^-)	W/F	Ion chromatography	5	95 - 105	0.008 mg-N/L
Sulfate (SO_4^{2-})	W/F	Ion chromatography	5	95 - 105	0.04 mg/L

Note: For more information on analytical methods and associated precision and accuracy objectives, see CASTNet Draft Quality Assurance Project Plan (QAPP) (Harding ESE, 1999).

W = wet or aqueous

F = filter

ICAP-AE = inductively coupled argon plasma-atomic emission

Table 2-3. Data Quality Objectives for Continuous Measurements

Measurement Parameter	Method	Objectives*	
		Precision	Accuracy
Wind Speed	Anemometer	± 0.5 m/s	The greater of ± 0.5 m/s for winds < 5 m/s or $\pm 5\%$ for winds > 5 m/s
Wind Direction	Wind Vane	5%	5°
Relative Humidity (Rh)	Hygrometer	$\pm 10\%$ (of full scale)	$\pm 5\%$, Rh $> 85\%$ $\pm 20\%$, Rh $> 85\%$
Solar Radiation	Pyranometer	$\pm 10\%$ (of reading)	10%
Precipitation	Tipping Bucket Rain Gauge	$\pm 10\%$ (of reading)	± 0.05 inch†
Ambient Temperature	Platinum RTD	$\pm 1.0^\circ\text{C}$	$\pm 0.5^\circ\text{C}$
Delta Temperature	Platinum RTD	$\pm 0.5^\circ\text{C}$	$\pm 0.5^\circ\text{C}$
Surface Wetness	Conductivity Bridge	Undefined	Undefined
Ozone (O ₃)	Ultraviolet (UV) Absorbance	$\pm 10\%$ (of reading)	$\pm 10\%$
Filter Pack Flow	Mass Flow Controller	± 0.15 Lpm	$\pm 5\%$

Note: °C = degrees Celsius
 Lpm = liters per minute
 m/s = meters per second
 RTD = resistance-temperature device

* Precision criteria apply to collocated instruments, and accuracy criteria apply to calibration of instruments.

† For target value of 0.50 inch.

Source: CASTNet Draft Quality Assurance Project Plan, Harding ESE (1999).

Table 2-4. Results From the QA Testing at ECN Facilities in the Netherlands

Run #	ECN Pall-Filters (mg/m ³)	ECN PVM-100 (mg/m ³)	RPD*	EPA-1 PVM-100 (mg/m ³)	RPD	EPA-2 PVM-100 (mg/m ³)	RPD	EPA Valente (mg/m ³)	RPD
1	883	808	-8.49	880	-0.34	904	2.38	1170	32.50
2	882	832	-5.67	896	1.59	930	5.44	1110	25.85
3	140	163	16.43	184	31.43	176	25.71	75	-46.43
3a	94	110	17.02	125	32.98	117	24.47	112	19.15
4	393	392	-0.25	423	7.63	439	11.70		
4a	412	412	0.00	446	8.25	462	12.14	510	23.79
5	345	361	4.64	388	12.46	402	16.52		
5a	352	369	4.83	395	12.22	410	16.48	472	34.09
6	360	360	0.00	386	7.22	401	11.39	477	32.50
7	687	686	-0.15	731	6.40	784	14.12	932	35.66
8	105	107	1.90	104	-0.95	110	4.76		
8a	97	94	-3.09	94	-3.09	98	1.03		
9	88	85	-3.41	86	-2.27	88	0.00	72	-18.18
9a	689	695	0.87	700	1.60	739	7.26		
10	675	681	0.89	687	1.78	725	7.41	823	21.93
10a	437	427	-2.29	433	-0.92	449	2.75		
10b	441	431	-2.27	436	-1.13	454	2.95	517	17.23
11	438	429	-2.05	435	-0.68	451	2.97	491	12.10
12	687	689	0.29	691	0.58	732	6.55	841	22.42
13	862	857	-0.58	836	-3.02	904	4.87	1034	19.95
13a	128	116	-9.38	118	-7.81	120	-6.25		
14	97	88	-9.28	88	-9.28	97	0.00	114	17.53
14a	388	406	4.64	409	5.41	426	9.79		
14b	383	401	4.70	404	5.48	419	9.40	482	25.85
14c	388	406	4.64	409	5.41	425	9.54	487	25.52
15	384	402	4.69	405	5.47	421	9.64	488	27.08
16a	647	680	5.10	676	4.48	716	10.66	837	29.37
16	114	120	5.26	123	7.89	126	10.53	121	6.14
Mean			1.04		4.60		8.36		18.20

* Relative percent difference (RPD) was calculated using the Pall filter concentrations as references.

Source: ECN

This page has been intentionally left blank.

Table 3-1. MADPro Cloud Frequency Summary (page 1 of 2)

		Whiteface Mountain						
		1994	1995	1996	1997	1998	1999	Total
May	% cloud frequency* samples** % completeness							
June	% cloud frequency Samples % completeness		14.31 720 100.00	48.96 527 73.00	33.88 546 76.00	40.68 708 98.00	20.11 378 53.00	34.46
July	% cloud frequency samples % completeness	42.09 335 45.00	48.92 738 99.00	48.01 579 78.00	26.32 475 64.00	37.56 639 86.00	33.24 737 99.00	41.93
August	% cloud frequency samples % completeness	57.46 717 96.00	40.80 549 74.00	45.24 714 96.00	42.86 686 92.00	35.67 600 81.00	38.01 734 99.00	43.34
September	% cloud frequency samples % completeness	64.21 693 96.00	41.63 699 97.00	50.43 704 98.00	57.89 596 83.00	45.15 660 92.00	33.09 556 77.00	48.73
October	% cloud frequency samples % completeness	31.51 384 52.00						
November	% cloud frequency samples % completeness							

Whitetop Mountain								
		1994	1995	1996	1997	1998	1999	Total
May	% cloud frequency	14.58	28.05		43.47	29.59	15.45	28.05
	samples	432	656		352	338	479	
	% completeness	58.00	88.00		47.00	45.00	64.00	
June	% cloud frequency	33.76	42.43	50.35	49.13	53.79	36.43	43.11
	samples	631	634	143	692	699	700	
	% completeness	88.00	88.00	20.00	96.00	97.00	97.00	
July	% cloud frequency		20.95	46.49	29.66	30.24	46.06	31.84
	samples		592	684	725	744	469	
	% completeness		80.00	92.00	97.00	100.00	93.00	
August	% cloud frequency	49.89	33.22	45.02	33.17	29.17	14.67	31.05
	samples	461	578	613	627	744	634	
	% completeness	62.00	78.00	82.00	84.00	100.00	85.00	
September	% cloud frequency	51.78	36.76	47.17	26.55	12.93	25.03	33.37
	samples	676	710	653	708	696	719	
	% completeness	94.00	99.00	91.00	98.00	97.00	100.00	
October	% cloud frequency	30.19	30.29	36.20	28.63	26.11		30.28
	samples	742	733	732	716	609		
	% completeness	100.00	99.00	98.00	96.00	82.00		
November	% cloud frequency			23.97	65.41			
	samples			292	266			
	% completeness			41.00	37.00			

Table 3-1. MADPro Cloud Frequency Summary (page 2 of 2)

Clingman's Dome								
		1994	1995	1996	1997	1998	1999	Total
May	% cloud frequency				81.78			
	samples				82			
	% completeness				11.00			
June	% cloud frequency				61.63	48.58	41.38	41.38
	samples				172	422	667	
	% completeness				24.00	59.00	93.00	
July	% cloud frequency		29.47	46.64	34.34	55.42	44.75	44.84
	samples		285	298	661	720	733	
	% completeness		38.00	40.00	89.00	97.00	99.00	
August	% cloud frequency		49.44		41.49	71.43	24.93	38.62
	samples		710		617	7	742	
	% completeness		95.00		93.00	1.00	100.00	
September	% cloud frequency	32.41	30.37		33.18	43.93	27.65	30.42
	samples	395	349		639	387	622	
	% completeness	55.00	48.00		89.00	54.00	86.00	
October	% cloud frequency	40.27		23.64	35.52	30.32		35.37
	samples	663		330	563	696		
	% completeness	89.00		44.00	76.00	94.00		
November	% cloud frequency				59.70			
	samples				67			
	% completeness				9.00			

* Cloud frequency is not used in subsequent analyses if the completeness criteria of greater than 70 percent is not met.

** Number of samples

Source: Harding ESE.

Table 3-2. Summary Statistics for Cloudwater Samples Collected at MADPro Sites from 1994 through 1999 (page 1 of 4)

1994	<u>Whiteface Mountain</u>					<u>Whitetop Mountain</u>					<u>Clingman's Dome</u>				
	n	mean	std dev	min	max	n	mean	std dev	min	max	n	mean	std dev	min	max
LWC	213	0.64	0.34	0.01	1.55	89	0.31	0.16	0.01	0.71	8	0.30	0.20	0.05	0.56
pH	223	3.97	0.69	2.73	5.71	141	3.80	0.45	2.81	5.36	9	4.36	0.71	3.82	6.14
Cond	221	166.35	182.97	4.00	1072.30	141	149.04	129.15	12.80	779.00	9	62.53	37.52	17.10	144.00
H ⁺	223	264.61	317.98	1.95	1862.09	141	244.72	240.07	4.37	1548.82	9	73.93	48.18	0.72	151.36
NH ₄ ⁺	235	210.26	256.10	0.56	1421.67	141	184.63	213.46	5.07	1349.99	9	126.36	125.30	5.93	422.14
SO ₄ ²⁻	235	379.37	471.04	2.29	2624.45	141	316.72	296.22	24.38	1606.25	9	169.28	153.67	55.21	556.25
NO ₃ ⁻	235	133.22	164.74	1.94	1078.95	141	143.66	130.35	11.07	828.58	9	61.21	35.13	20.71	110.00
NO ₂ ⁻	235	0.63	0.70	0.22	4.78	141	0.92	1.23	0.29	7.29	9	0.48	0.23	0.29	0.86
Ca ²⁺	235	24.82	41.21	0.00	227.54	141	20.16	22.10	0.15	124.85	9	29.21	30.89	6.64	100.45
Mg ²⁺	235	6.63	9.62	0.82	58.44	141	8.26	9.92	0.74	80.66	9	16.67	17.58	2.80	51.03
Na ⁺	235	3.29	4.89	0.87	51.76	141	16.46	36.76	0.78	323.01	9	50.54	65.26	1.35	184.99
K ⁺	235	2.37	3.27	0.26	39.13	141	6.15	25.19	0.43	296.68	9	3.79	4.43	0.97	15.35
Cl ⁻	235	10.29	13.07	0.56	94.50	141	27.39	38.37	1.55	301.83	9	43.28	55.41	2.48	172.07
1995	<u>Whiteface Mountain</u>					<u>Whitetop Mountain</u>					<u>Clingman's Dome</u>				
	n	mean	std dev	min	max	n	mean	std dev	min	max	n	mean	std dev	min	max
LWC	502	0.61	0.27	0.05	1.02	519	0.30	0.13	0.00	0.66	123	0.30	0.15	0.00	0.61
pH	523	3.92	0.63	2.57	6.57	550	3.84	0.48	2.59	5.23	136	3.87	0.63	2.67	6.27
Cond	524	137.90	159.24	1.91	1142.00	550	151.22	158.65	3.28	1590.00	136	156.46	159.37	4.50	1060.00
H ⁺	523	276.73	361.90	0.27	2691.53	550	241.28	259.82	5.89	2570.40	136	263.57	285.87	0.54	2137.96
NH ₄ ⁺	517	191.63	223.59	0.71	1314.29	550	200.06	221.74	0.71	1521.43	135	182.08	212.35	3.50	1571.43
SO ₄ ²⁻	519	334.29	429.31	1.81	3416.67	550	325.67	337.52	3.17	2395.83	135	361.34	440.63	4.73	3270.83
NO ₃ ⁻	519	136.08	162.00	0.71	1078.57	550	166.76	194.65	2.14	1992.86	135	132.33	131.15	2.00	850.00
NO ₂ ⁻	519	1.11	1.40	0.21	9.93	550	1.27	1.44	0.29	9.86	135	1.27	2.05	0.29	15.07
Ca ²⁺	516	24.39	41.29	0.25	292.70	548	24.64	33.36	0.18	336.41	133	27.68	53.19	0.36	349.09
Mg ²⁺	516	6.76	10.98	0.25	81.36	548	10.32	13.63	0.25	146.09	133	11.63	11.63	0.40	64.43
Na ⁺	516	5.10	13.58	0.13	235.85	548	20.81	39.29	0.23	278.54	133	28.73	33.58	0.69	264.15
K ⁺	516	2.34	3.17	0.08	18.28	548	7.54	22.16	0.53	375.78	133	2.83	2.77	0.21	17.87
Cl ⁻	519	11.59	16.27	0.08	134.84	550	33.46	46.95	0.79	420.31	135	38.17	35.62	0.56	252.19

Table 3-2. Summary Statistics for Cloudwater Samples Collected at MADPro Sites from 1994 through 1999 (page 2 of 4)

1996	Whiteface Mountain					Whitetop Mountain					Clingman's Dome				
	n	mean	std dev	min	max	n	mean	std dev	min	max	n	mean	std dev	min	max
LWC	549	0.54	0.26	0.01	1.02	191	0.36	0.14	0.06	0.74	29	0.21	0.10	0.06	0.42
pH	569	4.09	0.56	2.81	5.89	181	3.79	0.54	2.82	5.49	103	3.73	0.41	3.06	4.85
Cond	568	104.59	115.26	1.80	927.00	170	169.92	190.64	4.00	935.00	105	221.50	133.12	19.00	621.00
H ⁺	569	154.25	184.44	1.29	1548.82	181	282.79	292.70	3.24	1513.56	103	263.38	197.15	14.13	870.96
NH ₄ ⁺	557	124.34	159.10	0.71	1178.57	194	174.29	182.70	2.79	871.43	105	219.81	166.11	1.93	750.00
SO ₄ ²⁻	557	202.47	273.43	1.35	2479.17	194	342.84	388.19	6.27	2354.17	105	394.30	286.71	13.40	1189.58
NO ₃ ⁻	557	87.68	106.71	1.29	764.29	194	147.29	144.19	3.71	757.14	105	152.78	95.86	8.71	417.86
NO ₂ ⁻	557	0.93	1.16	0.29	12.21	194	1.46	1.83	0.29	10.86	105	1.82	1.67	0.29	9.21
Ca ²⁺	556	14.88	30.02	0.15	349.68	194	19.82	27.05	0.61	174.55	105	40.42	52.56	0.55	257.45
Mg ²⁺	556	3.76	6.00	0.25	47.55	194	7.35	9.20	0.47	52.05	105	12.97	15.30	0.25	85.10
Na ⁺	556	3.07	6.95	0.22	104.34	194	11.46	21.42	0.22	162.33	105	16.71	30.57	0.22	124.55
K ⁺	556	1.60	2.58	0.13	40.52	194	3.56	4.31	0.28	46.93	105	3.13	2.87	0.13	21.17
Cl ⁻	557	7.22	10.49	0.56	77.01	194	23.58	28.52	0.73	201.41	105	27.36	26.53	0.56	120.45
1997	Whiteface Mountain					Whitetop Mountain					Clingman's Dome				
	n	mean	std dev	min	max	n	mean	std dev	min	max	n	mean	std dev	min	max
LWC	335	0.57	0.26	0.09	1.02	464	0.39	0.17	0.06	1.01	283	0.38	0.19	0.01	0.98
pH	393	4.08	0.69	2.87	6.10	501	3.92	0.55	2.80	6.06	318	3.76	0.61	2.80	5.88
Cond	378	138.54	158.84	1.90	978.00	464	153.29	150.10	4.10	880.00	180	187.75	173.04	2.60	1080.00
H ⁺	393	199.73	236.27	0.79	1348.96	501	233.73	260.02	0.87	1584.89	318	323.89	296.52	1.32	1584.89
NH ₄ ⁺	382	184.38	261.86	0.71	1721.43	501	210.09	256.23	0.71	1721.43	318	245.71	246.39	1.07	1650.00
SO ₄ ²⁻	381	304.28	398.22	1.58	2916.67	501	331.41	360.97	1.83	2375.00	318	432.77	409.84	3.67	2791.67
NO ₃ ⁻	381	147.54	216.86	0.64	1900.00	501	157.58	182.21	2.86	1135.71	318	183.38	169.15	2.57	1007.14
NO ₂ ⁻	381	0.95	1.17	0.29	8.00	501	1.33	1.59	0.29	11.00	318	1.40	1.50	0.29	13.86
Ca ²⁺	376	36.44	75.38	0.15	739.77	501	20.77	31.56	0.21	303.49	318	41.65	59.72	0.15	512.48
Mg ²⁺	376	10.33	20.43	0.25	222.77	501	7.82	11.41	0.25	114.40	318	10.68	12.66	0.25	77.37
Na ⁺	376	8.04	22.18	0.28	231.63	501	14.50	35.69	0.22	419.56	318	16.32	27.61	0.22	244.89
K ⁺	376	2.52	3.48	0.13	35.88	501	2.95	5.31	0.13	69.92	318	2.89	3.12	0.13	20.74
Cl ⁻	381	11.28	16.40	0.56	110.01	501	26.29	47.46	0.56	547.25	318	24.41	27.32	0.56	204.51

Table 3-2. Summary Statistics for Cloudwater Samples Collected at MADPro Sites from 1994 through 1999 (page 3 of 4)

1998	Whiteface Mountain					Whitetop Mountain					Clingman's Dome				
	Total Records Accepted = 387					Total Records Accepted = 276					Total Records Accepted = 269				
	n	mean	std dev	min	max	n	mean	std dev	min	max	n	mean	std dev	min	max
LWC	362	0.59	0.26	0.07	1.02	265	0.28	0.17	0.01	0.95	223	0.36	0.17	0.03	0.78
pH	387	4.01	0.71	2.56	5.80	271	3.65	0.48	2.71	5.28	268	3.57	0.39	2.82	5.82
Cond	387	155.30	213.44	3.82	1353.00	271	198.79	164.60	19.00	908.00	268	201.89	139.92	7.10	793.00
H ⁺	387	282.98	406.05	1.58	2754.23	271	365.46	332.57	5.25	1949.84	268	373.82	302.60	1.51	1513.56
NH ₄ ⁺	387	198.50	280.13	1.86	1528.57	276	233.81	237.13	1.07	1457.14	267	279.24	202.93	3.93	1300.00
SO ₄ ²⁻	386	337.97	526.62	2.17	3499.27	276	467.18	418.92	7.83	2124.56	269	443.58	320.10	15.48	2030.83
NO ₃ ⁻	386	133.13	188.88	1.22	1329.48	276	189.74	170.47	4.79	1093.61	269	208.50	138.38	10.08	829.14
NO ₂ ⁻	386	0.68	0.57	0.29	6.07	276	1.30	1.35	0.29	8.00	269	0.83	0.88	0.29	7.43
Ca ²⁺	387	23.35	45.89	0.15	380.85	276	39.10	51.64	0.62	465.09	269	46.95	42.38	1.30	324.50
Mg ²⁺	387	6.89	12.20	0.25	122.52	276	13.62	19.42	0.46	202.28	269	13.27	10.47	0.43	75.42
Na ⁺	387	4.79	11.93	0.22	108.87	276	18.73	32.73	0.22	210.17	269	23.59	24.55	0.44	104.59
K ⁺	387	2.17	2.81	0.13	21.48	276	3.95	4.92	0.13	34.03	269	3.80	3.08	0.13	18.32
Cl ⁻	386	9.46	15.02	0.56	128.63	276	31.63	40.48	0.56	423.15	269	30.40	26.37	1.64	135.40
1999	Whiteface Mountain					Whitetop Mountain					Clingman's Dome				
	Total Records Accepted = 473					Total Records Accepted = 143					Total Records Accepted = 174				
	n	mean	std dev	min	max	n	mean	std dev	min	max	n	mean	std dev	min	max
LWC	395	0.50	0.22	0.05	1.00	141	0.38	0.12	0.09	0.67	171	0.41	0.26	0.02	1.02
pH	473	4.11	0.65	2.57	6.15	143	4.18	0.55	2.74	5.36	173	3.68	0.64	2.68	5.48
Cond	473	107.15	150.36	3.20	1230.00	143	89.79	121.36	0.13	978.00	173	211.12	213.90	3.70	1081.00
H ⁺	473	199.95	310.03	0.71	2691.53	143	138.85	218.52	4.37	1819.70	173	447.69	472.84	3.31	2089.30
NH ₄ ⁺	473	127.53	180.36	1.43	1600.00	143	106.63	119.09	1.43	632.86	174	203.36	219.44	1.43	1528.57
SO ₄ ²⁻	473	233.75	342.00	2.10	3020.35	143	201.17	244.58	4.42	1533.09	174	487.01	545.14	3.54	3686.91
NO ₃ ⁻	473	125.51	250.21	0.57	2251.54	143	96.59	144.52	2.72	1279.45	174	198.20	206.49	1.64	964.95
NO ₂ ⁻	473	1.00	0.77	0.71	7.64	143	1.03	0.59	0.71	4.14	174	0.90	0.56	0.71	5.00
Ca ²⁺	473	32.56	99.09	0.15	1277.44	143	16.02	22.99	0.20	103.79	174	72.89	119.92	0.15	793.41
Mg ²⁺	473	10.93	29.97	0.25	353.89	143	5.41	6.91	0.33	29.87	174	16.64	26.79	0.25	216.45
Na ⁺	473	10.41	28.78	0.22	276.23	143	4.29	9.78	0.22	56.55	174	9.17	15.33	0.22	127.02
K ⁺	473	2.32	3.94	0.13	35.54	143	1.92	2.12	0.13	10.82	174	3.57	5.15	0.13	42.19
Cl ⁻	473	10.48	22.97	0.56	184.78	143	9.88	15.86	0.56	131.18	174	14.34	17.81	0.56	128.36

Table 3-2. Summary Statistics for Cloudwater Samples Collected at MADPro Sites from 1994 through 1999 (page 4 of 4)

Note:

max = maximum
mean = arithmetic average
min = minimum
n = sample size used in calculations
std dev = sample standard deviation

All units are $\mu\text{eq/L}$ except for LWC (g/m^3), pH (unitless), and conductivity ($\mu\text{mhos/cm}$).

The following acceptance criteria were used, based on the cation and anion concentrations:

- (1) If both cation and anion sums were less than $100 \mu\text{eq/L}$, then the RPD (defined below) was ± 100 for a record to be accepted.
- (2) If either of the cation or anion sums were greater than $100 \mu\text{eq/L}$, then the RPD (defined below) was ± 25 for a record to be accepted.

RPD = The difference in cation and anion concentrations divided by the average of the cation and anion concentration multiplied by 100

Source: Harding ESE.

Table 3-3. Number of Records Accepted for Analysis

Site ID	Year	Total Number of Records	Number of Records Accepted	Percent Accepted
Clingman's Dome	1994	14	9	64%
	1995	142	136	96%
	1996	122	105	86%
	1997	334	324	97%
	1998	341	269	79%
	1999	174	174	100%
Whiteface Mountain	1994	279	235	84%
	1995	759	525	69%
	1996	644	597	93%
	1997	469	448	96%
	1998	445	387	87%
	1999	503	478	94%
Whitetop Mountain	1994	162	141	87%
	1995	573	550	96%
	1996	206	194	94%
	1997	552	501	91%
	1998	311	276	89%
	1999	156	143	92%

Source: Harding ESE.

Table 3-4. Mountain Cloud Linear Regression Results

Concentrations	Site ID	Two-sided p-values and directions of trend							
		H ⁺		NH ₄ ⁺		NO ₃ ⁻		SO ₄ ²⁻	
Normalized	CLD303	<i>0.0001</i>	<i>increase</i>	<i>0.0151</i>	<i>increase</i>	<i>0.0001</i>	<i>increase</i>	<i>0.0002</i>	<i>increase</i>
	WFM300	0.0956		<i>0.0002</i>	<i>decrease</i>	0.2159		<i>0.0078</i>	<i>decrease</i>
	WTM302	0.0650		0.6648		0.4650		<i>0.0305</i>	<i>increase</i>
Nonnormalized	CLD303	<i>0.0001</i>	<i>increase</i>	<i>0.0328</i>	<i>increase</i>	<i>0.0001</i>	<i>increase</i>	<i>0.0026</i>	<i>increase</i>
	WFM300	0.1046		<i>0.0015</i>	<i>decrease</i>	0.5332		<i>0.0029</i>	<i>decrease</i>
	WTM302	0.5097		0.3613		0.3594		0.4023	

Note: Bold italicized p-values indicate significant changes over time ($\alpha=0.05$).

No diagnostics were performed to check the adequacy of the linear models.

Source: Harding ESE, 2000

Table 3-5. Summary Statistics of Major Ion Concentrations for June through September 1994 through 1999

		H ⁺	NH ₄ ⁺	SO ₄ ²⁻	NO ₃ ⁻
Clingman's Dome	mean	358.92	237.09	445.52	182.31
	minimum	1.51	1.07	3.54	1.64
	maximum	2137.96	1650.00	3686.91	1007.14
	median	269.15	193.21	337.50	147.96
Whiteface Mountain	mean	224.70	167.69	288.77	125.12
	minimum	0.27	0.56	1.35	0.57
	maximum	2754.23	1721.43	3499.27	2251.54
	median	104.71	77.14	143.33	59.86
Whitetop Mountain	mean	297.63	215.74	391.96	174.70
	minimum	4.37	0.71	1.83	2.50
	maximum	2570.40	1721.43	2395.83	1992.86
	median	199.53	133.57	262.45	124.29

Source: Harding ESE.

Table 4-1. Monthly Deposition Estimates Produced with the CLOUD Model

Site	Year	Month	Deposition (kg/ha)				H ₂ O(cm)
			H ⁺	SO ₄ ²⁻	NO ₃ ⁻	NH ₄ ⁺	
Clingman's Dome	1994	10	0.43	1.30	0.52	0.82	6.43
	1995	8	1.33	3.11	1.12	1.30	9.83
	1996	--	--	--	--	--	--
	1997	7	2.28	4.71	1.55	2.01	5.54
		8	2.35	4.72	1.89	2.36	8.74
		9	1.78	3.70	1.02	1.58	10.43
		10	3.10	6.57	2.76	3.66	7.02
	1998	7	4.52	7.86	3.01	5.92	10.76
		10	2.16	3.93	2.22	2.35	9.10
Whiteface Mountain	1994	8	4.71	12.10	3.38	6.47	22.23
		9	8.56	--	7.84	11.33	50.83
	1995	7	5.51	11.10	4.10	6.36	23.47
		8	5.65	8.11	2.78	4.24	21.07
		9	3.93	5.41	3.12	3.42	19.85
	1996	6	3.34	7.50	2.13	4.63	27.17
		7	2.30	6.14	2.38	3.57	21.80
		8	2.75	6.76	2.36	3.77	17.77
	1997	9	2.21	4.45	2.16	2.48	21.70
		6	2.14	5.46	2.90	3.57	14.34
		8	2.75	5.31	1.72	2.09	17.87
	1998	9	5.76	12.40	4.71	5.86	23.78
		6	2.39	4.11	1.77	2.11	17.44
		7	3.05	5.38	1.75	2.81	17.89
		8	3.22	6.29	2.11	3.71	15.79
		9	5.70	10.02	4.08	5.77	20.90
Whitetop Mountain	1994	6	1.66	3.16	1.10	1.59	5.59
		9	2.25	3.52	1.80	2.86	10.27
		10	0.54	1.26	0.62	0.83	7.09
	1995	6	1.31	2.78	1.04	1.48	7.16
		7	1.01	2.44	1.02	1.27	2.07
		8	2.86	5.73	2.56	2.64	8.10
		9	1.71	3.40	1.55	1.68	5.64
	1996	10	0.68	1.37	0.85	0.79	6.55
		7	2.01	4.37	1.55	1.74	10.28
		8	7.99	15.91	5.17	5.15	10.21
		9	3.60	6.11	2.95	3.97	17.24
		10	2.24	5.18	2.34	3.20	11.65
	1997	6	3.46	7.30	3.11	4.02	13.77
		7	3.90	9.67	2.84	4.35	17.09
		8	2.56	5.46	2.06	2.70	7.79
		9	1.61	3.74	1.30	1.98	6.83
	1998	10	1.37	2.83	1.37	1.64	8.47
		6	5.00	10.56	4.03	4.35	16.43
		7	1.65	3.47	1.07	1.64	3.63
		8	2.07	3.82	1.22	1.79	4.40
		9	1.43	2.44	0.90	1.01	1.68
		10	2.49	0.88	0.37	0.27	5.63

Table 4-2. Seasonal Deposition Estimates Produced with the CLOUD Model*

Site	Year	H ⁺	SO ₄ ²⁻	NO ₃	NH ₄ ⁺
Clingman's Dome	1997	8.55	17.51	5.95	7.93
Whiteface Mountain	1995	20.12	32.83	13.33	18.69
	1996	10.60	24.85	9.03	14.45
	1997	14.20	30.89	12.44	15.36
	1998	14.36	25.80	9.71	14.40
Whitetop Mountain	1995	6.89	14.35	6.17	7.07
	1996	18.13	35.19	12.89	14.48
	1997	11.53	26.17	6.71	13.05
	1998	10.15	20.29	7.22	8.79

Note: All measurements are in kg/ha

- * Three of the four months were required to calculate seasonal deposition. Three-month depositions were multiplied by 4/3 to obtain seasonal depositions. Season is defined from June through September.

Table 4-3. Effect of Data Screening on Sample Retention

SITE-YR	Initial No.	Accept		INC*	ions<200		ions=>200		NO WS	NO LWC	NO DUR	>3hr DUR	Excess	
		No.	%		RD>100%	RD>25%	RD>25%	RD>25%					AN>25%	Excess CAT>25%
WFM-94	279	151	54.1	12	2	40	40	61	12	1	0	0	14	36
WFM-95	759	360	47.4	13	1	222	222	163	0	0	0	0	11	246
WFM-96	644	482	74.8	59	2	40	40	34	18	9	0	0	11	37
WFM-97	469	258	55.0	62	2	29	29	115	3	0	0	0	6	34
WFM-98	452	359	79.4	8	9	47	47	22	7	0	0	0	2	58
WTM-95	573	395	68.9	2	0	20	20	120	1	0	0	35	16	7
WTM-97	552	460	83.3	0	1	46	46	30	14	0	0	1	35	13
CLD-97	334	271	81.1	6	0	10	10	46	0	0	0	1	8	2

Note: INC* = incomplete chemical record; therefore, %RD could not be evaluated.

DUR = duration

AN = anion

CAT = cation

WS = wind speed

WFM = Whiteface Mountain

WTM = Whitetop Mountain




CLD = Clingman's Dome

RD = relative difference

Table 4-4. Combinations of Wind Speed and LWC Evaluated

	WS = 3.618 m/s	WS = 7.028 m/s	WS = 12.278 m/s
LWC = 0.263 g / m ³	✓	✓	✓
LWC = 0.418 g / m ³	✓	✓	✓
LWC = 0.833 g / m ³	✓	✓	✓

Table 4-5. Alternate Forest Canopy Descriptions

Effect of Tree Species 					
Species	observed	canopy	simple model	canopy*	
LAI = 10 m ² /m ² Height = 17 m	Broad Leaf = 16% of LAI Needle Leaf = 84% of LAI		Needle Leaf = 100% of LAI		
Effect of Height 					
Effect of Height	specified*			modeled	
LAI = 10 m ² /m ²	Height = 10 m	Height = 11 m	Height = 12 m	Height = 14 m	Height = 17 m
Effect of Leaf Area 					
Area	low	typical**		high	
Height = 10 m	LAI = 6	LAI = 8	LAI = 10	LAI = 12	

* A pure conifer canopy of 10-m height was specified.

** An observed LAI of 10 m²/m² value at 1,225 m was selected as typical of the forests of interest.

Table 4-6. MCLOUD Seasonal Deposition Estimates

Site	Year	kg/ha		
		SO ₄ ²⁻	NO ₃ ⁻	NH ₄ ⁺
Clingman's Dome	1997	9.4	3.2	4.3
	1999	21.3	7.3	7.9
Whiteface Mountain	1994	27.3	9.5	14.6
	1995	17.8	7.1	8.8
	1996	16.6	6.1	8.6
	1997	28.0	10.4	14.2
	1998	20.4	7.4	10.8
	1999	12.4	4.8	5.7
Whitetop Mountain	1995	13.1	6.1	6.8
	1997	18.7	6.6	8.8
	1999	6.7	2.4	2.7

Table 4-7. Summary of CLOUD Model Sensitivity, Potential Bias, and Expected Differences with MCLoud Modeling Results

Model Parameter	Scenario	Parameter Shift	Range of Response
General Model Sensitivity			
canopy type	pure fir canopy vs. fir+birch canopy		+1.5% to +2.5%
canopy height	10-m canopy height vs. typical observed 17-m height	-41%	-2.5% to -3.5%
leaf area index m^2/m^2	LAI range of 6 to 12 m^2/m^2 @ 10-m height	20%	-2.0% to +4.0%
		-40%	-9.8% to +1.8%
wind speed & LWC	6 $m s^{-1}$ vs. 12 $m s^{-1}$ @LWC = 0.26 $g m^{-3}$ WF drop size distribution	-50%	-48%
	6 $m s^{-1}$ vs. 12 $m s^{-1}$ @LWC = 0.83 $g m^{-3}$ WF drop size distribution	-50%	-34%
	6 $m s^{-1}$ vs. 12 $m s^{-1}$ @LWC = 0.26 $g m^{-3}$ WT drop size distribution	-50%	-49%
	6 $m s^{-1}$ vs. 12 $m s^{-1}$ @LWC = 0.83 $g m^{-3}$ WT drop size distribution	-50%	-39%
	met conditions shift 1150 - 1350-m a.s.l. w/o cloud frequency	-15%	-31%
	met conditions shift 1150 - 1350-m a.s.l. including cloud frequency	-15%	-65%
General Possibilities for Bias			
layer thickness	1-m layers vs. limit of progressively smaller layers		-8%
vertical distribution LAI	shift shape of curve + 1 meter	10%	12%
	shift shape of curve - 1 meter	-10%	-9%
LWC	effect of data screening procedure in some years		+6.6% to -6.6%
wind speed	effect of data screening procedure in some years		-0.7% to -5.1%
SO ₄ ²⁻ concentration	effect of data screening procedure in some years		+9.6% to +21%
met & chemistry	effect of completeness of record	unknown	possibly significant
Differences Between CLOUD and MCLoud Modeling			
vertical distribution LAI	CLOUD vs. MCLoud	unknown	at least $\pm 10\%$
drop size distribution	CLOUD vs. MCLoud for Whiteface Mountain	range of LWC & WS	-24% to +6%
	CLOUD vs. MCLoud for Whiteface Mountain	WFM-97 average	-3%
# drop size classes	CLOUD vs. MCLoud for CLD-97	20 to 500	-10%
wind speed height	CLOUD vs. MCLoud for Whiteface Mountain	3.2 vs. 1	-20%
pressure, temperature	CLOUD vs. MCLoud		$\pm < 1\%$

Table 4-8. Comparison of Deposition Velocities and Water Depositions

Deposition Velocity (cm/sec)			H ₂ O Deposition (cm)	
Month	CLOUD	M CLOUD	CLOUD	M CLOUD
Whiteface Mountain 1997			Whiteface Mountain 1997	
7	31.56	31.19	--*	--*
8	32.72	31.18	22.23	16.15
9	48.53	42.64	50.8	34.41
Clingman's Dome 1997			Clingman's Dome 1997	
7	18.74	15.70	5.54	3.81
8	21.96	16.22	8.74	6.16
9	23.55	16.56	10.43	6.7
10	25.05	19.08	7.02	5.07
Whitetop Mountain 1997			Whitetop Mountain 1997	
5	32.60	22.20	--*	6.25
6	28.10	20.00	13.77	9.96
7	30.80	21.50	17.09	12.1
8	27.20	19.80	7.79	5.46
9	28.10	20.30	6.83	4.88
10	33.20	23.40	8.47	5.99

* Not Available.

Table 4-9. Best Estimates of Seasonal Depositions

Site	Year	H ⁺	SO ₄ ²⁻	NO ₃ ⁻	NH ₄ ⁺
Clingman's Dome	1997	8.55	17.51	5.95	7.93
	1999*	22.04	30.89	10.58	11.45
Whiteface Mountain	1994*	34.94	38.22	13.78	21.17
	1995	20.12	32.83	13.33	18.69
	1996	10.60	24.85	9.03	14.45
	1997	14.20	30.89	12.44	15.36
	1998	14.36	25.80	9.71	14.40
	1999*	14.84	17.98	6.96	8.27
Whitetop Mountain	1995	6.89	14.35	6.17	7.07
	1996	18.13	35.19	12.89	14.48
	1997	11.53	26.17	6.71	13.05
	1998	10.15	20.29	7.22	8.79
	1999*	7.39	9.71	3.48	3.91

Note: All measurements in kg/ha.

- * All 1999 estimates and 1994 estimates for Whiteface Mountain were derived from MCLOUD model results.

The MCLOUD results were multiplied by 1.45 to account for the differences discussed in Section 4.3.

U.S. EPA Headquarters Library
Mail code 3201
1200 Pennsylvania Avenue NW
Washington DC 20460

Table 5-1. Summary of Cloud, Precipitation, Dry, and Total Deposition Estimates for Whiteface Mountain (page 1 of 2)

Total S Deposition (kg/ha/month)

		clddep	drydep				wetdep		Total	
		SO ₄ ²⁻ as S	SO ₂	SO ₂ as S (SO ₂ * 0.5011)	SO ₄ ²⁻	SO ₄ ²⁻ as S (SO ₄ ²⁻ * 0.3338)	Total DRYDEP ¹ (SO ₂ + SO ₄ ²⁻)	SO ₄ ²⁻	SO ₄ ²⁻ as S (SO ₄ ²⁻ * 0.3338)	S
Jun	1994							4.166	1.391	
Jul	1994		0.302	0.151	0.392	0.131	0.282	2.587	0.864	
Aug	1994	12.129						2.155	0.719	
Sep	1994	16.721	0.083	0.042	0.084	0.028	0.070	1.478	0.493	17.285
Jun	1995		0.098	0.049	0.134	0.045	0.094	1.032	0.345	
Jul	1995	11.121	0.090	0.045	0.184	0.062	0.107	2.868	0.957	12.185
Aug	1995	8.126	0.100	0.050	0.118	0.039	0.089	1.098	0.366	8.581
Sep	1995	5.418	0.077	0.039	0.062	0.021	0.059	0.831	0.277	5.755
Jun	1996	7.520	0.050	0.025	0.077	0.026	0.051	1.393	0.465	8.036
Jul	1996	6.155	0.125	0.063	0.140	0.047	0.109	1.238	0.413	6.678
Aug	1996	6.818	0.078	0.039	0.125	0.042	0.081	0.917	0.306	7.205
Sep	1996	4.463						0.912	0.305	
Jun	1997	5.475	0.255	0.128	0.275	0.092	0.220	1.225	0.409	6.103
Jul	1997		0.273	0.137	0.271	0.091	0.227	2.232	0.745	
Aug	1997	5.317	0.172	0.086	0.121	0.040	0.127	2.414	0.806	6.250
Sep	1997	12.430						1.101	0.368	
Jun	1998	4.117						1.877	0.626	
Jul	1998	5.391	0.233	0.117	0.203	0.068	0.185	1.759	0.587	6.163
Aug	1998	6.300	0.083	0.041	0.091	0.031	0.072	3.295	1.100	7.472
Sep	1998	10.048	0.209	0.105	0.132	0.044	0.149	3.819	1.275	11.472

¹Total Sulfur Dry Deposition = ((SO₂ * 0.5011) + (SO₄²⁻ * 0.3338))**Total N Deposition kg/ha/month**

		clddep	drydep				wetdep		Total	
		NO ₃ ⁻ as N	HNO ₃	HNO ₃ as N (HNO ₃ * 0.2223)	NO ₃ ⁻	NO ₃ ⁻ as N (NO ₃ ⁻ * 0.2260)	Total DRYDEP ¹ (HNO ₃ + NO ₃ ⁻)	NO ₃ ⁻	NO ₃ ⁻ as N (NO ₃ ⁻ * 0.2260)	N
Jun	1994							1.996	0.451	
Jul	1994		1.667	0.371	0.003	0.0006	0.371	1.607	0.363	
Aug	1994	3.380						0.975	0.220	
Sep	1994	7.839	0.915	0.203	0.003	0.0007	0.204	0.747	0.169	8.212
Jun	1995		1.569	0.349	0.004	0.0010	0.350	0.825	0.186	
Jul	1995	4.099	1.377	0.306	0.003	0.0007	0.307	1.706	0.386	4.792
Aug	1995	2.783	0.884	0.196	0.003	0.0006	0.197	1.219	0.275	3.255
Sep	1995	3.119	0.803	0.179	0.003	0.0006	0.179	0.683	0.154	3.452
Jun	1996	2.127	0.638	0.142	0.002	0.0003	0.142	1.093	0.247	2.516
Jul	1996	2.385	1.202	0.267	0.003	0.0007	0.268	1.067	0.241	2.894
Aug	1996	2.360	0.560	0.125	0.002	0.0003	0.125	0.631	0.143	2.627
Sep	1996	2.158						0.731	0.165	
Jun	1997	2.903	2.454	0.545	0.006	0.0014	0.547	0.920	0.208	3.658
Jul	1997		2.518	0.560	0.006	0.0013	0.561	1.365	0.309	
Aug	1997	1.722	1.210	0.269	0.003	0.0007	0.270	1.143	0.258	2.250
Sep	1997	4.714						0.639	0.144	
Jun	1998	1.769						1.552	0.351	
Jul	1998	1.755	1.735	0.386	0.003	0.0007	0.386	1.249	0.282	2.423
Aug	1998	2.106	1.004	0.223	0.002	0.0005	0.224	1.728	0.390	2.720
Sep	1998	4.082	1.484	0.330	0.004	0.0009	0.331	1.762	0.398	4.811

¹Total Nitrogen Dry Deposition = ((HNO₃ * 0.2223) + (NO₃⁻ * 0.2260))

Table 5-1. Summary of Cloud, Precipitation, Dry, and Total Deposition Estimates for Whiteface Mountain (page 2 of 2)

H⁺ Deposition (kg/ha/month)

		clddep	drydep			wetdep	Total
		H ⁺	H ⁺ from HNO ₃ (HNO ₃ * 0.0160)	H ⁺ from SO ₂ (SO ₂ * 0.0157)	Total DRYDEP ¹ (HNO ₃ + SO ₂)	H ⁺	H ⁺
Jun	1994					0.078	
Jul	1994		0.0267	0.0047	0.0314	0.060	
Aug	1994	0.474				0.042	
Sep	1994	0.863	0.0146	0.0013	0.0159	0.028	0.907
Jun	1995		0.0251	0.0015	0.0266	0.024	
Jul	1995	0.555	0.0220	0.0014	0.0234	0.063	0.641
Aug	1995	0.570	0.0141	0.0016	0.0157	0.015	0.600
Sep	1995	0.396	0.0129	0.0012	0.0141	0.023	0.433
Jun	1996	0.337	0.0102	0.0008	0.0110	0.034	0.382
Jul	1996	0.232	0.0192	0.0020	0.0212	0.026	0.279
Aug	1996	0.277	0.0090	0.0012	0.0102	0.021	0.309
Sep	1996	0.222				0.022	
Jun	1997	0.216	0.0392	0.0040	0.0433	0.027	0.287
Jul	1997		0.0403	0.0043	0.0446	0.046	
Aug	1997	0.277	0.0194	0.0027	0.0221	0.047	0.346
Sep	1997	0.581				0.023	
Jun	1998	0.241				0.042	
Jul	1998	0.308	0.0278	0.0037	0.0314	0.038	0.377
Aug	1998	0.325	0.0161	0.0013	0.0174	0.060	0.402
Sep	1998	0.575	0.0237	0.0033	0.0270	0.063	0.665

¹ Total H⁺ Dry Deposition = ((HNO₃ * 0.0160) + (SO₂ * 0.0157)) as documented by Miller (1993a)NH₄⁺ as N Deposition (kg/ha/month)

		clddep	drydep		wetdep		Total
		NH ₄ ⁺ as N	NH ₄ ⁺	NH ₄ ⁺ as N (NH ₄ ⁺ * 0.7765)	NH ₄ ⁺	NH ₄ ⁺ as N (NH ₄ ⁺ * 0.7765)	NH ₄ ⁺ as N
Jun	1994		NA		0.570	0.443	
Jul	1994		NA		0.255	0.198	
Aug	1994	6.474	NA		0.308	0.239	
Sep	1994	11.338	NA		0.218	0.169	
Jun	1995		NA		0.158	0.123	
Jul	1995	6.365	NA		0.427	0.331	
Aug	1995	4.241	NA		0.273	0.212	
Sep	1995	3.422	NA		0.099	0.077	
Jun	1996	4.630	NA		0.173	0.134	
Jul	1996	3.570	NA		0.232	0.180	
Aug	1996	3.776	NA		0.146	0.113	
Sep	1996	2.480	NA		0.128	0.100	
Jun	1997	3.563	NA		0.166	0.129	
Jul	1997		NA		0.253	0.197	
Aug	1997	2.092	NA		0.254	0.197	
Sep	1997	5.866	NA		0.123	0.096	
Jun	1998	2.109	NA		0.273	0.212	
Jul	1998	2.816	NA		0.204	0.159	
Aug	1998	3.708	NA		0.481	0.373	
Sep	1998	5.773	NA		0.628	0.488	

Source: Harding ESE.

Table 5-2. Summary of Cloud, Precipitation, Dry, and Total Deposition Estimates for Whitetop Mountain (page 1 of 2)

Total S Deposition (kg/ha/month)

		clddep	drydep				wetdep		Total	
		SO ₄ ²⁻ as S	SO ₂	SO ₂ as S (SO ₂ * 0.5011)	SO ₄ ²⁻	SO ₄ ²⁻ as S (SO ₄ ²⁻ * 0.3338)	Total DRYDEP ¹ (SO ₂ + SO ₄ ²⁻)	SO ₄ ²⁻	SO ₄ ²⁻ as S (SO ₄ ²⁻ * 0.3338)	S
Jun	1994	3.162								
Jul	1994									
Aug	1994									
Sep	1994	3.530								
Jun	1995	2.789								
Jul	1995	2.448						0.682	0.228	
Aug	1995	5.740						0.725	0.242	
Sep	1995	3.411						0.702	0.234	
Jun	1996									
Jul	1996	4.375	0.346	0.173	0.317	0.106	0.279	0.685	0.229	4.883
Aug	1996	15.943	0.212	0.106	0.469	0.157	0.263	0.915	0.305	16.511
Sep	1996	6.125	0.302	0.151	0.215	0.072	0.223	0.581	0.194	6.542
Jun	1997	7.312						1.094	0.365	
Jul	1997	9.695						1.620	0.541	
Aug	1997	5.476	0.4142	0.208	0.4564	0.152	0.360	1.115	0.372	6.208
Sep	1997	3.747	0.6365	0.319	0.3122	0.104	0.423	0.635	0.212	4.382
Jun	1998	10.582						2.370	0.791	
Jul	1998	3.476						0.838	0.280	
Aug	1998	3.825						0.716	0.239	
Sep	1998	2.448	0.587	0.294	0.413	0.138	0.432	0.306	0.102	2.982
Jun	1999		0.261	0.131	0.367	0.123	0.254			
Jul	1999		0.445	0.223	0.427	0.143	0.366			
Aug	1999		0.591	0.296	0.537	0.179	0.475			
Sep	1999		0.568	0.284	0.205	0.069	0.353			

¹Total Sulfur Dry Deposition = ((SO₂ * 0.5011) + (SO₄²⁻ * 0.3338))**Total N Deposition kg/ha/month**

		clddep	drydep				wetdep		Total	
		NO ₃ ⁻ as N	HNO ₃	HNO ₃ as N (HNO ₃ * 0.2223)	NO ₃ ⁻	NO ₃ ⁻ as N NO ₃ ⁻ * 0.2260	Total DRYDEP ¹ (HNO ₃ + NO ₃ ⁻)	NO ₃ ⁻	NO ₃ ⁻ as N (NO ₃ ⁻ * 0.2260)	N
Jun	1994	1.099								
Jul	1994									
Aug	1994									
Sep	1994	1.806								
Jun	1995	1.037								
Jul	1995	1.020						0.387	0.087	
Aug	1995	2.558						0.332	0.075	
Sep	1995	1.550						0.352	0.079	
Jun	1996									
Jul	1996	1.555	3.596	0.799	0.011	0.002	0.802	0.543	0.123	2.479
Aug	1996	5.174	3.483	0.774	0.004	0.001	0.775	0.557	0.126	6.075
Sep	1996	2.948	2.708	0.602	0.006	0.001	0.604	0.255	0.058	3.609
Jun	1997	3.109						0.584	0.132	
Jul	1997	2.844						0.786	0.178	
Aug	1997	2.056	3.600	0.800	0.014	0.003	0.803	0.532	0.120	2.980
Sep	1997	1.306	3.694	0.821	0.012	0.003	0.824	0.363	0.082	2.212
Jun	1998	4.034						1.287	0.291	
Jul	1998	1.070						0.409	0.092	
Aug	1998	1.218						0.334	0.075	
Sep	1998	0.897	3.188	0.709	0.012	0.003	0.711	0.097	0.022	1.631
Jun	1999		2.996	0.666	0.005	0.001	0.667			
Jul	1999		3.926	0.873	0.004	0.001	0.873			
Aug	1999		3.721	0.827	0.004	0.001	0.828			
Sep	1999		2.808	0.624	0.014	0.003	0.627			

¹ Total Nitrogen Dry Deposition = ((HNO₃ * 0.2223) + (NO₃⁻ * 0.2260))

Table 5-2. Summary of Cloud, Precipitation, Dry, and Total Deposition Estimates for Whitetop Mountain (page 2 of 2)

H⁺ Deposition (kg/ha/month)

		clddep	drydep			wetdep	Total
		H ⁺	H ⁺ from HNO ₃ (HNO ₃ * 0.0160)	H ⁺ from SO ₂ (SO ₂ * 0.0157)	Total DRYDEP ¹ (HNO ₃ + SO ₂)	H ⁺	H ⁺
Jun	1994	0.168					
Jul	1994						
Aug	1994						
Sep	1994	0.226					
Jun	1995	0.132					
Jul	1995	0.102				0.014	
Aug	1995	0.288				0.015	
Sep	1995	0.172				0.014	
Jun	1996						
Jul	1996	0.202	0.0575	0.0054	0.0630	0.017	0.282
Aug	1996	0.806	0.0557	0.0033	0.0590	0.021	0.886
Sep	1996	0.363	0.0433	0.0048	0.0481	0.015	0.426
Jun	1997	0.349				0.022	
Jul	1997	0.394				0.032	
Aug	1997	0.258	0.0576	0.0065	0.0641	0.022	0.344
Sep	1997	0.162	0.0591	0.0100	0.0691	0.014	0.245
Jun	1998	0.504				0.046	
Jul	1998	0.167				0.018	
Aug	1998	0.208				0.015	
Sep	1998	0.144	0.0510	0.0092	0.0602	0.005	0.209
Jun	1999		0.0479	0.0041	0.0520		
Jul	1999		0.0628	0.0070	0.0698		
Aug	1999		0.0595	0.0093	0.0688		
Sep	1999		0.0449	0.0089	0.0538		

¹ Total H⁺ Dry Deposition = ((HNO₃ * 0.0160) + (SO₂ * 0.0157)) as documented by Miller (1993a)NH₄⁺ as N Deposition (kg/ha/month)

		clddep	drydep		wetdep		TOTAL
		NH ₄ ⁺ as N	NH ₄ ⁺	NH ₄ ⁺ as N (NH ₄ ⁺ * 0.7765)	NH ₄ ⁺	NH ₄ ⁺ as N (NH ₄ ⁺ * 0.7765)	NH ₄ ⁺ as N
Jun	1994	1.591					
Jul	1994						
Aug	1994						
Sep	1994	2.858					
Jun	1995	1.481					
Jul	1995	1.268			0.126	0.098	
Aug	1995	2.644			0.286	0.222	
Sep	1995	1.684			0.082	0.064	
Jun	1996						
Jul	1996	1.739	0.064	0.050	0.000	0.000	1.789
Aug	1996	5.155	0.077	0.060	0.000	0.000	5.215
Sep	1996	3.976	0.039	0.030	0.039	0.030	4.036
Jun	1997	4.027			0.140	0.109	
Jul	1997	4.354			0.194	0.151	
Aug	1997	2.698	0.092	0.071	0.131	0.102	2.871
Sep	1997	1.983	0.069	0.053	0.084	0.066	2.102
Jun	1998	4.353			0.393	0.305	
Jul	1998	1.641			0.101	0.079	
Aug	1998	1.790			0.099	0.077	
Sep	1998	1.015	0.108	0.084	0.049	0.038	1.136
Jun	1999		0.097	0.075			
Jul	1999		0.075	0.059			
Aug	1999		0.116	0.090			
Sep	1999		0.057	0.044			

Source: Harding ESE.

Table 5-3. Summary of Cloud, Precipitation, Dry, and Total Deposition Estimates for Clingman's Dome (page 1 of 2)**Total S Deposition (kg/ha/month)**

		clddep	drydep				wetdep		Total
		SO ₄ ²⁻ as S	SO ₂	SO ₂ as S (SO ₂ * 0.5011)	SO ₄ ²⁻	SO ₄ ²⁻ as S (SO ₄ ²⁻ * 0.3338)	Total DRYDEP ¹ (SO ₂ + SO ₄ ²⁻)	SO ₄ ²⁻ as S (SO ₄ ²⁻ * 0.3338)	S
Jun 1994							3.994	1.333	
Jul 1994							2.388	0.797	
Aug 1994							3.659	1.221	
Sep 1994							1.127	0.376	
Jun 1995							4.600	1.536	
Jul 1995							2.528	0.844	
Aug 1995	3.117						2.855	0.953	
Sep 1995							1.767	0.590	
Jun 1996							2.149	0.717	
Jul 1996							1.763	0.588	
Aug 1996							4.988	1.665	
Sep 1996							2.756	0.920	
Jun 1997							2.365	0.789	
Jul 1997	4.717						4.041	1.349	
Aug 1997	4.725						3.169	1.058	
Sep 1997	3.705						1.024	0.342	
Jun 1998							1.074	0.358	
Jul 1998	7.877	0.248	0.124	0.277	0.092	0.217	2.555	0.853	8.946
Aug 1998		0.306	0.153	0.426	0.142	0.296	4.298	1.435	
Sep 1998							0.839	0.280	
Jun 1999							1.899	0.634	
Jul 1999		0.155	0.078	0.301	0.101	0.178	1.183	0.395	
Aug 1999		0.302	0.151	0.421	0.140	0.292			
Sep 1999		0.422	0.211	0.278	0.093	0.304			

¹ Total Sulfur Dry Deposition = ((SO₂ * 0.5011) + (SO₄²⁻ * 0.3338))² wetdep data taken from the NADP/NTN site at Mt. Mitchell, NC**Total N Deposition kg/ha/month**

		clddep	drydep				wetdep		Total
		NO ₃ ⁻ as N	HNO ₃	HNO ₃ as N (HNO ₃ * 0.2223)	NO ₃ ⁻	NO ₃ ⁻ as N (NO ₃ ⁻ * 0.2260)	Total DRYDEP ¹ (HNO ₃ + NO ₃ ⁻)	NO ₃ ⁻ as N (NO ₃ ⁻ * 0.2260)	N
Jun 1994							1.905	0.431	
Jul 1994							1.321	0.298	
Aug 1994							1.531	0.346	
Sep 1994							0.609	0.138	
Jun 1995							2.731	0.617	
Jul 1995							1.368	0.309	
Aug 1995	1.118						1.620	0.366	
Sep 1995							0.851	0.192	
Jun 1996							1.374	0.310	
Jul 1996							0.927	0.209	
Aug 1996							2.122	0.480	
Sep 1996							1.590	0.359	
Jun 1997							1.495	0.338	
Jul 1997	1.555						1.882	0.425	
Aug 1997	1.889						1.201	0.271	
Sep 1997	1.022						0.621	0.140	
Jun 1998							0.874	0.197	
Jul 1998	3.007	2.555	0.568	0.007	0.002	0.570	1.193	0.270	3.846
Aug 1998		2.324	0.517	0.007	0.002	0.518	1.715	0.387	
Sep 1998							0.346	0.078	
Jun 1999							1.091	0.246	
Jul 1999		2.367	0.526	0.002	0.001	0.527	0.552	0.125	
Aug 1999		2.930	0.651	0.003	0.001	0.652			
Sep 1999		2.898	0.644	0.010	0.002	0.646			

¹ Total Nitrogen Dry Deposition = ((HNO₃ * 0.2223) + (NO₃⁻ * 0.2260))² wetdep data taken from the NADP/NTN site at Mt. Mitchell, NC

Table 5-3. Summary of Cloud, Precipitation, Dry, and Total Deposition Estimates for Clingman's Dome (page 2 of 2)

H⁺ Deposition (kg/ha/month)

		clddep	drydep			wetdep	Total
		H ⁺	H ⁺ from HNO ₃ (HNO ₃ * 0.0160)	H ⁺ from SO ₂ (SO ₂ * 0.0157)	Total DRYDEP ¹ (HNO ₃ + SO ₂)	H ⁺	H ⁺
Jun	1994					0.082	
Jul	1994					0.055	
Aug	1994					0.076	
Sep	1994					0.027	
Jun	1995					0.106	
Jul	1995					0.052	
Aug	1995	0.135				0.070	
Sep	1995					0.039	
Jun	1996					0.049	
Jul	1996					0.038	
Aug	1996					0.110	
Sep	1996					0.063	
Jun	1997					0.054	
Jul	1997	0.230				0.078	
Aug	1997	0.237				0.055	
Sep	1997	0.179				0.025	
Jun	1998					0.018	
Jul	1998	0.456	0.0409	0.0039	0.0448	0.055	0.555
Aug	1998		0.0372	0.0048	0.0420	0.083	
Sep	1998					0.014	
Jun	1999					0.038	
Jul	1999		0.0379	0.0024	0.0403	0.025	
Aug	1999		0.0469	0.0047	0.0516		
Sep	1999		0.0464	0.0066	0.0530		

¹ Total H⁺ Dry Deposition = ((HNO₃ * 0.0160) + (SO₂ * 0.0157)) as documented by Miller (1993a)² wetdep data taken from the NADP/NTN site at Mt. Mitchell, NC**NH₄⁺ as N Deposition (kg/ha/month)**

		clddep	drydep		wetdep		Total
		NH ₄ ⁺ as N	NH ₄ ⁺	NH ₄ ⁺ as N (NH ₄ ⁺ * 0.7765)	NH ₄ ⁺	NH ₄ ⁺ as N (NH ₄ ⁺ * 0.7765)	NH ₄ ⁺ as N
Jun	1994				0.451	0.350	
Jul	1994				0.181	0.140	
Aug	1994				0.299	0.232	
Sep	1994				0.130	0.101	
Jun	1995				0.647	0.502	
Jul	1995				0.332	0.257	
Aug	1995	1.301			0.270	0.210	
Sep	1995				0.208	0.161	
Jun	1996				0.313	0.243	
Jul	1996				0.226	0.175	
Aug	1996				0.496	0.385	
Sep	1996				0.339	0.263	
Jun	1997				0.261	0.203	
Jul	1997	2.014			0.471	0.365	
Aug	1997	2.361			0.450	0.349	
Sep	1997	1.584			0.084	0.065	
Jun	1998				0.164	0.127	
Jul	1998	5.920	0.0603	0.047	0.308	0.239	6.206
Aug	1998		0.0839	0.065	0.503	0.391	
Sep	1998				0.125	0.097	
Jun	1999				0.218	0.169	
Jul	1999		0.0512	0.040	0.114	0.088	
Aug	1999		0.0875	0.068			
Sep	1999		0.0751	0.058			

¹ wetdep data taken from the NADP/NTN site at Mt. Mitchell, NC

Source: Harding ESE.

Table 5-4. Percent Composition of Total Deposition at the Three MADPro Sites

		Sulfur	Nitrogen	NH ₄ ⁺	H ⁺
Whiteface Mountain	Cloud Deposition	90.95	83.67	NA	87.61
	Wet Deposition	7.58	8.17	NA	7.90
	Dry Deposition	1.47	8.15	NA	4.49
Whitetop Mountain	Cloud Deposition	89.27	68.77	95.37	80.87
	Wet Deposition	3.96	2.96	1.80	3.94
	Dry Deposition	6.78	28.27	2.84	15.19
Clingman's Dome	Cloud Deposition	81.14	66.13	90.42	70.91
	Wet Deposition	14.54	11.43	7.97	13.29
	Dry Deposition	4.32	22.44	1.91	15.97

Note: Sulfur deposition includes SO₂ and/or SO₄²⁻.

Nitrogen deposition includes HNO₃ and/or NO₃⁻.

NH₄⁺ deposition is presented in terms of nitrogen (N).

Source: Harding ESE.

Table 5-5. Dry, Wet, and Total Seasonal Depositions (June through September) for Whiteface Mountain and Two Nearby CASTNet Sites for 1995 through 1998

		Sulfur			Nitrogen			H ⁺		
		WFM300	WST109	CTH110	WFM300	WST109	CTH110	WFM300	WST109	CTH110
Dry	1995	0.349	0.136	1.202	1.033	0.155	1.235	0.080	0.013	0.116
	1996	0.321	0.116	1.074	0.713	0.121	0.971	0.057	0.011	0.095
	1997	0.765	0.162	1.402	1.837	0.143	1.086	0.147	0.013	0.113
	1998	0.541	0.119	1.608	1.255	0.091	0.930	0.101	0.009	0.108
Wet	1995	1.945	2.762	3.325	1.001	1.250	1.594	0.125	0.196	0.203
	1996	1.489	2.822	3.765	0.796	1.234	1.615	0.103	0.188	0.231
	1997	2.328	2.996	2.857	0.919	1.335	1.249	0.143	0.196	0.154
	1998	3.588	2.944	3.398	1.421	1.297	1.490	0.203	0.189	0.200
Total	1995	35.180	2.898	4.527	15.360	1.405	2.828	2.230	0.942	1.490
	1996	26.770	2.938	2.840	10.540	1.355	2.586	1.230	0.840	1.484
	1997	34.060	3.158	4.259	15.210	1.478	2.335	1.720	0.903	1.229
	1998	29.990	3.063	5.006	12.390	1.387	2.420	1.750	0.932	1.301

Notes: WST109 is Woodstock, NH.
 CTH110 is Connecticut Hill, NY.
 All measurements are in kg/ha.

Source: Harding ESE, 1999.

Table 5-6. Dry, Wet, and Total Seasonal Depositions (June through September)
for Whitetop Mountain and Two Nearby CASTNet Sites for 1996

	WTM302	PNF126	VPI120
Dry Sulfur	1.020	0.980	1.319
Dry Nitrogen	2.908	0.942	1.312
Dry NH ₄ ⁺	0.187	0.201	0.196
Dry H ⁺	0.227	0.085	0.122
Wet Sulfur	0.971	1.772	3.475
Wet Nitrogen	0.409	0.655	1.218
Wet NH ₄ ⁺	0.040	0.567	0.799
Wet H ⁺	0.071	0.124	0.204
Total Sulfur	37.250	2.752	4.794
Total Nitrogen	16.220	1.597	2.530
Total NH ₄ ⁺	14.720	0.768	0.995
Total H ⁺	2.130	0.209	0.326

Note: PNF126 is Pisgah National Forest, NC
VPI120 is Horton Station, VA
All measurements are in kg/ha.

Source: Harding ESE.

Table 6-1. Warm Season Average Ion Concentrations for the Six MCCP Sites 1986 through 1988

Site	n	pH	NO ₃ ⁻	Cl ⁻	NH ₄ ⁺	SO ₄ ²⁻	H ⁺
Mt. Mitchell, NC	624	3.4	174	31	184	489	398
Whitetop, VA	656	3.76	144	16	152	321	174
Whiteface 1, NY*	987	3.77	73	5	97	205	171
Whiteface 2, NY**	120	3.59	92	7	157	352	255
Shenandoah, VA	230	3.77	94	13	93	176	171
Moosilauke, NH	328	3.58	132	16	107	257	263

All measurements are in µeq/L

* 1,485-m elevation.

** 1,250-m elevation.

Table 6-2. Comparison (RPD) of MCCP versus MADPro Average Ion Concentrations

Site	SO ₄ ²⁻	NO ₃ ⁻	NH ₄ ⁺	H ⁺
Whiteface Mountain	33.94	28.31	26.71	27.14
Whitetop Mountain	19.99	19.27	34.67	52.43
Clingman's Dome	- 9.31	4.66	25.22	-10.37

Note: RPD = relative percent difference based on MADPro concentrations

Table 6-3. Mean Chemical Composition Including Minima and Maxima of Cloudwater Collected at Mt. Brocken, Germany**

Year	n*	SO ₄ ²⁻	NO ₃ ⁻	Cl ⁻	TIC	NH ₄ ⁺	Na ⁺	Ca ²⁺	Mg ²⁺	H ⁺	TIC+	SO ₄ ²⁻ / NO ₃ ⁻
1992	37	331	387	127	845	391	156	147	40	39	773	0.86
	Min	41	21	6		9	< 1	10	1	< 0.1		
	Max	1194	1071	579		1007	854	1311	212	339		
1993	1054	265	280	68	613	410	60	54	26	83	633	0.95
	Min	4	0.5	0.3		2	2	3	5	< 0.1		
	Max	4169	5946	2401		8083	2444	2245	693	1500		
1994	847	342	408	126	876	545	124	141	40	146	996	0.84
	Min	1	0.5	0.3		2	2	3	5	< 0.1		
	Max	3922	3803	2065		6815	2765	4859	679	2884		

Note: TIC = total ionic concentration of anions.

TIC+ = total ionic concentration of cations.

All measurements are in µeq/L

* Number of events (sampling time resolution in 1992) and number of 1-hour samples (1993, 1994).

** Quality assurance program and instrumentation patterned after MCCP.

Table 6-4. Statistical Characterization of the Chemical Composition of Fog Samples from European Investigations

Location and Investigator	Cond.	pH	H ⁺	Na ⁺	K ⁺	NH ₄ ⁺	Mg ²⁺	Ca ²⁺	Cl ⁻	NO ₃ ⁻	SO ₄ ²⁻
Units	$\mu\text{S cm}^{-1}$			$\mu\text{eq L}^{-1}$							
Waldstein arithmetic mean (Wrzesinski & Klemm 2000)	151	4.3	89	65	11.5	669	19.5	69	54	481	497
median	142	4.3	52	30	9.7	547	10	40	31	409	421
mean derived from the logarithm	121	4.3	51	39	13.8	547	14.8	46	46	342	376
minimum	17	3.3	2	< 9	< 6.7	< 21	< 4.6	< 11	< 13	20	55
maximum	452	5.7	513	664	68.5	2580	152	493	389	1740	1800
standard deviation	95	0.5	91	124	10.5	498	29.6	84	74	370	360
Easterly mean derived from the logarithm	189	4.0(c)	101	(a)	(a)	788	14	74	(a)	596	690(c)
Westerly mean derived from the logarithm	100	4.4(c)	41	(a)	(a)	463	15.7	40	(a)	268	395(c)
Confidence level	>99%	>99%	>99%	(a)	(a)	>99%	(b)	>99.9%	(a)	>99%	>99%
Wulfersreuth ² arithmetic mean (Trautner 1988)	526	3.1	n.d.	92	80.2	1370	73.9	375	138	708	1440
minimum	58	2.4	n.d.	12	9	87	15.7	51	43	127	352
maximum	2500	4.9	n.d.	774	246	5420	584	3350	660	5600	9040
Ochsenkopf ³ arithmetic mean (Henerich 1987)	255	3.5	314	66	28	922	22	110	96	599	669
minimum	49	2.9	45	5	4	125	3	9	8	83	83
maximum	900	4.3	1190	213	80	2820	76	376	374	2610	2380
Ochsenkopf ¹ minimum (Verhoeven et al. 1987)	175	3.7	224	86	37	395	57	151	76	376	415
Landeshugel ⁴ minimum (Schrimpf et al. 1984)	69	2.5	n.d.	60	n.d.	n.d.	n.d.	50	60	80	310
maximum	1230	4.2	n.d.	970	n.d.	n.d.	n.d.	2530	1510	3000	2890
Rigi Staffel (Collett et al., 1993)											
Number of samples	n.d.	38	n.d.	40	40	40	40	40	40	40	40
arithmetic mean	n.d.	4.63	n.d.	34	8	660	12	46	53	490	300
standard deviation	n.d.	1.05	n.d.	75	7	930	19	78	99	800	390
volume weighted average	n.d.	5.05	n.d.	23	6	460	8	32	35	310	213
minimum	n.d.	6.88	n.d.	0	0	46	1	2	1	14	24
maximum	n.d.	2.95	n.d.	400	26	4600	88	330	540	3700	1800
Seeboden											
Number of samples	n.d.	20	n.d.	23	22	23	23	23	23	23	23
arithmetic mean	n.d.	5.28	n.d.	20	15	920	21	88	77	440	380
standard deviation	n.d.	0.96	n.d.	29	18	1680	64	240	120	880	630
volume weighted average	n.d.	5.22	n.d.	18	16	1100	24	98	88	520	430
minimum	n.d.	6.76	n.d.	0	0	150	0	6	2	19	37
maximum	n.d.	3.78	n.d.	120	76	6600	310	1100	440	3700	2500

¹50°03'54"N, 11°45'54"E, 650-680 m a.s.l.²50°01'07"N, 11°48'23"E, 1024 m a.s.l.³50°22.5'N, 11°38.5'E, 600-640 m a.s.l.

(a) Data are not normally or lognormally distributed. No calculations were performed.

(b) no significant difference.

(c) arithmetic mean

Notes:

< = below the given determination limit

* = standard deviation, confidence level for Student's t-test for different means

n.d. = no data

Table 6-5. Comparison of MADPro Cloudwater Deposition Estimates to Previous Studies

Site	Ref.	Water	H ⁺	NH ₄ ⁺	SO ₄ ²⁻	NO ₃ ⁻
Moosilauke	1	1.7	0.06	0.44	2.7	2
Whiteface	1	2.3	0.03	0.39	2.2	0.8
Mt. Mitchell	1	4.9	0.19	1.1	8.4	4
Whitetop (B)	1	11.5	0.37	3.3	20.1	9.9
Moosilauke (L) *	2	7	0.2	1.4	11.5	8.5
Whiteface (M) *	3	12.8	0.15	1.6	7.8	4.8
CLD	4	8.1	0.23	3	14.3	7.7
WFML	4	19.1	0.35	4.9	20.7	11.9
WTM	4	8.3	0.22	2.8	13.2	7.5

* Moosilauke (L) and Whiteface (M) are annual averages; MCCP data and this study are warm-season only.

Note: Water deposition rates are in cm/month, ion deposition rates are in kg/ha/month.
Results from MADPro are in bold.

References: 1 = Mohnen *et al.* (1990) (MCCP project report).

2 = Lovett *et al.* (1982).

3 = Miller *et al.* (1993).

4 = this study.

Table 6-6. A Summary of Cloudwater Chemical Deposition via Droplet Interception for the Eastern United States

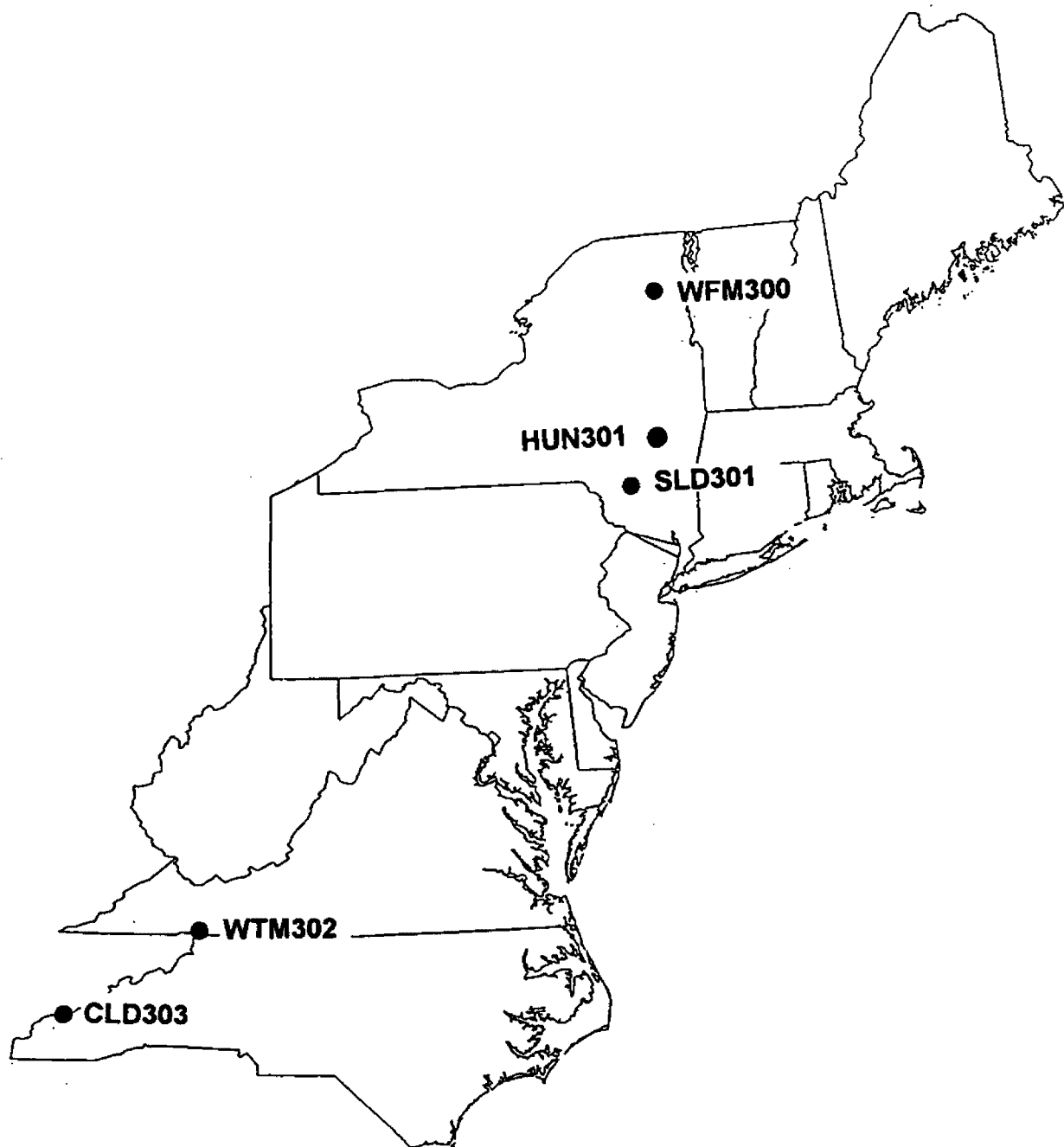
Author (Reference)	Site	Elevation (meters)	Year	Cloud droplet deposition (kg ha ⁻¹ month ⁻¹)				H ₂ O (cm yr ⁻¹)	Frequency of cloud (%)
				H ⁺	NH ₄ ⁺	NO ₃ ⁻	SO ₄ ²⁻		
Lovett <i>et al.</i> (1982, 1983)	Moosilauke, NH	1220	1980-81	0.2	1.4	8.5	11.5	68	40
Mueller & Weatherford (1988)	Whitetop, VA	1686	1986	-	-	4.1	7.2	-	-
Lindberg <i>et al.</i> (1988)	Great Smokey Mt., NC	1740	1986	0.14	1	2.2	7.2	-	25
Sigmon <i>et al.</i> (1989)	Shenandoah, VA	1014	1987	0.02	0.2	0.7	0.9	13	7
Saxena <i>et al.</i> (1989)	Mitchell, NC	2000	1986	0.17	1.2	3.2	9.8	35-77	25.52
Stogner & Saxena (1988)	Mitchell, NC	2000	1986	0.12	0.8	3.2	7.3	-	-
Dasch (1989)	Mitchell, NC	1987	1986	0.03	0.3	0.9	2.2	18	62
Mohnen (1988)	Moosilauke, NH	1000	1987	0.04	0.24	0.8	1.7	18	23
Mohnen <i>et al.</i> (1990)	Moosilauke, NH	1000	1987-88	0.06	0.44	2	2.7	20	19
Mohnen (1988)	Whiteface, NY	1483	1987	0.18	2.3	4.8	11.2	127	42
Mohnen (1988)	Whiteface, NY	1200	1987	0.05	0.8	3	7	-	27
Mohnen <i>et al.</i> (1990)	Whiteface, NY	1250	1986-88	0.03	0.39	0.8	2.2	28	24
Lindberg & Johnson (1988)	Whiteface, NY	1000	1986-88	0.04	0.5	1	2	13	-
Mohnen (1988)	Whitetop, VA	1686	1987	0.22	2.6	7.7	13.8	-	31
Mohnen (1988)	Whitetop, VA	1686	1987	0.2	11.8	10.4	13.1	-	31
Mohnen <i>et al.</i> (1990)	Whitetop, VA	1686	1986-88	0.22	2	6.1	12.1	90	30
Mohnen (1988)	Mitchell, NC	2000	1987	0.09	0.1	2.6	5.6	-	27
Mohnen (1988)	Mitchell, NC	2000	1987	0.13	1.1	2.2	8.9	-	27
Mohnen <i>et al.</i> (1990)	Mitchell, NC	2000	1986-88	0.19	1.1	4	8.4	59	29
Mohnen (1988)	Shenandoah, VA	1014	1987	0.04	0.3	1.3	1.3	-	7
Lindberg & Johnson (1988)	Great Smokey Mt., NC	1740	1986-88	0.05	0.5	1	4	37	-

Source: Vong *et al.*, 1991.

Table 6-7. Comparison of the Proportion of Total Ion Deposition Delivered by the Dry, Cloudwater, and Precipitation Deposition Estimates for Whiteface Mountain at an Elevation of 1,050 m

Ion	Percent of total deposition		
	Precipitation	Cloudwater	Dry deposition
SO ₄ ²⁻	45	46	9
NO ₃ ⁻	38	42	20
NH ₄ ⁺	41	58	1
H ⁺	46	36	17

Figures



WFM300	Whiteface Mountain
SLD301	Slide Mountain
HUN301	Hunter Mountain
WTM302	Whitetop Mountain
CLD303	Clingman's Dome

Figure 2-1. Locations of Mountain Acid Deposition Sites

Source: Harding ESE.

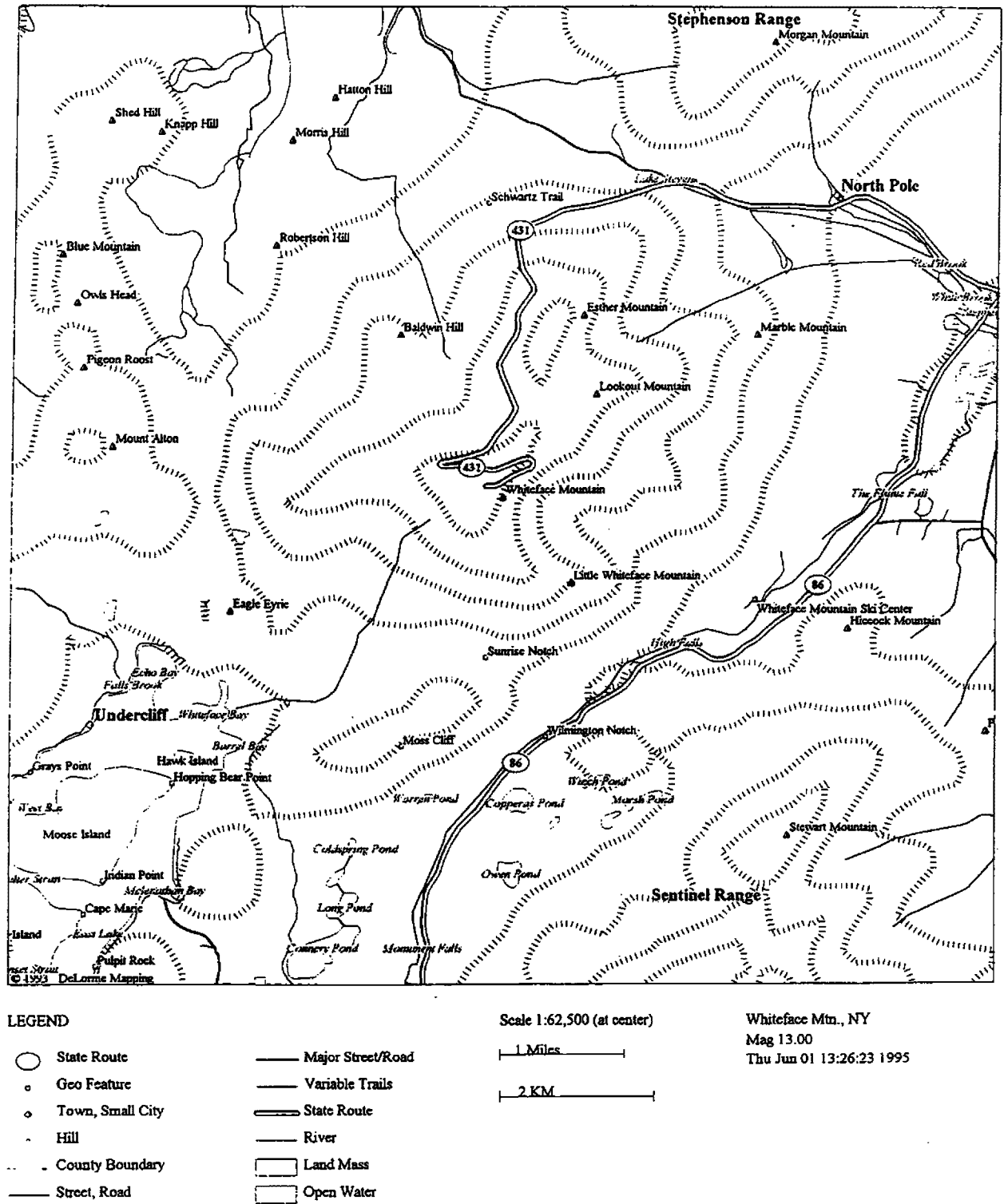
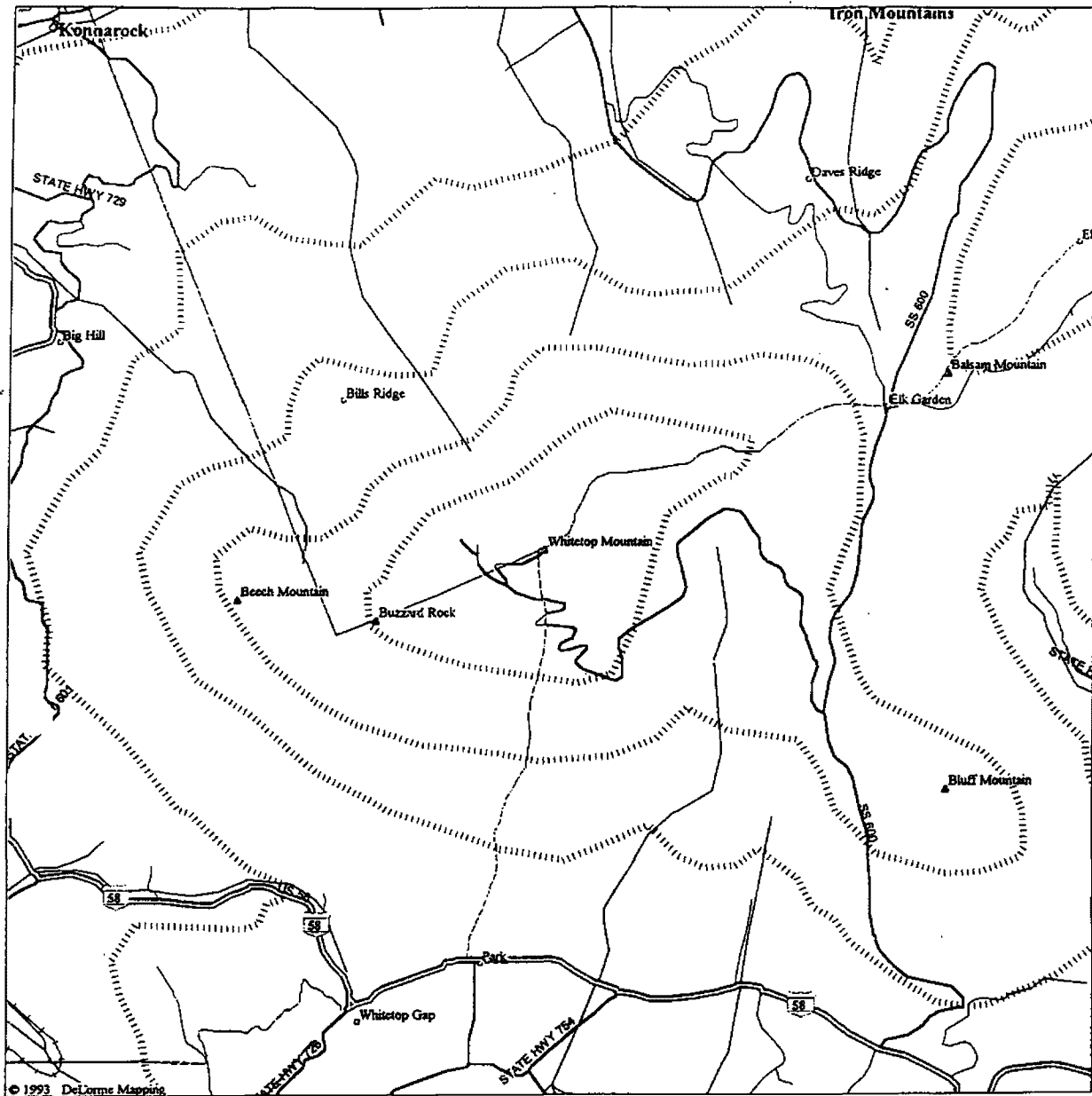


Figure 2-2. Regional Map for Whiteface Mountain, NY

Source: Harding ESE.



LEGEND

- | | |
|-----------------------|----------------------|
| ○ Geo Feature | — Major Street/Road |
| ● Town, Small City | — US Highway |
| ▲ Hill | — Railroad |
| — US Highway | — River |
| - - - County Boundary | — Intermittent River |
| — Street, Road | ... Contours |

Scale 1:31,250 (at center)

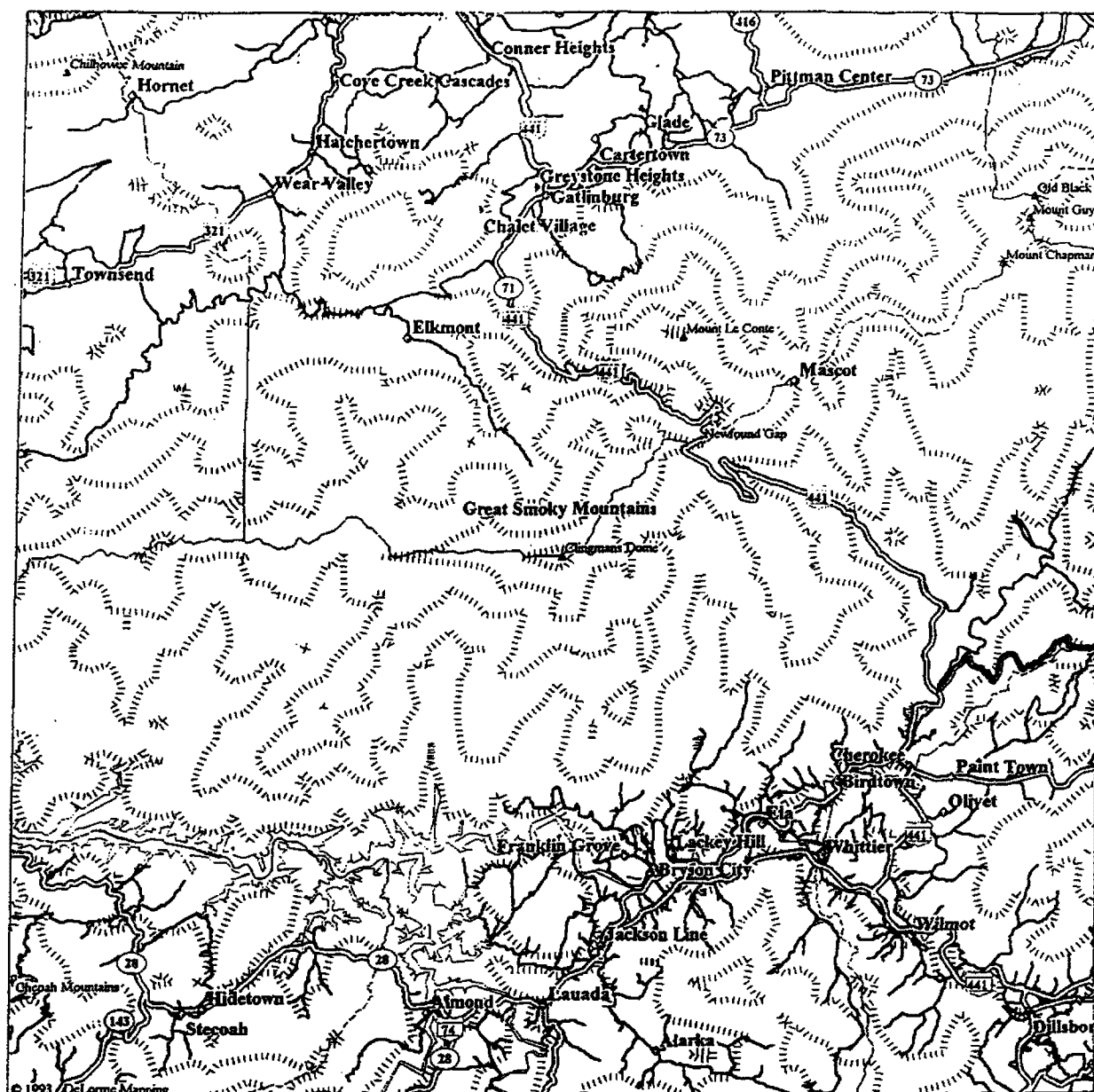
2000 Feet

1000 Meters

Whitetop Mtn, VA
Mag 14.00
Thu Jun 01 13:52:11 1995

Figure 2-3. Regional Map for Whitetop Mountain, VA

Source: Harding ESE.



LEGEND

○ State Route	Population Center	Land Mass
◦ Geo Feature	Major Street/Road	Open Water
◊ Town, Small City	Interstate Highway	Contours
- Hill	State Route	
US Highway	US Highway	
County Boundary	Airfield	

Clingman's Dome, TN
 Mag 11.00
 Thu Jun 01 13:13:02 1995

Scale 1:250,000 (at center)

5 Miles

5 KM

Figure 2-4. Regional Map for Clingman's Dome, TN

Source: Harding ESE.

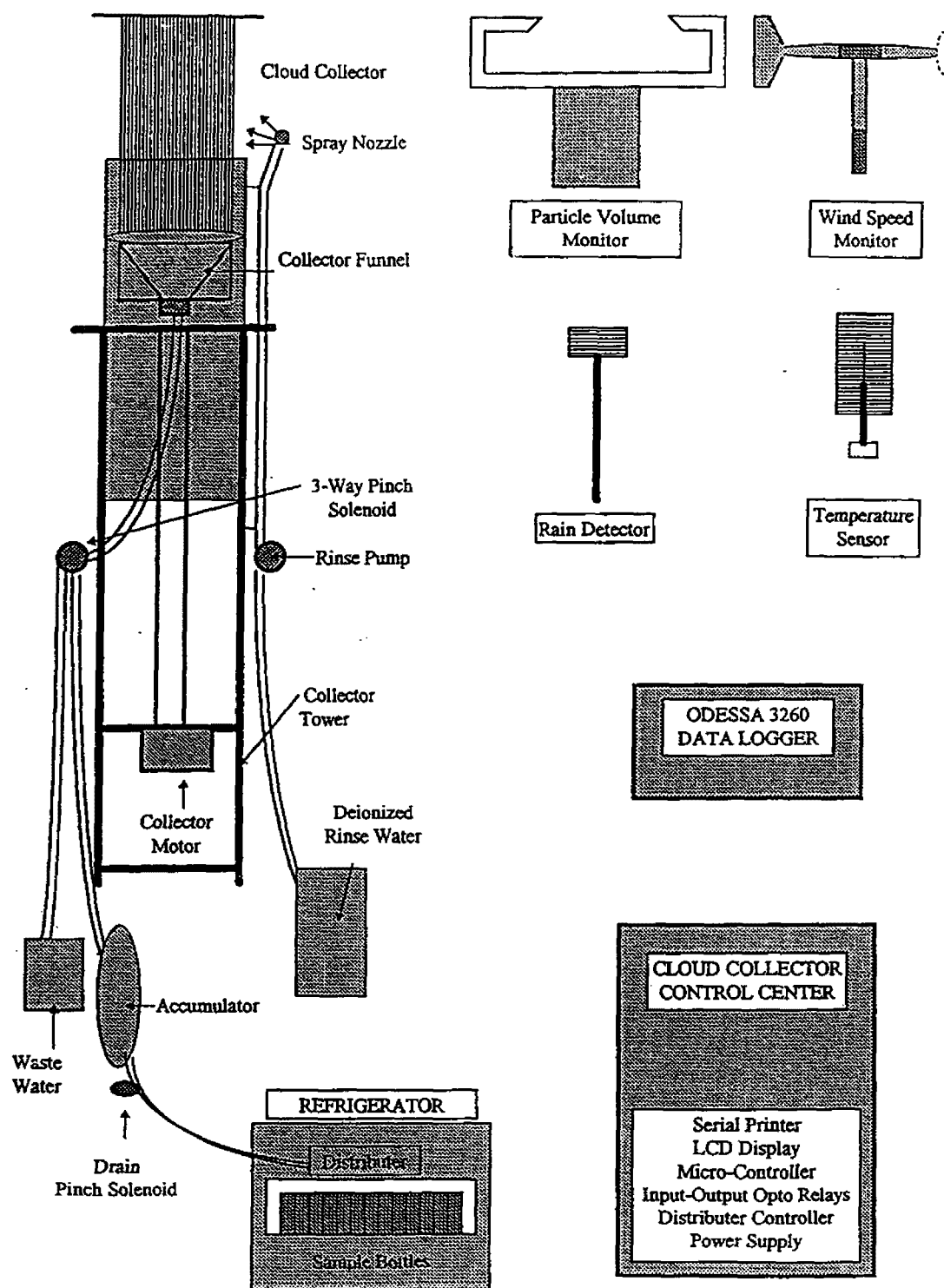
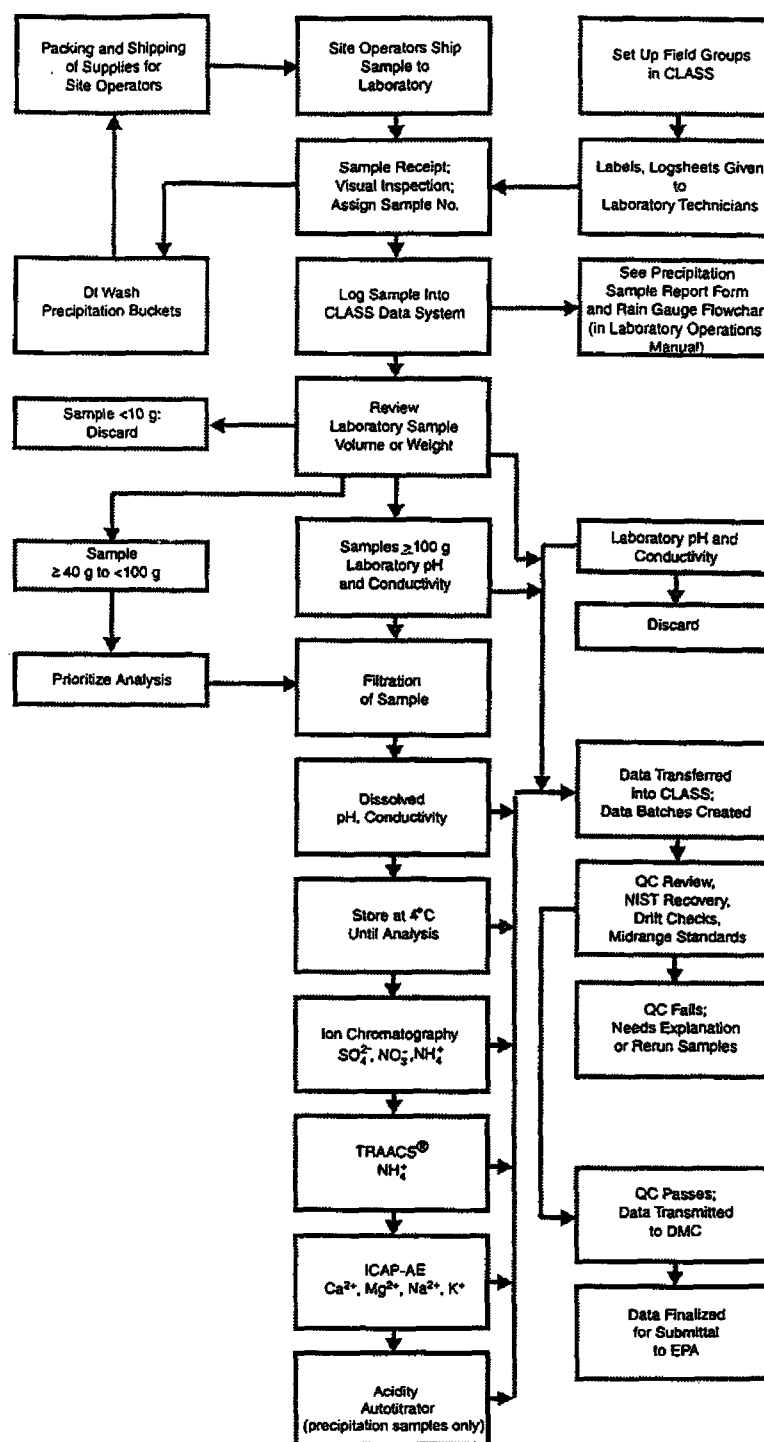


Figure 2-5. MADPro Sampling System
Source: Harding ESE.



vol3/castnet_prop98/fig27.A1

Figure 2-6. Flowchart of Laboratory Operations for Cloudwater and Precipitation Sample Analyses
Source: Harding ESE.

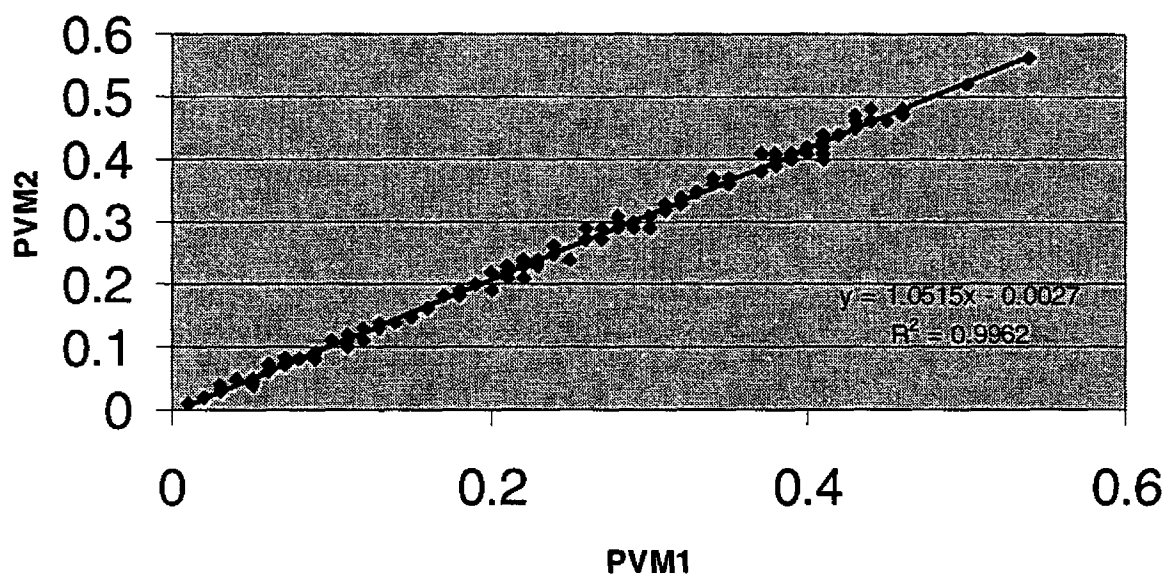


Figure 2-7. PVM-100 Intercomparison at Whitetop Mountain, VA, 1998
Source: Harding ESE.

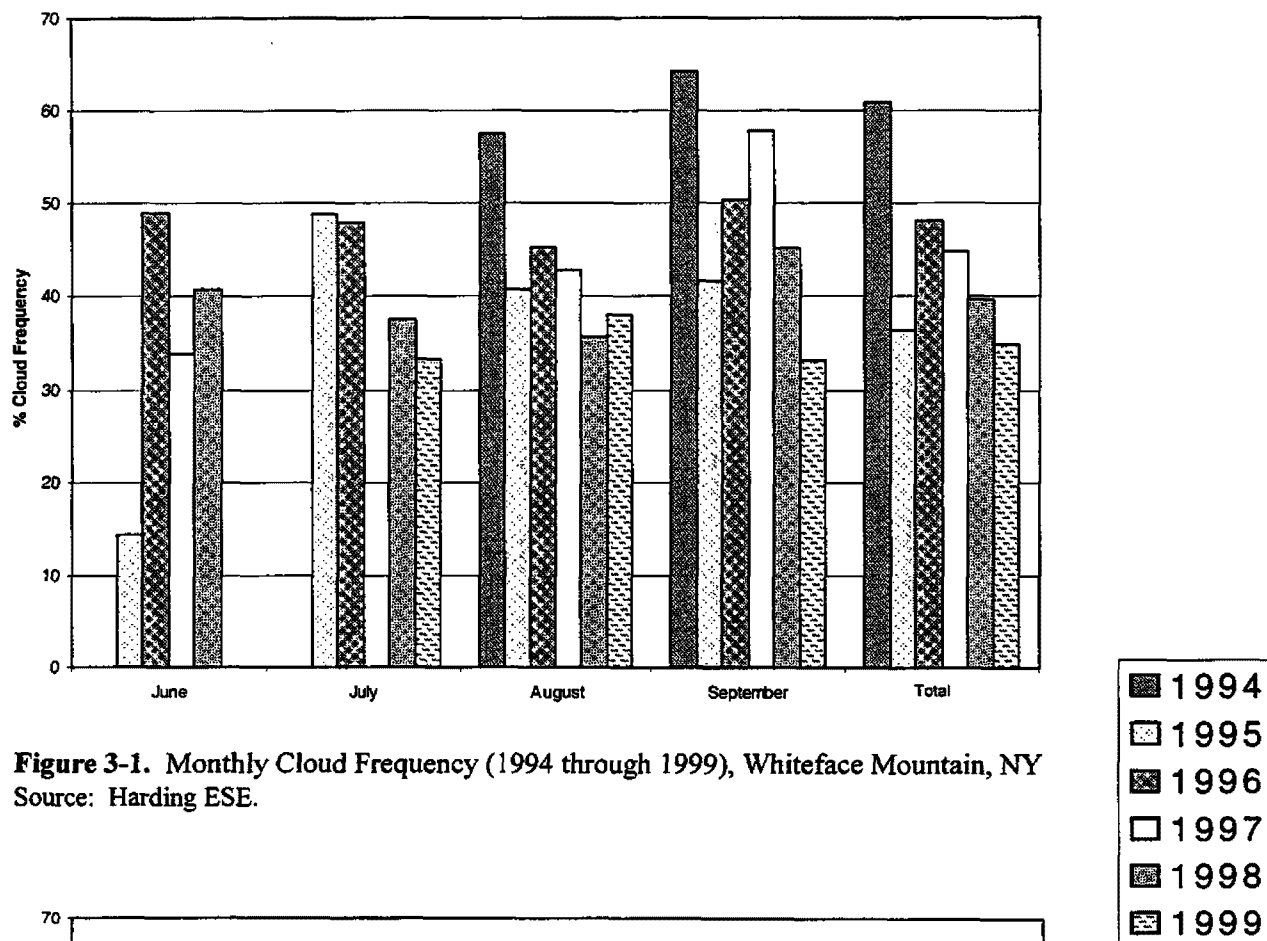


Figure 3-1. Monthly Cloud Frequency (1994 through 1999), Whiteface Mountain, NY
Source: Harding ESE.

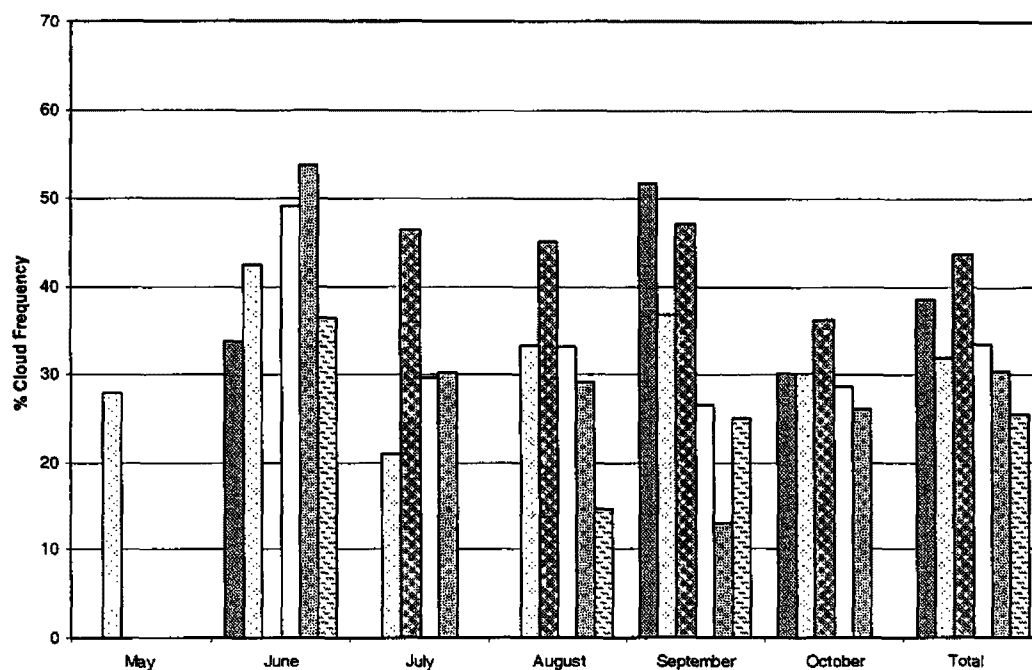


Figure 3-2. Monthly Cloud Frequency (1994 through 1999), Whitetop Mountain, VA
Source: Harding ESE.

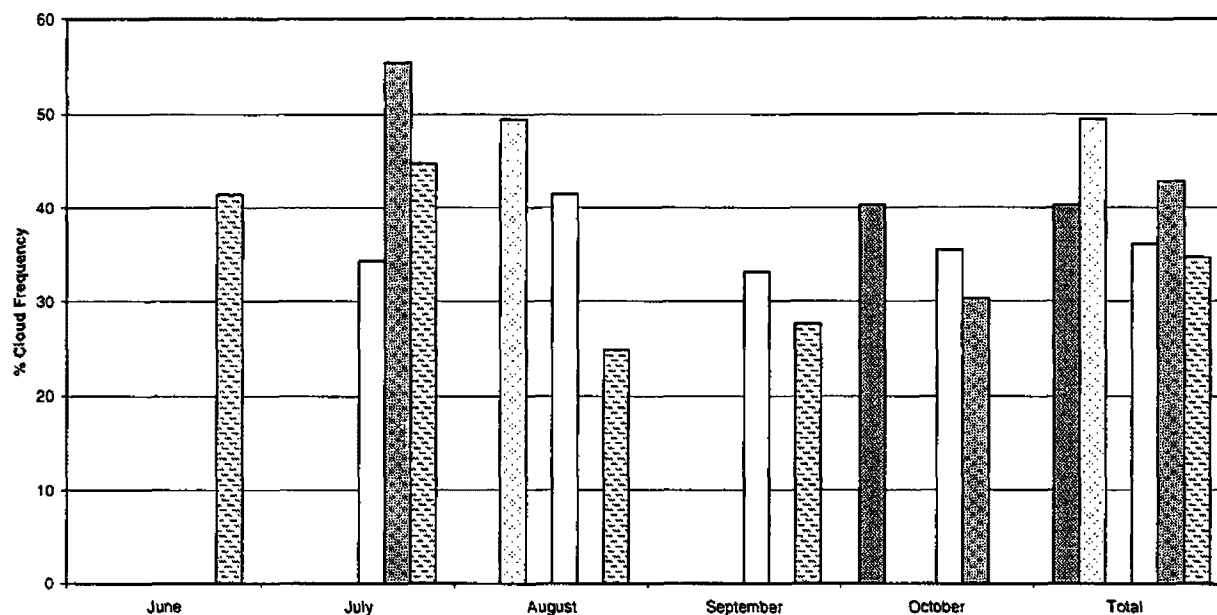


Figure 3-3. Monthly Cloud Frequency (1994 through 1999), Clingman's Dome, TN
Source: Harding ESE.

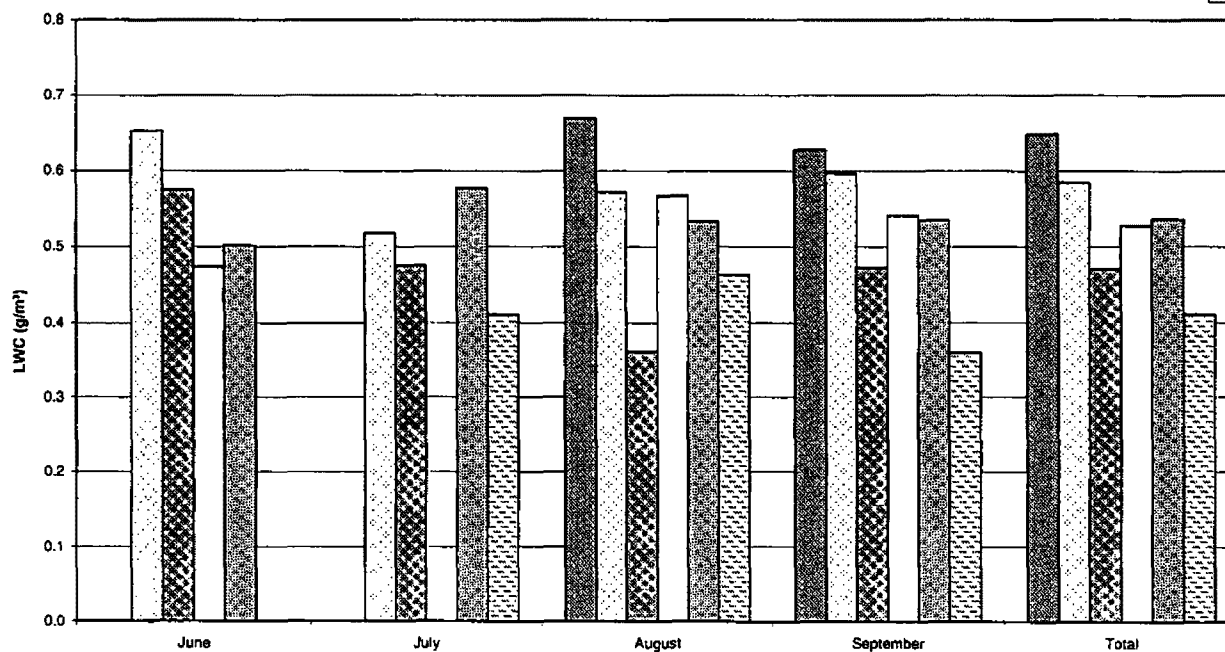
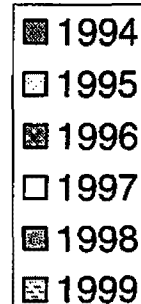


Figure 3-4. Mean Liquid Water Content of Clouds (1994 through 1999), Whiteface Mountain, NY
Source: Harding ESE.

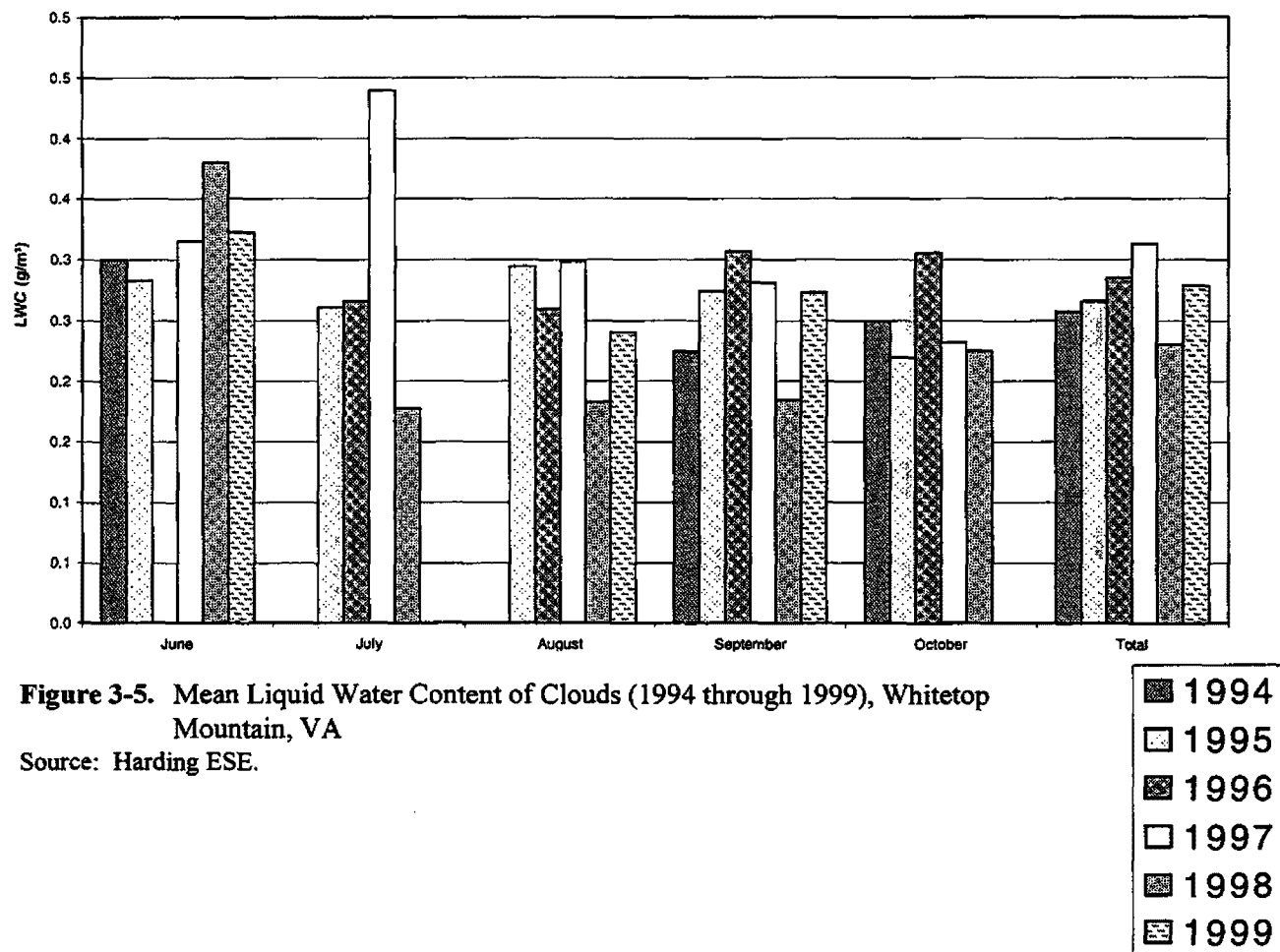


Figure 3-5. Mean Liquid Water Content of Clouds (1994 through 1999), Whitetop Mountain, VA

Source: Harding ESE.

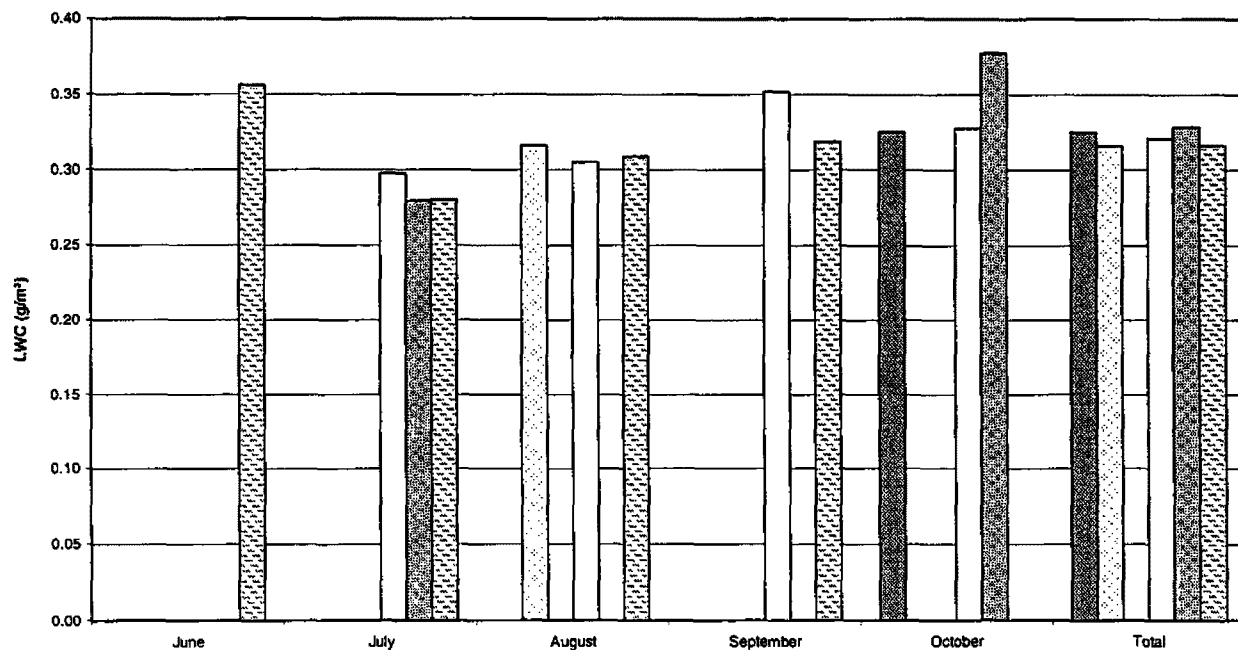


Figure 3-6. Mean Liquid Water Content of Clouds (1994 through 1999), Clingman's Dome, TN

Source: Harding ESE.

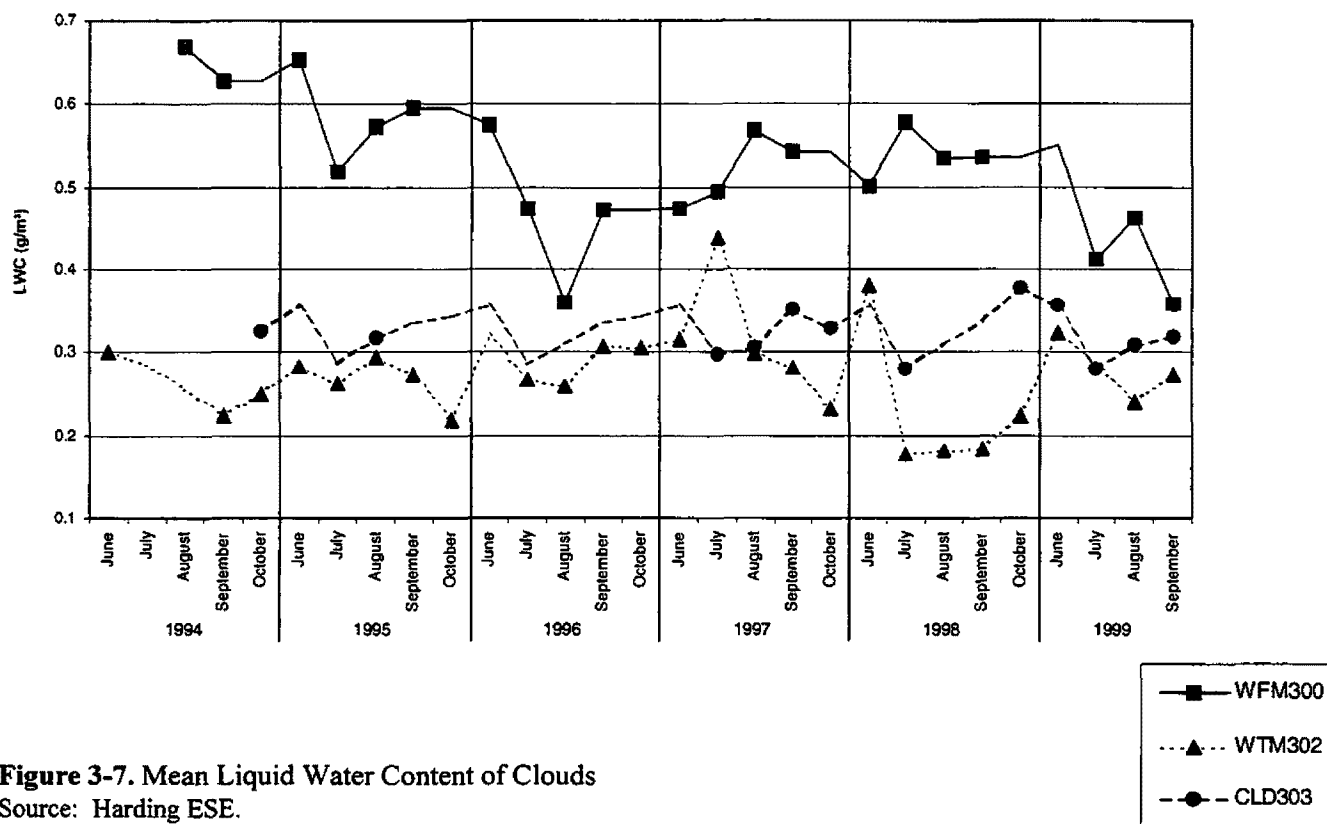


Figure 3-7. Mean Liquid Water Content of Clouds
Source: Harding ESE.

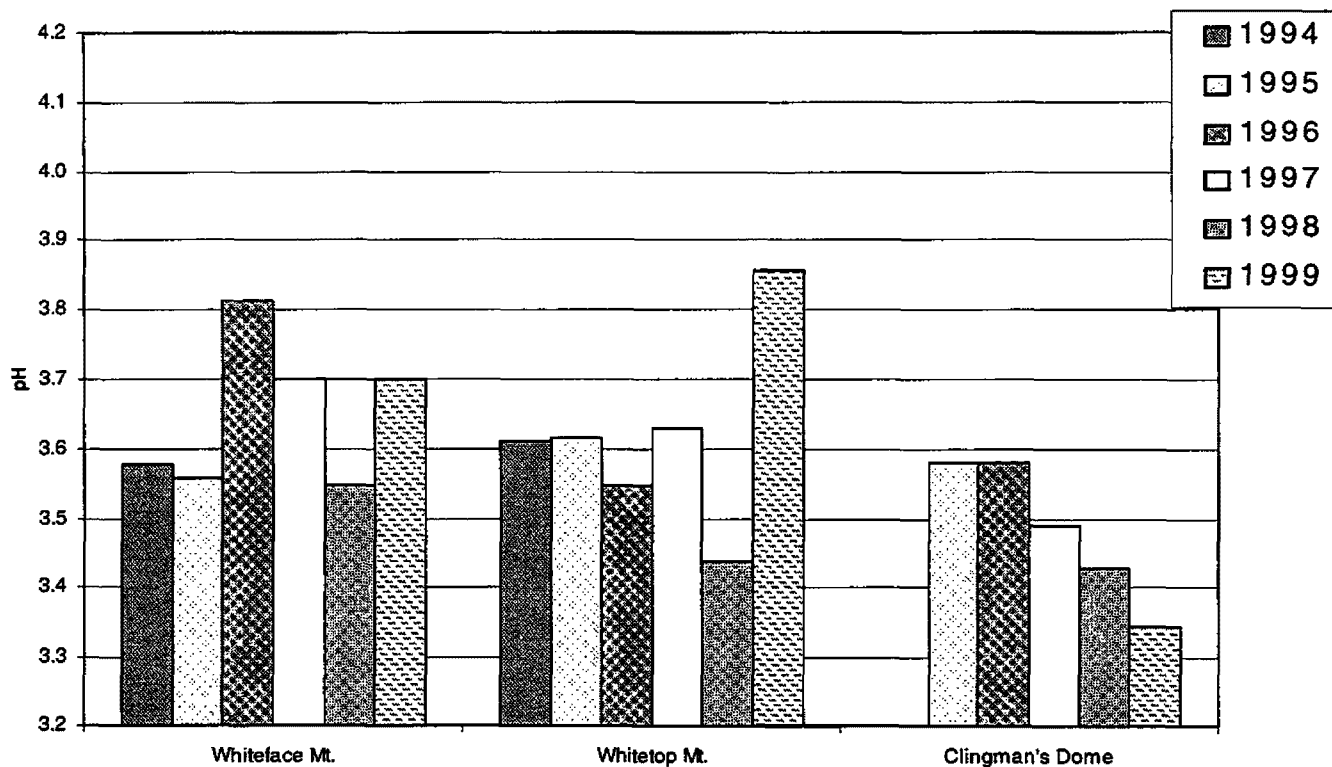


Figure 3-8. Mean pH of Cloudwater Samples at MADPro Sites (1994 through 1999)
Source: Harding ESE.

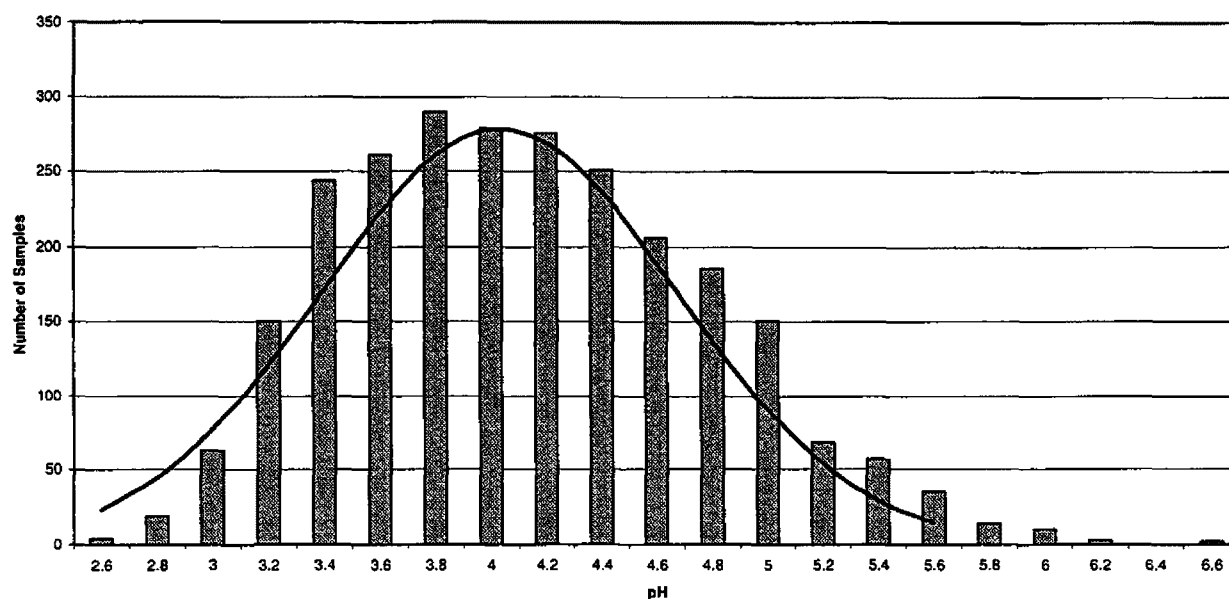


Figure 3-9. Frequency Distribution for Cloudwater pH at Whiteface Mountain, NY
(1994 through 1999)
Source: Harding ESE.

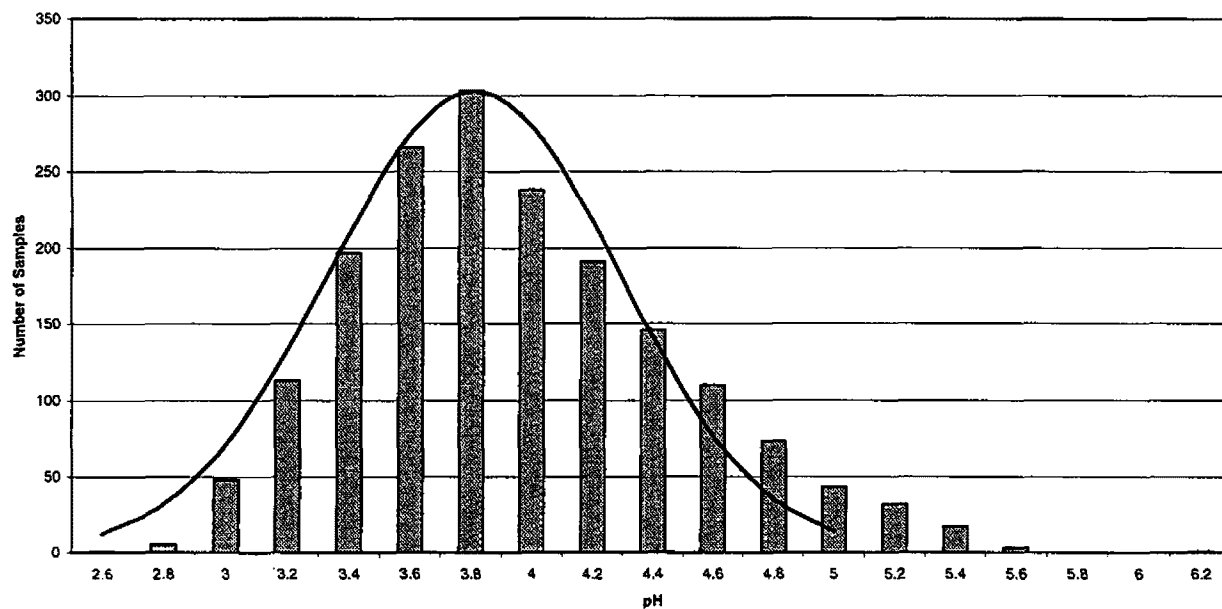


Figure 3-10. Frequency Distribution for Cloudwater pH at Whitetop Mountain, VA (1994 through 1999)

Source: Harding ESE.

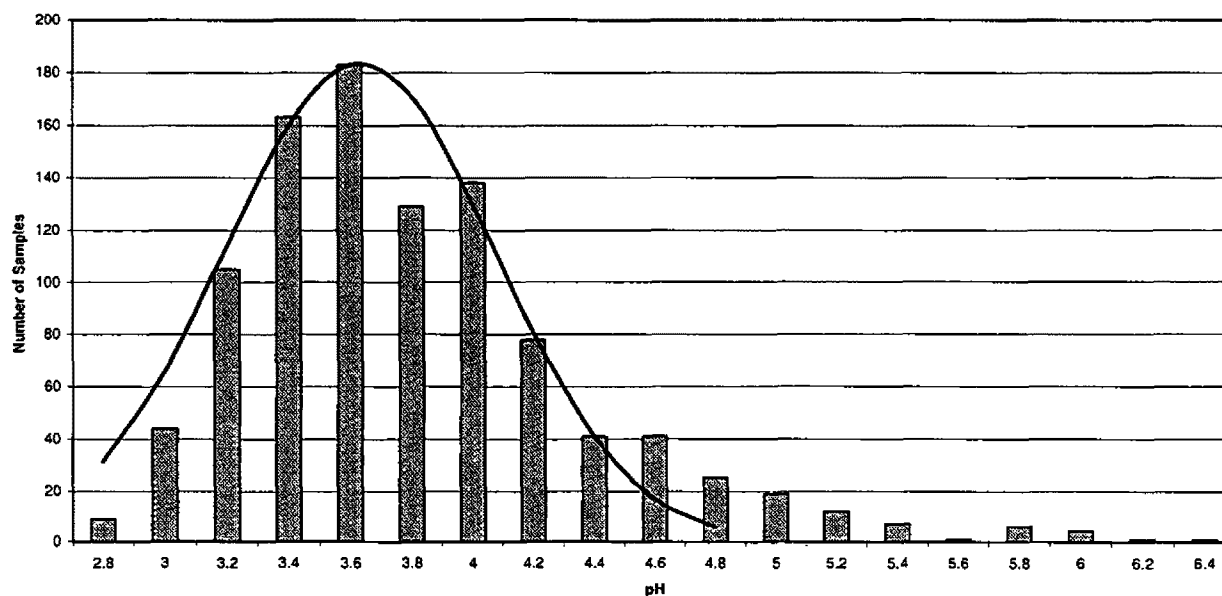


Figure 3-11. Frequency Distribution for Cloudwater pH at Clingman's Dome, TN (1994 through 1999)

Source: Harding ESE.

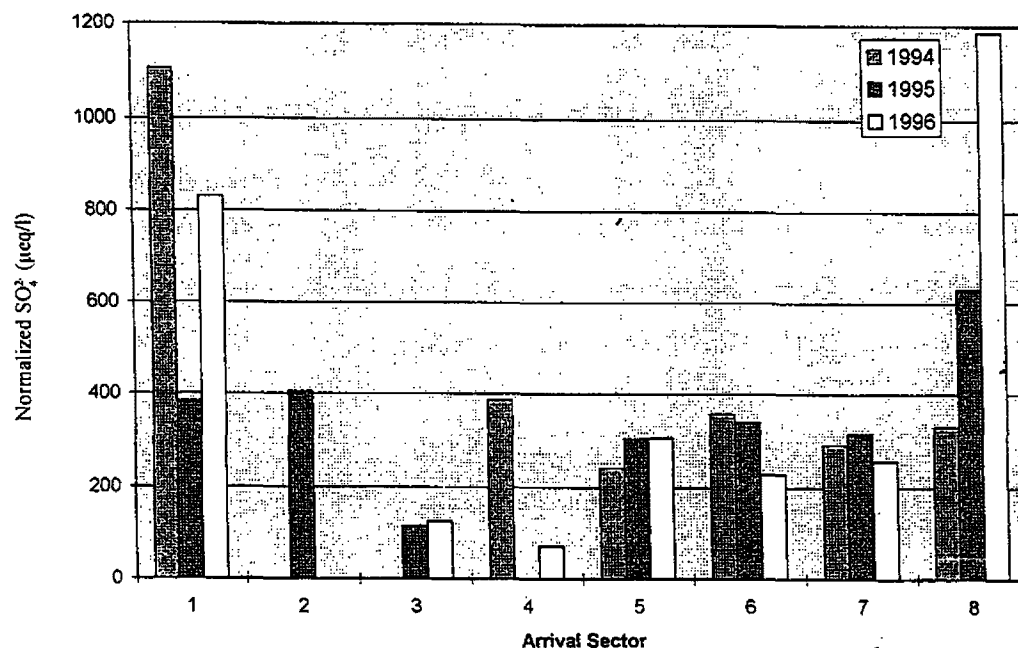


Figure 3-12. Normalized SO_4^{2-} Concentrations in Cloudwater at Whitetop Mountain, 1994 through 1996 -- Calculated as LWC Weighted Means versus Arrival Sector

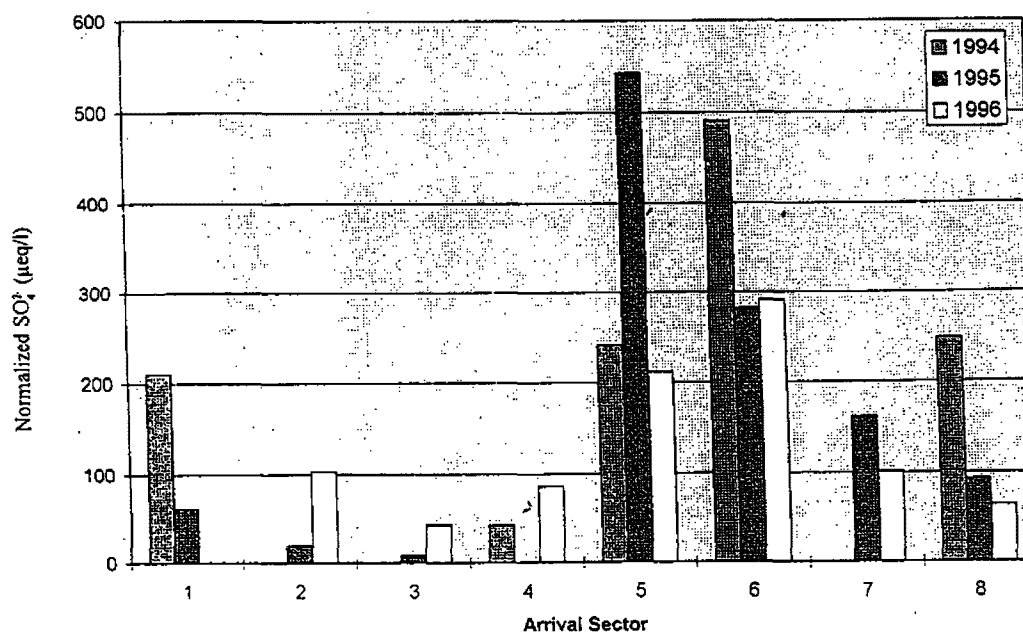


Figure 3-13. Normalized SO_4^{2-} Concentrations in Cloudwater at Whiteface Mountain, 1994 through 1996 -- Calculated as LWC Weighted Means versus Arrival Sector

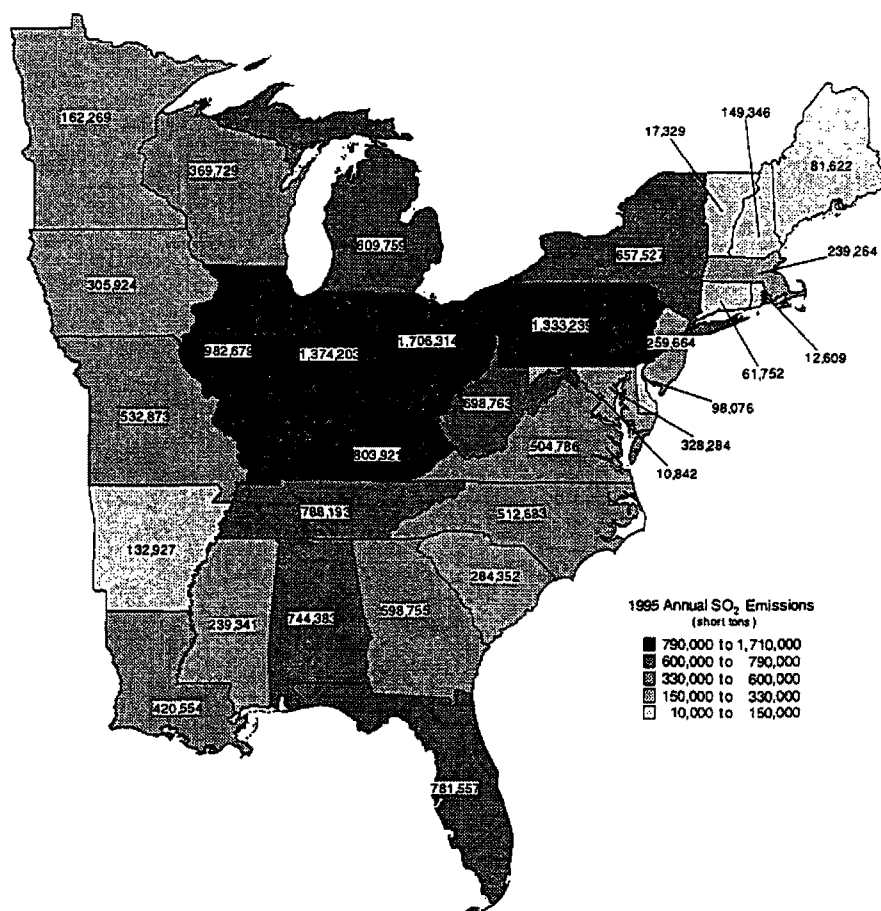


Figure 3-14. Annual SO₂ Emissions for 1995

WFM300 Whiteface Mountain
WTM302 Whitetop Mountain
CLD303 Clingman's Dome

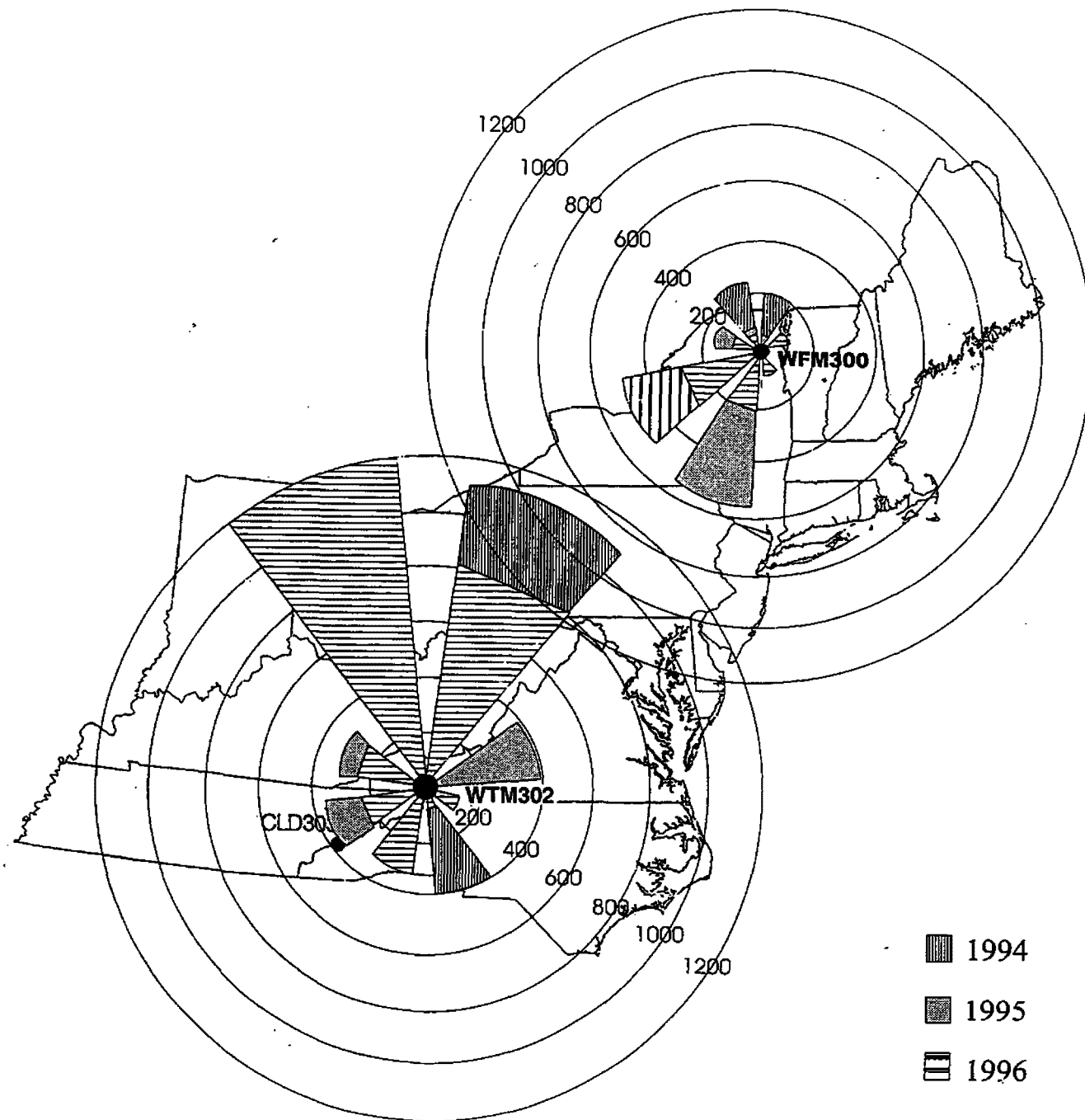


Figure 3-15. Mean Normalized SO₂ Concentrations (µeq/L) Segregated by; Back Trajectory Arrival Sector

This page has been intentionally left blank.

100

101

102

103

104

105

106

107

108

109

110

111

112

113

114

115

116

117

118

119

120

121

122

123

124

125

126

127

128

129

130

131

132

133

134

135

136

137

138

139

140

141

142

143

144

145

146

147

148

149

150

151

152

153

154

155

156

157

158

159

160

161

162

163

164

165

166

167

168

169

170

171

172

173

174

175

176

177

178

179

180

181

182

183

184

185

186

187

188

189

190

191

192

193

194

195

196

197

198

199

200

201

202

203

204

205

206

207

208

209

210

211

212

213

214

215

216

217

218

219

220

221

222

223

224

225

226

227

228

229

230

231

232

233

234

235

236

237

238

239

240

241

242

243

244

245

246

247

248

249

250

251

252

253

254

255

256

257

258

259

260

261

262

263

264

265

266

267

268

269

270

271

272

273

274

275

276

277

278

279

280

281

282

283

284

285

286

287

288

289

290

291

292

293

294

295

296

297

298

299

300

301

302

303

304

305

306

307

308

309

310

311

312

313

314

315

316

317

318

319

320

321

322

323

324

325

326

327

328

329

330

331

332

333

334

335

336

337

338

339

340

341

342

343

344

345

346

347

348

349

350

351

352

353

354

355

356

357

358

359

360

361

362

363

364

365

366

367

368

369

370

371

372

373

374

375

376

377

378

379

380

381

382

383

384

385

386

387

388

389

390

391

392

393

394

395

396

397

398

399

400

401

402

403

404

405

406

407

408

409

410

411

412

413

414

415

416

417

418

419

420

421

422

423

424

425

426

427

428

429

430

431

432

433

434

435

436

437

438

439

440

441

442

443

444

445

446

447

448

449

450

451

452

453

454

455

456

457

458

459

460

461

462

463

464

465

466

467

468

469

470

471

472

473

474

475

476

477

478

479

480

481

482

483

484

485

486

487

488

489

490

491

492

493

494

495

496

497

498

499

500

501

502

503

504

505

506

507

508

509

510

511

512

513

514

515

516

517

518

519

520

521

522

523

524

525

526

527

528

529

530

531

532

533

534

535

536

537

538

539

540

541

542

543

544

545

546

547

548

549

550

551

552

553

554

555

556

557

558

559

560

561

562

563

564

565

566

567

568

569

570

571

572

573

574

575

576

577

578

579

580

581

582

583

584

585

586

587

588

589

590

591

592

593

594

595

596

597

598

599

600

601

602

603

604

605

606

607

608

609

610

611

612

613

614

615

616

617

618

619

620

621

622

623

624

625

626

627

628

629

630

631

632

633

634

635

636

637

638

639

640

641

642

643

644

645

646

647

648

649

650

651

652

653

654

655

656

657

658

659

660

661

662

663

664

665

666

667

668

669

670

671

672

673

674

675

676

677

678

679

680

681

682

683

684

685

686

687

688

689

690

691

692

693

694

695

696

697

698

699

700

701

702

703

704

705

706

707

708

709

710

711

712

713

714

715

716

717

718

719

720

721

722

723

724

725

726

727

728

729

730

731

732

733

734

735

736

737

738

739

740

741

742

743

744

745

746

747

748

749

750

751

752

753

754

755

756

757

758

759

760

761

762

763

764

765

766

767

768

769

770

771

772

773

774

775

776

777

778

779

780

781

782

783

784

785

786

787

788

789

790

791

792

793

794

795

796

797

798

799

800

801

802

803

804

805

806

807

808

809

810

811

812

813

814

815

816

817

818

819

820

821

822

823

824

825

826

827

828

829

830

831

832

833

834

835

836

837

838

839

840

841

842

843

844

845

846

847

848

849

850

851

852

853

854

855

856

857

858

859

860

861

862

863

864

865

866

867

868

869

870

871

872

873

874

875

876

877

878

879

880

881

882

883

884

885

886

887

888

889

890

891

892

893

894

895

896

897

898

899

900

901

902

903

904

905

906

907

908

909

910

911

912

913

914

915

916

917

918

919

920

921

922

923

924

925

926

927

928

929

930

931

932

933

934

935

936

937

938

939

940

941

942

943

944

945

946

947

948

949

950

951

952

953

954

955

956

957

958

959

960

961

962

963

964

965

966

967

968

969

970

971

972

973

974

975

976

977

978

979

980

981

982

983

984

985

986

987

988

989

990

991

992

993

994

995

996

997

998

999

1000

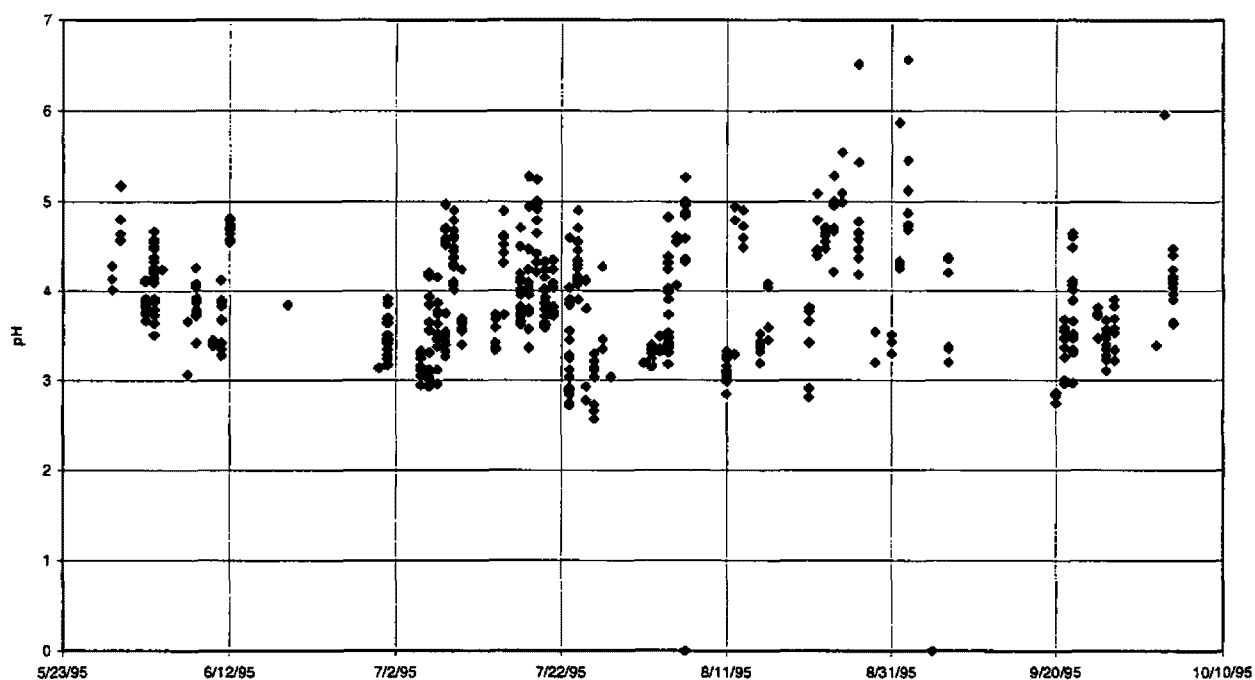


Figure 3-16. pH of Cloudwater Samples, Whiteface Mountain, NY (1995)
Source: Harding ESE.

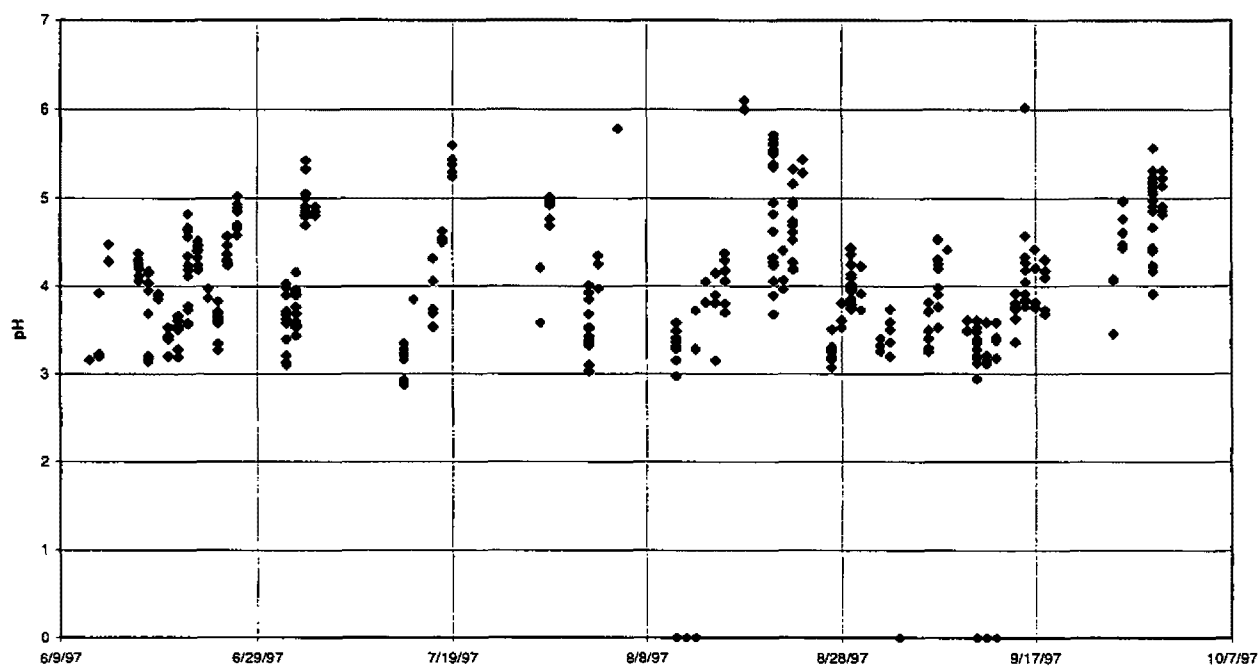


Figure 3-17. pH of Cloudwater Samples, Whiteface Mountain, NY (1997)
Source: Harding ESE.

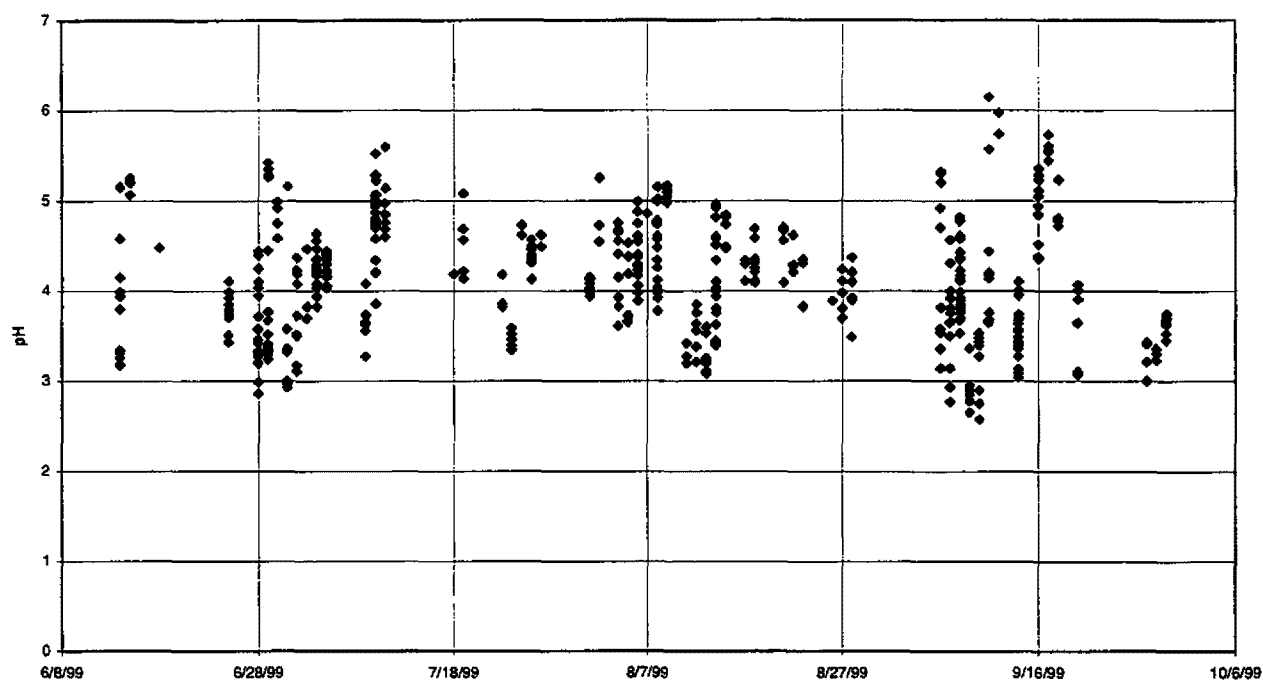


Figure 3-18. pH of Cloudwater Samples, Whiteface Mountain, NY (1999)
Source: Harding ESE.

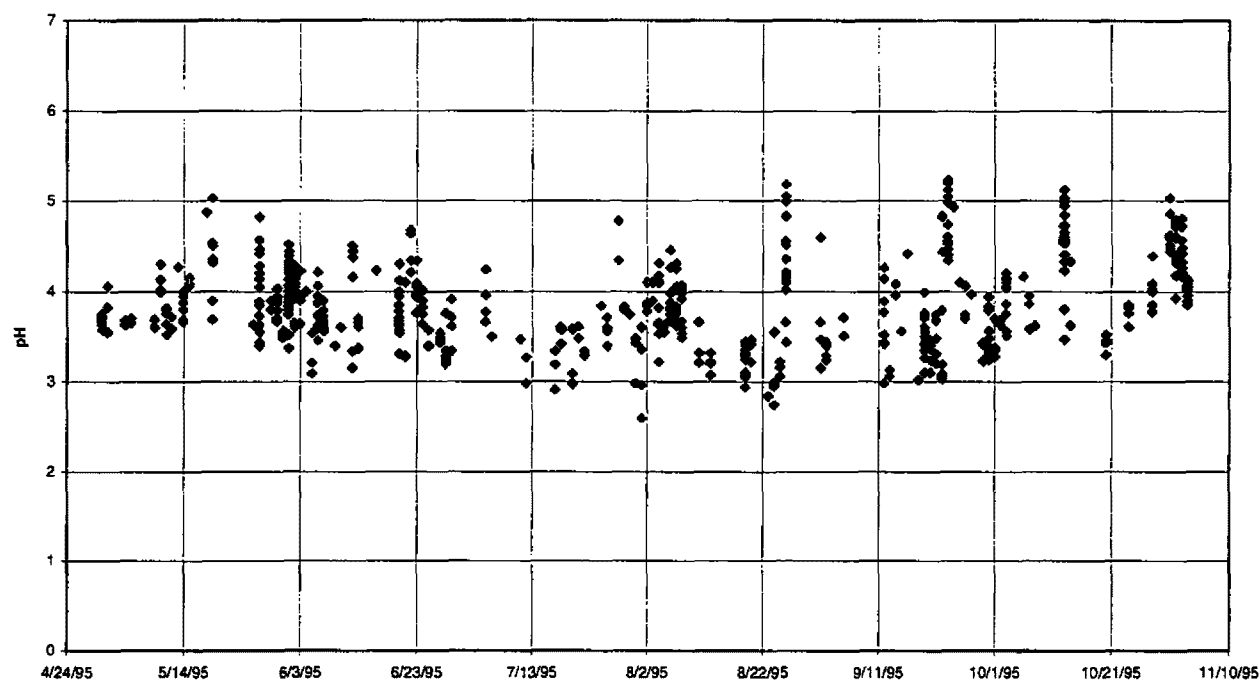


Figure 3-19. pH of Cloudwater Samples, Whitetop Mountain, VA (1995)
Source: Harding ESE.

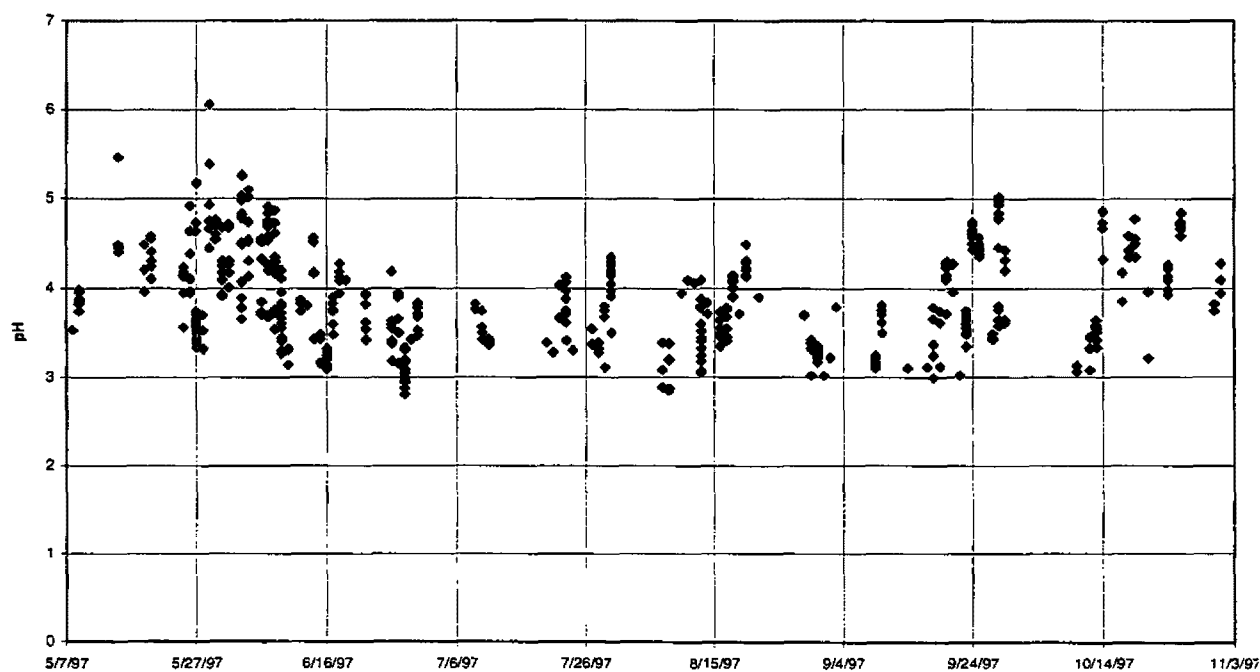


Figure 3-20. pH of Cloudwater Samples, Whitetop Mountain, VA (1997)
Source: Harding ESE.

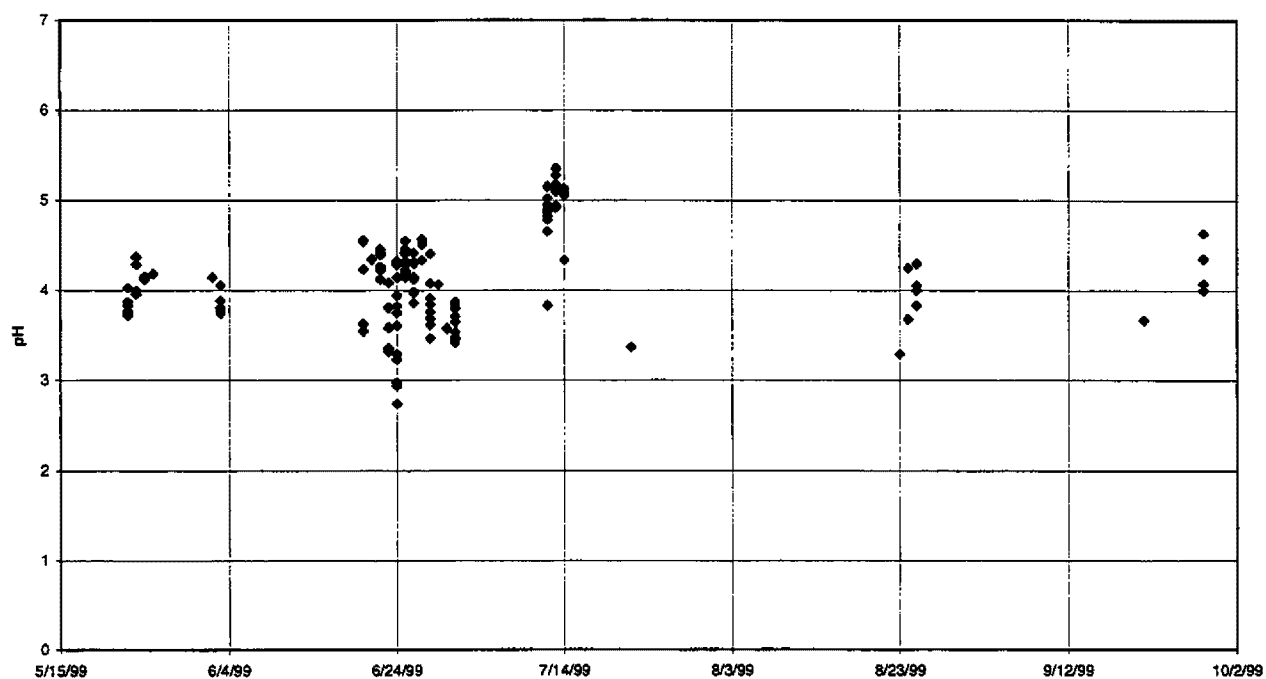


Figure 3-21. pH of Cloudwater Samples, Whitetop Mountain, VA (1999)
Source: Harding ESE.

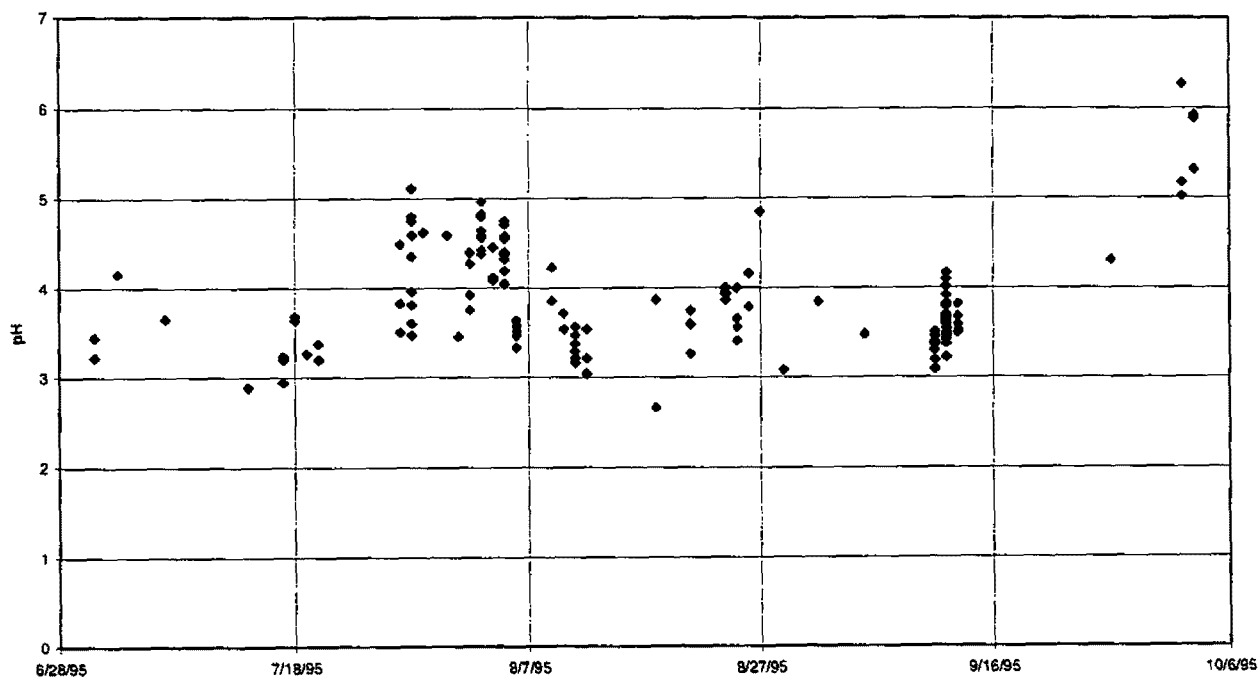


Figure 3-22. pH of Cloudwater Samples, Clingman's Dome, TN (1995)
Source: Harding ESE.

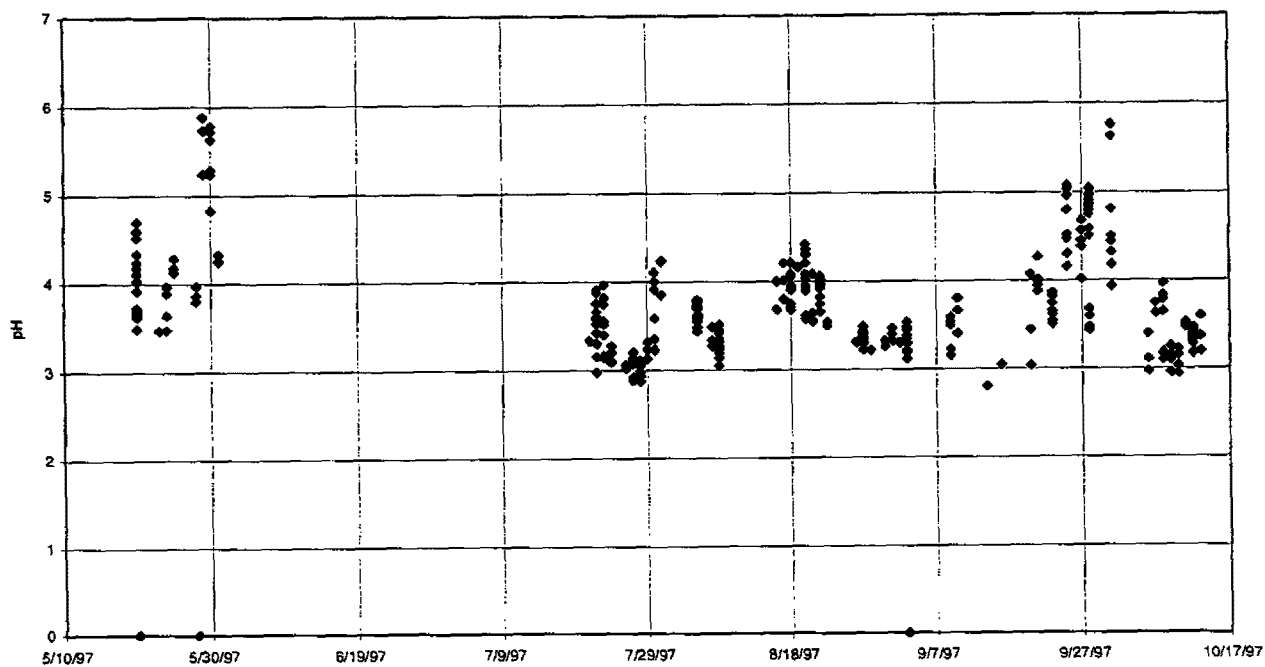


Figure 3-23. pH of Cloudwater Samples, Clingman's Dome, TN (1997)
Source: Harding ESE.

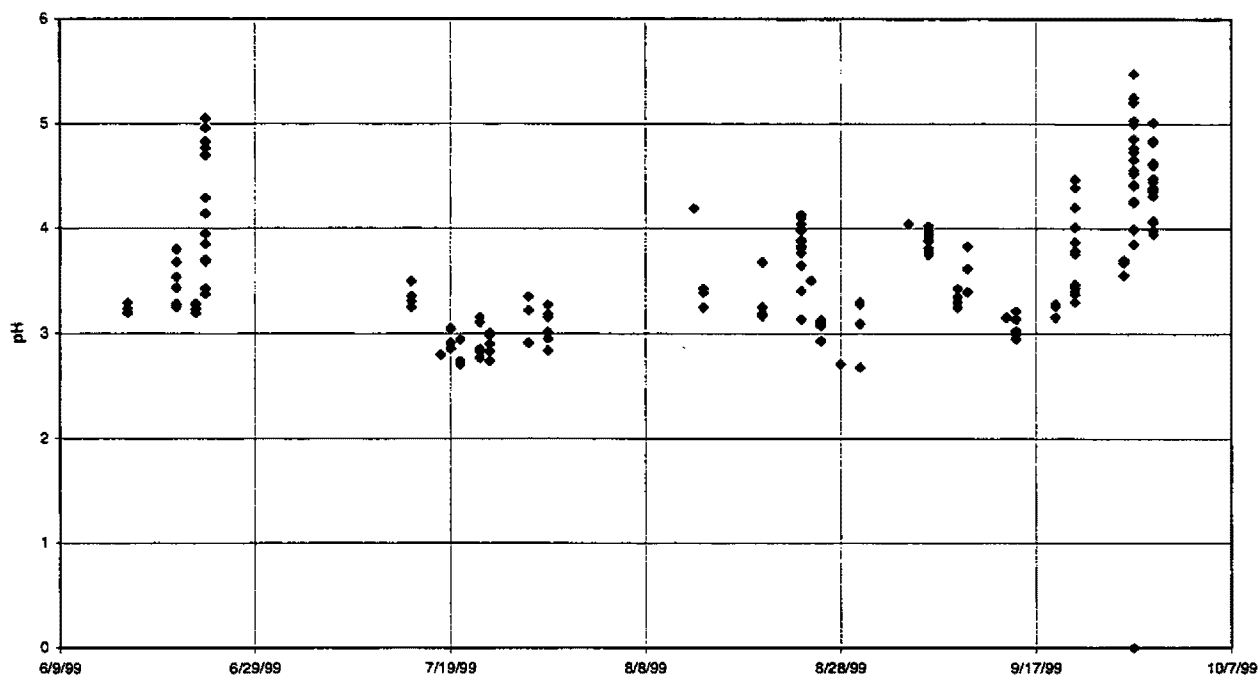


Figure 3-24. pH of Cloudwater Samples, Clingman's Dome, TN (1999)
Source: Harding ESE.

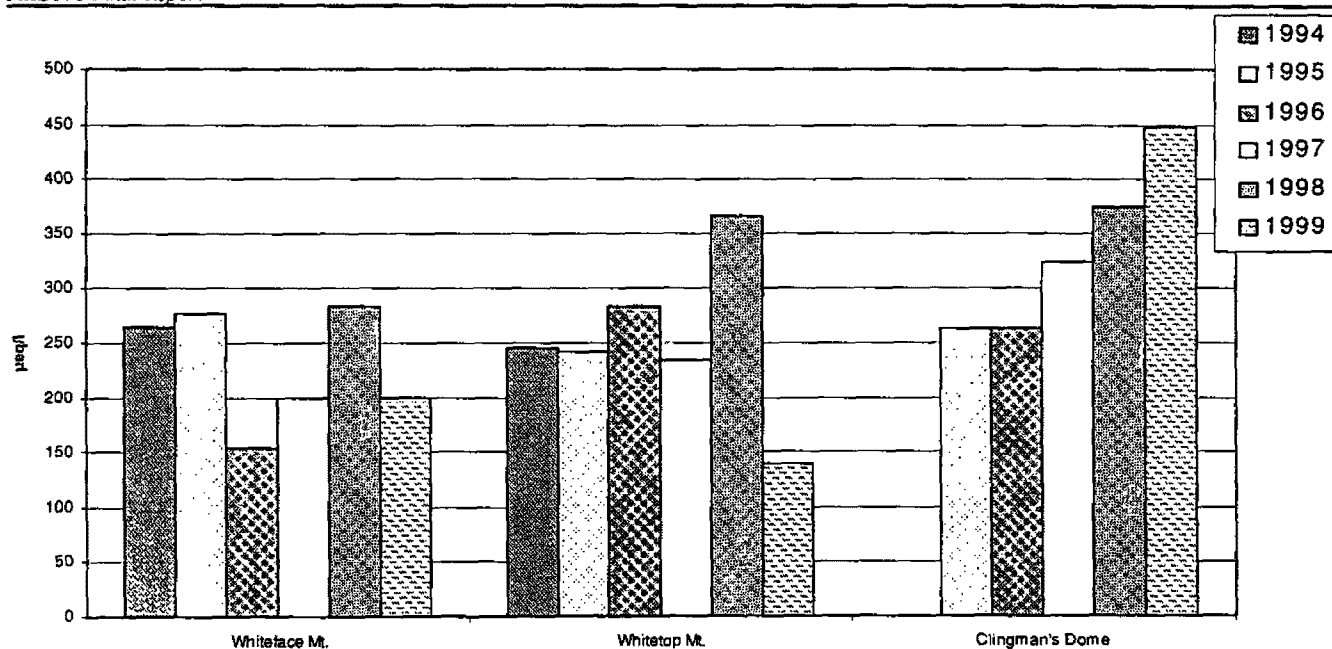


Figure 3-25. Mean Hydrogen Ion Concentrations of Cloudwater Samples at MADPro Sites (1994 through 1999)

Source: Harding ESE.

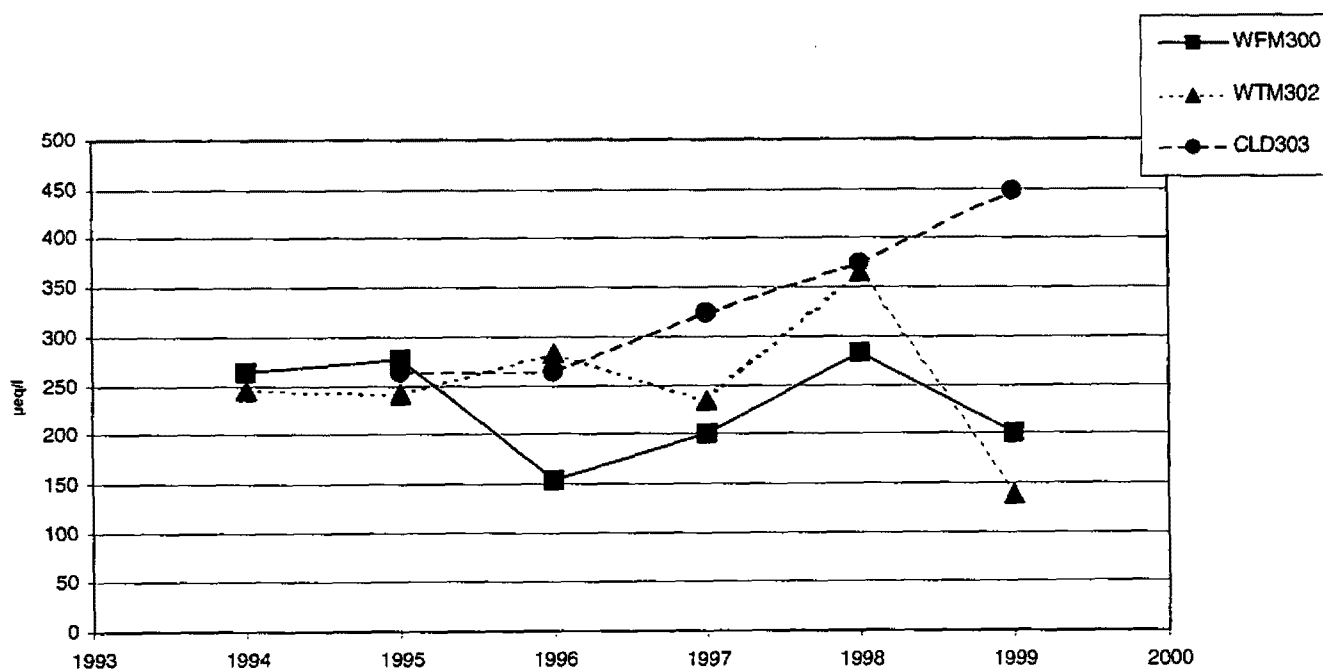


Figure 3-26. Mean Hydrogen Ion Concentrations of Cloudwater Samples at MADPro Sites (1994 through 1999)

Source: Harding ESE.

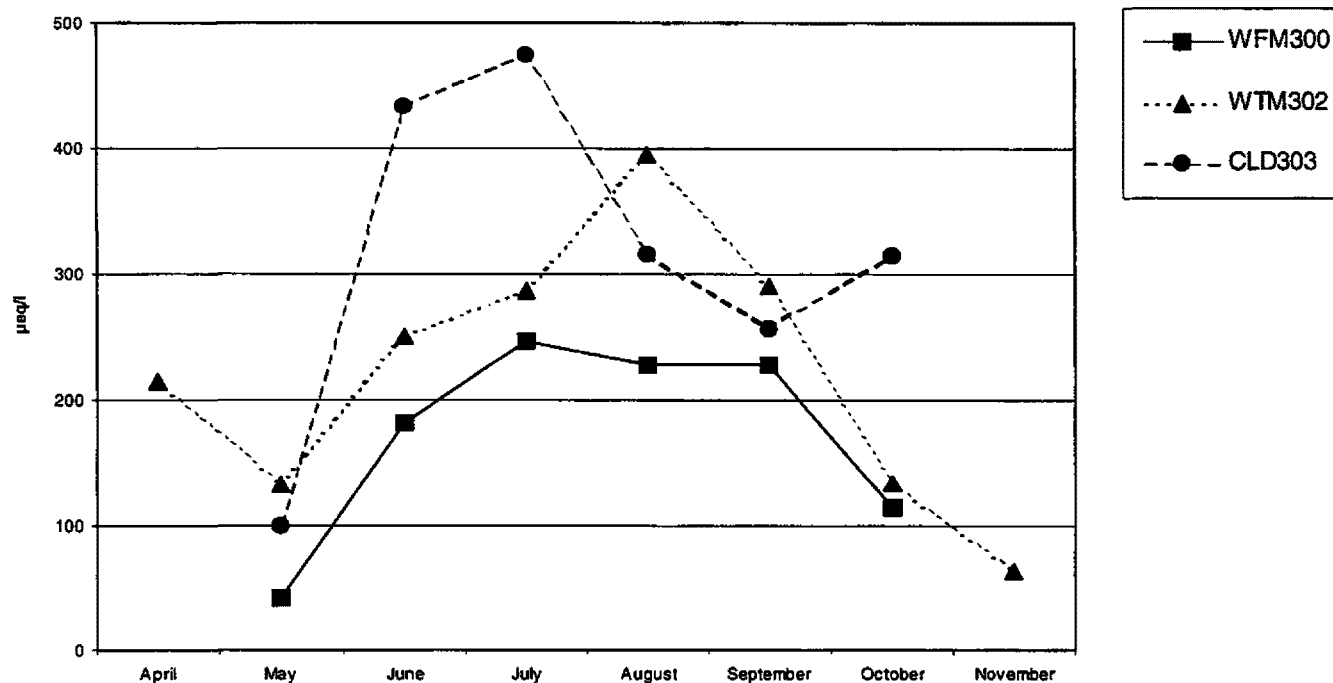


Figure 3-27. Monthly Variation in H⁺ Concentration in Cloudwater
(Means Across All Years, 1994 through 1999)

Source: Harding ESE.

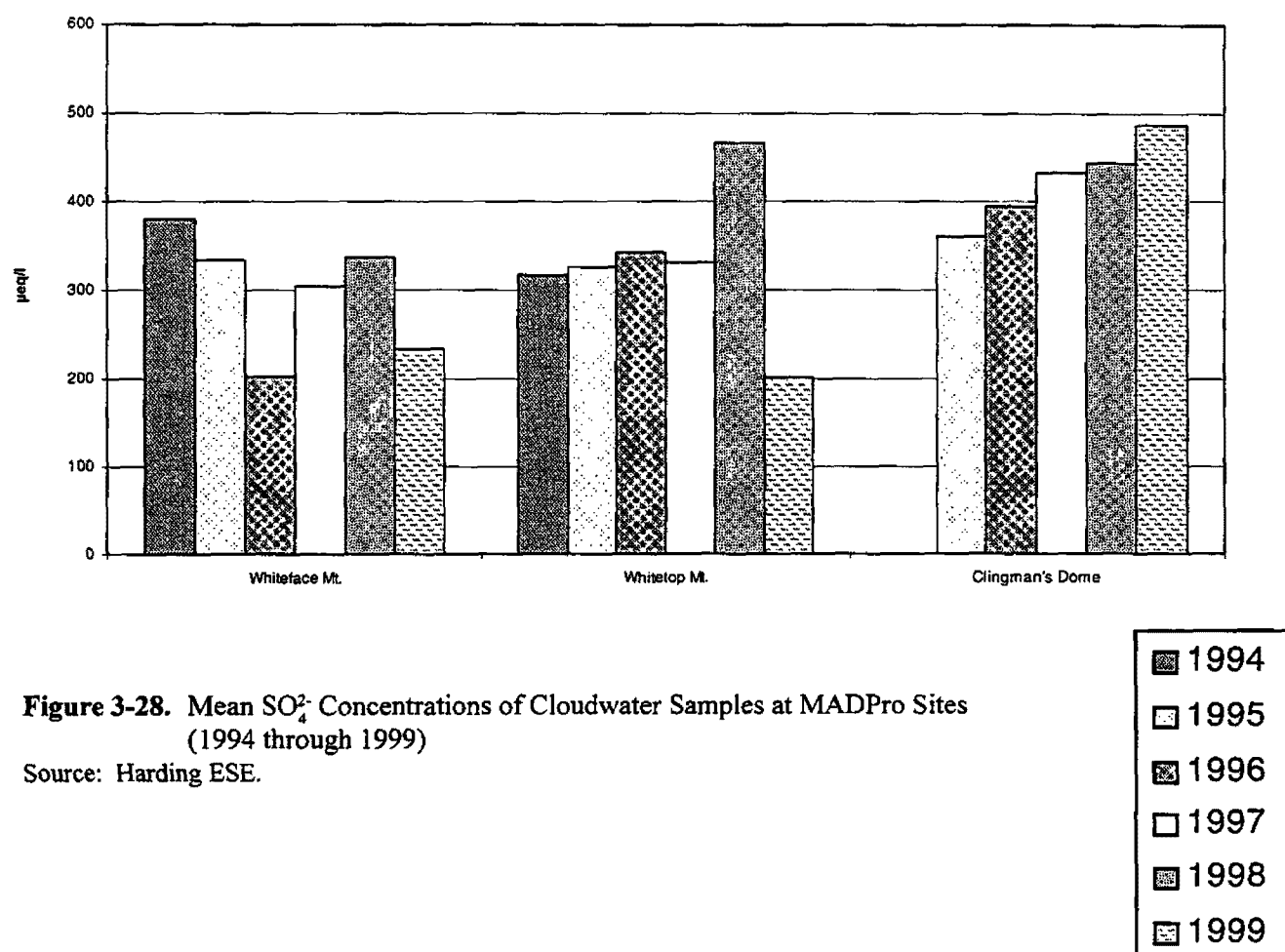


Figure 3-28. Mean SO_4^{2-} Concentrations of Cloudwater Samples at MADPro Sites (1994 through 1999)

Source: Harding ESE.

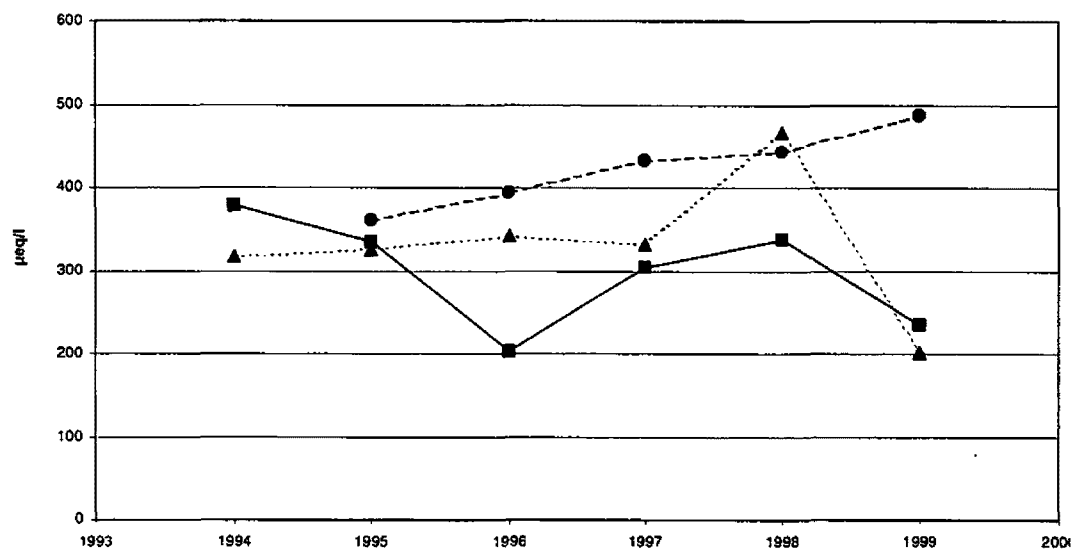


Figure 3-29. Mean SO_4^{2-} Concentrations of Cloudwater Samples at MADPro Sites (1994 through 1999)

Source: Harding ESE.

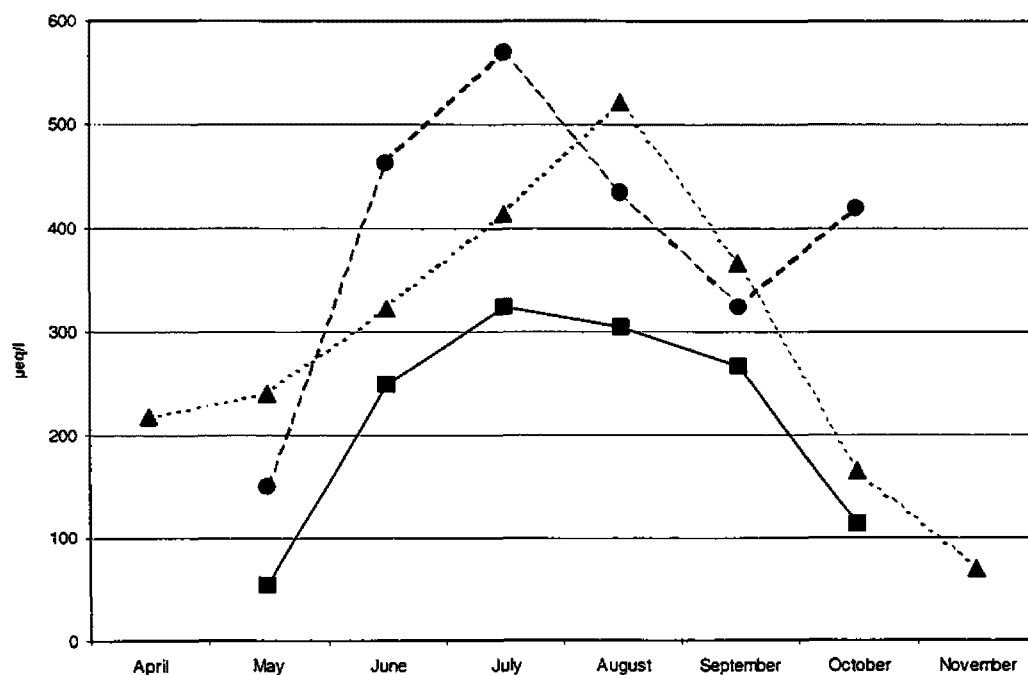


Figure 3-30. Monthly Variation in SO_4^{2-} Concentrations in Cloudwater (Means Across All Years, 1994 through 1999)

Source: Harding ESE.

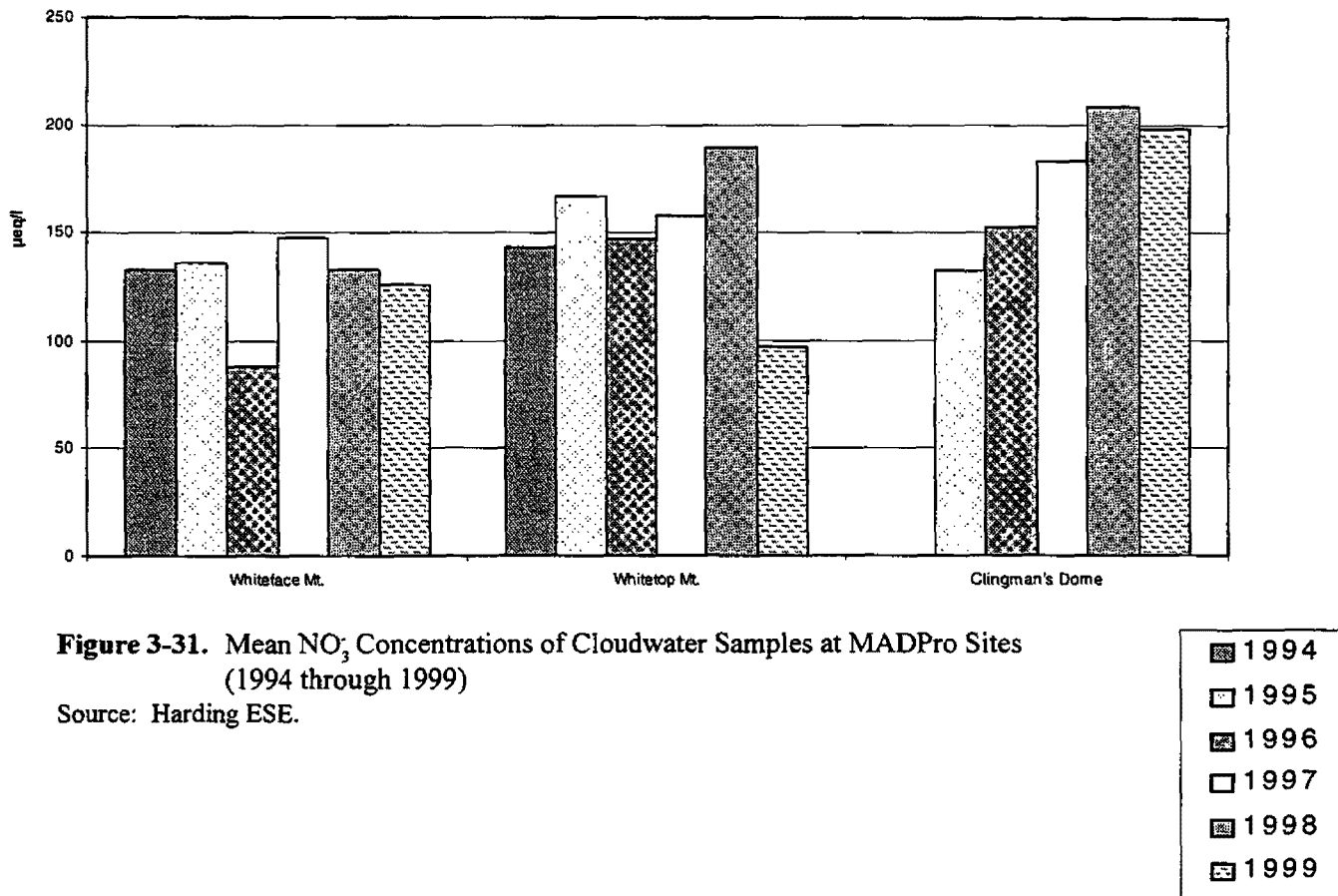


Figure 3-31. Mean NO₃⁻ Concentrations of Cloudwater Samples at MADPro Sites (1994 through 1999)

Source: Harding ESE.

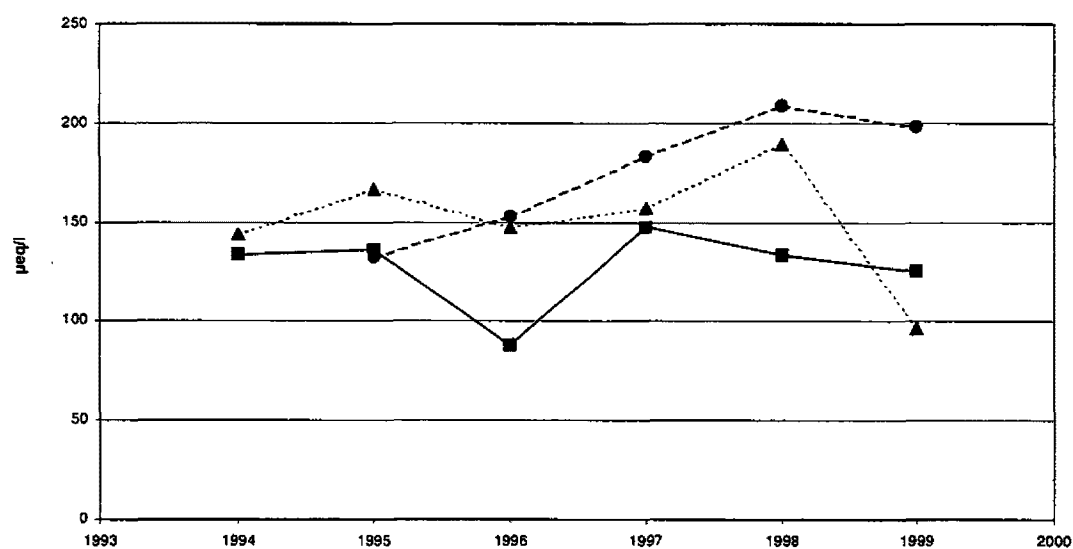


Figure 3-32. Mean NO_3 Concentrations of Cloudwater Samples at MADPro Sites (1994 through 1999)

Source: Harding ESE.

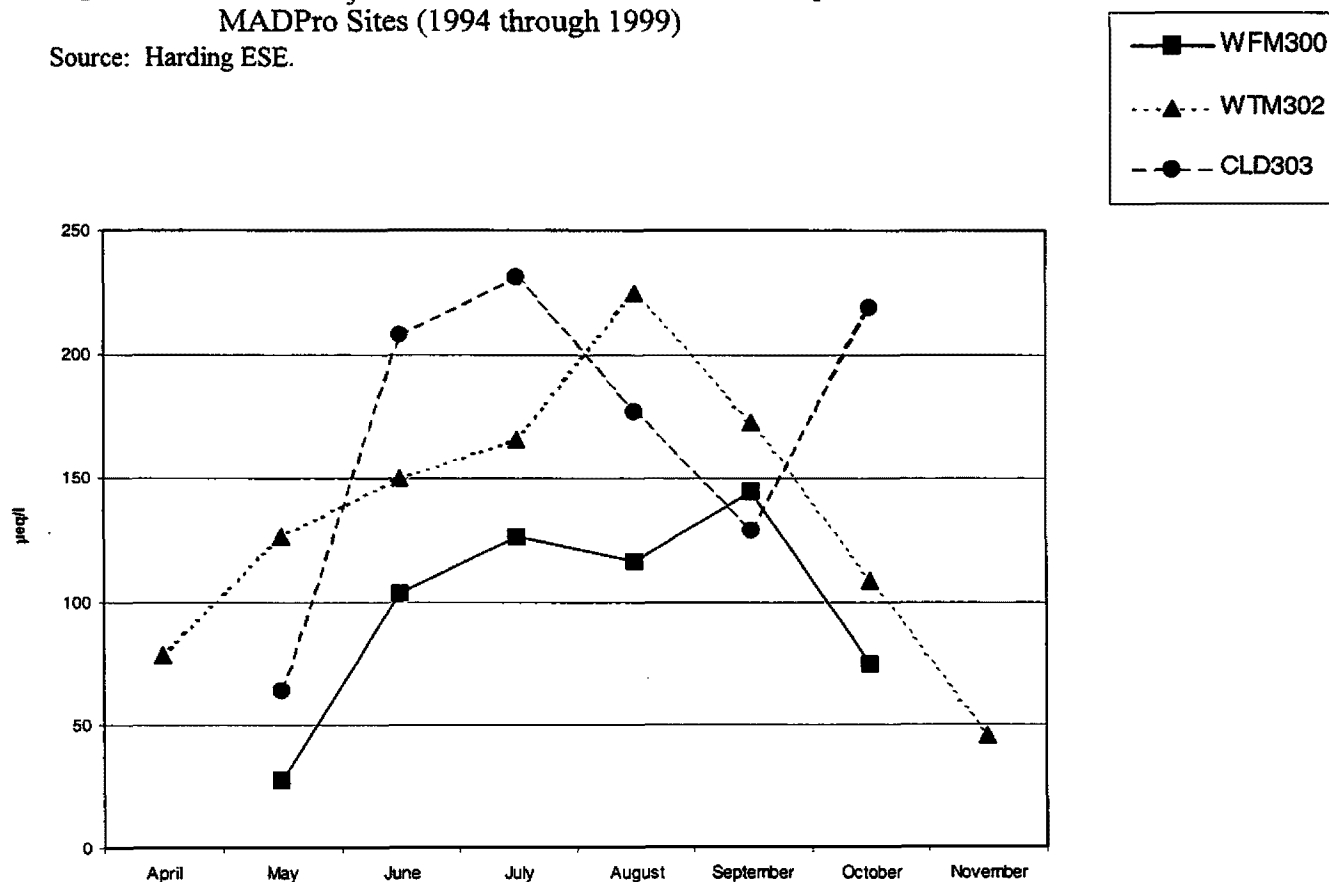
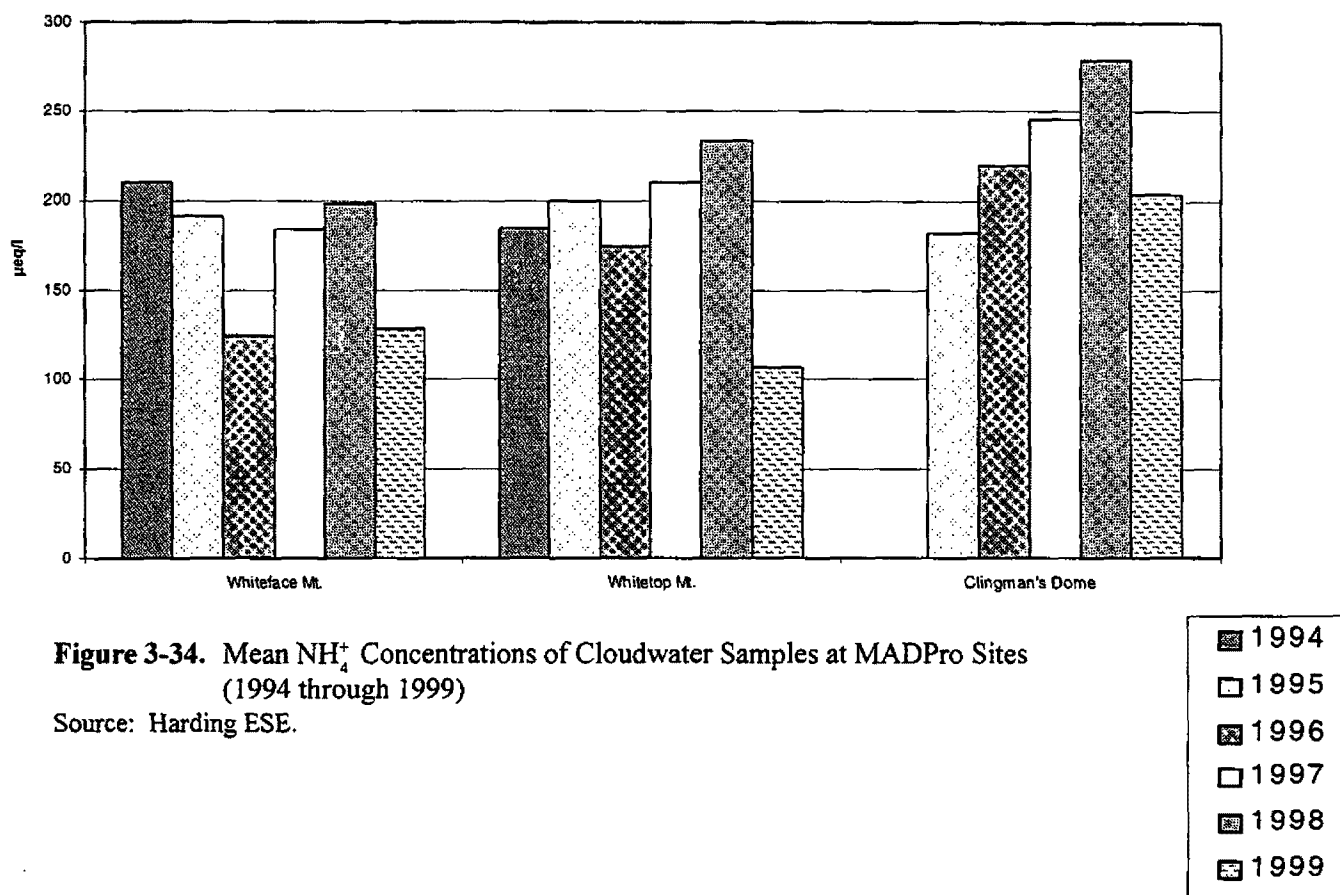


Figure 3-33. Monthly Variation in NO_3 Concentrations in Cloudwater (Means Across All Years, 1994 through 1999)

Source: Harding ESE.



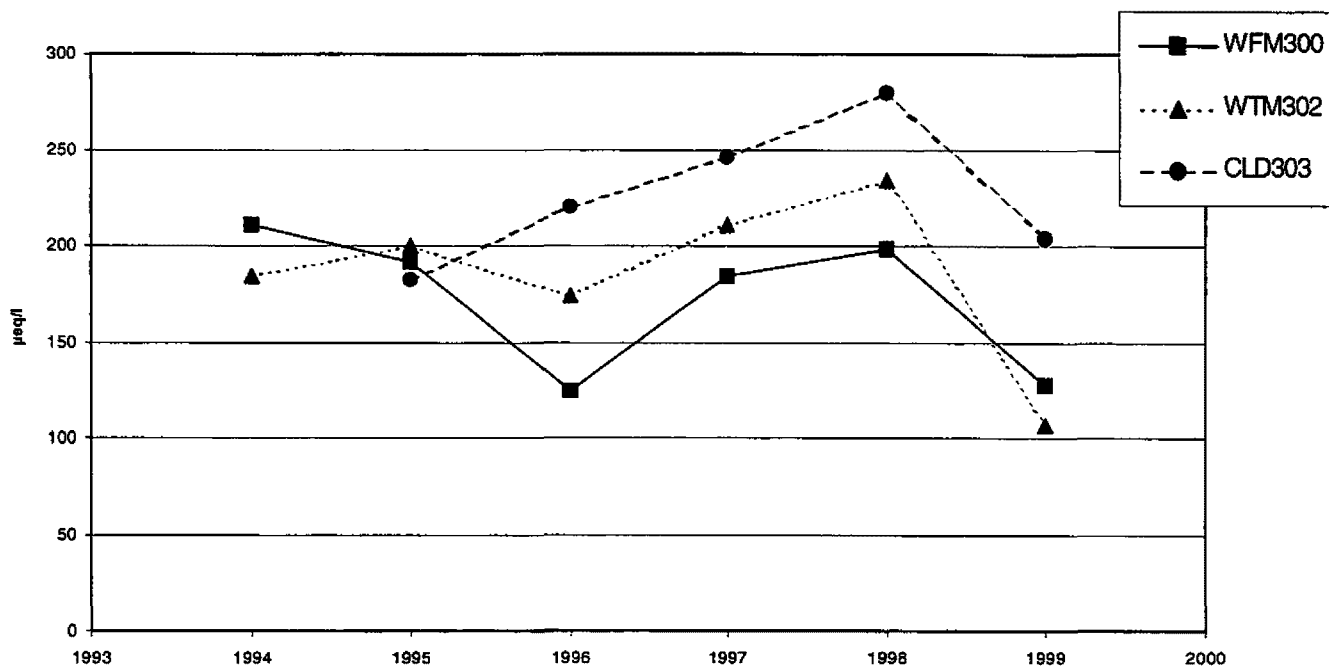


Figure 3-35. Mean NH_4^+ Concentrations of Cloudwater Samples at MADPro Sites (1994 through 1999)

Source: Harding ESE.

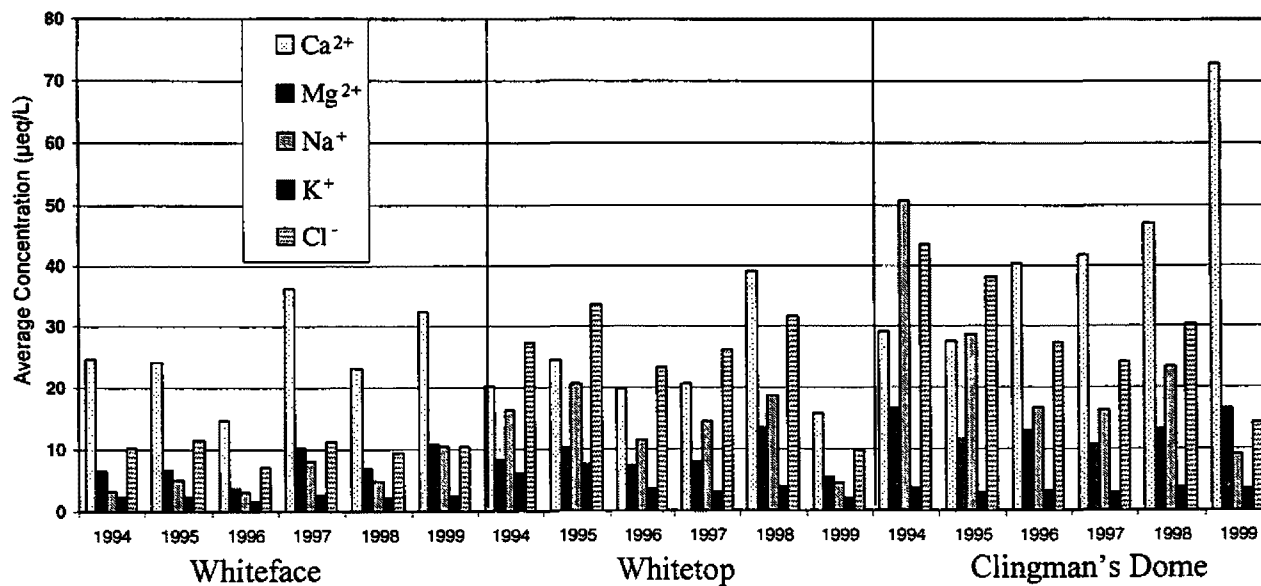


Figure 3-36. Average Minor Ion Concentrations from 1994 to 1999

Source: Harding ESE.

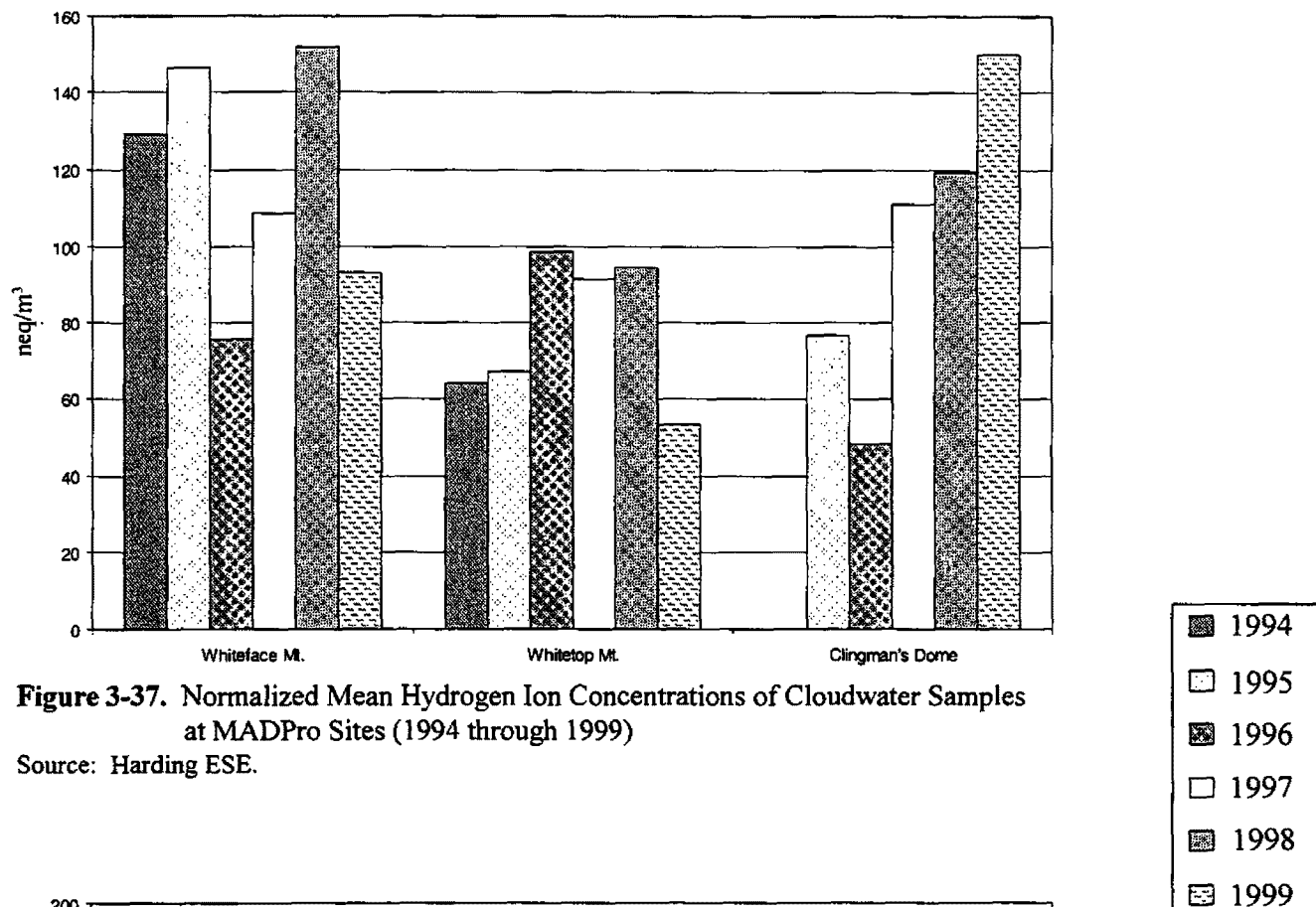


Figure 3-37. Normalized Mean Hydrogen Ion Concentrations of Cloudwater Samples at MADPro Sites (1994 through 1999)

Source: Harding ESE.

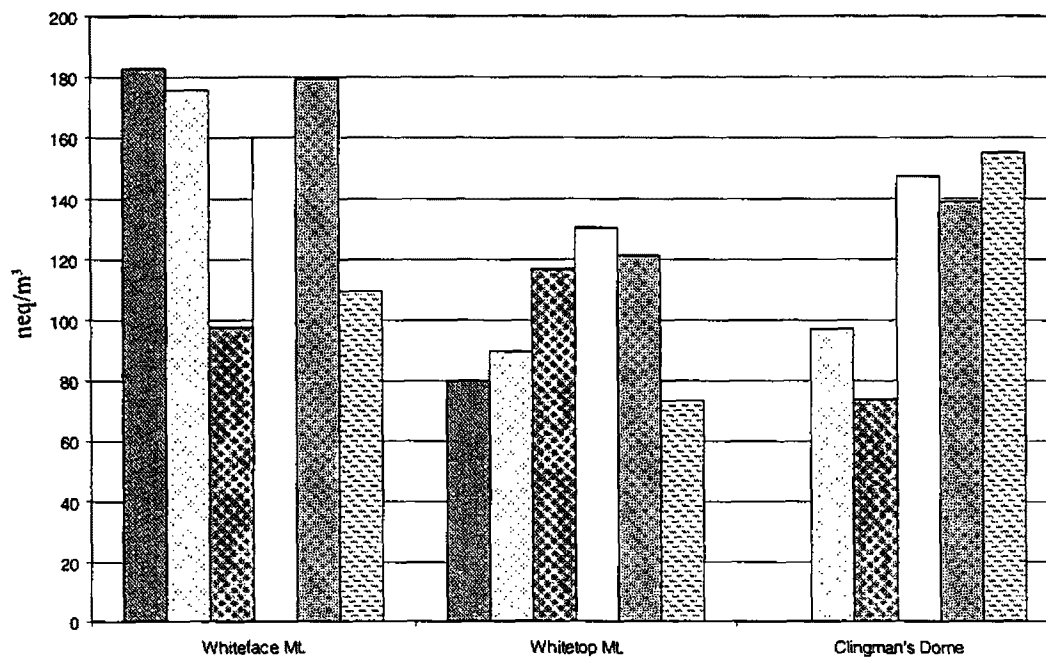


Figure 3-38. Normalized Mean SO₄²⁻ Concentrations of Cloudwater Samples at MADPro Sites (1994 through 1999)

Source: Harding ESE.

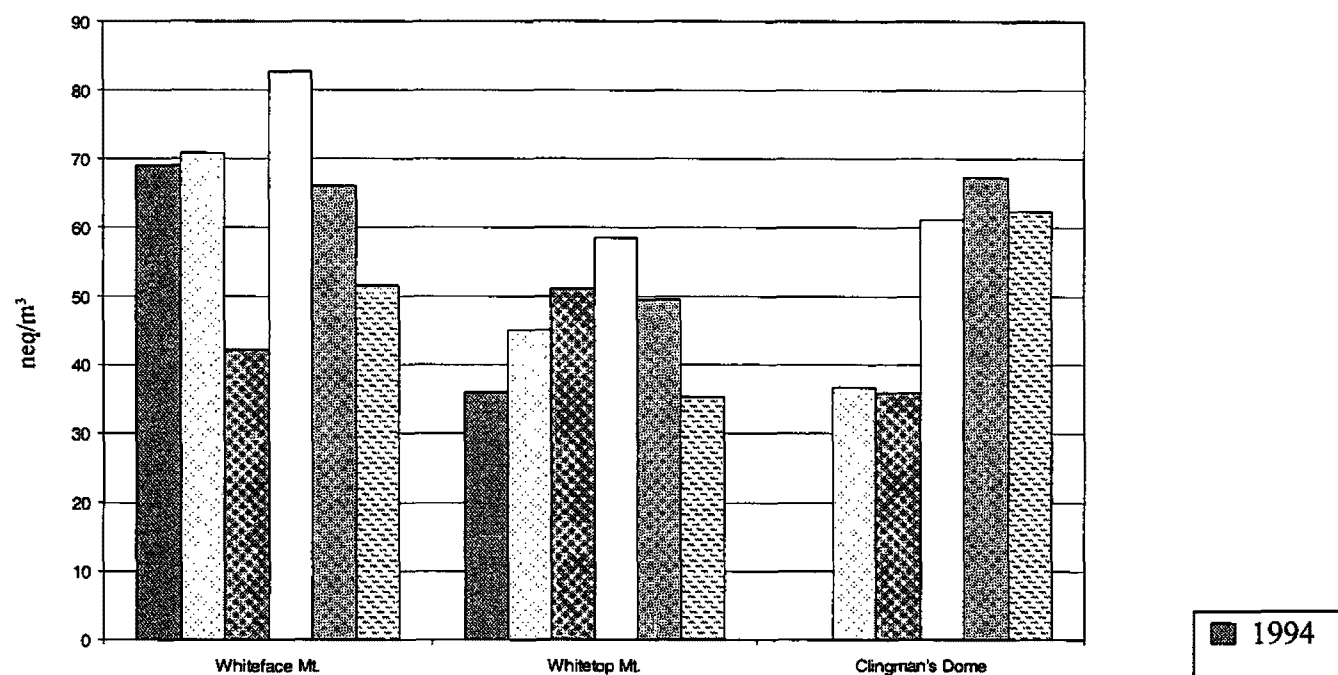


Figure 3-39. Normalized Mean NO_3^- Concentrations of Cloudwater Samples at MADPro Sites (1994 through 1999)

Source: Harding ESE.

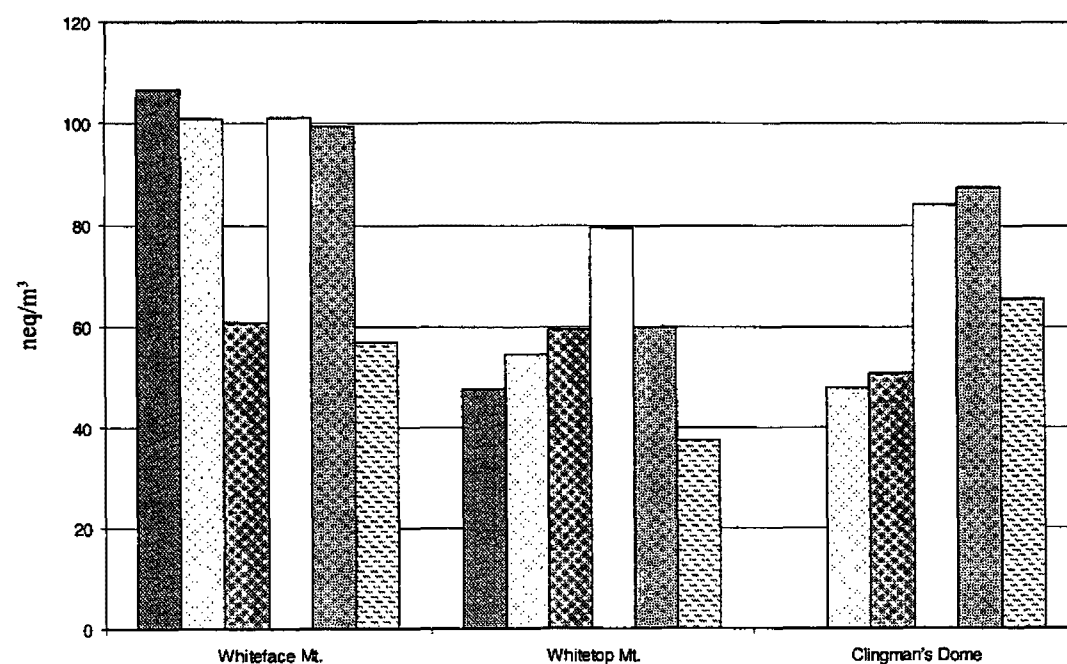


Figure 3-40. Normalized Mean NH_4^+ Concentrations of Cloudwater Samples at MADPro Sites (1994 through 1999)

Source: Harding ESE.

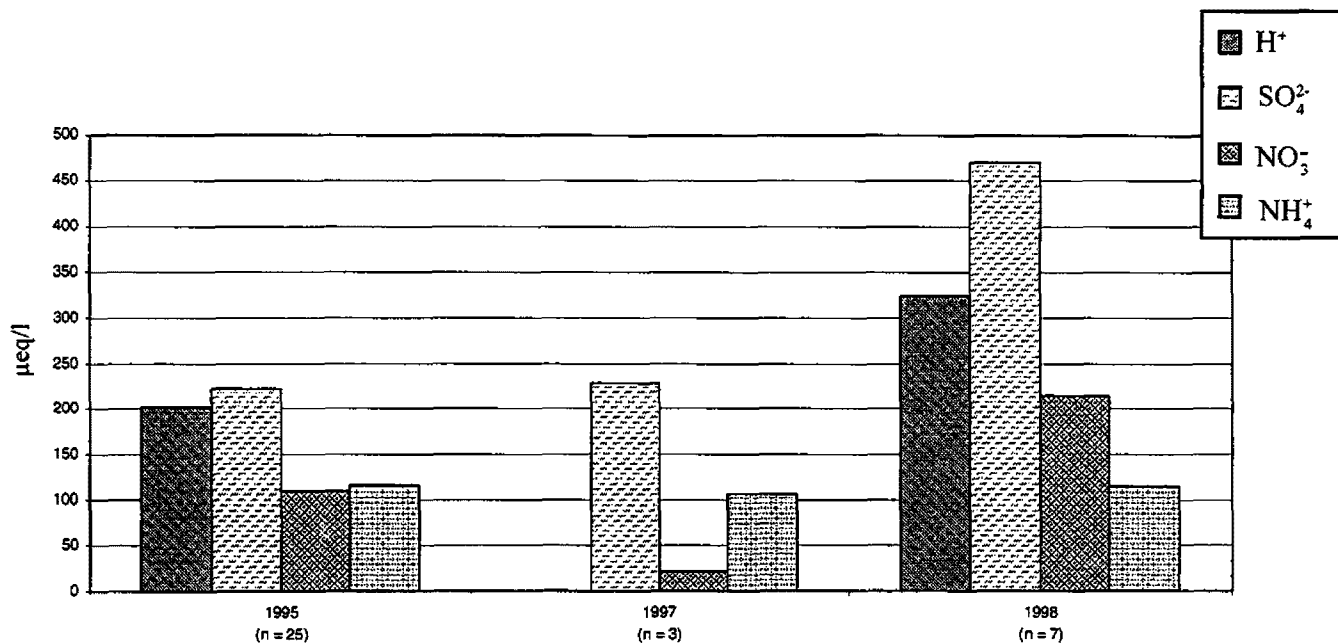


Figure 3-41. Concentrations for SLD/HUN301 (1995, 1997, 1998)

Source: Harding ESE.

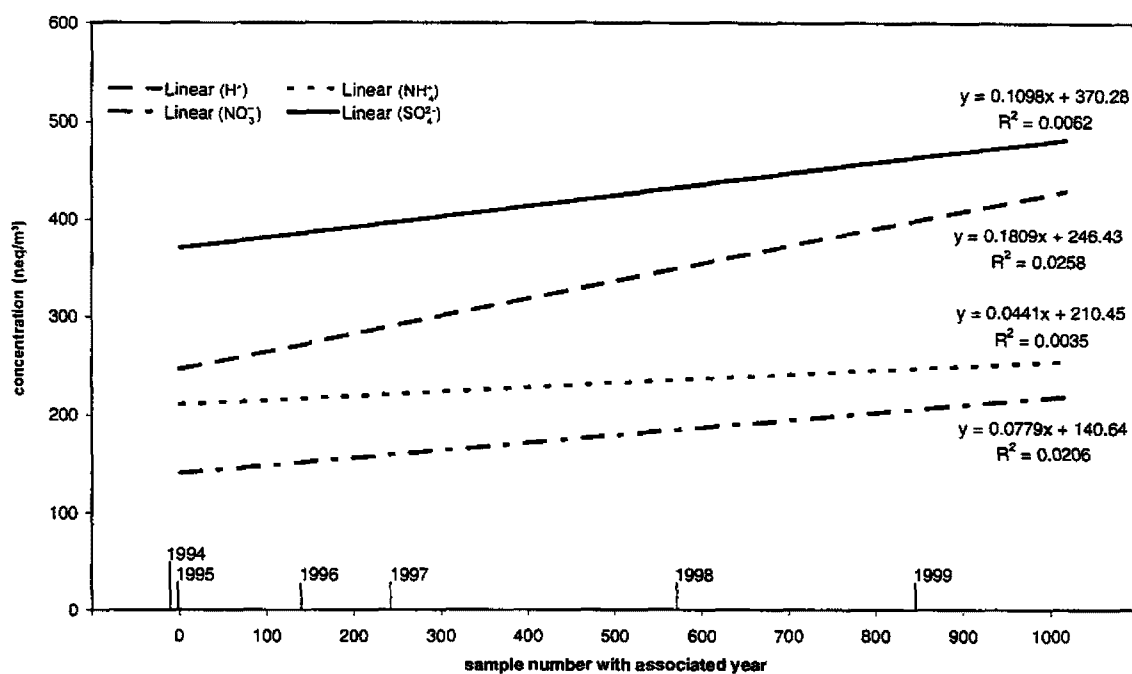


Figure 3-42. CLD303 1994 through 1999 Regressions Using All Data Points - Non-Normalized Concentrations

Source: Harding ESE.

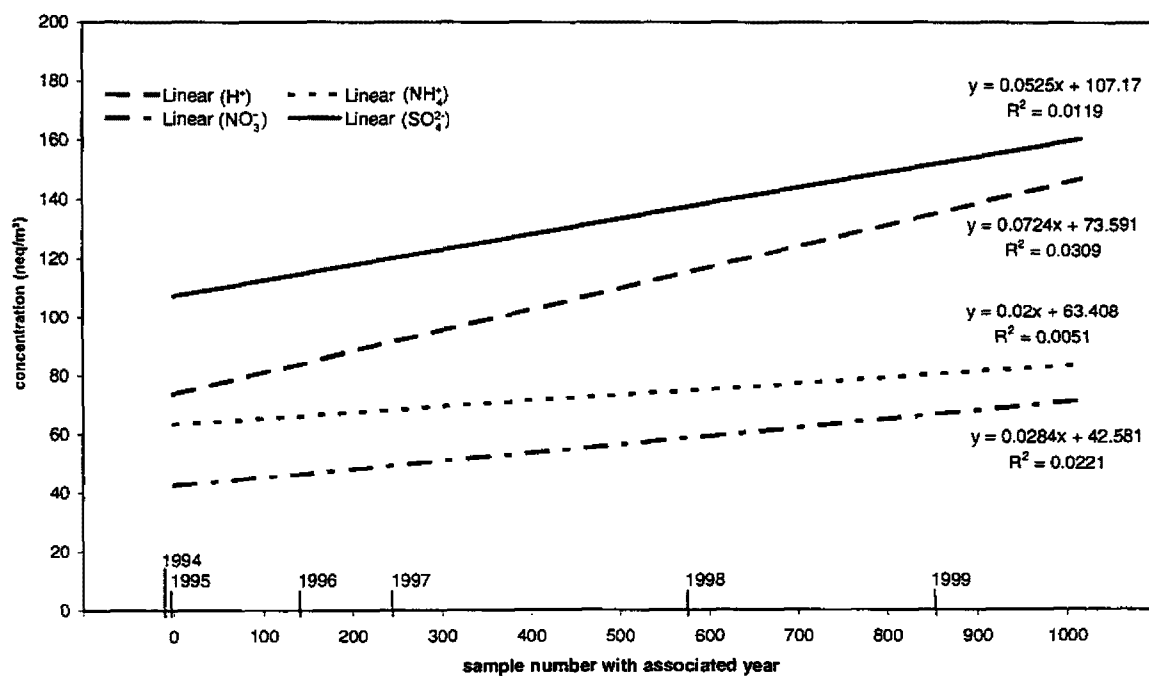


Figure 3-43. CLD303 1994 through 1999 Regressions Using All Data Points - Normalized Concentrations

Source: Harding ESE.

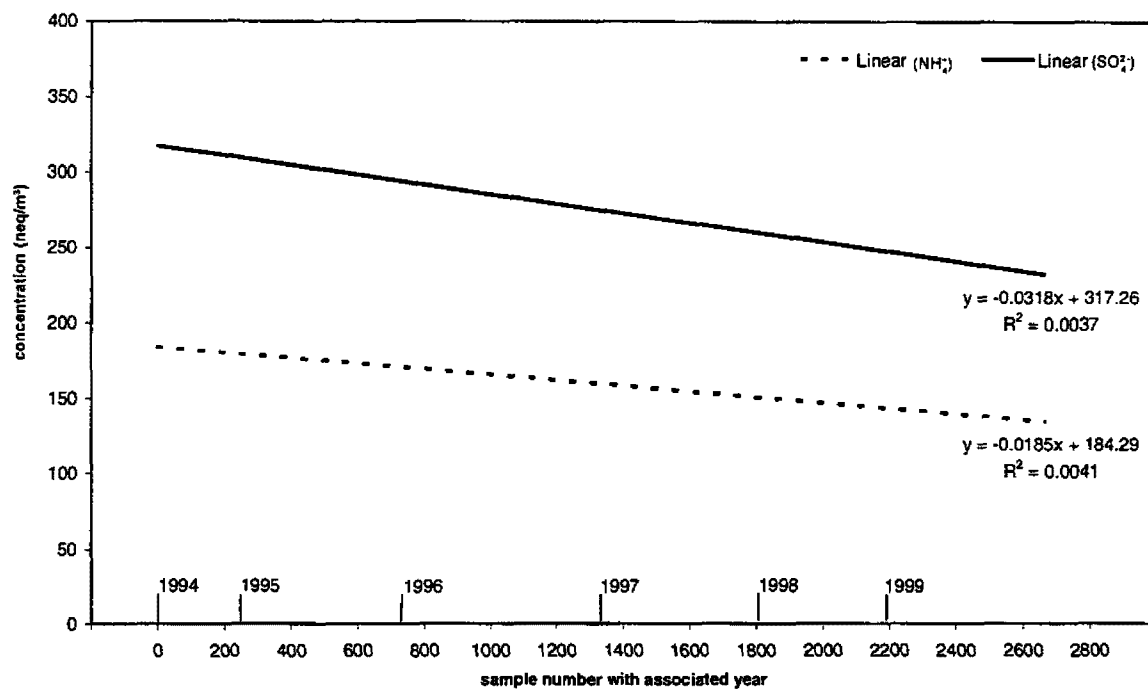


Figure 3-44. WFM300 1994 through 1999 Regressions Using All Data Points - Non-Normalized Concentrations

Source: Harding ESE.

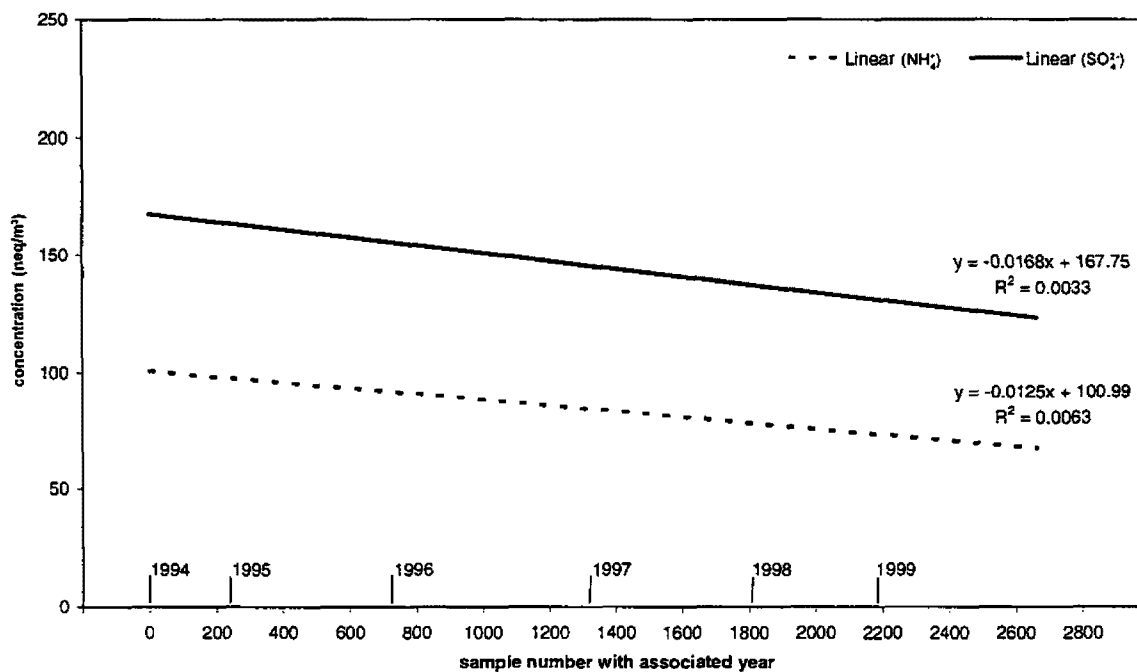


Figure 3-45. WFM300 1994 through 1999 Regressions Using All Data Points - Normalized Concentrations

Source: Harding ESE.

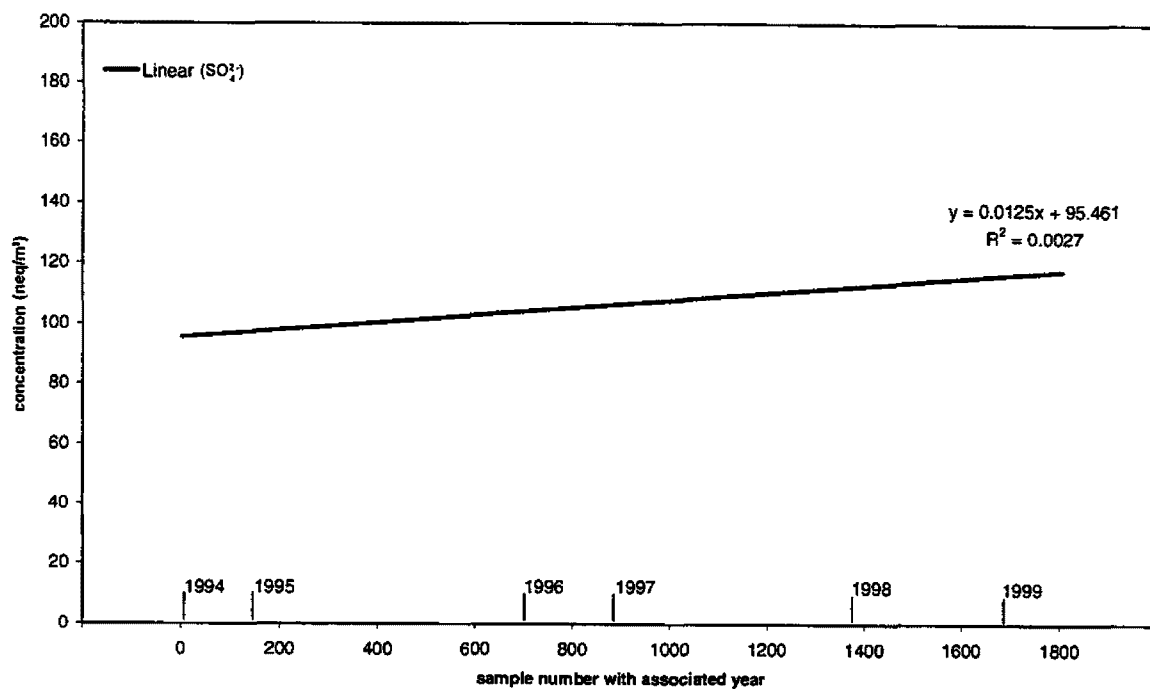


Figure 3-46. WTM302 1994 through 1999 Regressions Using All Data Points - Normalized Concentrations

Source: Harding ESE.

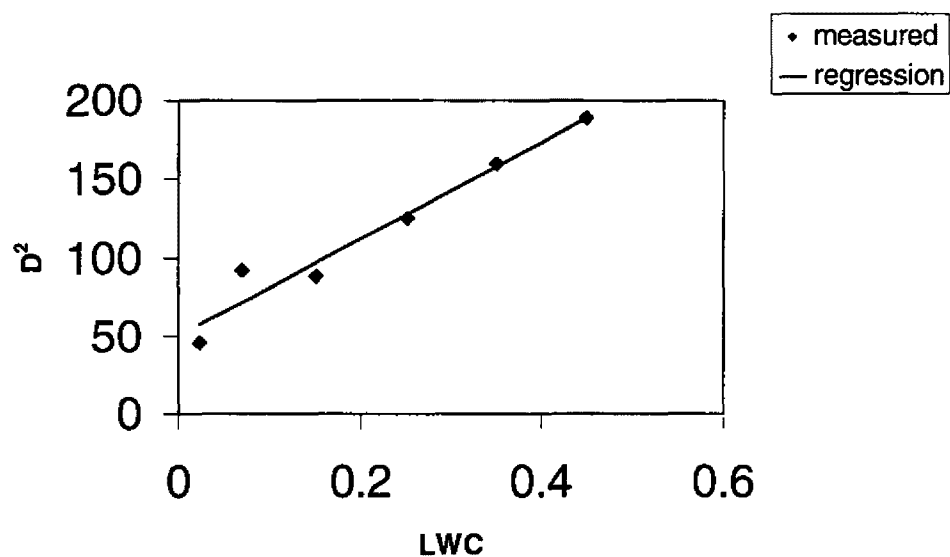


Figure 4-1. Relationship Between Square of the Mean Droplet Diameter (D) and LWC for Clouds on Whitetop Mountain

Note: Data are from Figure 2 of Joslin *et al.*, 1990.

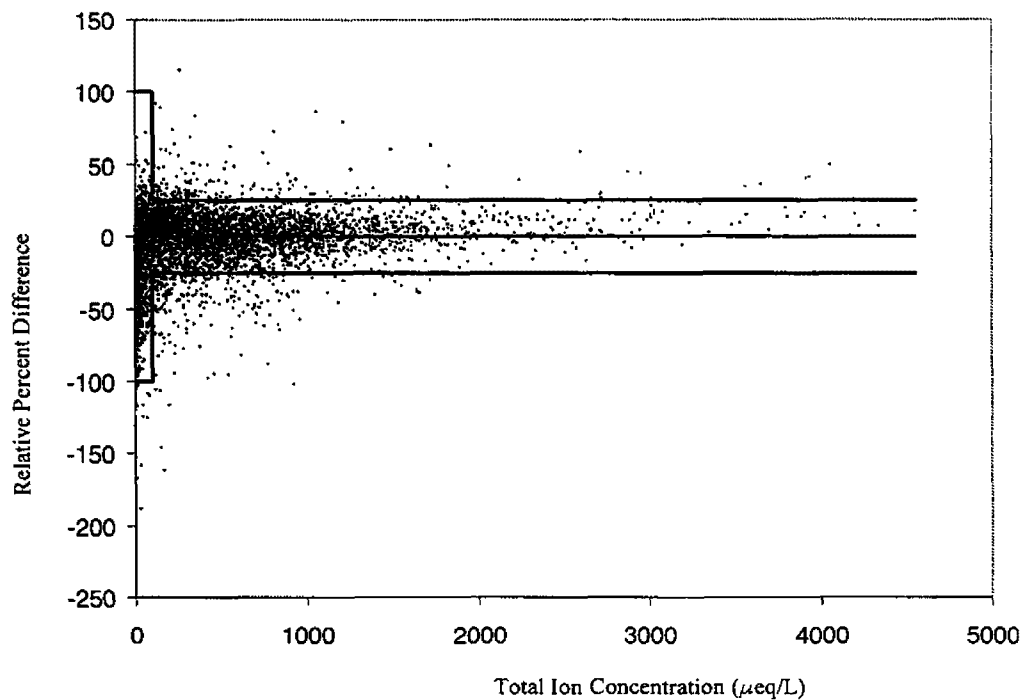


Figure 4-2. Relative Percent Difference Versus Total Anion Concentration for Each Sample

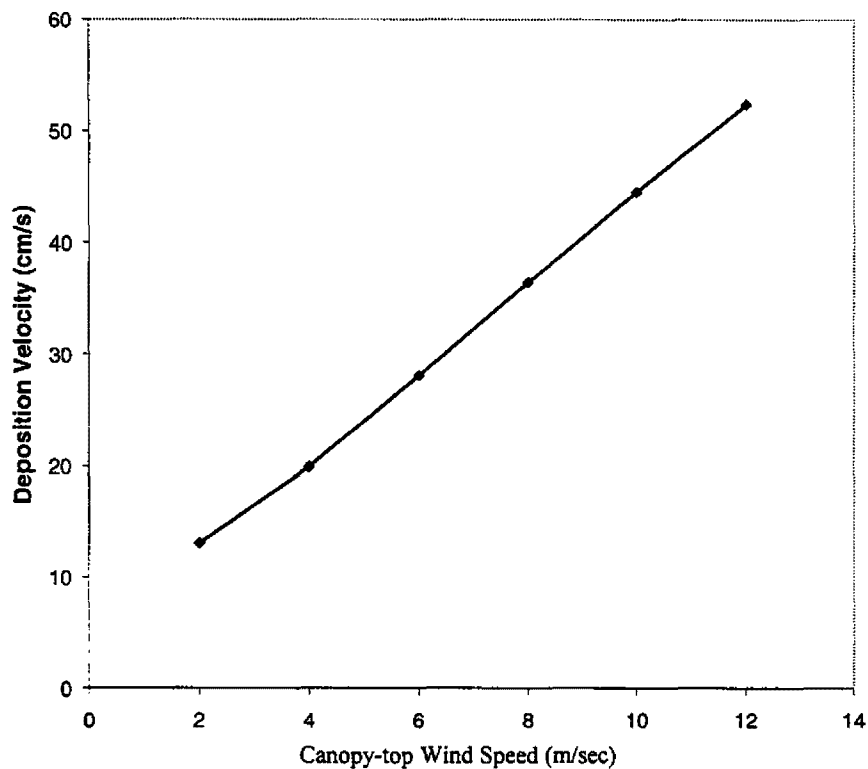


Figure 4-3. Sensitivity of Deposition Velocity to Wind Speed

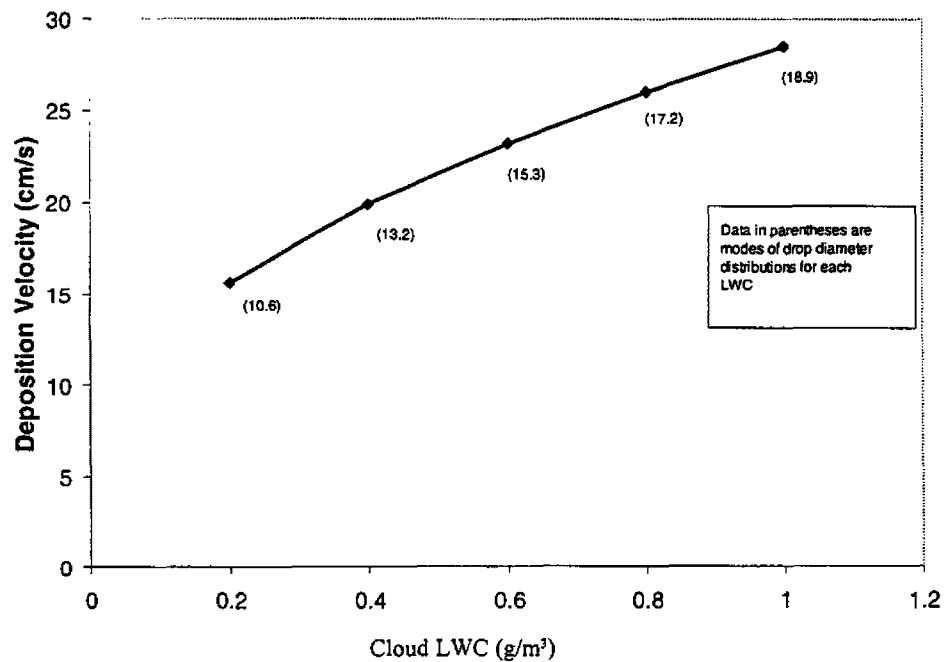


Figure 4-4. Sensitivity of Deposition Velocity to LWC

Note: For these simulations, the wind speed was set at 4 m/sec.

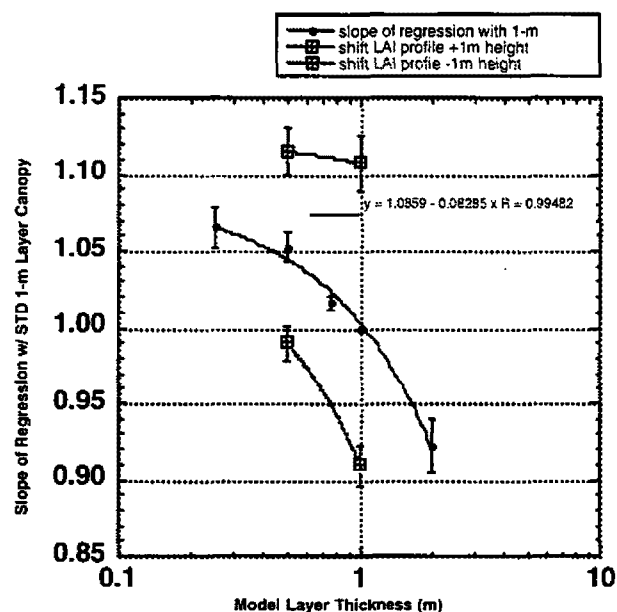


Figure 4-5. Results of Numerical Experiments with Model Layer Thickness and Shifts in the Vertical Distribution of Leaf Area.

Note: X-Axis is log scale. Y-axis represents the ratio of average model performance with a given scenario versus average performance with 1-m layers and the CASTNet standard leaf area profile.

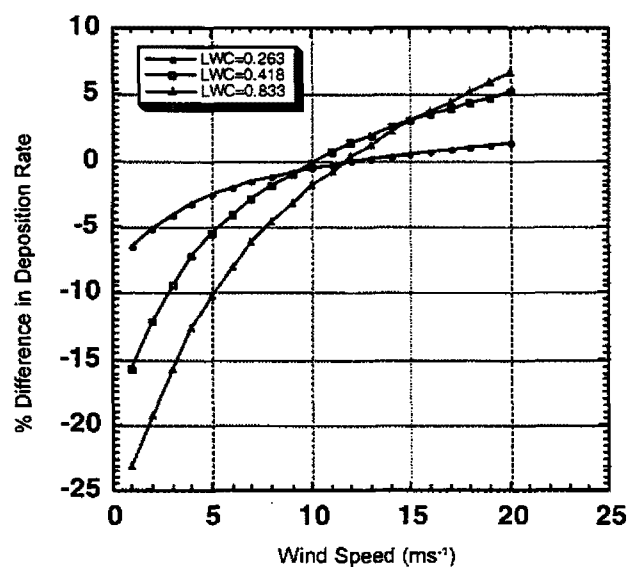


Figure 4-6. Difference in Cloudwater Deposition Rate Between Model Runs Using the Whitetop Mountain Cloud Droplet Size Distribution and the Whiteface Mountain Cloud Droplet Size Distribution for a Range of LWC and Wind Speed

Note: Percent deviations are calculated with respect to the Whiteface Mountain distribution results.

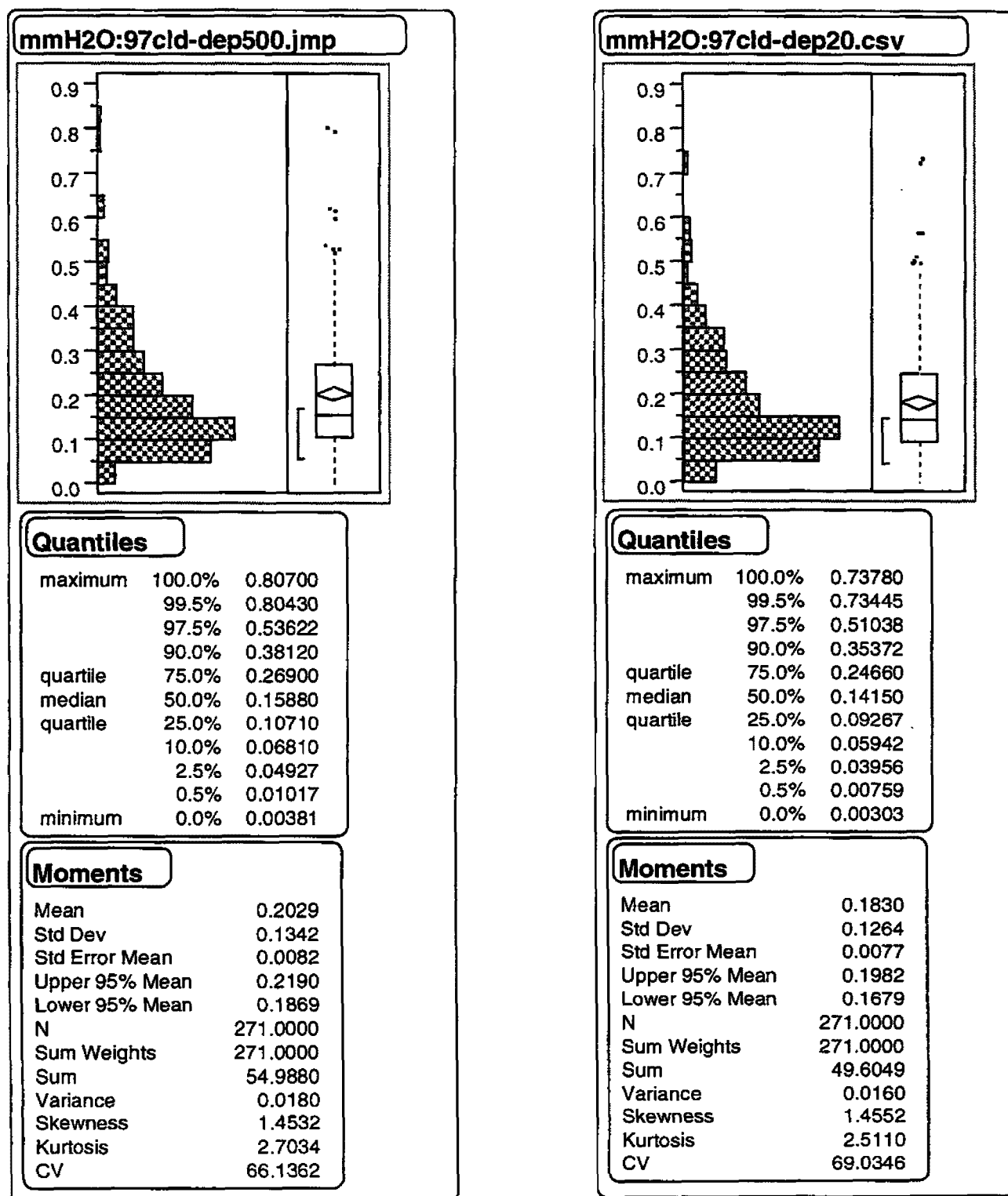
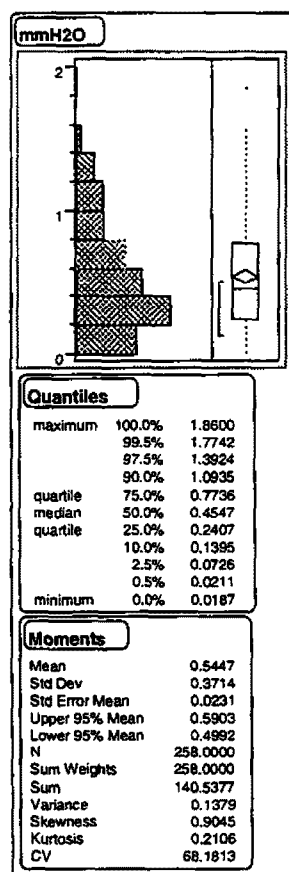
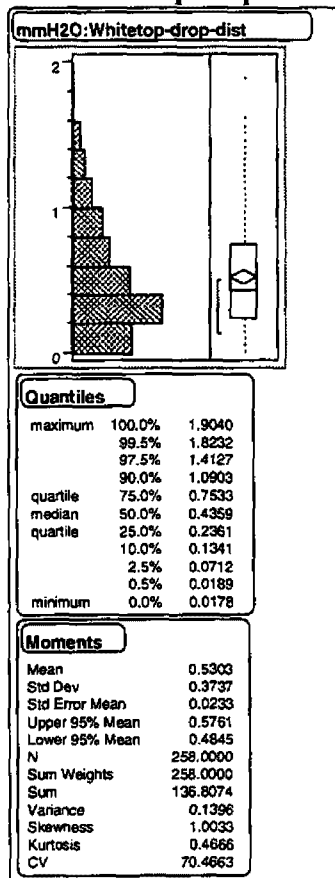


Figure 4-7. Frequency Distribution of Sample Water Deposition for Clingman's Dome 1997 Data Set Calculated with Either 500 or 20 Droplet Size Classes Representing the Continuous Droplet Size Distribution

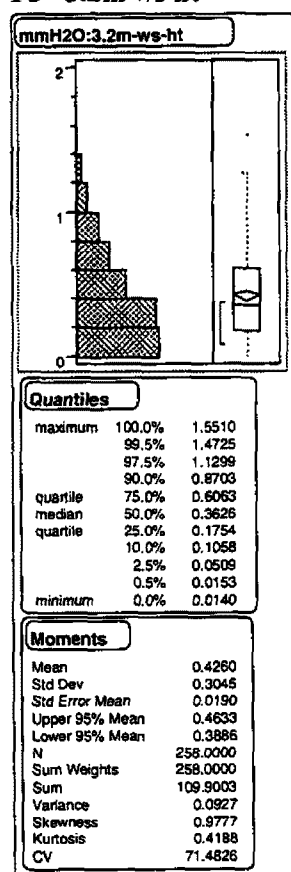
P1- standard MCLLOUD



P2- Whitetop drop sizes



P3- 3.2m ws ht



P4-summit WS & LWC

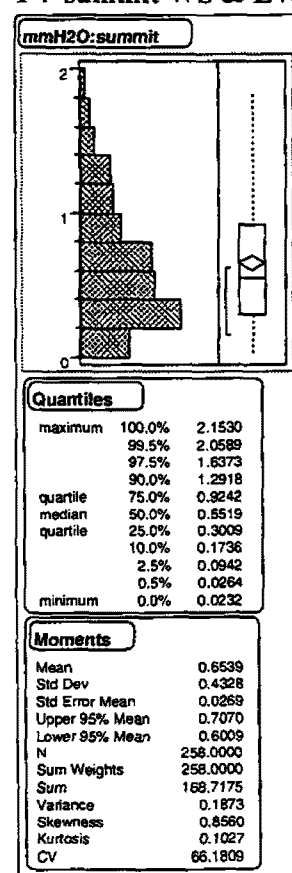


Figure 4-8. Comparison of Estimated Cloudwater Fluxes Using Four Potential Model Scenarios at Whiteface Mountain, 1997

Note: P1 - MCLLOUD Model, P2 - using the Whitetop, VA droplet size distribution, P3 - using 3.2 meters as the height of the windspeed measurement above the canopy, P4 - applying (uncorrected) summit WS and LWC to the 1,350-m elevation site.

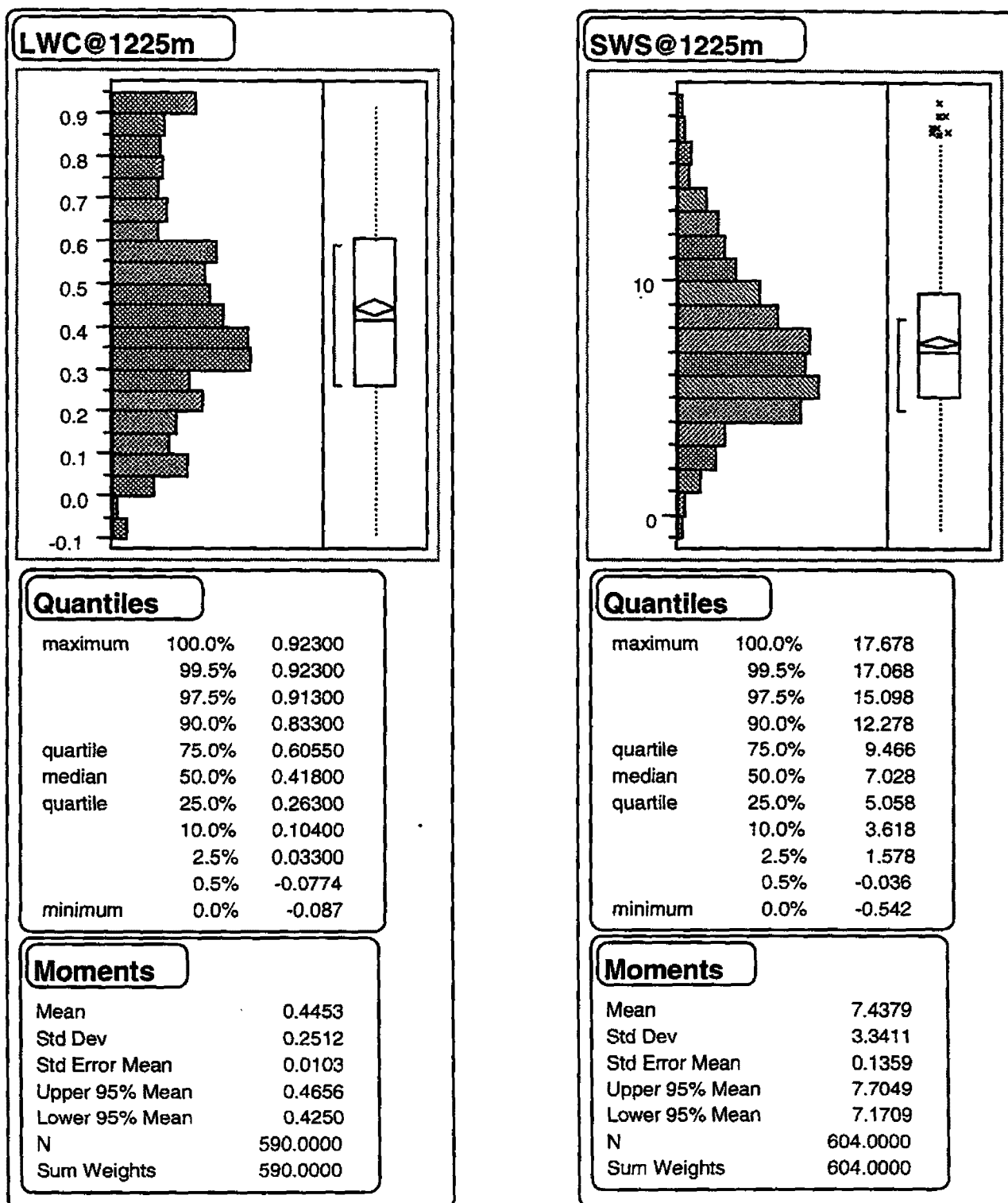


Figure 4-9. Frequency Distributions of LWC and Wind Speed Scaled to Values Representative of 1,225-m Elevation on Whiteface Mountain

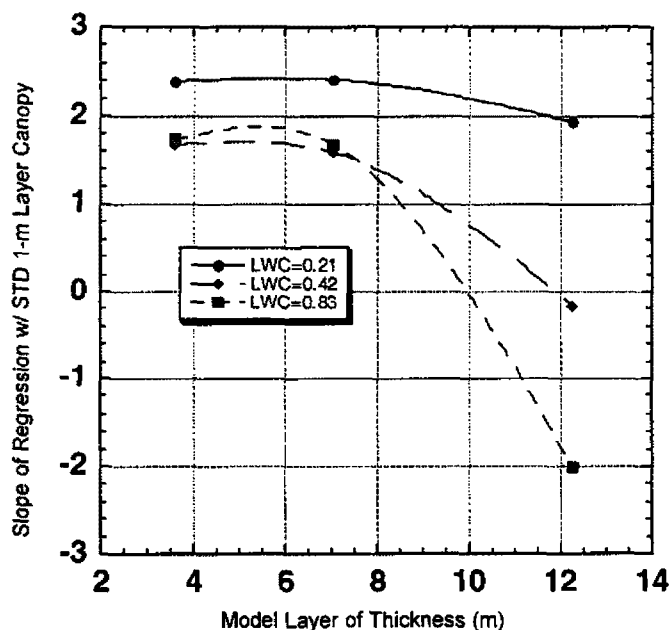


Figure 4-10. Percent Deviation of Model Response to a Hypothetical Pure Balsam Fir Canopy from Model Response to an Observed Average Canopy at 1,225-m Elevation on Whiteface Mountain over a Range of Wind Speed and LWC Values.

Note: In both cases, the canopy height was 17 m and LAI = $10 \text{ m}^2/\text{m}^2$.

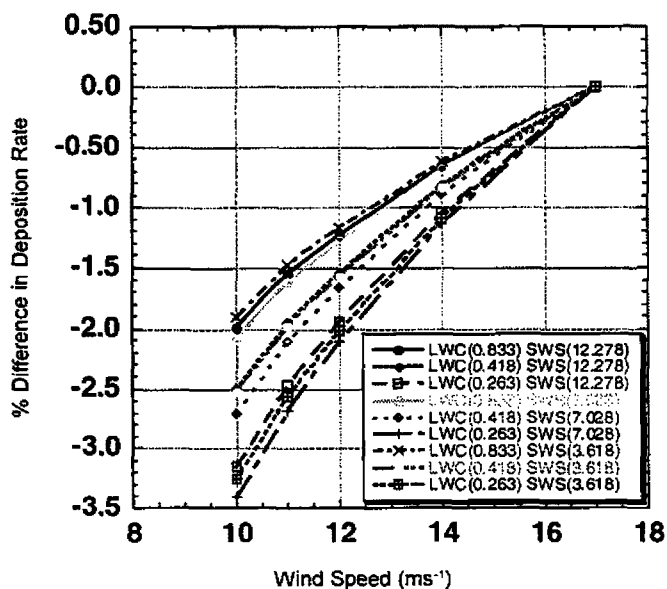


Figure 4-11. Percent Deviation of Model Response to Several Canopy Height Specifications from Model Response to the Observed Height of 17 m at 1,225-m Elevation.

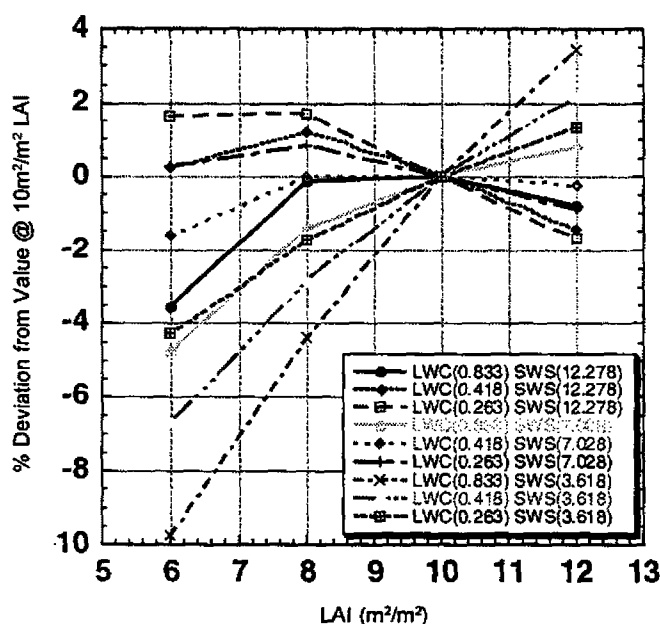


Figure 4-12. Percent Deviation of Model Response to Variations in LAI with a Constant Canopy Height of 10 m

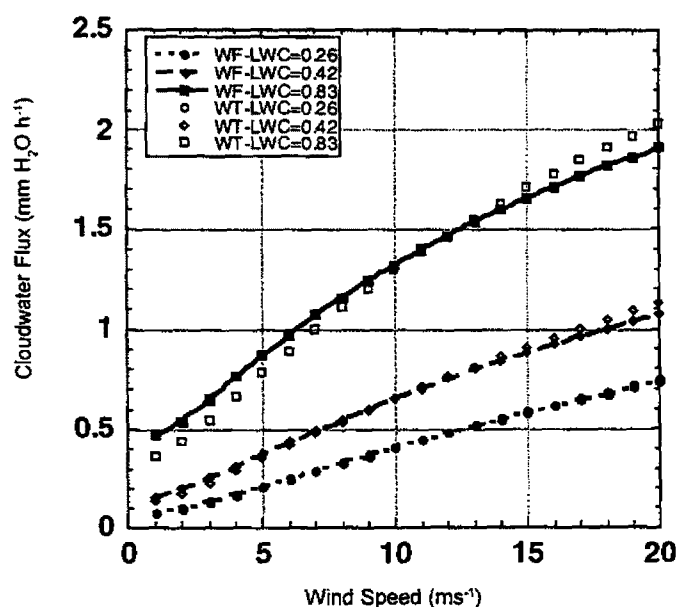


Figure 4-13. Model Response (Hourly Water Flux) to Variation in Wind Speed for a Range of Cloud LWC

Note: Solid symbols with solid lines are model response using the Whiteface Mountain cloud droplet size distribution (WF). Open symbols are model response using a droplet size distribution representative of Whitetop Mountain (WT).

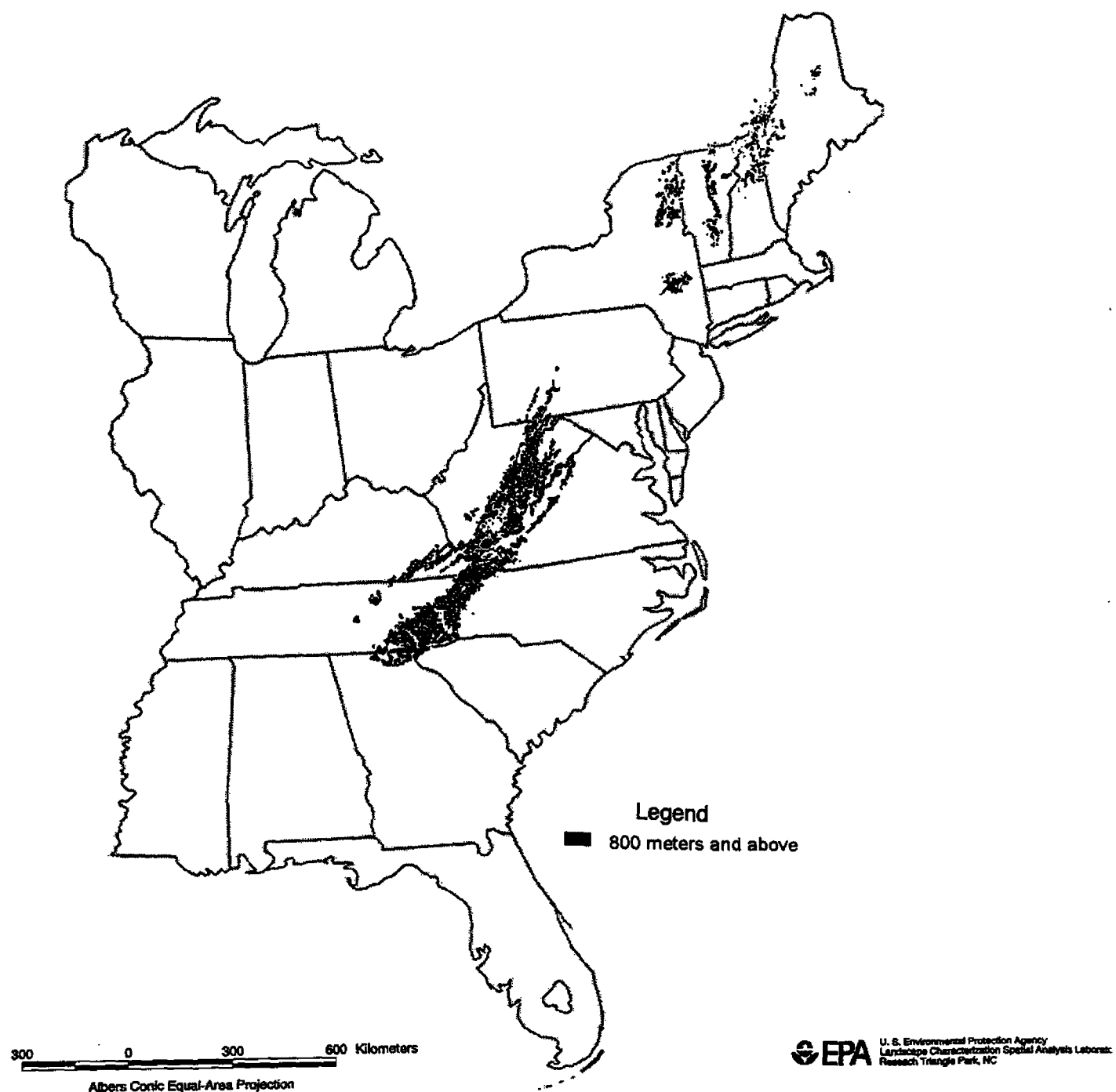


Figure 5-1. Areas in the Eastern United States with Elevations Above 800 Meters

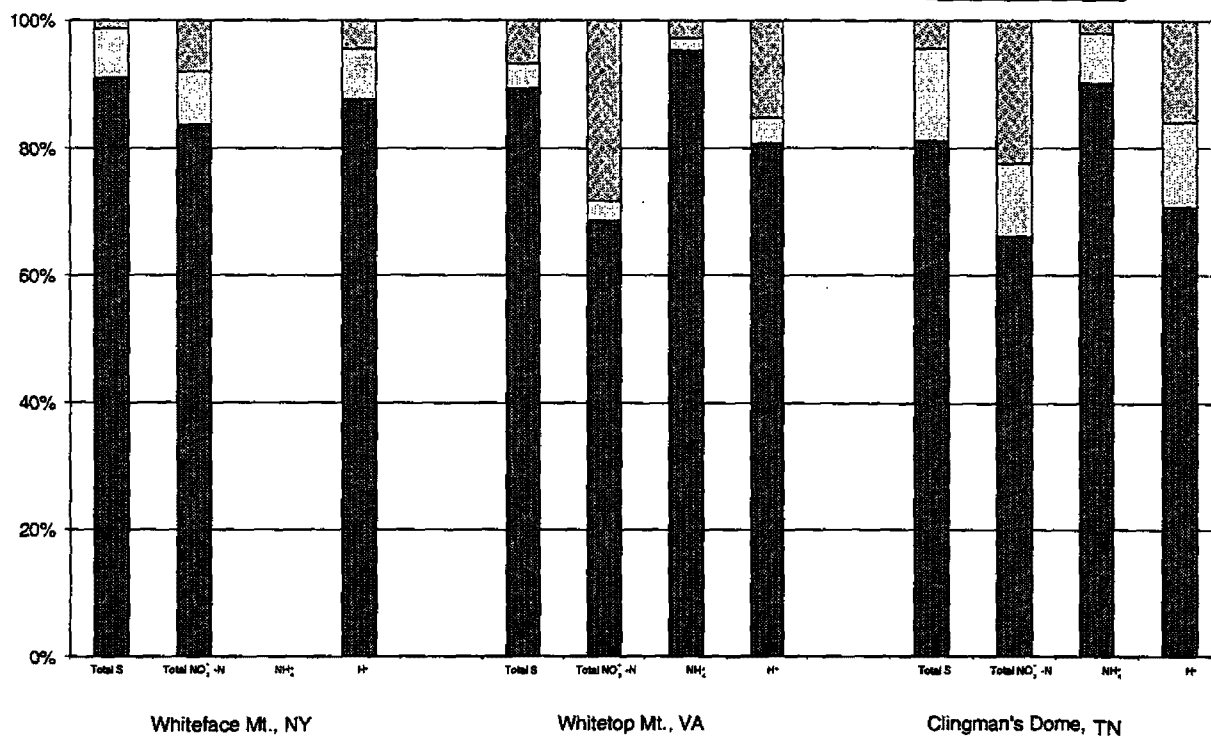
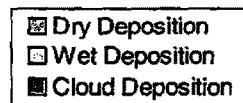
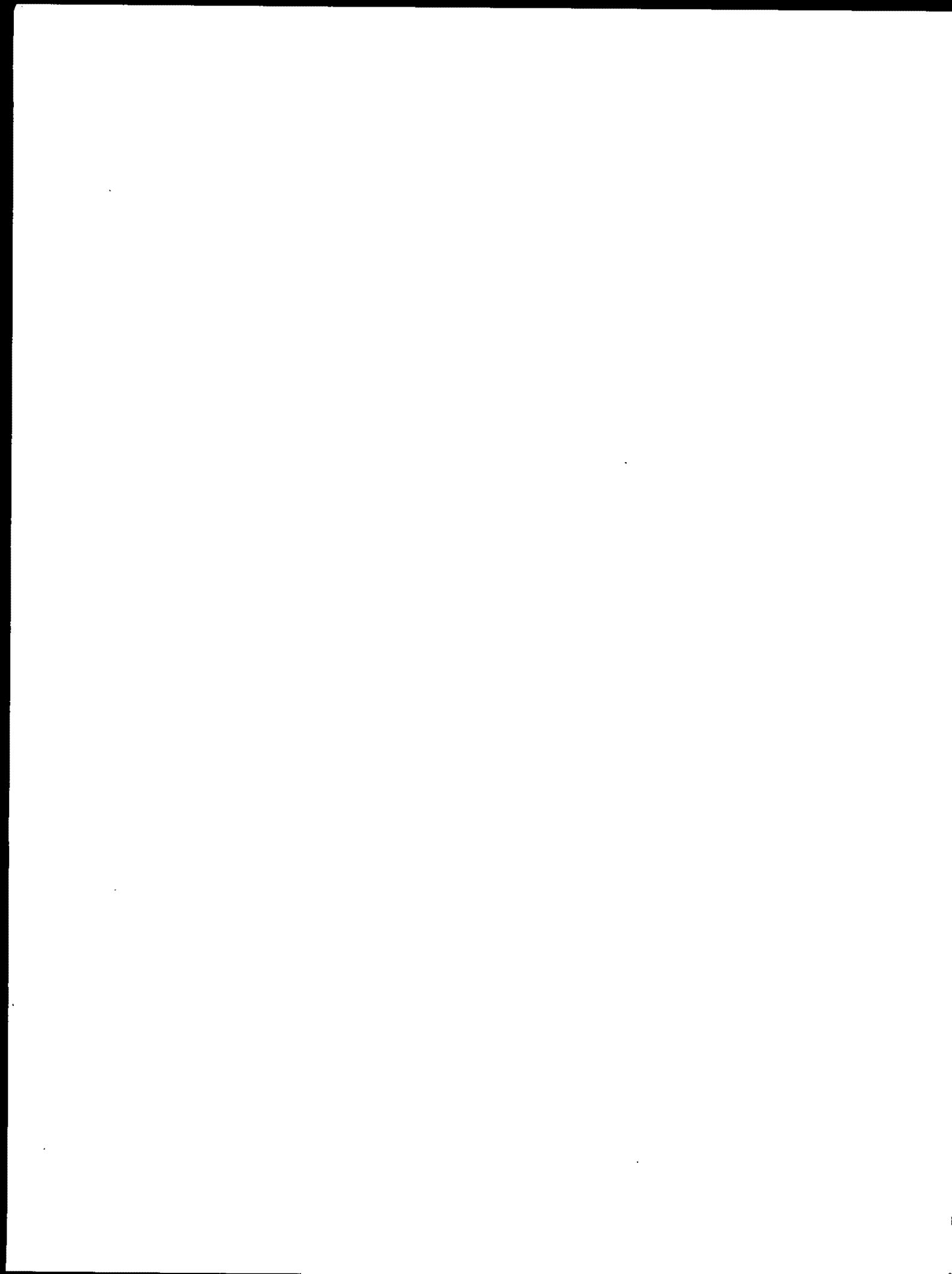


Figure 5-2. Percent Composition of Total Deposition Estimates at MADPro Sites
Source: Harding ESE.



Appendix



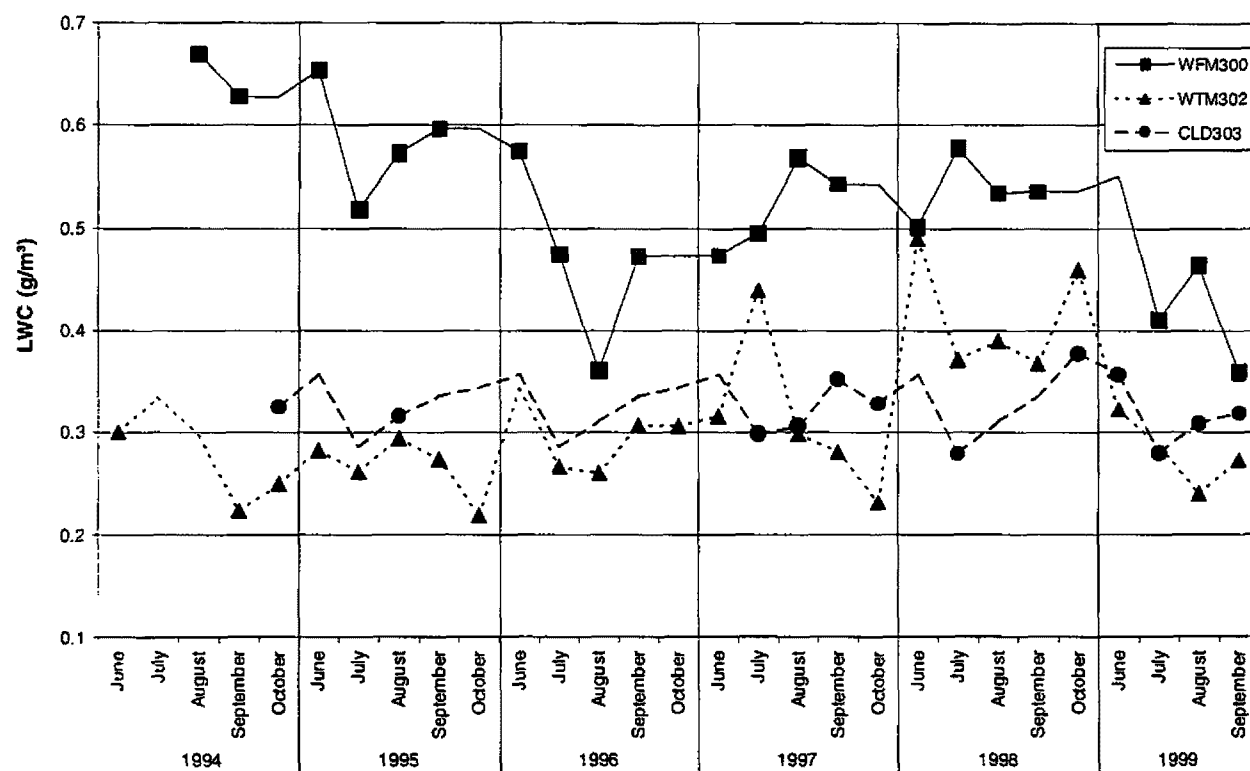


Figure A-1. Mean Liquid Water Content of Clouds with Scaled 1998 WTM LWC
Source: Harding ESE.

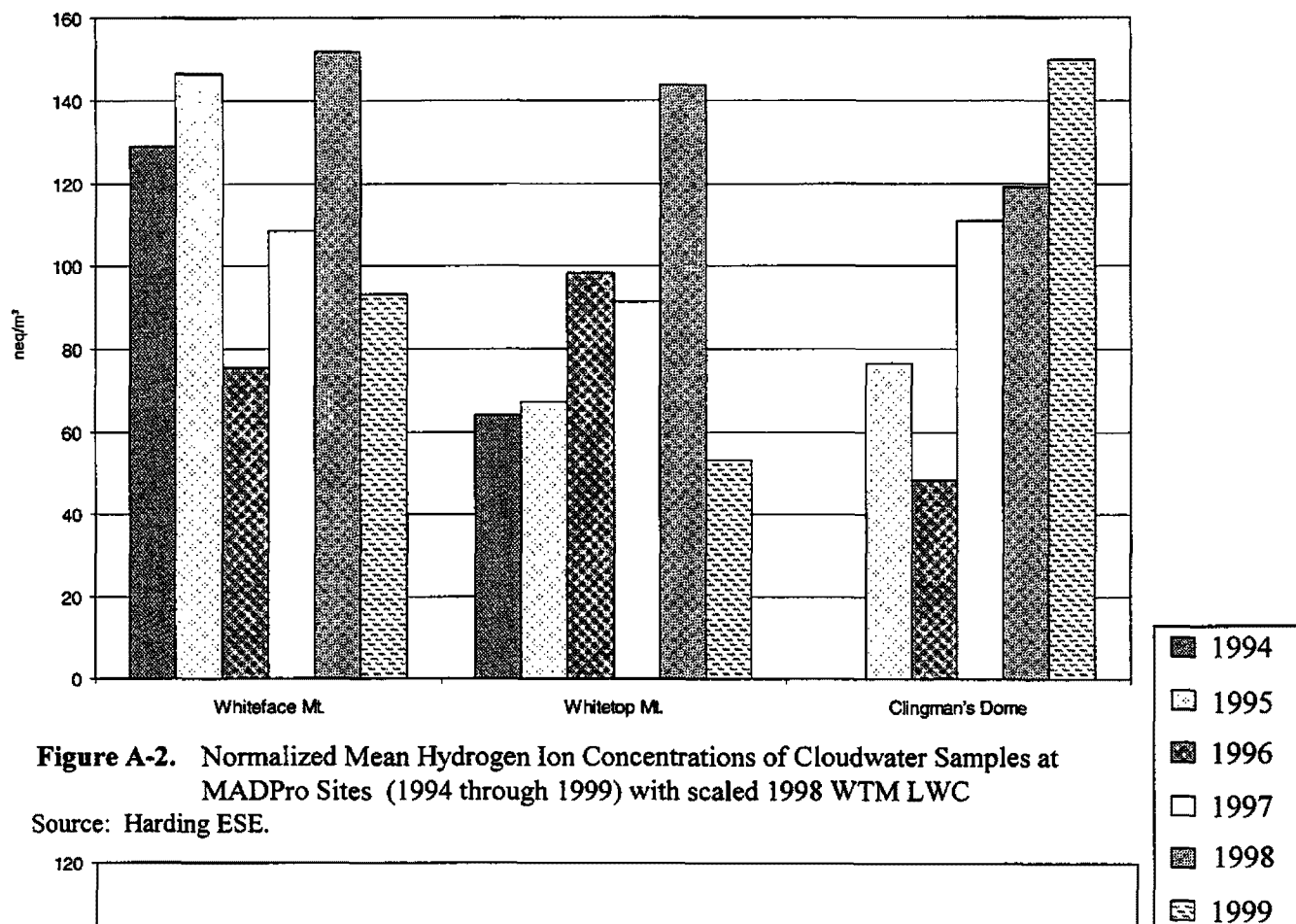


Figure A-2. Normalized Mean Hydrogen Ion Concentrations of Cloudwater Samples at MADPro Sites (1994 through 1999) with scaled 1998 WTM LWC

Source: Harding ESE.

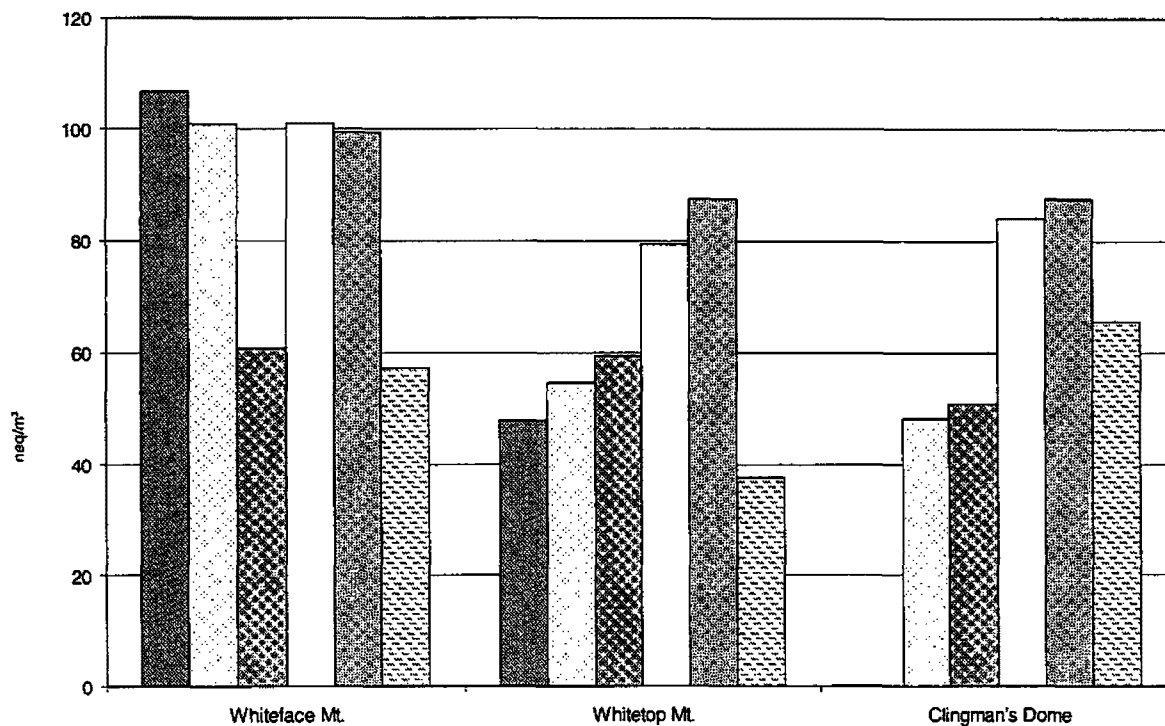


Figure A-3. Normalized Mean NH_4^+ Concentrations of Cloudwater Samples at MADPro Sites (1994 through 1999) with 1998 WTM LWC

Source: Harding ESE.

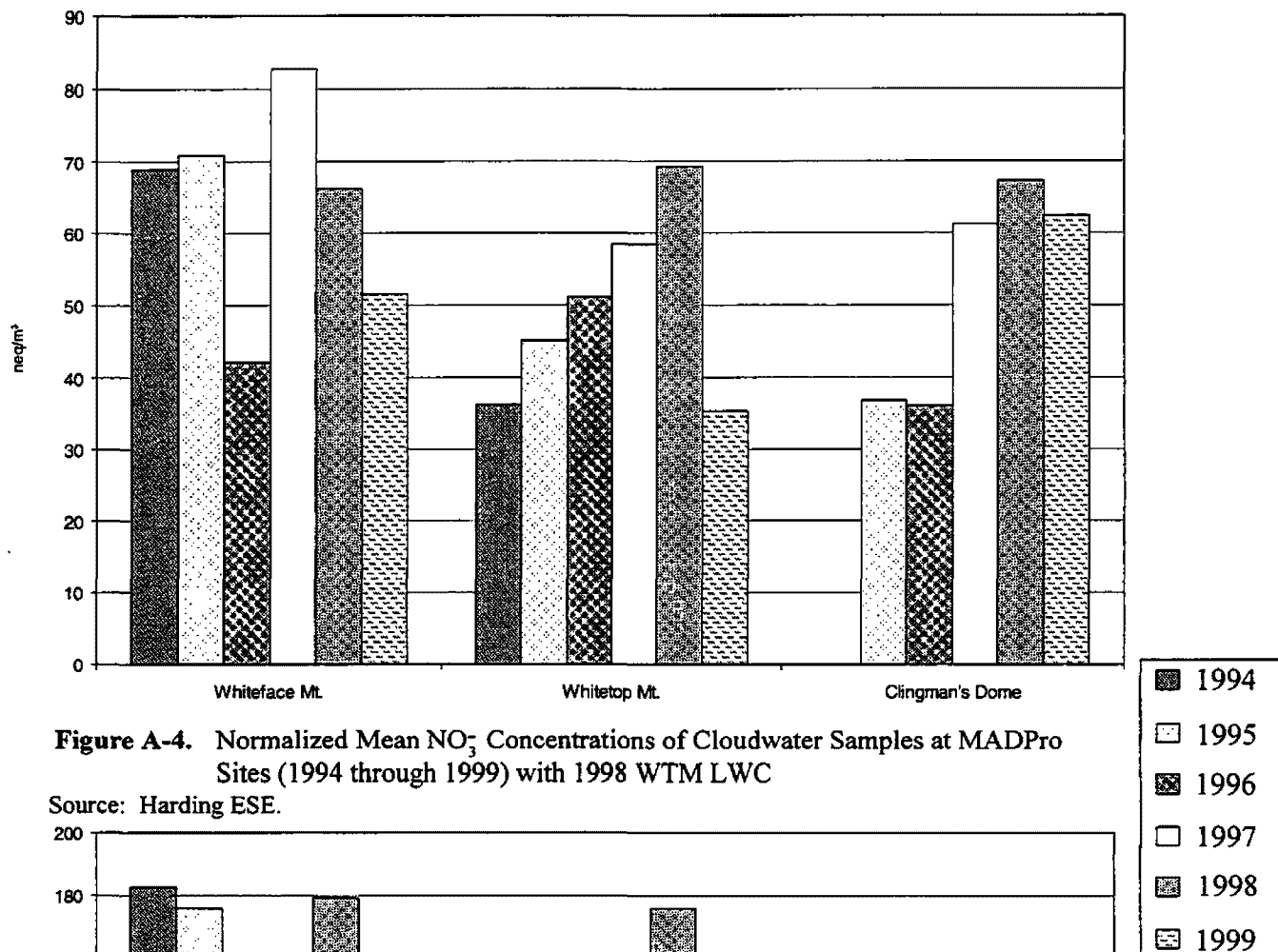


Figure A-4. Normalized Mean NO₃⁻ Concentrations of Cloudwater Samples at MADPro Sites (1994 through 1999) with 1998 WTM LWC

Source: Harding ESE.

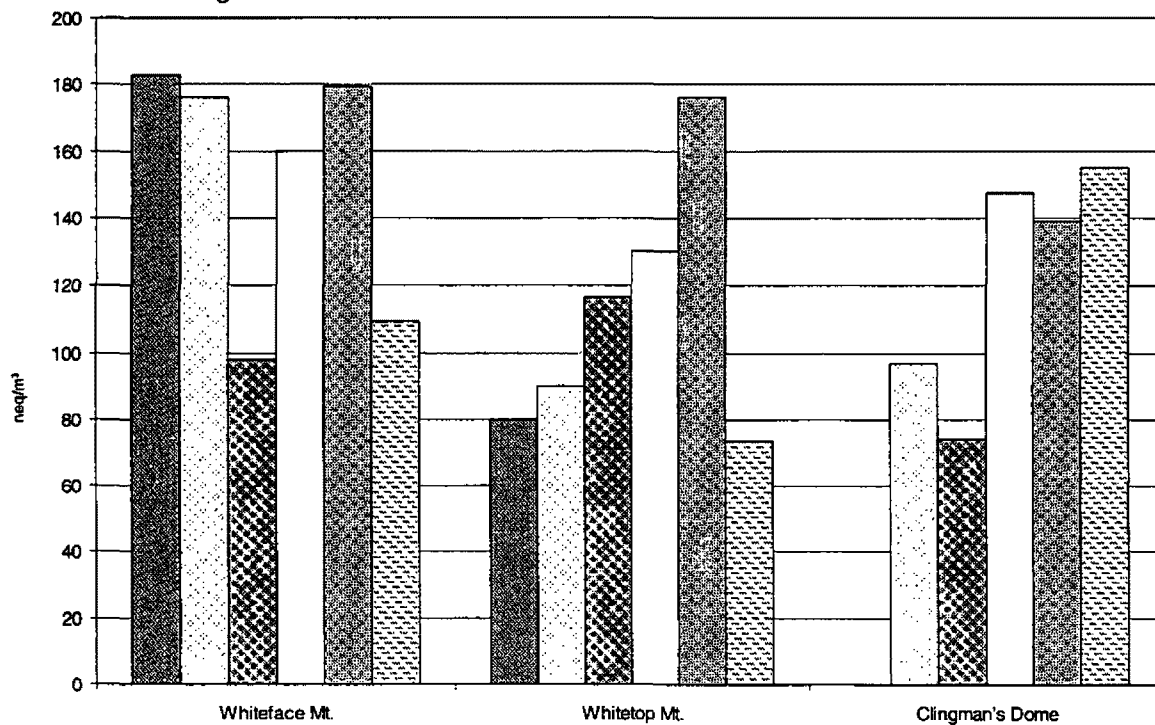


Figure A-5. Normalized Mean SO₄²⁻ Concentrations of Cloudwater Samples at MADPro Sites (1994 through 1999) with 1998 WTM LWC

Source: Harding ESE.

